

LONDON  
SCHOOL of  
HYGIENE  
& TROPICAL  
MEDICINE



**Investigation of the Role of Bile Salts in the  
Biogenesis and Virulence of *Campylobacter jejuni*  
Outer Membrane Vesicles**

**Cadi Hazel Mary Davies**

Thesis submitted in accordance with the requirements for the degree of  
Doctor of Philosophy  
of the  
University of London

March 2022

**Department of Infection Biology**

**Faculty of Infectious and Tropical Diseases**

**LONDON SCHOOL OF HYGIENE & TROPICAL MEDICINE**

Funding details - No funding received

## **Declaration**

I, Cadi Davies, confirm that the work presented in this thesis is my own. Where information has been derived from other sources, I confirm that this has been indicated in the thesis.

## Data contributed by others

The following datasets were produced either by others, or with help from others.

**Chapter 3:** The *Campylobacter jejuni* 11168 *miaA* mutant and 11168H *miaA* complement strains were provided by Dr Aidan Taylor in collaboration with Professor David Kelly at the University of Sheffield.

**Chapter 3:** Whole genome sequencing of *Campylobacter jejuni* strains was performed by Dr Ozan Gundogdu at the London School of Hygiene and Tropical Medicine.

**Chapter 3:** 3,3'-Dipropylthiadicarbocyanine Iodide (DiSC3) membrane permeability assay was performed by Dr Aidan Taylor in collaboration with Professor David Kelly at the University of Sheffield.

**Chapter 3:** Nanoparticle tracking analysis was performed by myself and Dr Jody Winter at Nottingham Trent University.

**Chapter 4:** RNAs-Seq bioinformatic analysis was performed by Dr Umer Zeeshan Ijaz at the University of Glasgow.

## Abstract

*Campylobacter jejuni* is a leading cause of foodborne bacterial gastroenteritis worldwide. As *C. jejuni* lacks the classical virulence-associated secretion systems of other enteric pathogens for the delivery of effector proteins into host cells, outer membrane vesicles (OMVs) may have a particularly important role in virulence. The bile salt sodium taurocholate (ST) has previously been shown to stimulate *C. jejuni* OMV production and enhance pathogenic properties of OMVs through an unknown mechanism. The maintenance of lipid asymmetry (MLA) pathway has been shown to play a role in the regulation of OMV production in other bacteria. Mutation of *miaA* in *C. jejuni* increased OMV production independent of changes to membrane stability. Additionally, OMV production of the *miaA* mutant was not stimulated by ST. RNA-Seq was performed to further characterise the transcriptional responses of *C. jejuni* to bile salts and identify key genes as a starting point for further hypothesis driven research. The transcriptional response of *C. jejuni* to biologically relevant concentrations of ST and sodium deoxycholate (SDC) was investigated. The uncharacterised gene *Cj0561c* demonstrated the greatest transcriptional response and was selected for further investigation. *C. jejuni* *Cj0561c* mutants were constructed in two wild-type strains. Given the link between *Cj0561c* and the multidrug efflux pump CmeABC through the transcriptional regulator CmeR, *cmeB* mutant and *cmeB Cj0561c* double mutants were also constructed. A range of phenotypic assays were carried out but no clear function for *Cj0561c* was elucidated. However, *Cj0561c* appeared to play a role in OMV cytotoxicity and lauryl sulfobetaine sensitivity. This study furthered the knowledge of the role of bile salts in *C. jejuni* OMV-mediated virulence. As the gut bile composition is impacted by both diet and microbiota, this study also highlights the potential importance of diet and lifestyle factors on the varying disease presentations associated with gut pathogen infections.

## Table of contents

Declaration .....	2
Data contributed by others.....	3
Abstract .....	4
Table of contents .....	5
Acknowledgements .....	9
List of abbreviations .....	10
Chapter One: Introduction.....	15
1.1 <i>Campylobacter jejuni</i> .....	15
1.1.1 Characteristics .....	15
1.1.2 <i>Campylobacter</i> Genus.....	15
1.1.3 Epidemiology .....	16
1.1.4 Infection .....	17
1.2 Pathogenesis .....	18
1.2.1 Flagella.....	18
1.2.2 Cytolethal distending toxin.....	19
1.2.3 Capsular polysaccharide .....	19
1.2.4 Lipooligosaccharide .....	19
1.2.5 Glycosylation .....	20
1.2.6 Adhesins .....	21
1.3 Bile salts and bacteria virulence .....	22
1.3.1 Bile salts background .....	22
1.3.2 Bile salt composition in the human gut.....	23
1.3.3 Bile salts and bacterial virulence.....	24
1.3.4 <i>C. jejuni</i> interactions with bile salts .....	26
1.4 Outer membrane vesicles (OMVs).....	30
1.4.1 Background and roles .....	30
1.4.2 Biogenesis.....	30
1.4.3 The maintenance of lipid asymmetry pathway (MLA) .....	32
1.4.4 Role of OMVs in bacterial virulence .....	34
1.4.5 <i>C. jejuni</i> OMVs .....	35
1.5 Aims and objectives.....	37
Chapter 2: Materials and Methods .....	38
2.1 Bacterial strains and growth conditions .....	38
2.2 Assays.....	39

2.2.1	Growth kinetics.....	39
2.2.2	Motility.....	39
2.2.3	Detergent sensitivity.....	40
2.2.4	Antibiotic sensitivity.....	40
2.2.5	3,3'-dipropylthiadicarbocyanine Iodide (DiSC3) permeability assay.....	41
2.2.6	Heat shock.....	41
2.2.7	Osmotic stress.....	41
2.2.8	Carbonyl cyanide <i>m</i> -chlorophenylhydrazone (CCCP) efflux pump inhibition assay..	42
2.3	OMV isolation and characterisation.....	43
2.3.1	OMV isolation.....	43
2.3.2	Protein quantification – Bicinchoninic acid (BCA) assay.....	43
2.3.3	Lipid quantification (KDO).....	43
2.3.4	Nanoparticle tracking analysis particle counts and size.....	44
2.4	Cell culture.....	45
2.4.1	Cell lines and conditions.....	45
2.4.2	Interaction, invasion, intracellular survival and IL-8 secretion assays.....	45
2.4.3	Treatment of intestinal epithelial cells with outer membrane vesicles.....	46
2.4.4	Interleukin-8 (IL-8) enzyme-linked immunosorbent assay (ELISA).....	47
2.5	<i>Galleria mellonella</i> larvae model of infection.....	48
2.5.1	<i>Galleria mellonella</i> larvae infection with live <i>C. jejuni</i> cells.....	48
2.5.2	<i>Galleria mellonella</i> larvae inoculation with outer membrane vesicles.....	48
2.6	Molecular techniques.....	49
2.6.1	Genomic DNA isolation.....	49
2.6.2	PCR.....	49
2.6.3	Mutagenesis.....	50
2.6.4	Natural transformation.....	56
2.6.5	Complementation.....	56
2.6.6	Whole genome sequencing.....	57
2.6.7	RNA isolation.....	58
2.6.8	qRT-PCR.....	58
2.6.9	RNA-Seq.....	60
2.6.10	Primers used in this study.....	70
2.7	Statistical analysis.....	73
<b>Chapter 3: Sodium taurocholate stimulates <i>Campylobacter jejuni</i> outer membrane vesicle production via down-regulation of the maintenance of lipid asymmetry pathway.....</b>		
3.1	Preface.....	74

3.1.1	Aims and objective .....	74
3.1.2	Assay optimisation data.....	76
3.2	Publication: Sodium Taurocholate Stimulates <i>Campylobacter jejuni</i> Outer Membrane Vesicle Production via Down-Regulation of the Maintenance of Lipid Asymmetry Pathway .....	86
Chapter Four:	RNA-Seq analysis of the transcriptional response of <i>C. jejuni</i> to the bile salts sodium taurocholate and sodium deoxycholate .....	112
4.1	Introduction .....	112
4.2	Results.....	114
4.2.1	Experimental design .....	114
4.2.2	Biologically relevant concentrations of sodium taurocholate or sodium deoxycholate did not cause significant changes to the overall transcriptional profile of wild-type strains. ....	115
4.2.3	Differentially expressed genes identified by DESeq analysis.....	116
4.2.4	Differentially expressed genes identified by SPLS-DA.....	121
4.2.5	Final gene list of differentially expressed genes .....	139
4.2.6	Verification of differentially expressed genes by qRT-PCR.....	141
4.3	Discussion.....	143
4.3.1	Sampling conditions.....	143
4.3.2	Differentially expressed genes identified by DESeq .....	143
4.3.3	Differentially expressed genes identified by sPLS-DA .....	144
4.3.4	Final list of differentially expressed genes .....	144
4.4	Conclusion .....	148
Chapter Five:	Phenotypic characterisation of bile salt response gene <i>Cj0561c</i> .....	149
5.1	Introduction .....	149
5.2	Results.....	151
5.2.1	<i>Cj0561c</i> is an outer membrane $\beta$ -barrel protein with a DUF2860 domain .....	151
5.2.2	The regulation of <i>Cj0561c</i> by sodium taurocholate and sodium deoxycholate .....	163
5.2.3	<i>Cj0561c</i> does not have a major role in resistance to heat shock or osmotic stress. ....	165
5.2.4	<i>Cj0561c</i> does not appear to play a role in antibiotic resistance .....	168
5.2.5	<i>Cj0561c</i> is not involved with bile salt sensitivity or active transport.....	170
5.2.6	<i>Cj0561c</i> does not have a general role in detergent sensitivity. ....	174
5.2.7	Transcriptional response of <i>Cj0561c</i> and <i>cmeABC</i> to LSB and taurine.....	177
5.2.8	<i>CmeABC</i> does not mask a <i>Cj0561c</i> detergent stress phenotype.....	179
5.2.9	<i>Cj0561c</i> has no clear role during bacterial interactions with host cells .....	182
5.2.10	<i>Cj0561c</i> plays a role in OMV related cytotoxicity in the <i>Galleria mellonella</i> larvae model of infection.....	187
5.3	Discussion.....	194

5.4	Conclusion .....	205
Chapter Six: Final Discussion .....		206
6.1	Summary .....	206
6.2	Future work .....	207
6.2.1	OMV production in the presence of sodium taurocholate at 42°C .....	207
6.2.2	Further characterisation of the transcriptional response of <i>C. jejuni</i> to bile salts using additional timepoints. ....	207
6.2.3	Determining the crystal structure of Cj0561c .....	209
6.2.4	Investigation into the specificity of the <i>Cj0561c</i> mutant sulfobetaine phenotype .	210
6.2.5	Characterisation of interaction and invasion of <i>C. jejuni</i> co-inoculated with <i>C. jejuni</i> wild-type and <i>Cj0561c</i> mutant outer membrane vesicles .....	210
6.2.6	Characterisation of <i>C. jejuni</i> wild-type and <i>Cj0561c</i> mutant outer membrane vesicles produced in the presence or absence of sodium taurocholate .....	210
References .....		212
Appendices .....		240
Appendix 1	.....	241
Appendix 2	.....	253
Appendix 3	.....	254
Appendix 4	.....	255
Appendix 5	.....	256
Appendix 6	.....	257
Appendix 7	.....	258
Appendix 8	.....	259
Appendix 9	.....	260

## Acknowledgements

I would like to thank everyone who made my PhD journey possible. Firstly, I would like to express my gratitude to my supervisor Professor Nick Dorrell for his support, guidance, and encouragement. Without the opportunities you have provided me with over the years I would not be where I am today. I would also like to thank Dr Ozan Gundogdu for all this support and guidance, and for shaping my appreciation for good coffee. I am also grateful for the knowledge and training provided by Dr Abdi Elmi. I would also like to thank Professor Brendan Wren; I am so fortunate to have had the opportunity to work in your group.

I would like to thank other past and present members of the *Campylobacter* group. I am very grateful for the friendship and support from Dr Janie Liaw, Geunhye (Gemma) Hong and Zahra Omole. Your friendship significantly ( $p < 0.001$ ) enhanced my PhD experience. I Couldn't have asked for more supportive lab buddies. I am so grateful to have gone through this experience with all of you! I would also like to thank Dr Fauzy Nasher, Dr Mahjanah Hussein and Dr Sherif Abouelhadid for their advice.

I would also like to thank Dr Anna Grabowska for sharing her *Campylobacter* knowledge and Dr Catherine Hall for all her support. I am also grateful to everyone else in the Wren group, past and present, for all the support, advice, conversation and friendship over the years. I would like to thank Dr Esmeralda Valiente for everything she taught me leading up to the start of my PhD.

I would like to give special thanks to my collaborators. I am grateful to Professor David Kelly and Dr Aidan Taylor at the University of Sheffield, and Dr Jody Winter at Nottingham Trent University for all the help with the MLA work. I also appreciate all the help and advice with the RNA-Seq work from Dr Umer Zeeshan Ijaz at the University of Glasgow.

Finally, I would like to thank my family and friends for the part they have played in getting me to where I am today. I would like to thank my amazing friends Liam, Laura, Lucy and Marrielle for all the support over the years. I would like to thank my partner Shahriyar for his patience and support throughout. Thank you to my Mam, Dad and Bampy Davies for everything they did to put me on the right path, and thank you to my Grandmother, Bampy Caspall and Sister for everything you have done to support me throughout my studies.

## List of abbreviations

%	Percentage
5'	5 prime
$\alpha$	Alpha
$\beta$	Beta
$\mu\text{g}$	Microgram
$\mu\text{M}$	Micromolar
$\sigma$	Sigma
ABACAS	Algorithm-Based Automatic Contiguation of Assembled Sequences
ABC	ATP-binding cassette
ACT	Artemis Comparison Tool
Act D	Actinomycin D
ATP	Adenosine triphosphate
BA	Blood agar
BCA	Bicinchoninic acid
BLAST	Basic Local Alignment Search Tool
BLASTP	Protein Basic Local Alignment Search Tool
bp	Base pair
BSA	Bovine serum albumin
BWA	Burrows-Wheeler aligner
CA	Cholic acid
Caco-2	Human colonic epithelial cells
Cam <sup>r</sup>	Chloramphenicol resistance cassette
CCCP	Carbonyl cyanide <i>m</i> -chlorophenylhydrazone
CDC	Centers for Disease Control and Prevention
CDCA	Chenodeoxycholic acid
cDNA	Complementary deoxyribonucleic
CDT	Cytolethal distending toxin
CFU	Colony-forming units
CHAPS	3-cholamidopropyl dimethylammonio 1-propanesulfonate
Cia	<i>Campylobacter</i> invasion antigen
CLR	Centred log ratio
cm	Centimetre
Cme	<i>Campylobacter</i> multidrug efflux

CO <sub>2</sub>	Carbon dioxide
COG	Cluster of orthologous groups
C <sub>T</sub>	Cycle threshold
DEPC	Diethyl Pyrocarbonate
DiSC3	3,3'-dipropylthiadicarbocyanine Iodide
DMEM	Dulbecco's Modified Eagle's Medium
DMSO	Dimethyl sulfoxide
DNA	Deoxyribonucleic acid
dNTP	Deoxynucleoside triphosphate
ds-cDNA	Double stranded complementary deoxyribonucleic
dsDNA	Double stranded deoxyribonucleic
DTT	Dithiothreitol
EBF	Electroporation buffer
EDTA	Ethylenediaminetetraacetic acid
ELISA	Enzyme-linked immunosorbent assay
Ery <sup>r</sup>	Erythromycin resistance cassette
ETEC	Enterotoxigenic <i>E. coli</i>
FBS	Foetal bovine serum
FSA	Food Standards Agency
G	Gram
GBS	Guillain-Barré syndrome
GCA	Glycocholate
GCDC	Sodium glycochenodeoxycholate
GDC	Glycodeoxycholate
gDNA	Genomic deoxyribonucleic acid
GLM	Generalised linear model
GS	Gene specific
H <sub>5</sub> IO <sub>6</sub>	Periodate reagent
HA	Homology arm
HeLA	Human cervical epithelial cells
HEp-2	Human cervical epithelial cells
HICs	Higher income countries
HRP	Horseradish peroxidase
IBD	Inflammatory bowel disease
IBS	Irritable bowel syndrome

IEC	Intestinal epithelial cells
IL-8	Interleukin-8
IM	Inner membrane
IPTG	Isopropyl $\beta$ - d-1-thiogalactopyranoside
ISA	Isothermal assembly
Kan	Kanamycin
kb	Kilobase
KCl	Potassium chloride
kDa	Kilodalton
KDO	2-Keto-3-deoxyoctonate acid
kV	Kilovolt
LASSO	Least absolute shrinkage and selection operator
LB	Lysogeny broth
LCA	Lithocholic acid
LDAO	Lauryldimethylamine oxide
LEE	Locus of enterocyte effacement
LMIC	Low- or middle-income country
LOO	Leave one out cross validation
LOS	Lipooligosaccharide
LPS	Lipopolysaccharide
LSB	Lauryl sulfobetaine
LSB-OMVs	Outer membrane vesicles produced in the presence of lauryl sulfobetaine
M	Molar
mA	Milliampere
MCE	Mammalian cell entry
MgCl <sub>2</sub>	Magnesium chloride
MH	Mueller Hinton
ml	Millilitre
MLA	Maintenance of lipid asymmetry
mM	Millimolar
MOI	Multiplicity of infection
mRNA	Messenger ribonucleic acid
N	Normality
N <sub>2</sub>	Nitrogen
NaCl	Sodium chloride

NaOH	Sodium hydroxide
NCBI	National Center for Biotechnology Information
ng	Nanogram
nm	Nanometer
nM	Nanomolar
NTA	Nanoparticle tracking analysis
O <sub>2</sub>	Oxygen
OD	Optical density
OM	Outer membrane
OMP	Outer membrane protein
OMPdb	Outer membrane protein database
OMV	Outer membrane vesicle
ORF	Open reading frame
PBS	Phosphate buffered saline
PCoA	Principal coordinate analysis
PCR	Polymerase chain reaction
PERMANOVA	Permutational multivariate analysis of variance
PL	Phospholipid
PLS-DA	Partial least squares discriminant analysis
pM	Picomolar
PQS	<i>Pseudomonas</i> quinolone signal
PRED-TMBB	Prediction of transmembrane beta-barrels
qRT-PCR	Quantitative reverse transcription polymerase chain reaction
RNA	Ribonucleic acid
RNA-Seq	Ribonucleic acid sequencing
RND	Resistance-nodulation-division
ROS	Reactive oxygen species
RPKM	Reads per kilobase of transcript per million mapped reads
rpm	Revolutions per minute
rRNA	Ribosomal ribonucleic acid
RT	Reverse transcriptase
RT-PCR	Reverse transcription polymerase chain reaction
SDC	Sodium deoxycholate
SDS	Sodium dodecyl sulfate
SOC	Super optimal broth with catabolite repression

SOE PCR	Splicing by overlap extension polymerase chain reaction
sPLS-DA	Sparse partial least squares discriminant analysis
ST	Sodium taurocholate
stOMV	Outer membrane vesicles produced in the presence of sodium taurocholate
T0SS	Type 0 secretion system
T3SS	Type III secretion system
T6SS	Type VI secretion system
T84	Human colonic epithelial cells
TAE	Tris-acetate-ethylenediaminetetraacetic acid
TCDB	Transporter classification database
TCDC	Sodium taurochenodeoxycholate
TDC	Taurodeoxycholate
TLR4	Toll-like receptor 4
TMB	Tetramethylbenzidine
Tris-HCl	Tris(hydroxymethyl)aminomethane hydrochloride
TSS	Total sum scaling
Tween 20	Polyoxyethylene (20) sorbitan monolaurate
U	Unit
UDCA	Ursodeoxycholic acid
UK	United Kingdom
USA	United States of America
V	Volt
v/v	Volume per volume
VBNC	Viable but non-culturable cells
VPI	<i>Vibrio</i> pathogenicity island
w/v	Weight per volume
WGS	Whole genome sequencing
X-Gal	5-bromo-4-chloro-3-indolyl-beta-D-galacto-pyranoside

## Chapter One: Introduction

### 1.1 *Campylobacter jejuni*

#### 1.1.1 Characteristics

*Campylobacter jejuni* is considered the leading bacterial cause of foodborne gastroenteritis worldwide (Kirk *et al.*, 2015; WHO, 2020). *C. jejuni* is a Gram-negative, microaerophilic, spiral or curved-rod shaped motile bacteria with amphitrichous flagella (Peard, 1979; Vandamme and De Ley, 1991; Young *et al.*, 2007; Balaban and Hendrixson, 2011). The cell size of *C. jejuni* can vary from 0.2 to 0.9  $\mu\text{m}$  wide and 0.5 to 5  $\mu\text{m}$  long. Depending on environmental conditions the cell morphology may alter to become coccoid (Vandamme and De Ley, 1991). *C. jejuni* is non-spore forming but can enter a viable but non-culturable (VBNC) state after exposure to non-favourable conditions, such as low temperature or nutrient starvation (Rollins and Colwell, 1986; Vandamme and De Ley, 1991; Oliver, 2010). *C. jejuni* is thermophilic with an optimal growth temperature of 42°C (avian body temperature) but can readily grow at 37°C (human body temperature) and is able to grow at temperatures as low as 30°C. When approaching minimum or maximum growth temperatures, *C. jejuni* exhibits a rapid rather than gradual reduction in growth rate. Despite being unable to grow at low temperatures, respiration, protein synthesis, chemotaxis and aerotaxis have all been observed at temperatures as low as 4°C (Hazeleger *et al.*, 1998; Stintzi, 2003). Despite the availability of many whole genome sequences of diverse *C. jejuni* strains, the mechanisms of pathogenesis are still poorly understood.

#### 1.1.2 *Campylobacter* Genus

The *Campylobacter* genus contains both pathogenic and non-pathogenic species and is part of the *Campylobacteraceae* family within the class of *Epsilonproteobacteria* (Lastovica *et al.*, 2014). The genus *Campylobacter* was originally proposed by Sebald and Veron in 1963 due to the diversity of characteristics, such as DNA base composition and growth requirements, present in the *Vibrio* genus which members of the *Campylobacter* genus were originally classified under (Sebald and Veron, 1963; Basden *et al.*, 1968). There are currently 32 species within the *Campylobacter* genus (Parte, 2018). Members of the *Campylobacter* genus are able to colonise a range of hosts including mammals, reptiles and birds (Lastovica *et al.*, 2014). The main species of *Campylobacter* responsible for human disease are *C. jejuni* and *C. coli*, with *C. jejuni* thought to cause around 90% of cases (CDC, 2019). Other less common species causing human infection include *C. concisus*, *C. rectus*, *C. hyointestinalis*, *C. insulaenigrae*, *C. sputorum*, *C. helveticus*, *C. lari*, *C. fetus*, *C. mucosalis*, *C. upsaliensis* and *C. ureolyticus* contributing to clinical manifestations such as gastroenteritis,

meningitis, sepsis, endocarditis and soft tissue abscesses in humans (Man, 2011; Kaakoush *et al.*, 2015; Heredia and García, 2018).

### 1.1.3 Epidemiology

Foodborne illness in the United Kingdom causes an estimated annual financial burden of £1.8 billion (FSA, 2013), with *Campylobacter* species the leading cause of infection. In 2018 there were nearly 70,000 laboratory confirmed cases of *Campylobacter* infection in the UK, although the actual number of infections is thought to be far higher. This was more than the collective total laboratory confirmed cases of the other leading causes of bacterial foodborne disease in the UK with *Escherichia coli* O157 totalling near 900 cases, *Salmonella* totalling near 10,000 cases and *Listeria monocytogenes* totalling around 170 cases (FSA, 2019a).

It is thought that between 50-75% of campylobacteriosis cases in the UK have chicken origins, either through consumption, cross contamination of raw or undercooked meat, or animal handling (FSA, 2019b). Other routes of transmission include unpasteurised milk, contaminated water and raw or undercooked pork or beef (Young *et al.*, 2007; Kaakoush *et al.*, 2015). A Food Standards Agency (FSA) survey in 2017 sampling fresh whole chicken from both large and small retailers in the UK found 56% were contaminated with *Campylobacter* species, and 7% were contaminated with more than 1,000 colony forming units (CFU)/g of neck skin (FSA, 2019c). *Campylobacter* infection rates in the UK peak during the summer months (Louis *et al.*, 2005; FSA, 2019b), which could in part be due to seasonal variation in *Campylobacter* carriage in chickens. Previous investigations into *Campylobacter* carriage in chickens saw increases associated with increased seasonal temperature, as well as an increase in the proportion of chicken meat contaminated with higher levels of *Campylobacter* during summer months (Wallace *et al.*, 1997; FSA, 2019c). Increases in cases of human infection correlate with seasonal temperature increases (Djennad *et al.*, 2019; Rushton *et al.*, 2019). A survey by the FSA observed an overall drop in the number of highly contaminated whole retail chicken (more than 1,000 CFU/g of neck skin) between 2014 and 2018, dropping from 18.4% to less than 5% (FSA, 2019b); however, despite this drop there has been an increase in the total laboratory confirmed cases of *Campylobacter* infection since 2016 (FSA, 2019a). This indicates that seasonal variation in infection may also be linked to human behaviour that are correlated to low rainfall and higher temperatures, such as travel to the countryside and agricultural land, and consumption of barbecued chicken during the summer months (Rushton *et al.*, 2019).

In low- and middle- income countries (LMICs) *Campylobacter* infection tends to be endemic rather than showing the seasonal fluctuation observed in higher income countries (HICs). In contrast to HICs where symptomatic infection is not linked to age, in LMICs the incidence of symptomatic infection

tends to decrease with age (Blaser, 1997; Coker *et al.*, 2002). *Campylobacter* is a leading cause of diarrhoeal disease in children under five, with many children experiencing multiple symptomatic *Campylobacter* infections per year during the first few years of life (Coker *et al.*, 2002; Lee *et al.*, 2014; Amour *et al.*, 2016). In LMICs diarrhoeal disease is a major cause of morbidity and mortality particularly for young children, causing around 10% of deaths for children under five, and around a quarter of the deaths linked to infectious causes for children under five (Liu *et al.*, 2012). Malnutrition linked to diarrhoeal disease during the early years of life has been linked to reduced physical and cognitive development, impacting opportunities and health later in life (Walker *et al.*, 2000; Victora *et al.*, 2008).

#### **1.1.4 Infection**

The infectious dose of *C. jejuni* is thought to be as low 500-800 CFU based on human infection studies (Robinson, 1981; Black *et al.*, 1988), however outbreak studies have suggested the infectious dose could be lower. For example, an outbreak study by Hara-Kudo and Takatori calculated the likely number of CFU consumed by an infected individual during an outbreak caused by undercooked beef liver at a restaurant was 360 CFU (Hara-Kudo and Takatori, 2011). Clinical symptoms of *C. jejuni* infection include headache, malaise, myalgia, fever, abdominal cramps and acute often bloody diarrhoea in HICs (Blaser, 1997; Coker *et al.*, 2002; Skirrow, 2003). Patients in LMICs tend to present with non-inflammatory watery diarrhoea or often asymptomatic infections (Figueroa *et al.*, 1989; Coker *et al.*, 2002).

*C. jejuni* infection tends to be self-limiting with symptoms generally resolving within a week (Blaser, 1997), however in a small number of cases, long term or fatal complications can occur. Infection complications can include bacteraemia or septicaemia (Meyer *et al.*, 1997; Nielsen *et al.*, 2010), myocarditis (Florkowski *et al.*, 1984; Hannu *et al.*, 2005), reactive arthritis (Locht and Krogfelt, 2002; Schonberg-Norio *et al.*, 2010), irritable bowel syndrome (Thornley *et al.*, 2001; Keithlin *et al.*, 2014) and the potentially fatal autoimmune disorder Guillain-Barré syndrome (GBS). GBS is linked to around 1 in 1,000 *C. jejuni* infections and is a potentially fatal neuropathy that affects the peripheral nerves, causing an ascending paralysis and leading to permanent neurological impairments in around 15-20% of GBS patients (Allos, 1997; Nachamkin *et al.*, 1998). Miller Fisher syndrome, a variant of GBS, may also occur in a small number of cases and can cause ophthalmoplegia and facial or bulbar palsy (Hughes, 2004). Fatal infections are mainly associated with young children, the elderly or people with other underlying health problems and are mainly a result of severe dehydration or GBS (Pacanowski *et al.*, 2008).

## 1.2 Pathogenesis

### 1.2.1 Flagella

*C. jejuni* is motile via amphitrichous unsheathed flagella and can swim at speeds of over 100  $\mu\text{m}/\text{second}$ , with higher speeds reached in a moderately viscous medium than in a low viscosity medium. *C. jejuni* is able to swim through the mucus barrier in the gut due to its 'cork-screw' motility (Ferrero and Lee, 1988; Chaban *et al.*, 2018). The flagella are crucial for both motility and chemotaxis as well as being an important virulence factor and colonisation determinant (Nachamkin *et al.*, 1993; Jones *et al.*, 2004). The flagella filament is composed of FlaA and FlaB subunits which are encoded on adjacent genes and have a high degree of sequence identity to each other but are under the control of different promoters and sigma factors (Nuijten *et al.*, 1990). The major flagellin subunit *flaA* is under control of  $\sigma^{28}$  encoded by *fliA*, and the minor flagellin subunit *flaB* is under control of  $\sigma^{54}$  encoded by *rpoN* (Hendrixson *et al.*, 2001). The flagella filament is attached to the basal body via a hook protein and the genes encoding both the basal body and hook protein are also under the regulation of  $\sigma^{54}$  (Kinsella *et al.*, 1997; Hendrixson and DiRita, 2003).

*C. jejuni* lacks the classical virulence associated secretion systems of other enteric pathogens that deliver effectors directly to target cells (Parkhill *et al.*, 2000), however a Type VI secretion system (T6SS) has been identified in a proportion of strains (Bleumink-Pluym *et al.*, 2013; Ugarte-Ruiz *et al.*, 2015). It has been proposed that the *C. jejuni* flagella can function as a Type III secretion system (T3SS) to secrete both flagella components during flagella assembly and also non-flagella proteins. Konkel *et al.* (2004) proposed that the *Campylobacter* invasion antigens (Cia) require the flagella for secretion. Since this, several other proteins have been linked with flagella secretion including FspA (flagella secreted protein) and FedB (flagella co-expressed determinants) (Poly *et al.*, 2007; Barrero-Tobon and Hendrixson, 2012). Comparison of the secretome from a wild-type strain and a *flgG* knock-out mutant was performed by Scanlan *et al.* (2017a) to characterise the flagella dependent secretome. The majority of secreted proteins did not change in abundance between the wild-type and mutant, however eight proteins showed reduced abundance and 17 proteins were absent from the secretome of the mutant (Scanlan *et al.*, 2017a). Increased invasion associated with increased flagella protein secretion resulting from relaxing of DNA supercoiling in *C. jejuni* has also been observed. Deletion mutants of the known *C. jejuni* adhesins *cadF* and *flpA*, which have been shown to be secreted in outer membrane vesicles (OMVs) (Elmi *et al.*, 2012), show significant reductions in invasiveness compared to respective wild-type strains. However, both the adhesin knock-out mutants and the wild-type strains demonstrate increasing invasiveness in response to induction of relaxation of DNA supercoiling

(Scanlan *et al.*, 2017b). More recently the *C. jejuni* flagella has been linked to the ability of certain *C. jejuni* phages to infect cells (Sacher *et al.*, 2021).

### **1.2.2 Cytolethal distending toxin**

The cytolethal distending toxin (CDT) was first described by Johnson and Lior in 1988 (Johnson and Lior, 1988). CDT is a heat-labile AB<sub>2</sub> toxin with the three subunit components encoded by *ctdA*, *ctdB* and *ctdC* which are located in an operon. CdtB is the active subunit with CtdA and CtdC facilitating entry of CdtB to the cell. All three subunits are crucial for toxin activity (Pickett *et al.*, 1996; Lara-Tejero and Galan, 2001; Lee *et al.*, 2003). CdtB has DNase I activity, causing double-strand DNA breaks in the target cell DNA which leads to cell cycle arrest at the G<sub>2</sub>/M stage and cell distention. CDT induces the secretion of pro-inflammatory cytokine interleukin-8 (IL-8), leading to localised inflammatory responses (Hickey *et al.*, 2000). CDT activity has also been linked to the development of colorectal cancer and changes in gut microbiome composition (He *et al.*, 2019).

### **1.2.3 Capsular polysaccharide**

The first whole genome sequence annotation of *C. jejuni* strain 11168 allowed the controversy surrounding the existence of a *C. jejuni* capsule to be resolved (Karlyshev *et al.*, 1998; Parkhill *et al.*, 2000; Karlyshev *et al.*, 2000). The presence of a capsule was then also biochemically and visually demonstrated using Alcian blue and electron microscope visualisation (Karlyshev *et al.*, 2001). The capsule polysaccharide is the determinant for the Penner serotyping of *C. jejuni* strains (Karlyshev *et al.*, 2000). The capsule biosynthesis genes are encoded by a number of phase variable genes (Bacon *et al.*, 2001) leading to within population capsule variation, as well as variations in sugar composition and modifications driving differences between strains. Variations have been linked to changes in virulence and immune evasion (McNally *et al.*, 2005; Champion *et al.*, 2010). The capsule polysaccharide of *C. jejuni* also plays a role in host colonisation, adhesion and invasion of host intestinal epithelial cells (IECs), and serum resistance (Bacon *et al.*, 2001; Keo *et al.*, 2011; Maue *et al.*, 2013).

### **1.2.4 Lipooligosaccharide**

Lipooligosaccharide (LOS) is a phosphorylated variable surface exposed glycolipid analogous to lipopolysaccharide (LPS). LOS consists of a lipid A molecule and an inner and outer core region but lacks the terminal O-antigen present on LPS molecules (Gilbert *et al.*, 2008). LOS is an essential component of the outer leaflet of the outer membrane (OM), functioning in reducing cell permeability, maintaining structural stability and evasion of the host immune response (Karlyshev *et al.*, 2005; Abellon-Ruiz *et al.*, 2017b). The *C. jejuni* LOS biosynthesis genes are located in a region of low G+C

content in the *C. jejuni* genome and some contain hypervariable sequences (Parkhill *et al.*, 2000). The genes encoding the inner core are relatively conserved between strains, however the terminal outer region varies considerably between strains, with certain variants able to mimic human gangliosides causing GBS (Moran, 1997; Gilbert *et al.*, 2000; Dorrell *et al.*, 2001).

### 1.2.5 Glycosylation

Protein glycosylation is the process of covalently attaching a glycan to a protein. *C. jejuni* possesses two protein glycosylation systems. *C. jejuni* modifies flagella proteins by *O*-linked glycosylation and modifies a significant number of periplasmic, membrane and secreted proteins by *N*-linked glycosylation (Szymanski *et al.*, 1999; Thibault *et al.*, 2001; Young *et al.*, 2002). The flagellin proteins of *C. jejuni* are extensively glycosylated with pseudaminic acid in regions that are surface exposed on the flagella filament. In *C. jejuni* strain 81-176, 19 threonine and serine residues in flagellin proteins are glycosylated (Thibault *et al.*, 2001). The proteins responsible for *N*-linked glycosylation in *C. jejuni* are encoded in the 12 gene *pgl* locus. The *N*-linked glycosylation pathway of *C. jejuni* involves the *en bloc* attachment of the heptasaccharide glycan to the asparagine residue in the target sequon, D/E-X1-N-X2-S/T (where X1 and X2 are any amino acid except proline), by the oligosaccharyltransferase PglB on the periplasmic side of the inner membrane (IM) (Kowarik *et al.*, 2006; Young *et al.*, 2007; Alemka *et al.*, 2013).

Loss of *N*-glycosylation results in reduced adhesion to and invasion of IECs (Szymanski *et al.*, 2002); reduced colonisation of mice and chickens (Szymanski *et al.*, 2002; Hendrixson and DiRita, 2004; Kelly *et al.*, 2006) and changes in immunogenicity (Szymanski *et al.*, 1999). The mechanisms causing these phenotypes are difficult to interpret due to the pleiotropic effects that removing *N*-linked glycosylation will have. Roles of individual *N*-glycoproteins include antimicrobial resistance via the CmeABC multidrug efflux pump (Scott *et al.*, 2011; Abouelhadid *et al.*, 2019a); zinc acquisition through the zinc ABC transporter protein ZnuA (Davis *et al.*, 2009) and chick colonisation (Scott *et al.*, 2009; Abouelhadid *et al.*, 2019a).

*C. jejuni* PglB has since its discovery been utilised in the field of glycoengineering due to its ability to transfer a relatively broad range of polysaccharide structures to acceptor proteins while expressed in *E. coli* (Wacker *et al.*, 2002). This has formed the basis for Protein Glycan Coupling Technology (or bioconjugation) which is able to transform bacterial cells into glycoconjugate vaccine production factories which can reduce time and cost of glycoconjugate production in comparison to traditional methods (Langdon *et al.*, 2009; Terra *et al.*, 2012; Kay *et al.*, 2019a) with the potential for use of these strains as live attenuated vaccines. This cost reduction opens the potential for the use of this

technology in vaccine production for LMICs and veterinary use (Kay *et al.*, 2019a; Mauri *et al.*, 2021; Terra *et al.*, 2022).

### 1.2.6 Adhesins

Adherence is important to enable bacteria to colonise the gut by preventing bacteria from being cleared by peristalsis or the flow of fluids through the gut, as well as being crucial to enable invasion of host cells. *C. jejuni* possess three well characterised adhesins with known cellular binding targets which are CadF, FlpA and JlpA. Other putative adhesins and adhesion-related proteins or structures include the flagella (Grant *et al.*, 1993; Yao *et al.*, 1994; Freitag *et al.*, 2017), capsular polysaccharide (Bachtiar *et al.*, 2007; van Alphen *et al.*, 2014), PEB1 (Pei *et al.*, 1998; Flanagan *et al.*, 2009; Novik *et al.*, 2010), PEB2 (Hao *et al.*, 2016), PEB3 (Rangarajan *et al.*, 2007; Rubinchik *et al.*, 2014), PEB4 (Rathbun *et al.*, 2009), CapA (Ashgar *et al.*, 2007), TlyA (Sałamaszyńska-Guz and Klimuszko, 2008; Sałamaszyńska-Guz *et al.*, 2020), PorA (MOMP Major OM Protein) (Moser *et al.*, 1997; Mahdavi *et al.*, 2014) and FbpA (Flanagan *et al.*, 2009).

CadF and FlpA are fibronectin binding proteins which bind to fibronectin in the extracellular matrix (Konkel *et al.*, 1997). CadF is an OmpA-like protein, and FlpA contains FN-type III domains. Both CadF and FlpA have an important role in colonisation, with deletion mutants showing reduced ability to colonise chickens (Ziprin *et al.*, 1999; Flanagan *et al.*, 2009), and demonstrating reduced adherence to both chicken and human IECs (Monteville *et al.*, 2003; Flanagan *et al.*, 2009; Konkel *et al.*, 2010).

JlpA is a surface exposed lipoprotein. Disruption of JlpA reduces adhesion to HEp-2 cells *in vitro* (Jin *et al.*, 2001). Jin *et al.* (2003) found purified JlpA bound to surface exposed HSP90 (Heat Shock Protein 90) on Hep-2 cells. Flanagan *et al.* (2009) did not observe a reduction in adhesion *in vitro* to chicken LMH hepatocellular epithelial cells, or a colonisation defect in broiler chickens (Flanagan *et al.*, 2009). Novik *et al.* (2010) was also unable to confirm a role in adhesion, with a wild-type and a *jlpA* deletion mutant showing comparable levels of adhesion to T84 cells. HSP90 upregulation has been associated with stress and surface exposed HSP90 has been associated with pathogen-associated molecular patterns (PAMPs), therefore it could be possible adhesion to HSP90 by JlpA may be restricted to certain conditions, cell lines or strains (Finlayson-Trick *et al.*, 2019).

## 1.3 Bile salts and bacteria virulence

### 1.3.1 Bile salts background

Bile salts are important molecules for signalling and metabolism for both the host and the gut microbiota. Bile salts also aid digestion while exerting antimicrobial properties preventing microbial overgrowth in the gut (Lorenzo-Zúñiga *et al.*, 2003). Bile salts are able to disrupt bacterial membranes, denature proteins, cause oxidative stress, induce DNA damage and chelate iron and calcium (Urdaneta and Casadesús, 2017). Many enteric bacteria have developed methods of tolerating bile stress, with some pathogens, such as *C. jejuni* and *Salmonella enterica*, even able to withstand the high concentrations of bile salts found in the gallbladder. *S. enterica* is able to colonise the human gall bladder causing repeated release of the pathogen into the lumen of the small intestine to cause chronic infection (Urdaneta and Casadesús, 2017).

In the human gut, the main primary bile acids produced as the initial product of cholesterol metabolism in the liver are cholic acid (CA) and chenodeoxycholic acid (CDCA). These are then conjugated to either glycine or taurine creating more soluble bile acids before they are transported to the gallbladder and released into the aqueous environment of the small intestine. Physiological pH then ionises the bile acids to form bile salts (Sung *et al.*, 1993; Russell, 2003). Bile salts stored in the gallbladder are released into the duodenum in response to food consumption. In a healthy person, around 95% of bile salts will be reabsorbed by the small intestine to be recycled and recirculated (Zwicker and Agellon, 2013). The remaining bile salts will reach the large intestine where some reabsorption will take place, however due to the extensive modification of bile salts in the large intestine creating a more hydrophobic bile pool profile, bile salts can precipitate and be subsequently excreted (Russell, 2003; Ridlon *et al.*, 2006). The more hydrophobic unconjugated bile salts, such as sodium deoxycholate (SDC), have greater detergent and antimicrobial properties than the conjugated and more hydrophilic bile salts, such as sodium taurocholate (ST) (Sung *et al.*, 1993).

The bile salt pool composition varies considerably between species and so the source of bile used to study gut microbe and bile interactions should be carefully considered and factored into the interpretation of the final data sets. Differences in both host genetics and host microbiome genetics influence this variation. The production of primary bile acids in the liver depend on the host enzymes. For example, the main human primary bile acids produced in the liver are CA and CDCA; however, mice are able to produce  $\beta$ -muricholic acid; pigs can produce hyocholic acid; and birds avicholic acid (Hofmann *et al.*, 2010). Host factors will also determine the conjugation of these primary bile acids. For example, cats exclusively conjugate primary bile acids to taurine (Markwell and Earle, 1995); mice almost exclusively conjugate to taurine (Alnouti *et al.*, 2008); the proportion of glycine to taurine

conjugation in humans can vary greatly based on dietary consumption of taurine (Sjövall, 1959; Hardison, 1978; Ridlon *et al.*, 2016), and some mammals such as sloths exclusively conjugate primary bile acids to glycine (Hagey *et al.*, 2010). Glycine conjugation in non-mammals is less common (Hofmann *et al.*, 2010). The species of bacteria present in the gut and the enzyme pool created by these species will influence the pool of secondary bile salts produced (Ridlon *et al.*, 2006). This means the gut bile pool composition and concentration will vary not only between species and individuals of the same species but also within an individual. Bile salts can vary based on location in the gut; changes in diet; use of antibiotics; health status; if a meal has recently been consumed, as well as other lifestyle factors over the course of an individual's life (Northfield and McColl, 1973; Hardison, 1978; Ridlon *et al.*, 2015; Dawson, 2016). It is thought that targeting the gut microbial composition to modulate the bile metabolites could improve human health as changes in the gut microbiota-bile axis are now recognised to impact human health (Long *et al.*, 2017).

### **1.3.2 Bile salt composition in the human gut**

The profile of bile salts will vary along the length of the human gut, with the small intestine containing a higher proportion of primary conjugated bile salts, compared to the large intestine which has higher proportion of secondary unconjugated bile salts (Northfield and McColl, 1973; Perez de la Cruz Moreno *et al.*, 2006). The main bile salts found in faeces will be secondary unconjugated bile salts, predominantly lithocholic acid (LCA) and SDC (Ridlon *et al.*, 2006). The main primary conjugated bile salts released into the small intestine of humans are ST, sodium glycocholate (GCA), sodium taurochenodeoxycholate (TCDC) and sodium glycochenodeoxycholate (GCDC) formed by the conjugation of either glycine or taurine to CA or CDCA (Ridlon *et al.*, 2006). Once released into the intestine bile salts can undergo biotransformations carried out by the gut microbiota to form secondary bile salts. In the small intestine bile salts can undergo deconjugation by a range of host gut bacterial species to form unconjugated bile salts (Ridlon *et al.*, 2006; Dawson, 2016). However, in the small intestine only a small proportion of bile salts will become deconjugated by the time they reach the distal part of the small intestine (Northfield and McColl, 1973; Ridlon *et al.*, 2006). More extensive biotransformations are carried out in the large intestine where the bacterial density is higher but the bile salt concentration lower. In the upper small intestine a bacterial density higher than  $10^3$ - $10^4$  CFU/ml is considered bacterial overgrowth. The bacterial density increases along the length of the small intestine and can exceed  $10^{11}$  in the large intestine (Ridlon *et al.*, 2006). Once in the large intestine, the initial modification experienced by bile salts will be deconjugation (Dawson, 2016). As the bile salts pass through the large intestine other modification such as oxidation of hydroxy groups and  $7\alpha/\beta$ -dehydroxylation are carried out. Shifts in the host-microbiota bile salt metabolome have been linked to the onset of health conditions such as irritable bowel syndrome (IBS) (Hou *et al.*, 2021).

Modifications such as 7 $\alpha$ -dehydroxylation are predominantly performed in the large intestine and are required to form SDC, meaning the composition in addition to concentration of bile salts is dependent on gut location (Ridlon *et al.*, 2006; Monte *et al.*, 2009).

In the human gut the overall concentration of bile found in the small intestine can vary greatly based on food consumption and health, however it is thought to fluctuate between 0.2-2% (w/v). This concentration will reduce along the length of the gut with the large intestine and lower small intestine containing much lower concentrations of bile salts compared to the upper small intestine (Van Deest *et al.*, 1968; Northfield and McColl, 1973; Hofmann and Eckmann, 2006; Kristoffersen *et al.*, 2007; Dawson, 2016). Northfield and McColl found that unconjugated bile salts were near absent from the jejunal fluids but increased in prevalence along the length of the small intestine. With the exception of the distal end of the small intestine, unconjugated bile salts formed only a fraction of the total bile pool in the small intestine (Northfield and McColl, 1973). A more recent study by Moreno *et al.* (2006) analysed the bile salt composition of duodenal and jejunal fluids from fasted state healthy volunteers simultaneously aspirated with separate catheters. ST was the most prevalent bile salt forming on average around 45% of the total bile pool. The secondary bile salt SDC formed less than 0.2% of the total bile pool (Perez de la Cruz Moreno *et al.*, 2006). Hamilton *et al.* (2007) examined the bile salt profile in the cecum of individuals that had died due to trauma. The average total bile concentration was estimated to be around 0.015% (w/v), more than 10-fold less than the lower end of the range expected for the small intestine under fasted conditions. Unconjugated bile salts made up just under 90% of the bile profile on average, and near 100% in some individuals. Of the unconjugated bile salts identified, SDC was the most prevalent forming around 30% of the bile pool on average, but up to 50% in some individuals. Other prevalent bile salts included CDCA and LCA, each forming around a fifth of the total bile pool. Primary conjugated bile salts such as ST and GCA formed on average less than 1.5% of the total bile pool (Hamilton *et al.*, 2007).

### **1.3.3 Bile salts and bacterial virulence**

The interaction of gut microbes with the bile salt pool is a dynamic relationship. The bile salt pool composition will affect the composition and behaviour of the gut microbiome, and the behaviour and composition of the gut microbiome will affect the composition of the bile pool. Pre-incubation in sub-lethal concentrations of bile salts have been shown to affect the ability of bacteria to survive subsequent exposure to higher concentrations of bile, indicating gut bacteria have regulated mechanisms of bile tolerance. Schmidt and Zink observed that 30 minutes exposure to 0.1% (w/v) bile salts (ox gall) caused a 21-fold increase in survival of *Bifidobacteria* cells subsequently exposed to 0.4% (w/v) bile salts (Schmidt and Zink, 2000). Flahaut *et al.* (1996) observed an increase from 0.05%

survival to 87.4% survival for *Enterococcus faecalis* cells primed with 0.08% (w/v) bile salts (1:1 mixture of CA and SDC) for 15 seconds prior to exposure to 0.3% (w/v) bile salt. Interactions between gut-colonising bacteria have also been implicated in alterations in bile sensitivity. For example, 'prey-triggered' activation of the *C. jejuni* T6SS has been suggested to increase susceptibility to bile salts due to increased bile salt influx through the T6SS (Lertpiriyapong *et al.*, 2012; Gupta *et al.*, 2021).

Bile salts have been well characterised to play a role in virulence in several enteric pathogens. Enteric pathogens have also demonstrated transcriptional responses specific to individual bile salts or classes of bile salts. A study by Pope *et al.* (1995) characterising the effect of bile on the virulence of *Shigella* species observed that the secondary unconjugated bile salts SDC or CDCA significantly increase invasion of human IECs *in vitro*. However, the conjugated bile salts taurodeoxycholate (TDC) and glycodeoxycholate (GDC) only slightly but not significantly increased invasion of IECs, and the primary bile salts cholate and GCA did not alter invasion (Pope *et al.*, 1995). Furthering the work by Pope *et al.* (1995), Faherty *et al.* (2012) linked the bile salt stimulated increased IEC adhesion to the upregulation of the surface exposed proteins OspE1 and OspE2 in *Shigella flexneri*. Another study demonstrating the specificity of transcriptional changes to specific bile salts was carried out by Yang *et al.* (2013) who measured the activation of *V. cholerae* major virulence factor *tcpA* as an indicator of virulence activation. Expression was strongly stimulated by the primary bile salts ST and GCA even at very low biological concentrations (<0.005% w/v). CA moderately activated *tcpA*, however the secondary bile salts SDC and CDCA did not activate expression of *tcpA*. Interestingly homogenates of the small intestine (where the concentration of primary bile salts are higher) of mice strongly activated *tcpA* expression, however homogenates of the large intestine (where the concentration of secondary bile salts are higher) only moderately activated *tcpA*. This is indicative of site-specific responses to host gut factors. The study also elucidated that the virulence gene upregulation in response to bile salts observed was due to changes in disulphide bond formation of TcpP, causing dimerization of TcpP and triggering a cascade to upregulate virulence gene expression (Yang *et al.*, 2013). Other examples of bile salt related virulence include up regulation of the locus of enterocyte effacement (LEE) pathogenicity island, chemotaxis related genes and iron scavenging in *E. coli* O157:H7 (Hamner *et al.*, 2013); increase of antibiotic resistance gene transfer by *Salmonella enterica* serovar typhimurium (He and Ahn, 2014); induction of sporulation of *Clostridium perfringens* and *Clostridium difficile* (Sorg and Sonenshein, 2008; Yasugi *et al.*, 2016), and upregulation of the type 3 secretion (T3SS) system and T3SS related virulence factor in *Vibrio parahaemolyticus* and *Shigella* species (Letchumanan *et al.*, 2017; Bernard *et al.*, 2017).

### 1.3.4 *C. jejuni* interactions with bile salts

*C. jejuni* is considered to have a high bile tolerance and has been implicated in a small number of gallbladder infections, however this is a rare complication of *C. jejuni* infection (Vaughan-Shaw *et al.*, 2010). The ability to survive bile salt stress varies between *C. jejuni* isolates, and it has been suggested higher bile salt tolerance is associated with strains causing human infection (Van Deun *et al.*, 2007). Growth in the presence of bile salts can induce cell stress. For example Negretti *et al.* (2017) demonstrated that growth in the presence of SDC induced the production of reactive oxygen species (ROS); decreased succinate dehydrogenase activity; increased catalase activity, and caused DNA strand breaks. Early investigations into the regulation of *C. jejuni* virulence by bile salts were performed by Doig *et al.* (1996) who proposed SDC stimulated the production of pili which aided in adhesion, invasion and virulence in the ferret model of diarrhoeal disease. Pili formation was also observed in the presence of CDCA and crude bile but not for other bile salts (Doig *et al.*, 1996). It was later demonstrated that incubating SDC with growth media would produce the pili-like structures even in the absence of bacteria, indicating the structures were just an artifact of mixing the bile salts with growth media (Gaynor *et al.*, 2001; Rivera-Amill *et al.*, 2001). SDC has since been shown to form a variety of structures based on environmental conditions, including nanotubes, rods and fibres (Jover *et al.*, 2021). More recent studies have observed biologically relevant concentrations of SDC to cause dramatic proteome variations; increase adherence and invasion of human intestinal epithelial Caco-2 cell line; and induction of the TcyP transport protein (Man *et al.*, 2020). Rivera-Amill *et al.* (2001) also investigated the potential role of bile salts in adhesion and invasion. Rivera-Amill *et al.* (2001) observed SDC, CA, and CDCA stimulated the synthesis of Cia proteins, indicating a link between bile salts at physiological concentrations and the upregulation of virulence (Rivera-Amill *et al.*, 2001). The link between bile salts and *C. jejuni* virulence has been further demonstrated by *C. jejuni* OMVs produced by strains grown in the presence of bile exhibiting enhanced virulence. Bile salt induced OMVs have previously been shown to have enhanced proteolytic activity, cytotoxicity, immunogenicity, adhesion to IEC *in vitro* and differing protein abundances (Elmi *et al.*, 2018; Taheri *et al.*, 2018). Bile salts have also been shown to enhance the promoter activity of *flaA*; are thought to play a role in chemotaxis; and enhance expression of the cytolethal distending toxin (Allen and Griffiths, 2001; Elmi *et al.*, 2018). Lin *et al.* (2002) characterised a then putative efflux system identified in the first whole genome sequence of *C. jejuni*, which showed homology to multidrug efflux transporters belonging to the RND superfamily. Mutants of components of this efflux pump demonstrated increased susceptibility to a range of antibiotics, heavy metals, bile salts, sodium dodecyl sulphate, ethidium bromide and other antimicrobial agents. Components of the efflux pump were termed CmeABC (*Campylobacter* multidrug efflux) (Parkhill *et al.*, 2000; Lin *et al.*, 2002; Pumbwe and Piddock, 2002; Gibreel *et al.*,

2007). Since this study, the CmeABC multidrug efflux pump has been well characterised and shown to play a role in bile salt resistance, as well as being upregulated in response to bile salts in *C. jejuni* (Lin *et al.*, 2003; Lin *et al.*, 2005a). Expression of the genes encoding CmeABC are repressed by the transcriptional regulator CmeR, which binds to the promoter region of *cmeABC*. It is thought bile salts prevent binding of CmeR to the promoter region of *cmeABC*, preventing transcriptional repression and thereby increasing expression of *cmeABC*. Bile salts are not thought to affect expression of *cmeR*. Both conjugated and non-conjugated bile salts inhibit the binding of *cmeR* (Lin *et al.*, 2005a; Lin *et al.*, 2005b; Su *et al.*, 2007). The oxidative stress response regulator CosR also represses *cmeABC* expression, however to a lesser extent than CmeR (Grinnage-Pulley *et al.*, 2016). The involvement of CosR in the regulation of *cmeABC* may be to counteract the oxidative stress induced by bile salt stress. The expression of another gene, *Cj0561c*, which encodes a protein of unknown function, is strongly stimulated by bile salts and demonstrates greater expression changes in response to *cmeR* mutation than is seen for *cmeABC*. The promoter region of *Cj0561c* contains two CmeR binding sites, but does not contain a binding site for CosR (Guo *et al.*, 2008; Dzieciol *et al.*, 2011; Grinnage-Pulley *et al.*, 2016). Bile salt induced expression of *cmeABC* increases the tolerance of *C. jejuni* to a range of antibiotics. *C. jejuni* strains that are more resistant to certain antibiotics can have a higher tolerance for bile salt stress (Mavri and Smole Možina, 2013a; Mavri and Smole Možina, 2013b). The reduced resistance to antimicrobials observed in *cmeABC* mutants has also been observed in strains with point mutations in the *N*-glycosylation sites of *cmeA*. This indicates *N*-linked glycosylation is also important to the function of this efflux pump, perhaps playing a role in the stability of the CmeABC complex (Dubb *et al.*, 2019; Abouelhadid *et al.*, 2019b). It is thought unconjugated bile salts can enter the bacteria cell through the T6SS in T6SS positive *C. jejuni* strains. The expression of *cmeABC* is thought to be coordinated with the expression of the T6SS to counteract the effect of bile influx to the cell (Lertpiriyapong *et al.*, 2012). SDC has also been shown to enhance biofilm formation of *C. jejuni*, potentially as a mechanism of stress tolerance during human infection (Svensson *et al.*, 2009; Svensson *et al.*, 2014).

CbrR is an orphan response regulator thought to contribute to bile tolerance of *C. jejuni*. Raphael *et al.* (2005) identified *Cj0643* which encodes a response regulator in the *C. jejuni* strain F38011, and observed significant reduction in growth of *Cj0643* mutants grown in the presence of 0.05% (w/v) SDC. This reduction in growth was also observed to a lesser extent for CDCA, CA, ox bile extract, Triton X-100, Tween 20 and SDS but there were no significant differences in growth in the presence of tetracycline, gentamicin or osmotic stress. Due to this, the gene was termed *cbrR* (*Campylobacter* bile resistance regulator). Mutation of *cbrR* also reduced the ability of strains to colonise chickens (Raphael *et al.*, 2005). Despite the apparent role in bile salt survival, *cbrR* is not thought to be involved in the

activation of *cmeABC* (Lin *et al.*, 2005a). Hoang *et al.* (2012) later observed that *cbrR* mutants exhibited reduced resistance to fowlicidin-1, an antimicrobial peptide found in the chicken gut. Kreuder *et al.* (2017) analysed transcriptional changes of a highly virulent sheep abortion strain IA3902 *in vivo* in the host gallbladder environment as well as in *in vitro* in the presence of ovine bile. Statistically significant transcriptional changes of *cbrR* were only observed *in vivo* after 24 hours, where *cbrR* was upregulated (Kreuder *et al.*, 2017). Masanta *et al.* (2019) saw decreased abundance of CbrR in the proteome of *C. jejuni* exposed to SDC, CDCA and GCA at sublethal concentrations for 12 hours *in vitro*. Capsular modifications and production of full length LOS have also been shown to impact bile tolerance, with mutants of *mlghB* or *mlghC*, which play a role in heptose modification in the capsule, and mutants of *Cj1136* which produce truncated LOS molecules, having increased susceptibility to bile salt stress (Javed *et al.*, 2012; Wong *et al.*, 2015).

#### **1.3.4.1 Omics-based studies investigating *C. jejuni* interactions with bile salts**

Several omics-based studies have demonstrated bile salts can induce transcriptional changes and alterations in the resultant proteome in *C. jejuni*. Fox *et al.* (2007) used mass spectrometry to analyse differences in protein abundance of *C. jejuni* cells grown in the presence or absence of ox bile *in vitro*. Cells were grown either in the presence or absence of 2.5% or 5% (w/v) ox bile for 18 hours. There were 19 proteins with differing abundances which included proteins involved in chemotaxis (CheV), flagella filament structure (FlaA, FlaB) and heat shock (GroEL) (Fox *et al.*, 2007). Masanta *et al.* (2019) examined the protein profile of *C. jejuni* 81-176 grown in the presence of subinhibitory concentrations of a range of bile salts. CmeABC was enriched in response to all bile salts tested and ROS detoxification proteins KatA and TpX were induced for more than one bile salt. The wider proteome however did vary between bile salt treatments. SDC and CDCA showed similar abundance patterns, as did CA compared to ST. SDC and CDCA triggered aerobic respiration pathways whereas other bile salts did not. SDC and CDCA also triggered the expression of different chemoreceptors compared to CA, ST, ursodeoxycholic acid (UDCA) and LCA. This indicates that as well as a general bile stress response, there are also distinct responses towards different bile salts. General COG pathways enriched in response to bile salts were translation, membrane transport, cell motility and energy metabolism (Masanta *et al.*, 2019).

Kreuder *et al.* (2017) examined the transcriptional response of a sheep abortion *C. jejuni* isolate exposed to ovine bile both *in vitro* and *in vivo* in the sheep gallbladder at either 2 or 24 hours. After two hours exposure, 388 and 112 chromosomal protein coding genes were differentially expressed *in vivo* and *in vitro* respectively. After 24 hours exposure, 516 and 302 chromosomal protein coding genes were differentially expressed *in vivo* and *in vitro* respectively. Genes identified included genes

previously characterised to play a role in bile stress such as *cmeABC*. Significant changes in the transcriptional regulators *cmeR* and *cbrR* were only differentially expressed after 24-hour exposure. *ciaB* and *flaA* were not identified as differentially expressed despite previous studies identifying these genes as bile regulated (Rivera-Amill *et al.*, 2001; Allen and Griffiths, 2001). COG functional categories identified in at least one condition as significantly enriched were cell motility; secondary metabolite biosynthesis and intracellular trafficking and secretion. COG categories significantly decreased were energy production and conversion; amino acid transport and metabolism; signal transduction mechanisms; carbohydrate transport and metabolism, and inorganic ion transport and metabolism. A number of non-coding RNAs were also identified as differentially expressed (Kreuder *et al.*, 2017). Negretti *et al.* (2017) using RNA-Seq, analysed the transcriptional response of *C. jejuni* strains 81-176, F38011 and 11168 grown in the presence of 0.05% (w/v) SDC for 16 or 18 hours compared to each strain grown in the absence of bile salt for 12 hours. A total of 90 genes were upregulated, and 80 genes downregulated in the presence of SDC for all three strains. The COG functional categories identified as significantly enriched in the presence of SDC were energy production and conversion, and cell motility (Negretti *et al.*, 2017). Due to the variation in timepoints; numbers of biological replicates used; strains used; and bile concentration or source selected, further work is needed to better understand the interaction of *C. jejuni* with bile salts to better understand its behaviour within the human gut.

## 1.4 Outer membrane vesicles (OMVs)

### 1.4.1 Background and roles

OMVs are small spherical membrane-bound structures formed from the OM of Gram-negative bacteria. OMV range in size from 10-500 nm and enable secretion of cargo in concentrated selectively packaged parcels, protected from the extracellular environment with the ability to target receptors on recipient cells (Kuehn and Kesty, 2005; Bomberger *et al.*, 2009; Bonnington and Kuehn, 2014; Schwechheimer and Kuehn, 2015; Bitto *et al.*, 2017; Davies *et al.*, 2019). Despite being metabolically expensive, OMV production is evolutionarily conserved in both pathogenic and non-pathogenic Gram-negative bacteria (Kulp and Kuehn, 2010; Roier *et al.*, 2016). OMV production has been observed under a range of conditions (Mashburn-Warren *et al.*, 2008; Elmi *et al.*, 2012; Altindis *et al.*, 2014; Zakharzhevskaya *et al.*, 2017; Davies *et al.*, 2019); both on solid and in liquid media (Schooling and Beveridge, 2006; Schwechheimer and Kuehn, 2015), and in the presence or absence of stress (Schwechheimer and Kuehn, 2015). Neither specific conditions nor gene mutations resulting in the absence of OMVs have been identified. OMVs have been suggested to have a variety of functions important in survival and virulence via processes such as competition for growth (Manning and Kuehn, 2011; Kulkarni *et al.*, 2015), immunomodulation (Koeppen *et al.*, 2016; Tsatsaronis *et al.*, 2018; Mehdi *et al.*, 2021), biofilm formation (Schooling and Beveridge, 2006; Zhao *et al.*, 2022), bacterial communication (Mashburn and Whiteley, 2005; Mashburn-Warren *et al.*, 2008; Zhao *et al.*, 2022), transfer of genetic material (Aktar *et al.*, 2021), and the delivery of biomolecules such as toxins (Bielaszewska *et al.*, 2017; Elmi *et al.*, 2018; Dhital *et al.*, 2021). OMV cargo can be selectively enriched or depleted, suggesting OMVs can be produced and packaged through a regulated process (Veith *et al.*, 2021). Characterisation of OMV proteomes have shown OMVs can have differing protein abundances relative to the OM and periplasmic fractions of the parent cell (Veith *et al.*, 2014). It is thought that OMVs produced under different conditions or by different OMV biogenesis mechanisms form distinct OMV populations with differing cargo (Haurat *et al.*, 2011; Toyofuku *et al.*, 2019). OMVs with differing cargo have been shown to induce differing host cell proteomic changes (Wei *et al.*, 2021). Understanding the mechanisms for biogenesis and cargo selection is of great importance for the study of Gram-negative bacterial pathogenesis.

### 1.4.2 Biogenesis

Previously proposed OMV biogenesis models include alterations in cell wall to OM linkages, stress, creation of defined genetic mutants, cell death or a species specific mechanism. It is thought that the build-up of cellular components (such as misfolded proteins, or peptidoglycan fragments due to cell

wall remodelling defects) at the OM result in bulging and subsequent blebbing (Zhou *et al.*, 1998; McBroom and Kuehn, 2007). However, OMVs can also contain biologically active cargo in addition to cell waste (Mashburn and Whiteley, 2005; Bielaszewska *et al.*, 2017; Elmi *et al.*, 2018). OMVs may also be released from cell division sites with high frequency. This is due to a reduction in cell wall to OM interaction to allow cell division. The reduction in cell wall to OM interactions can cause areas prone to blebbing (Kulp and Kuehn, 2010). However, OMV release is not restricted to cell division sites (Elhenawy *et al.*, 2016). Deatherage *et al.* (2009) studied the effect of removing cell wall to OM linkages on OMV production, and reported that removal of OmpA linkages increased OMV production independent of membrane defects. Removal of other linkages (Lpp, TolA, TolB, and Pal) did cause membrane defects (Deatherage *et al.*, 2009). However, down-regulation of *ompA* is associated with the membrane stress sigma factor,  $\sigma^E$  (Song *et al.*, 2008). Other studies have also reported a loss of membrane integrity in *ompA* mutants (Wang, 2002; Nevermann *et al.*, 2019). It is possible however that transient reductions in OM to cell wall linkages could provide a mechanism for OMV production, such as the mechanism described by Nevermann *et al.* (2019) for Nlpl, a protein thought to play a role in cell division and formation of OM to peptidoglycan linkages (Nevermann *et al.*, 2019; Banzhaf *et al.*, 2020). LPS has also been reported to play a role in OMV biogenesis, with genetically altered strains with altered LPS structure or charge in various bacteria reporting variations in both OMV size and protein content. One example being a *Pseudomonas aeruginosa* CPA mutant, which is only able to synthesize negatively charged LPS, produced OMVs with altered size (Nguyen *et al.*, 2003). Haurat *et al.* (2011) also reported differing protein profiles in a *Porphyromonas gingivalis waaL* mutant. A further mechanism has been identified in the OM of *P. aeruginosa*. *P. aeruginosa* has increased OM fluidity compared to the OM of other Gram-negative bacteria. *P. aeruginosa* produces a quorum sensing molecule PQS (pseudomonas quinolone signal) which induces membrane curvature through interactions with lipid A to stabilize and reduce fluidity of the OM. PQS-induced OMV production is specific to *P. aeruginosa* cells (Mashburn and Whiteley, 2005; Mashburn-Warren *et al.*, 2008).

More recently, Roier *et al.* (2016) have proposed a new general regulatory model based on the maintenance of lipid asymmetry (MLA) pathway that could be widely applicable to Gram-negative bacteria (Roier *et al.*, 2016). The MLA pathway is a lipid transport pathway which has been shown to play a role in the retrograde trafficking of phospholipids (PLs) from the outer leaflet of the OM to the IM. The pathway consists of an IM ABC (ATP binding cassette) transporter consisting of MlaBDEF (MlaB is absent in  $\alpha$  and  $\epsilon$  proteobacteria), a periplasmic chaperone MlaC, and the OM lipoprotein MlaA. The core components of this pathway are highly conserved in Gram-negative bacteria (Malinverni and Silhavy, 2009). Roier *et al.* (2016) proposed that *Haemophilus influenzae* utilises the MLA pathway to regulate OMV production. It was described that downregulation of the pathway leads to an

accumulation of PLs in the OM leading to an asymmetric expansion which eventually results in the formation of an OMV. Roier *et al.* (2016) demonstrated increased OMV production in *mfa* mutants, as well as reduced *mfa* gene expression in *H. influenzae* under iron-limiting conditions.

### 1.4.3 The maintenance of lipid asymmetry pathway (MLA)

The MLA pathway was proposed by Malinverni and Silhavy (2009) who described the pathway as an ABC transport system involved in the retrograde trafficking of PLs from the OM to the IM which prevents PL accumulation in the OM and functions in the absence of obvious extracellular stress (Malinverni and Silhavy, 2009). Two other systems which play a role in modifying PLs in the OM have been described in Gram-negative bacteria, these are PagP and PldA. Both PagP and PldA are expressed at low levels and are dormant unless triggered by cell stress. PldA remains in the membrane as dormant monomers but is triggered to dimerise into an active form upon sensing PLs in the OM. PagP is induced by the PhoPQ regulated stress response pathway. Both pathways modify PLs and do not directly remove the PL from the OM, however it is thought PldA also generates lipid messenger molecules that trigger additional pathways to restore cell membrane homeostasis (Jia *et al.*, 2004; May and Silhavy, 2018).

MlaA, also known as VacJ, is an OM lipoprotein which has been identified as a virulence factor in several Gram-negative bacteria (Suzuki *et al.*, 1994; Cuccui *et al.*, 2007; Carpenter *et al.*, 2014). MlaA is thought to form a channel in the OM and interact with OmpC or OmpF to form a complex (Yeow *et al.*, 2018). Despite some degree of conservation in the MlaA binding region of OmpC and OmpF, only OmpC is thought to be essential for MlaA function (Abellon-Ruiz *et al.*, 2017a; Yeow *et al.*, 2018). The MlaA/OmpC association is not fully understood. One hypothesis is the interaction functions either in placement of or stability of MlaA in the OM (Chong *et al.*, 2015; Abellon-Ruiz *et al.*, 2017a; Yeow *et al.*, 2018). However the requirement of OmpC for function, in addition to experimental evidence demonstrating OM lipid asymmetry being impacted by a point mutation in the OmpC/MlaA binding region (Arg92), which also impacts OmpC gating, suggests a functional rather than a support role (Yeow *et al.*, 2018). The pore size of MlaA at the inner leaflet of the OM is thought to be too small to allow inner leaflet PLs to diffuse in. The pore size at the outer leaflet is thought to be sufficient to permit diffusion of PLs but not molecules as large as LPS or LOS to enter the channel. It is thought a conformational change occurs, possibly triggered by MlaC, that allows the outer leaflet PLs that have diffused into the MlaA pore to move through to the inner leaflet (Abellon-Ruiz *et al.*, 2017a). More recent studies have detailed the presence of a hairpin loop structure in MlaA which could function as a gate for the MlaA channel (Yeow *et al.*, 2018).

MlaA passes the PL to the periplasmic chaperone MlaC which binds the hydrophobic tails leaving the hydrophilic head exposed (Huang *et al.*, 2016; Abellon-Ruiz *et al.*, 2017a). The transfer of PLs from MlaA to MlaC is thought to be driven by the high affinity of MlaC to PLs (Tang *et al.*, 2021; Low and Chng, 2021). MlaC transports the PL to the IM ABC transporter composed of MlaBDEF. MlaD receives the PL from MlaC. MlaD is a single MCE (mammalian cell entry) domain protein which forms a ring structure associated with the IM ABC transporter (Ekiert *et al.*, 2017). Other multi-MCE domain proteins exist in Gram-negative bacteria, such as PqiB and YebT in *E. coli*. PqiB and YebT are predicted to belong to pathways which form channels composed of stacked MCE rings that are able to bridge across the periplasmic space and are thought to enable lipid transport between the OM and the IM (Nakayama and Zhang-Akiyama, 2017; Ekiert *et al.*, 2017). PqiB is encoded in the *pqiABC* (paraquat inducible) operon and contains three MCE domains. YebT is encoded along with YebS in an operon and contains seven MCE domains (Nakayama and Zhang-Akiyama, 2017). To date, *mld* is the only identified MCE domain protein present in *C. jejuni*. PLs returned to the IM are thought to be recycled to a general PL pool (Abellon-Ruiz *et al.*, 2017a).

It has been suggested the MLA pathway could function in the anterograde trafficking of PLs from the IM to the OM (Kamischke *et al.*, 2019; Hughes *et al.*, 2019). This hypothesis is in part backed by the high affinity of MlaC for PLs, which is thought to enable ATP-independent passing of PLs from MlaD to MlaC (Hughes *et al.*, 2019). Two more recent reviews provide compelling arguments supporting the involvement of the MLA pathway in retrograde trafficking of PLs (Powers and Trent, 2019; Shrivastava and Chng, 2019). Both reviews suggest that there is insufficient data to support the anterograde trafficking hypothesis due to limitations in the experimental design in previous publications. These reviews also suggest that the MLA pathway, if involved in anterograde trafficking of PLs, is unlikely to be the only method of anterograde PL transport (Powers and Trent, 2019; Shrivastava and Chng, 2019). More recently, a study working with *Acinetobacter baumannii* found no evidence of anterograde PL transport defects in MLA mutants (Powers *et al.*, 2020), in addition to a further study providing experimental evidence for ATP-dependent retrograde trafficking of PLs in *E. coli* (Tang *et al.*, 2021). Tang *et al.* (2021) explained that the coupling of MlaD to ATPases provides the energy necessary to overcome the high affinity of MlaC to PLs.

Disruption of the MLA pathway has not been shown to disrupt the structural integrity of the OM. However, various studies have reported increases in permeability to certain molecules. This is likely due to the creation of transient PL bilayer patches reducing the barrier function to molecules able to diffuse across PL bilayers. For example, Abellon-Ruiz *et al.* (2017a) reported differences in susceptibility of *E. coli mla* mutants to the small molecules doxycycline and chlorpromazine; Malinverni and Silhavy (2009) observed increased sensitivity of *E. coli mla* mutants to SDS in

combination with EDTA, but not to SDS alone; Roier *et al.* (2016) did not observe any obvious membrane defects for *H. influenzae mla* mutants in response to detergent stress, however Bernier *et al.* (2018) observed differences in susceptibility to Gram-positive but not Gram-negative antibiotics for *Burkholderia cenocepacia mla* mutants (Malinverni and Silhavy, 2009; Roier *et al.*, 2016; Abellon-Ruiz *et al.*, 2017a; Bernier *et al.*, 2018).

#### 1.4.4 Role of OMVs in bacterial virulence

OMVs have well characterised roles in bacterial virulence (Ellis and Kuehn, 2010). For example, OMVs have been demonstrated to harbour secreted virulence factors which can contribute to cytotoxic effects in the *Galleria mellonella* model of infection (McMahon *et al.*, 2012; Elmi *et al.*, 2018), as well as OMVs being able to induce an inflammatory response of human IECs (Elmi *et al.*, 2012; Lee *et al.*, 2018). OMVs have also been associated with toxin secretion, including secretion of Shiga toxin by enterohemorrhagic *E. coli* O157:H7 (Yokoyama *et al.*, 2000); the pore-forming cytotoxin ClyA by *E. coli* K-12 (Wai *et al.*, 2003); cholera toxin by *V. cholerae* (Chatterjee and Chaudhuri, 2011); and CDT by *C. jejuni* and *S. enterica* (Lindmark *et al.*, 2009; Elmi *et al.*, 2012; Guidi *et al.*, 2013). Other secreted virulence factors include proteases (Choi *et al.*, 2011; Elmi *et al.*, 2016), adhesins (Elmi *et al.*, 2016; Gasperini *et al.*, 2018), and immunomodulatory molecules (Perez Vidakovic *et al.*, 2010). The selective enrichment of OMVs with virulence factors provides evidence that OMVs can function as a regulated virulence secretion mechanism rather than just a by-product of cell growth or lysis.

In addition to the direct impact of virulence factors secreted within OMVs, OMVs can impact the virulence potential of the parent cell. For instance, Rolhion *et al.* (2010) demonstrated that mutation of *ompA* in the *E. coli* strain LF82 reduced invasion of Intestine-407 epithelial cells. However, pre-treatment of Intestine-407 epithelial cells with OMVs produced by the wild-type *E. coli* LF82 strain were able to increase invasion of the LF82 isogenic *ompA* mutant. Analysis of OMVs produced by *Porphyromonas gingivalis* revealed the presence of haemagglutinins that were able to increase host adhesion and contribute to the formation of dental plaque through enhancing bacterial aggregation (Ellen and Grove, 1989; Bélanger *et al.*, 2012). *V. cholerae* utilises OMVs to accelerate adaption of the OM during host infection by upregulating OMV production in response to sensing to the host gut environment. The accelerated removal of OM in the form of OMVs functioned to increase the speed of accumulation of glycine-modified LPS and removal of porins which are permissive to entry of harmful compounds (Zingl *et al.*, 2020). Collectively, previous research indicates OMVs have a significant role in bacterial virulence.

#### 1.4.5 *C. jejuni* OMVs

OMVs were proposed to play a role in virulence of *C. jejuni* by Logan and Trust in 1982 (Logan and Trust, 1982). Almost three decades later in 2009, biologically active CDT was discovered to be released in *C. jejuni* OMVs, supporting the earlier suspicion by Logan and Trust that OMVs could function in toxin secretion, and providing the first evidence that *C. jejuni* utilises OMVs for virulence factor secretion (Lindmark *et al.*, 2009). A range of virulence factors have been identified within *C. jejuni* OMVs, including the CDT; adhesins CadF, FlpA; PEB3; colonisation related proteins such as Cj0561c; Cas9 nuclease; and virulence-associated proteases that contribute to *C. jejuni* invasion into IECs (Lindmark *et al.*, 2009; Elmi *et al.*, 2012; Elmi *et al.*, 2016; Elmi *et al.*, 2018; Backert *et al.*, 2018; Saha *et al.*, 2020). Over 150 proteins, including at least 16 *N*-linked glycoproteins, have been identified in *C. jejuni* OMVs. These proteins mainly originate from the OM and periplasm but also from the IM and cytoplasm (Elmi *et al.*, 2012; Jang *et al.*, 2014; Elmi *et al.*, 2018; Taheri *et al.*, 2019; Zamora *et al.*, 2020). *N*-linked glycosylation has been shown to be important in *C. jejuni* OMV function (Zamora *et al.*, 2020). Zamora *et al.* (2020) observed alterations in protein profiles and enrichment of proteases in a glycosylation impaired 11168 *pglE* mutant. *C. jejuni* OMVs isolated at 37°C (human body temperature) have also been shown to differ in protein abundance compared to OMVs isolated at 42°C (avian body temperature), suggesting *C. jejuni* can alter cargo in response to host signals (Taheri *et al.*, 2019).

Previous characterisation of *C. jejuni* OMVs by our group has demonstrated that *C. jejuni* OMVs contain numerous proteins representative of around 10% of the total *C. jejuni* proteome, and includes OM associated, periplasmic and cytoplasmic proteins (Elmi *et al.*, 2012). Amongst these proteins were 16 *N*-linked glycoproteins; HtrA, Cj0511 and Cj1365c which exhibit serine protease activity; and CDT. HtrA and Cj1365c were also shown to contribute to the cleavage of E-cadherin and occludin, which are proteins associated with adherens junctions and tight junctions of eukaryotic cells (Elmi *et al.*, 2012; Elmi *et al.*, 2016). The most predominant population of proteins identified by Elmi *et al.* (2012) within *C. jejuni* OMVs had no determined function. Elmi *et al.* (2012) also demonstrated that *C. jejuni* OMVs can induce IL-8, IL-6, TNF- $\alpha$  and hBD-3 secretion from T84 IECs as well as exhibiting cytotoxicity towards both T84 IECs and *G. mellonella* larvae. Additionally, *C. jejuni* OMVs were able to enhance invasion of T84 IECs when co-inoculated with live *C. jejuni* cells (Elmi *et al.*, 2012; Elmi *et al.*, 2016).

An important feature of a pathogen is the ability to sense the environment and to appropriately alter and co-ordinate the regulation of virulence factors. Our group has previously reported that the bile salt ST has a role in OMV production and OMV-mediated virulence in *C. jejuni* (Elmi *et al.*, 2018). OMVs produced in the presence of ST (stOMVs) also had an increased number of proteins within the OMV cargo proteome. A total of 34 proteins were found to be exclusive to the stOMV proteome, including

*Campylobacter* invasion antigen (Cial); bile salt response protein Cj0561c; and Cj0628 which is thought to play a role in adhesion and colonisation. stOMVs also exhibited increased proteolytic activity, cytotoxicity, and immunogenicity towards IECs, as well as increased cytotoxicity in *G. mellonella* larvae (Elmi *et al.*, 2018).

## 1.5 Aims and objectives

The aim of this study was to investigate the interaction of *C. jejuni* with bile salts at physiological concentrations found in the human gut, and to investigate the link between bile salts and OMV related virulence of *C. jejuni*.

Objectives:

1. Investigate the role of ST and the MLA pathway in the biogenesis of *C. jejuni* OMVs.
2. Investigate transcriptional changes caused by growth in biologically relevant concentrations of either ST or SDC.
3. To characterise key genes identified as transcriptionally regulated by bile salts.

## Chapter 2: Materials and Methods

### 2.1 Bacterial strains and growth conditions

The *C. jejuni* wild-type strains used in this study were NCTC 11168 (the widely studied human clinical isolate), 11168H (a hypermotile derivative of NCTC 11168) (Karlyshev *et al.*, 2002) and 488 (a Brazilian human isolate obtained from Dr Daiani Teixeira da Silva)(Liaw *et al.*, 2019). Mutant and complement strains constructed from these wild-type strains are listed in Table 2.1. Unless otherwise stated, *C. jejuni* cultures were grown in a microaerobic chamber (Don Whitley Scientific, Bingley, United Kingdom) containing 85% (v/v) N<sub>2</sub>, 10% (v/v) CO<sub>2</sub>, and 5% (v/v) O<sub>2</sub> at 37°C either on blood agar (BA) plates containing Columbia agar base (Oxoid, Basingstoke, United Kingdom), 7% (v/v) horse blood in Alsever's (TCS Microbiology, Botolph Claydon, United Kingdom), and Skirrow *Campylobacter* Selective Supplement (Oxoid), or in Brucella broth (BD Diagnostics, Wokingham, United Kingdom) shaking at 75 rpm. Brucella broth was pre-incubated under microaerobic conditions in a vented tissue culture flask for 24 hours prior to inoculation. *C. jejuni* strains were grown on BA plates for 24 hours prior to experiments unless otherwise stated. *E. coli* XL2-Blue competent cells (Stratagene, San Diego, USA) and *E. coli* SCS110 competent cells (Agilent, Santa Clara, USA) used for cloning were grown at 37°C in aerobic conditions either in lysogeny broth (LB) (Oxoid) shaking at 200 rpm or on LB agar plates (Oxoid). When required, ampicillin (100 µg/ml), kanamycin (50 µg/ml), apramycin (60 µg/ml), chloramphenicol (50 µg/ml for *E. coli* or 10 µg/ml for *C. jejuni*), or erythromycin (75 µg/ml for *E. coli* or 2 µg/ml for *C. jejuni*) were added to cultures.

**Table 2.1.** *C. jejuni* mutant and complement strains used in this study.

Strain	Selection marker	Mutagenesis method
<b>11168 <i>mlaA</i> mutant</b>	Kanamycin	Replacement of ORF with kanamycin resistance cassette (Taylor <i>et al.</i> , 2017).
<b>11168 <i>mlaA</i><sup>+</sup></b>	Chloramphenicol	pRRA complementation construct (Taylor <i>et al.</i> , 2017).
<b>488 <i>mlaA</i> mutant</b>	Kanamycin	Natural transformation using gDNA from 11168 <i>mlaA</i> mutant.
<b>488 <i>mlaA</i><sup>+</sup></b>	Chloramphenicol	pCJC1 complementation construct (Gundogdu <i>et al.</i> , 2011; Jervis <i>et al.</i> , 2015).
<b>11168H <i>Cj0561c</i> mutant</b>	Kanamycin	Replacement of the centre of the ORF with kanamycin resistance cassette by SOE PCR.
<b>488 <i>Cj0561c</i> mutant</b>	Kanamycin	Replacement of the centre of the ORF with kanamycin resistance cassette by SOE PCR.

<b>488 <i>Cj0561c</i><sup>+</sup></b>	Chloramphenicol	pCJC1 complementation construct (Gundogdu <i>et al.</i> , 2011; Jervis <i>et al.</i> , 2015)
<b>488 <i>cmeB</i> mutant</b>	Erythromycin	Interruption of ORF with erythromycin resistance cassette (Gundogdu <i>et al.</i> , 2011; Jervis <i>et al.</i> , 2015)
<b>488 <i>Cj0561c cmeB</i> double mutant</b>	Kanamycin, erythromycin	Replacement of the centre of the <i>Cj0561c</i> ORF with kanamycin resistance cassette by SOE PCR. Interruption of <i>cmeB</i> ORF with erythromycin resistance cassette (Gundogdu <i>et al.</i> , 2011; Jervis <i>et al.</i> , 2015)
<b>11168H <i>cmeB</i> mutant</b>	Erythromycin	Interruption of ORF with erythromycin resistance cassette (Gundogdu <i>et al.</i> , 2011; Jervis <i>et al.</i> , 2015)
<b>11168H <i>Cj0561c cmeB</i> double mutant</b>	Kanamycin, erythromycin	Replacement of the centre of the <i>Cj0561c</i> ORF with kanamycin resistance cassette by SOE PCR. Interruption of <i>cmeB</i> ORF with erythromycin resistance cassette (Gundogdu <i>et al.</i> , 2011; Jervis <i>et al.</i> , 2015)

The 11168 *mIaA* mutant and complement strains were kindly provided by Professor David Kelly and Dr Aidan Taylor at the University of Sheffield. All other strains were produced during this study. ORF = open reading frame; SOE PCR = splicing by overlap extension polymerase chain reaction.

## 2.2 Assays

### 2.2.1 Growth kinetics

*C. jejuni* cells were harvested from a 24 hour BA plate culture and resuspended in 1 ml of sterile phosphate buffered saline (PBS). The OD<sub>600</sub> was measured on a Spectronic Spectrophotometer (Thermo Fisher Scientific, Massachusetts, USA) using 100 µl of bacterial suspension diluted in 900 µl PBS. The suspension was used to inoculate 10 ml of pre-incubated Brucella broth to an OD<sub>600</sub> of 0.1 using the following calculation:

$$\left( \frac{\text{required OD}_{600}}{\text{suspension OD}_{600} \times \text{dilution factor}} \right) \times \text{culture volume (ml)} \times 1000 = \text{volume required (}\mu\text{l)}$$

Broth cultures were incubated at 37°C under microaerobic conditions shaking at 75 rpm. OD<sub>600</sub> readings were taken every two hours over an 18 hour period. For CFU/ml counts, culture samples were diluted 10-fold to 10<sup>-7</sup> then 10 µl of dilutions 10<sup>-5</sup> to 10<sup>-7</sup> were spotted in triplicate onto BA plates and grown for two days before CFUs were counted.

### 2.2.2 Motility

Brucella semi-solid agar motility plates were prepared by adding 0.4% (w/v) bacteriological agar (Sigma-Aldrich, United Kingdom) to Brucella broth. *C. jejuni* cells were harvested from a 24 hour BA plate into 1 ml of PBS. The bacterial suspension was adjusted to an OD<sub>600</sub> of 1.0, and 5 µl was

inoculated into the centre of a motility plate. Each strain was inoculated in triplicate onto separate agar plates. The diameter and characteristics of halos were measured every 24 hours for 72 hours.

### **2.2.3 Detergent sensitivity**

Sensitivity to biologically relevant concentrations of the bile salt ST was analysed by performing ST supplemented growth kinetics. ST growth kinetics was performed as described in Section 2.2.1 with the addition of ST to the pre-incubated broth to a final concentration of 0.2% (w/v). Fresh 10% (w/v) ST stock solutions were prepared for each assay in Brucella broth and filter sterilised using a 0.22 µm membrane filter. Sensitivity to ST at high concentrations was analysed by comparing the OD<sub>600</sub> and CFU/ml of late-log phase broth cultures grown in the presence or absence of 2% (w/v) ST. Sensitivity to ST at both biologically relevant concentrations and stress concentrations on agar was also carried out by preparing Brucella agar (1.5% (w/v) bacteriological agar in Brucella broth) supplemented with 0.04% - 2% (w/v) ST. A suspension of *C. jejuni* from a 24 hour BA plate culture was prepared to an OD<sub>600</sub> of 1.0 and a 10-fold serial dilution to 10<sup>-7</sup> was performed. 10 µl of each dilution was spotted onto assay plates. Plates were incubated under microaerobic conditions for three days prior to counting CFUs. Sensitivity to the bile salt sodium SDC was analysed on Brucella agar as described for ST using 0.001 or 0.5% (w/v) SDC.

Sensitivity to lauryl sulfobetaine (LSB) (Sigma-Aldrich), 3-((3-Cholamidopropyl)dimethylammonium)-1-propanesulfonate (CHAPS) (Sigma-Aldrich) and sodium dodecyl sulfate (SDS) (Sigma-Aldrich) was analysed by comparing CFU/ml of *C. jejuni* cultures 10-fold serially diluted to 10<sup>-7</sup> and spotted onto Brucella agar with or without supplementation of LSB (0.2 - 1.5 mM final concentration), CHAPS (0.5% (w/v) final concentration) or SDS (500 µg/ml final concentration). *C. jejuni* cultures were obtained from either mid-log phase broth cultures (see Section 2.2.1), or cells harvested from a 24 hour BA plate culture into 1 ml of sterile PBS and adjusted to OD<sub>600</sub> of 1.0.

### **2.2.4 Antibiotic sensitivity**

Sensitivity to polymyxin B was analysed by comparing CFU/ml of mid-log phase cultures 10-fold serially diluted to 10<sup>-7</sup> and spotted in triplicate onto BA plates either with or without supplementation of polymyxin B (2.5 µg/ml final concentration). CFU/ml were counted after 2-4 days once colonies were visible.

Sensitivity to a range of antimicrobials was analysed using the disk diffusion method. *C. jejuni* cells were harvested from a 24 hour BA plate into PBS, and the optical density adjusted to an OD<sub>600</sub> of 0.1 (approximately McFarland 0.5 or 2 x 10<sup>8</sup> CFU/ml). A sterile cotton swab was used to create a lawn on BA plates (prepared without Skirrow) and plates were allowed to dry for five minutes. Antimicrobial

disks with ampicillin (10 µg), tetracycline (30 µg) and polymyxin B (300 U) (Oxoid) were added to each bacterial lawn plate. Additional antibiotic disks were prepared for ampicillin and erythromycin by adding 100 µg total for ampicillin or 2 µg total for erythromycin to sterile blank antimicrobial susceptibility disks (Oxoid). Plates were incubated for 24 hours at 37°C under microaerobic conditions. Zones of inhibition were recorded.

### 2.2.5 3,3'-dipropylthiadicarbocyanine Iodide (DiSC3) permeability assay

DiSC3 is a potentiometric fluorescent probe which accumulates on and translocates into hyperpolarised lipid bilayers and can be used to measure membrane permeability. Fluorescence was monitored at Ex/Em wavelength of 622/670 nm in a Cary Eclipse fluorescence spectrophotometer (Agilent). *C. jejuni* cells were washed in 20 mM sodium phosphate buffer, pH 7.4, containing 10 mM KCl, and adjusted to an OD<sub>600</sub> of 0.1. DiSC3 was added to 5 µM final concentration and fluorescence emission followed for two minutes to establish the baseline. Polymyxin B was then added (100 µM final concentration) and emission followed for a further 1 minute, before the addition of SDS (20 mM final concentration) to give the maximum fluorescence value. Percentage incorporation of the dye into the membrane was calculated by:

$$100 - \left( \frac{\text{emission after polymyxin B (minus baseline)}}{\text{maximum emission after SDS (minus baseline)}} \right) \times 100$$

= % membrane incorporation

(Davies *et al.*, 2019)

### 2.2.6 Heat shock

A suspension of *C. jejuni* from a 24 hour BA plate culture was prepared in sterile PBS to an OD<sub>600</sub> of 1.0 in 200 µl (see Section 2.2.1). The suspension was incubated at 55°C for three minutes in a water bath, put on ice for 15 seconds, then plated for CFU/ml as described in Section 2.2.1.

### 2.2.7 Osmotic stress

Osmotic stress agar plates were prepared by supplementing Mueller Hinton (MH) agar with 0% to 2% (w/v) of NaCl. A bacterial suspension was prepared from a 24 hour BA plate into Brucella broth then used to inoculate 10 ml of pre-incubated Brucella broth to an OD<sub>600</sub> of 0.1 as described in Section 2.2.1. Bacterial cultures were grown for eight hours to mid-log phase. Bacterial cells were pelleted by centrifugation at 3,000 × g for 10 minutes at room temperature. The supernatant was discarded and the pellet was resuspended in 10 ml of sterile PBS. The cells were pelleted by centrifugation as described above and the pellet was resuspended in sterile PBS to an OD<sub>600</sub> of 0.1. The bacterial suspension was 10-fold serially diluted to 10<sup>-6</sup> and 10 µl of each dilution was spotted in triplicate onto

osmotic stress agar plates. Plates were incubated under microaerobic conditions at 37°C for 48 hours before CFU/ml were counted as described in Section 2.2.1.

### **2.2.8 Carbonyl cyanide *m*-chlorophenylhydrazone (CCCP) efflux pump inhibition assay**

CCCP is an efflux pump inhibitor with inhibition achieved by uncoupling oxidative phosphorylation and disrupting the proton gradient of the IM. CCCP was used to analyse efflux pump activity in the presence of stress. *C. jejuni* cells were harvested from a 24 hour BA plate culture into 1 ml of sterile PBS, adjusted to OD<sub>600</sub> of 1.0, 10-fold serially diluted to 10<sup>-7</sup> and spotted in triplicate onto Brucella agar plates with or without supplementation of 0.2 - 1.5 mM LSB with CCCP (0.05 or 0.1 µg/ml). CFUs were counted after four days once colonies were visible.

## **2.3 OMV isolation and characterisation**

### **2.3.1 OMV isolation**

*C. jejuni* OMVs were isolated as previously described (Elmi *et al.*, 2012; Davies *et al.*, 2019). Briefly, *C. jejuni* cells from a 24 hour BA plate were resuspended in Brucella broth and used to inoculate 50 ml of pre-incubated Brucella broth to an OD<sub>600</sub> of 0.1. Cultures were grown to late-log phase with the exact timepoints determined by the growth kinetics for each strain. OD<sub>600</sub> values were normalised to OD<sub>600</sub> of 1.0 and the sterile supernatants were obtained by pelleting cells and filter-sterilising supernatants through a 0.22 µm membrane filter. The supernatants were then concentrated to 2 ml using an Ultra-4 Centrifugal Filter Unit with a nominal 10 kDa cut-off (Millipore). The concentrated filtrate was ultra-centrifuged at 150,000 × g for 3 hour at 4°C using a TLA 100.4 rotor (Beckman Coulter, California, USA). The resulting OMV pellet was washed by resuspending in particle-free PBS without calcium chloride and magnesium chloride (Sigma) and then pelleted by ultra-centrifugation as described above. Particle-free PBS without calcium chloride and magnesium chloride is used to minimise clumping of OMVs which could impact nanoparticle tracking (NTA) analysis measurements. The resulting OMV pellet was resuspended in 200 µl PBS and used immediately unless otherwise used for nanoparticle tracking analysis (NTA) in which case OMV aliquots were stored at –20°C. All isolation steps were performed on ice.

### **2.3.2 Protein quantification – Bicinchoninic acid (BCA) assay**

The protein concentration of OMV preparations was quantified using a commercial bicinchoninic-acid (BCA) assay kit according to the manufacturer's protocol (Thermo Fisher Scientific), using Bovine Serum Albumin (BSA) as the protein standard. Briefly, BSA standards dilution series was prepared ranging from 25 µg/ml to 2,000 µg/ml in PBS and stored at 4°C until use. The working reagent was prepared using 50 parts BCA reagent A to 1 part BCA reagent B. Each OMV preparation was diluted 1 in 10 in PBS and 10 µl of each OMV preparation or BSA standard was pipetted in triplicate to separate wells of a flat bottom 96 well plate. 200 µl of working reagent was pipetted using a multi-channel pipette into each assay well. Each well was mixed by pipetting, taking care not to introduce bubbles. The assay plate was wrapped with foil and incubated at 37°C for 30 minutes. Results were recorded using ELx800 Absorbance Microplate Reader (BioTek, Swindon, United Kingdom) at 590 nm. Protein concentration was calculated using a standard curve generated from the BSA standards readings.

### **2.3.3 Lipid quantification (KDO)**

The LOS of OMV preparations was quantified by measuring 2-Keto-3-deoxyoctonate acid (KDO) content as described previously (Lee and Tsai, 1999). Briefly, 50 µl of OMV preparations were

hydrolysed with 50  $\mu$ l sulphuric acid (0.5 N) at 100°C for 15 min, then mixed with 50  $\mu$ l 0.1 M periodate reagent ( $H_5IO_6$ ) and incubated at room temperature for 10 min. 200  $\mu$ l of 4% (w/v) sodium arsenite reagent ( $NaAsO_2$ ) then 800  $\mu$ l 0.6% (w/v) thiobarbituric acid was added and samples heated again to 100°C for 15 min. Samples were mixed with 1 ml dimethyl sulfoxide (DMSO) to stabilise the chromophore and  $OD_{548}$  measurements were taken. 2-Keto-3-deoxyoctonate ammonium salt (Sigma-Aldrich) was used as the KDO standard to generate a standard curve (Davies *et al.*, 2019).

#### **2.3.4 Nanoparticle tracking analysis particle counts and size**

NTA was conducted using a ZetaView PMX 110 instrument (Particle Metrix GmbH, Germany) following the manufacturer's instructions. The instrument was calibrated against a known concentration of PS100 nanoparticles with 100 nm diameter (Applied Microspheres B. V., The Netherlands). Nanostandards and OMV samples were suspended in particle-free PBS and diluted appropriately before analysis. Suitable dilution concentrations of samples based on protein content are between 0.1-0.2  $\mu$ g/ml. Each sample was counted and sized across two cycles of 11 frames per cycle with a flow cell sensitivity of 80% (Davies *et al.*, 2019).

## **2.4 Cell culture**

### **2.4.1 Cell lines and conditions**

Cell culture media unless otherwise stated contained Dulbecco's Modified Eagle's Medium (DMEM) with GlutaMax (Thermo Fisher Scientific) supplemented with 10% (v/v) foetal bovine serum (FBS) (Thermo Fisher Scientific), 1% (v/v) non-essential amino acids (Thermo Fisher Scientific) and 1% (v/v) penicillin-streptomycin (Thermo Fisher Scientific). Media was pre-incubated at 37°C in a CO<sub>2</sub> incubator with 5% CO<sub>2</sub> prior to use. Cell lines used were human colonic adenocarcinoma intestinal epithelial cell (IEC) lines T84 (ECACC 88021101) cells and Caco-2 cells (ECACC 86010202).

Frozen cell lines were revived by briefly thawing at 37°C in a water bath for one minute then resuspending in pre-incubated cell culture media. Cells were added to a 25 cm<sup>2</sup> filter cap tissue culture flask and incubated at 37°C in a CO<sub>2</sub> incubator until cells were semi-confluent. Spent tissue culture media was replaced every 1-3 days. Once semi-confluent growth was reached, the media was removed and cells were washed three times with 10 ml of pre-incubated PBS. 3 ml of pre-incubated trypsin-EDTA was added and flasks were then incubated in a CO<sub>2</sub> incubator at 37°C for 10 minutes. If a large proportion of cells remained attached the flask was incubated for up to a further five minutes. 15 ml of tissue culture media was added to the detached cells and the contents of the flask was transferred to a 50 ml sterile falcon tube. Cells were centrifuged at 180 × g for 10 minutes. The supernatant was discarded, pellet was gently resuspended in 25 ml of pre-incubated tissue culture media then added to a 75 cm<sup>2</sup> tissue culture flask. The flask was incubated at 37°C in a CO<sub>2</sub> incubator until semi-confluent growth was reached. Once semi-confluent growth was reached, cells were split by washing and detaching cells as described above then splitting 50 ml of cells between two 75 cm<sup>2</sup> tissue culture flasks.

### **2.4.2 Interaction, invasion, intracellular survival and IL-8 secretion assays**

IECs were seeded into the central eight wells of a 24-well tissue culture plate from a 75 cm<sup>2</sup> flask with semi-confluent growth. Cells were washed and detached as described in Section 2.4.1 then resuspended in 10 ml of pre-incubated tissue culture media. 100 µl of cell suspension was diluted 1:10 in 800 µl of tissue culture media with 100 µl of Trypan blue. 20 µl of diluted cell suspension was loaded onto a haemocytometer (Weber Scientific, United Kingdom) and viable cells from the four corner 4x4 grids were counted. Cells were diluted in tissue culture media to a cell density of 1 × 10<sup>5</sup> cells/ml using the following equation:

Cell suspension density:

$$\text{Average grid count} \times \text{dilution factor} \times 10^4 = \text{Cells/ml}$$

\* Haemocytometer grid volume is  $10^{-4}$  ml.

Volume of cell suspension required for dilution:

$$\left( \frac{\text{Required cell density}}{\text{Cell density of cell suspension}} \right) \times \text{Required volume (ml)} \times 1000 = \text{Volume required } (\mu\text{l})$$

To each well 1 ml of diluted cell suspension was added. The plate was incubated at 37°C in a CO<sub>2</sub> incubator for seven days until semi-confluent growth was reached. The tissue culture media was changed every 2-3 days. 24 hours prior to infection tissue culture media was replaced with infection media. Infection media lacks the penicillin-streptomycin supplement.

A *C. jejuni* cell suspension was prepared from a 24 hour BA plate as described in Section 2.2.1 in 1 ml of tissue culture infection media. The bacterial suspension was adjusted to an OD<sub>600</sub> of 0.2 (approximately  $2 \times 10^8$  CFU/ml). 100  $\mu\text{l}$  of suspension was 10-fold serially diluted to count for CFU/ml as described in Section 2.2.1. IEC monolayers in the 24-well plate were washed with pre-incubated infection media and 1 ml of bacterial suspension in infection media was added to each well. This gave an multiplicity of infection (MOI) value of 200:1. IEC were incubated with the bacterial suspension in a CO<sub>2</sub> incubator for 3 or 24 hours. As a growth control, 100  $\mu\text{l}$  of infection supernatant was 10-fold serially diluted to count for CFU/ml as described in Section 2.2.1. For interaction assays infected monolayers were washed three times with 1 ml PBS then incubated with 0.5 ml 0.1% (v/v) Triton X-100 (Thermo Fisher) for 20 minutes at room temperature followed by pipetting for one minute to lyse IECs. Lysed cells were serially diluted and plated for CFUs as described in Section 2.2.1. For invasion assays, washed cells were treated with gentamicin (150  $\mu\text{g/ml}$ ) for two hours, washed three times with pre-warmed PBS then lysed with 0.1% (v/v) Triton X-100 and plated for CFUs as described above. For intracellular survival assays, washed cells were incubated with gentamicin (150  $\mu\text{g/ml}$ ) as described above, washed three times with pre-warmed PBS followed by incubation with gentamicin (10  $\mu\text{g/ml}$ ) for a further 18 hours. Cells were then washed, lysed and plated for CFUs as described above.

### **2.4.3 Treatment of intestinal epithelial cells with outer membrane vesicles**

Semi-confluent T84 cells were prepared and washed as described in Section 2.4.2. To each well 1 ml of preincubated infection media was added. OMVs were prepared as described in Section 2.3.1. and quantified using the BCA assay as described in Section 2.3.2. To minimise the potential of OMV components to denature prior to inoculation, OMVs were added directly from tubes on ice and were

prepared fresh on the day of inoculation. To prevent cold shock of IECs, OMVs were added in a total volume of 50 µl to the 1 ml infection media in each well. 100 µg total of OMVs were added to replicate wells and mixed by washing supernatant over monolayers once. IECs were incubated with OMVs in a CO<sub>2</sub> incubator for 24 hours. The total supernatant was then aspirated and stored at -80°C prior to IL-8 quantification (see Section 2.4.4).

#### **2.4.4 Interleukin-8 (IL-8) enzyme-linked immunosorbent assay (ELISA)**

Stimulation of IL-8 secretion by IECs during infection with *C. jejuni* whole cells or treatment with OMVs was assessed using the Human IL-8 Uncoated ELISA kit (Thermo Fisher Scientific) according to the manufacturer's protocol. IECs were seeded into 24-well tissue culture plates, grown until semi-confluent, then infected with either *C. jejuni* for 3 or 24 hours as described in Section 2.4.2 or treated with 100 µg of *C. jejuni* OMVs for either 3 or 24 hours as described in Section 2.4.3. Cell supernatants were collected and stored at -80°C for up to one month.

To coat the 96-well ELISA plate, the capture antibody (anti-human IL-8) was diluted 1:250 in coating buffer and 100 µl was added to each well. The 96-well ELISA plate was incubated overnight at 4°C. The coating antibody was removed and each well was washed three times with 260 µl wash buffer (PBS with 0.05% (v/v) Tween-20), allowing the wash buffer to sit for one minute before aspirating. Wells were blocked with 200 µl of ELISA/ELISPOT diluent (diluted to 1X in deionised water) at room temperature for one hour with agitation then wells were washed once with 200 µl wash buffer. The Human IL-8 standard was prepared fresh for each assay. The Human IL-8 standard was reconstituted in distilled water for 20 minutes then a 2-fold serial dilution was performed in ELISA/ELISPOT diluent to create an 8-point standard curve. 100 µl of IL-8 standard, sample or ELISA/ELISPOT blank were added to replicate wells of the ELISA 96-well plate. The plate was sealed and incubated at room temperature for two hours with agitation, wells were then aspirated and washed four times with wash buffer as previously described. The detection antibody (biotin-conjugated anti-human IL-8) was diluted 1:250 in ELISA/ELISPOT diluent and 100 µl was added to each well. The plate was sealed and incubated at room temperature for one hour with agitation. The detection antibody was aspirated and wells washed four times as previously described. The Avidin-HRP (horseradish peroxidase) enzyme was diluted 1:250 in ELISA/ELISPOT diluent and 100 µl was added to each well. The plate was sealed and incubated at room temperature for 30 minutes with agitation. The Avidin-HRP was aspirated and wells washed six times as previously described allowing each wash to sit for two minutes before removing. 100 µl of substrate solution (Tetramethylbenzidine (TMB) solution) was added to each well. The plate was sealed and incubated at room temperature for 15 minutes with agitation.

100 µl of stop solution (2 N sulfuric acid) was added to each well. The plate was read at 450 nm on a SpectraMax M3 Multi-Mode Microplate reader (Molecular Devices, San Jose, USA).

## **2.5 *Galleria mellonella* larvae model of infection**

*G. mellonella* larvae were purchased from Livefoods Direct (Sheffield, United Kingdom). Larvae were stored in a dormant state at 4°C for up to two weeks. Larvae without visible melanisation and of a similar size (0.18 g to 0.26 g) were selected for experiments. Prior to experiments larvae were kept at room temperature for one hour until larvae had regained total motility. A 25 µl gastight syringe (Hamilton, Giarmata, Romania) was used to inject 10 µl total inoculum into the right foremost leg. The syringe was washed with 20 µl of 100% (v/v) ethanol three times, then with 20 µl of sterile PBS three times prior to all experiments and when switching between inoculum within experiments.

### **2.5.1 *Galleria mellonella* larvae infection with live *C. jejuni* cells**

A *C. jejuni* cell suspension of each strain was prepared from a 24 hour BA plate as described in Section 2.2.1 to an OD<sub>600</sub> of 0.1 in sterile PBS. For each strain 10 larvae were injected with 10 µl of bacterial suspension. Additional larvae were injected with sterile PBS as controls. A total of four biological replicates were performed, and all strains were injected in a single session from the same larvae batch for each biological replicate to minimise batch variation. Larvae were incubated at 37°C under aerobic conditions for five days. The health and viability of larvae was recorded every 24 hours. Larvae were recorded as deceased if they were no longer responsive to touch. Larvae were recorded as live but unhealthy if larvae were responsive to touch but had visible melanisation. Larvae were recorded as healthy if there were no visible signs of melanisation.

### **2.5.2 *Galleria mellonella* larvae inoculation with outer membrane vesicles**

OMVs were prepared as described in Section 2.3.1. fresh on the day of inoculation for each biological replicate. OMVs were quantified using a BCA assay as described in Section 2.3.2. and diluted to 1.5 µg/µl in sterile ice-cold PBS. To ensure OMVs were not denatured prior to the assay, OMVs were kept on ice and were taken up into a gastight syringe directly from tubes kept on ice. A total of 15 µg of OMVs in 10 µl was injected per larvae. A total of 10 larvae were injected for each OMV sample. All OMVs from a single wild-type and its respective mutant or complement strains were injected in a single session from the same larvae batch for each biological replicate to minimise batch variation. A total of four biological replicates were performed. Additional larvae were injected with ice cold sterile PBS as controls. Larvae were incubated at 37°C under aerobic conditions for three days. Health and viability of larvae was recorded as described in Section 2.5.1. after 12, 24, 48 and 72 hours.

## 2.6 Molecular techniques

### 2.6.1 Genomic DNA isolation

*C. jejuni* genomic DNA was isolated using the PureLink Genomic DNA Mini Kit (Thermo Fisher Scientific). *C. jejuni* cells were harvested from 24 BA plate and gDNA isolated according to the manufacturer's protocol for Gram-negative bacteria. Briefly, cells were suspended in 180 µl of PureLink Genomic Digestion Buffer with 20 µl Proteinase K. The cells were lysed at 55°C for 30 minutes. 20 µl of RNaseA was added and the lysate was incubated at room temperature for two minutes. 200 µl PureLink Genomic Lysis/Binding Buffer and 200 µl of 100% (v/v) ethanol was added to the lysate tube then the lysate was vortexed to produce a homogenous solution. The solution was added to a PureLink spin column and centrifuged at 10,000 x g for 1 minute. The collection tube was replaced and the column washed with 500 µl of PureLink Wash Buffer 1 then 500 µl of PureLink Wash Buffer 2. gDNA was eluted with 40 µl of DEPC-treated water. DNA concentrations were quantified using a NanoDrop ND-1000 spectrophotometer (NanoDrop Technologies, Delaware, USA). gDNA was stored at -20°C.

### 2.6.2 PCR

Primers were designed manually then checked for homodimers, heterodimers and hairpin-loops using the OligoAnalyzer Tool (Integrated DNA Technologies, Coralville, USA). Primers were diluted to a final concentration of 100 pmol/µl using DEPC-treated water and stored at -20°C. Primers used in this study are listed in Table 2.2 (see Section 2.6.10). Unless otherwise stated, PCRs were performed using MyTaq Red mastermix (Bioline, London, United Kingdom) using 0.25 µl of each forward and reverse primer, 1 µl of DNA template (200-400 ng/µl) and 98.5 µl of 1x PCR mastermix. Unless otherwise stated, PCRs were carried out using the following program:

35 cycles:

Denature	- 94°C for 15 seconds
Anneal	- temperature primer dependent, 1 minute
Extension	- 72°C for 1 minute per 1.5 kb
Final extension step	- 72°C for 7 minutes

PCRs were run on 1% (w/v) TAE agarose gels supplemented with GelRed (Sigma-Aldrich) to 1X final concentration. Reactions were run alongside 5 µl DNA HyperLadder 1kb (Bioline) at 120 V and 500 mA for 40 minutes.

## 2.6.3 Mutagenesis

### 2.6.3.1 Mutagenesis strategies

The *C. jejuni* 11168 *miaA* mutant was kindly provided by Professor David Kelly and Dr Aidan Taylor at the University of Sheffield. Briefly, *miaA* was inactivated by deletion of the reading frame by homologous cross-over and replacement with a kanamycin resistance cassette. The mutation vector was created using the Gibson isothermal assembly method as previously described (Taylor *et al.*, 2017). The *C. jejuni* 488 *miaA* mutant strain was constructed by natural transformation (see Section 2.6.4) using gDNA from the 11168 *miaA* mutant strain.

The 11168H and 488 *Cj0561c* genes were inactivated by insertion of a kanamycin resistance cassette into the centre of the open reading frame (ORF) by homologous recombination. The mutation vector was created as previously described (Gundogdu *et al.*, 2011) with the addition of SOE PCR (see Section 2.6.3.2) to replace the centre of the *Cj0561c* reading frame with a BglII restriction site leaving around 200 bp of homology either side of the kanamycin integration site to allow for homologous recombination.

The 488 *cmeB* gene was inactivated by insertion of an erythromycin resistance cassette into the centre of the ORF by homologous recombination. The mutation vector was created as previously described (Gundogdu *et al.*, 2011). The centre 1 kb of the *cmeB* ORF was amplified by PCR (See Section 2.6.2). The amplicon was cloned into pGEM-T vector by TA cloning (see Section 2.6.3.2) and contained a single BclI restriction site for integration the erythromycin resistance cassette. The 488 *Cj0561c cmeB* double mutant was constructed using the mutation vectors described previously for the *Cj0561c* and *cmeB* single mutant strains.

### 2.6.3.2 SOE PCR

Gene specific Splicing by Overlap Extension (SOE) PCR primers were designed to amplify approximately 200 bp homology arms within *Cj0561c* ORF at both the 5' and 3' end as shown in Figure 2.1. The internal primers (the reverse primer of the 5' homology arm, and the forward primer of the 3' homology arm) contained part of the BglII restriction site and a 6 bp region of overlap to the opposite homology arm. Regions of overlap were designed to have melting temperatures appropriate for the melting temperature of the primers.

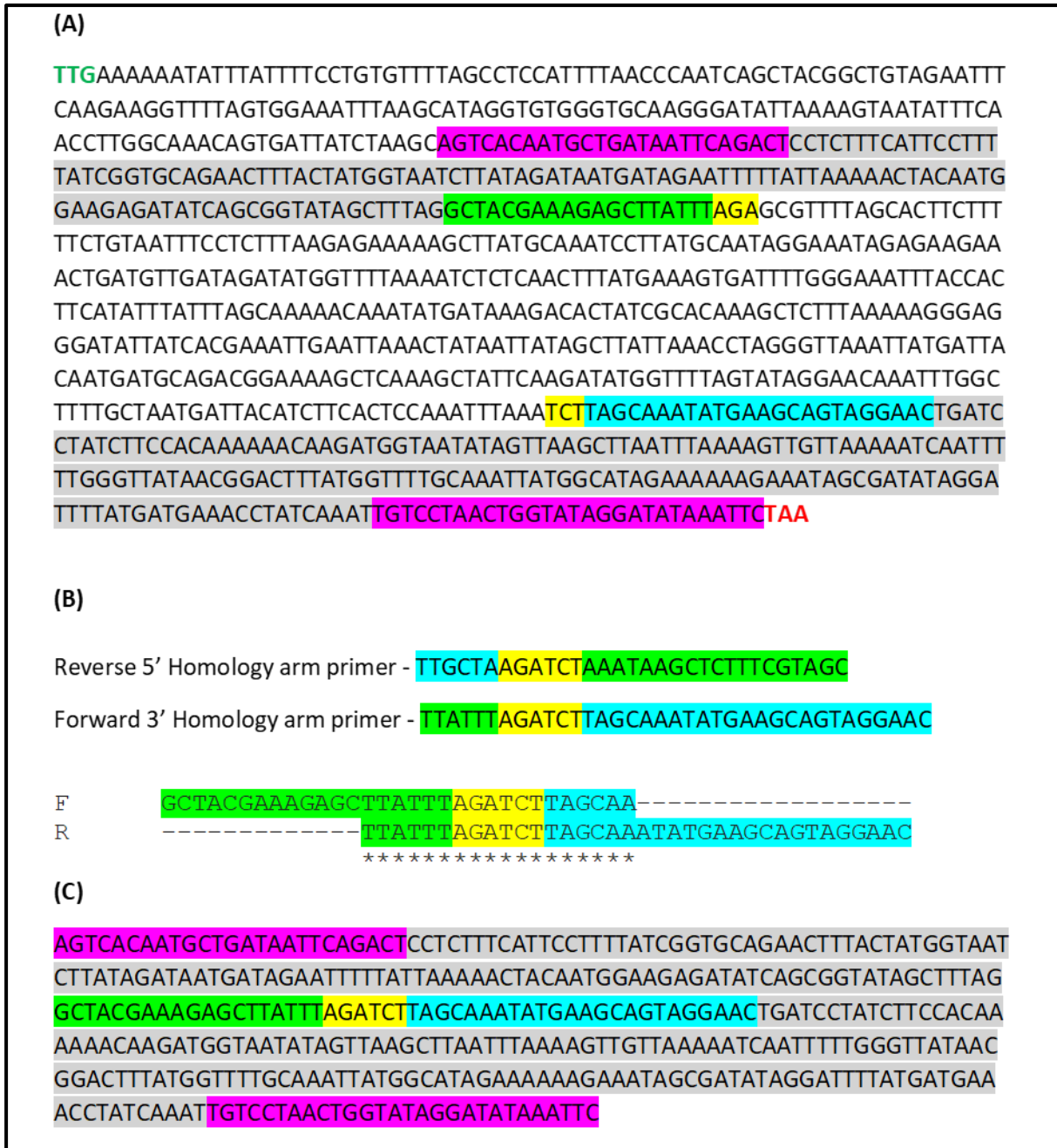


**Figure 2.1.** SOE PCR primer design. **(A)** Regions highlighted in grey represent the 5' and 3' homology arms within the *Cj0561c* coding sequence. The regions highlighted in purple represent the target sequence of the SOE PCR external primers; 5' homology arm forward primer and 3' homology arm reverse primer. The regions highlighted in green or blue represent the target sequence of the SOE PCR internal primers, 5' homology arm reverse primer and 3' homology arm forward respectively. The regions highlighted in yellow represent the BglIII restriction site. The start codon is in green text and the stop codon is in red text. **(B)** The region of overlap between the internal SOE PCR primers. **(C)** The SOE PCR product.

The homology arms were amplified using Phusion High-Fidelity DNA Polymerase Master Mix with HF buffer (Thermo Fisher Scientific). 50 µl reactions were set up using 25 µl of 2X Phusion Master Mix, 0.5 µl of each forward and reverse primer (100 pmol/µl), 1 µl of gDNA and 23 µl of DEPC-treated water. The homology arm PCR used the following thermal cycles:

Initial denaturation – 30 seconds

35 cycles:

Denature	- 98°C for 10 seconds
Anneal	- 51°C* for 30 seconds
Extension	- 72°C for 30 seconds per kb

Final extension step - 72°C for 5 minutes

\* Annealing temperature is primer dependent.

Homology arm PCRs were PCR purified using the QIAquick PCR Purification Kit (Qiagen) and used as the template for the SOE PCR. The SOE PCR was setup using Phusion High-Fidelity DNA Polymerase Master Mix with HF buffer as described above using the homology arm PCR products as the template. Equal concentrations of each homology arm were used for the SOE PCR. Of note, splicing efficiency can be improved by running a 10 cycle PCR without primers prior to the 35 cycle SOE PCR with primers. The SOE PCR was analysed on a 1% (w/v) agarose gel and the SOE PCR product purified using the Monarch DNA Gel Extraction Kit (New England Biolabs, Ipswich, USA) and eluted in 20 µl of DEPC-treated water. The SOE PCR was A-Tailed to enable cloning into the pGEM-T vector by TA cloning. 20 µl of SOE PCR product was added 20 µl of 2X MyTaq Red master mix and incubated at 70°C for 20 minutes then chilled on ice for two minutes. The reaction was purified using the QIAquick PCR Purification Kit and eluted in 20 µl of DEPC-treated water. The SOE PCR product was ligated into the pGEM-T vector in a 3:1 molar ratio of insert to vector using the following ligation reaction and calculation:

Reaction set up:

2X Rapid Ligation Buffer	5 µl
pGEM-T vector (50 ng)	1 µl
SOE PCR product (20 ng)	X µl
T4 DNA Ligase (3 Weiss units/µl)	1 µl
DEPC treated water	to a final reaction volume 10 µl

Incubated at room temperature for 1 hour.

$$\frac{\text{ng of vector} \times \text{kb size of insert}}{\text{kb size of vector}} \times \text{insert:vector molar ratio} = \text{ng of insert}$$

### **2.6.3.3 Transformation of *E. coli***

Blue/white screening agar plates were prepared by adding IPTG (final concentration of 0.16 pmol/ml), X-Gal (0.004% w/v final concentration) and ampicillin (final concentration 100 µg/ml) to LB agar. The PCR/pGEM-T ligation mixture was briefly centrifuged then 2 µl was added to a 1.5 ml microcentrifuge tube and chilled on ice. 2 µl of β-mercaptoethanol (1.22 M) was added to a 100 µl aliquot of XL2-Blue Ultracompetent Cells (Agilent Technologies), or SCS110 Competent Cells (Dam methylase deficient for Bcl1 restriction digests), cells were mixed gently by tapping the tube, then incubated on ice for 10 minutes with occasional mixing. 50 µl of competent cells were transferred to a tube containing the PCR ligation reaction, gently mixed then incubated on ice for 30 minutes. Cells were heat shocked at 42°C for 30 seconds then put back on ice for two minutes. Cells were then recovered by adding 900 µl of pre-warmed SOC broth and incubating at 37°C shaking at 200 rpm for 45 minutes. 100 µl, 200 µl and 400 µl of recovered cells were plated onto separate blue/white screening agar plates and incubated overnight at 37°C. White colonies were selected for screening by colony PCR (see Section 2.6.3.4).

### **2.6.3.4 Vector screening by colony PCR**

Selected colonies were re-streaked onto LB agar plates supplemented with appropriate antibiotics and incubated overnight at 37°C. A single colony from the overnight plate was suspended in 50 µl of DEPC-treated water, vortexed, heated at 95°C for 10 minutes then centrifuged at 13,000 rpm for 10 minutes. PCRs were set up using the MyTaq Red PCR Master Mix as previously described (see Section 2.6.2) with gene specific (SOE PCR external) forward and reverse primers and 1 µl of colony supernatant. PCR positive transformants were verified by sequencing using gene specific primers via cycle sequencing using the Eurofins Mix2Seq sequencing service.

### **2.6.3.5 Insertion of the kanamycin or erythromycin resistance cassette into mutation vector**

The pGEM-T vector containing the cloned PCR product, the pJMK30 vector (van Vliet *et al.*, 1998) containing the kanamycin resistance cassette or the pDH20 vector containing the erythromycin resistance cassette were harvested from overnight *E. coli* cultures using the QIAprep Spin Miniprep Kit (Qiagen). Plasmid preparations were eluted in 30 µl of DEPC-treated water and concentrations analysed using a NanoDrop ND-1000 spectrophotometer. The kanamycin resistance cassette was isolated from the pJMK30 vector and the erythromycin resistance cassette was isolated from pDH20 vector using the following restriction digest:

Reaction set up:

Plasmid mini prep	1 µg
10X NEBuffer 3.1	5 µl
BamHI	1 µl
DEPC treated water	to 50 µl

Incubated at 37° for 15 minutes.

The resistance cassette restriction digest reactions were run on a 1% (w/v) TAE agarose gel supplemented with GelRed (1X final concentration) alongside DNA HyperLadder 1kb (Bioline) at 120 V and 500 mA for one hour. The resistance cassette bands were cut from the gel and purified using the Monarch DNA Gel Extraction Kit. The vectors containing the cloned PCR products were linearised using either BglII or BclI to create sticky ends complementary to the BamHI digested resistance cassettes using the following restriction digest reaction:

Reaction set up:

Plasmid mini prep	1 µg
10X NEBuffer 3.1	5 µl
BglII or BclI (10 units/µl)	1 µl
DEPC treated water	to 50 µl

Incubated at 37°C for 15 minutes, purified using the QIAquick PCR purification kit.

The BamHI digested resistance cassettes were ligated into the BglII or BclI digested vectors in a 3:1 insert to vector molar ratio using the following ligation reaction and equation detailed in Section 2.6.3.2:

Reaction set up:

BglII or BclI digested vector	50 ng
BamHI digested resistance cassette	X ng
10X T4 DNA Ligase buffer	2 µl
T4 DNA Ligase	1 µl
DEPC treated water	to 20 µl

Incubated at room temperature for 10 minutes.

Heat inactivated at 65°C for 10 minutes.

The ligation reaction was transformed into XL2-Blue Ultracompetent Cells as previously described (see Section 2.6.3.3) and plated onto LB ampicillin/kanamycin plates then incubated overnight at 37°C. Colonies were screened as previously described (see Section 2.6.3.4) using gene specific primers

(external primers for SOE PCR products) to check for integration of the resistance cassette. Correct orientation of the cassette was screened for using the gene specific forward primer (external forward primer for SOE PCR products) and the resistance cassette specific forward-out primer (Table 2.2) which is a reverse primer located 0.38 kb from the start of the kanamycin resistance cassette or 0.33 kb from the start of the erythromycin resistance cassette. PCR positive clones were verified by DNA sequencing as previously described (see Section 2.6.3.4) using the resistance cassette specific forward-out and reverse-out primers which will sequence the plasmid in the 3' to 5' direction from the start of the resistance cassette and in the 5' to 3' direction from the end of the resistance cassette respectively.

#### **2.6.3.6 Transformation of *C. jejuni* by electroporation**

*C. jejuni* glycerol stocks were plated onto BA plates and grown for 24 hours. EBF buffer (Electroporation Buffer) was prepared by mixing sucrose (final concentration 10% w/v) and glycerol (final concentration 15% v/v) in Milli-Q water then filter sterilising using a 0.22 µm membrane. *C. jejuni* cells were harvested from 24 hour plates and suspended into 10 ml of ice cold EBF buffer. The suspension was centrifuged at 3,000 x g at 4°C for 10 minutes and the supernatant was discarded. Cells were resuspended in 1 ml of ice cold EBF buffer then centrifuged at 17,000 x g for two minutes and the supernatant was discarded. This was repeated once before resuspending cells in 250 µl of EBF buffer. The cell suspension was separated into 50 µl aliquots and either used immediately for transformation or stored at -80°C until use.

Transformations were performed by mixing 2.5 µg of mutation vector with 50 µl of electrocompetent *C. jejuni* cells in EBF buffer. Cells were incubated on ice for 10 minutes then transferred to a pre-chilled 2 mm gap electroporation cuvette (Bio-Rad Laboratories, California USA). Electroporations were performed using a GenePulser Xcell (Bio-Rad Laboratories) using 2.5 kV, 25 µFD and 200 Ω settings. Immediately following electroporation, cells were mixed with 100 µl of pre-warmed SOC broth and plated onto BA plates. Plates were then incubated at 37°C under microaerobic conditions for 24 hours. Cells were then harvested and suspended in 500 µl Brucella broth. 100-400 µl of cell suspension was then spread onto BA plates supplemented with kanamycin or erythromycin. Plates were incubated for up to seven days under microaerobic conditions.

#### **2.6.3.7 Screening and verification of *C. jejuni* mutants**

Kanamycin-resistant or erythromycin-resistant *C. jejuni* colonies were restreaked onto BA plates supplemented with kanamycin or erythromycin and grown for 24 hours at 37°C under microaerobic conditions. Single colonies were suspended in 50 µl of DEPC treated water, vortexed, heated at 95°C for 10 minutes then centrifuged at 17,000 x g for 10 minutes. PCRs were set up using the MyTaq Red PCR Master Mix as previously described (see Section 2.6.2) and resistant colonies screened for

insertion and correct orientation of the resistance cassette as previously described (see Section 2.6.3.5). PCR products were run on a 1% (w/v) TAE agarose gel supplemented with GelRed X1 final concentration alongside the DNA HyperLadder 1kb (Bioline) at 120 V and 500 mA for one hour. Bands which had the correct expected size were cut from the gel and purified using the Monarch DNA Gel Extraction Kit. Purified PCR products were confirmed by DNA sequencing as previously described (see Section 2.6.3.5).

#### **2.6.4 Natural transformation**

*C. jejuni* is naturally competent meaning mutated gene copies can be transferred between strains by natural transformation. The gene sequences of both *m1aA* and *Cj0561* between the 11168H and 488 wild-type strains are highly similar making these genes suitable for mutation via natural transformation. gDNA was extracted as previously described (see Section 2.6.1) from a *C. jejuni* strain containing the desired gene knockout. Glycerol stocks of wild-type strains were plated onto BA plates and grown for two days. Wild-type strains were then restreaked onto MH agar plates (Oxoid) and grown for 15 hours. 1 µl loopful of *C. jejuni* cells from the overnight plate culture were smeared into 1 cm diameter circles on a MH agar plate. 5 µl of gDNA ranging from 40-200 ng/µl was spotted onto separate *C. jejuni* smears. *C. jejuni* cells were incubated with the gDNA on MH agar for five hours at 37°C under microaerobic conditions. *C. jejuni* smears were pooled into 200 µl of sterile PBS and diluted 10-fold to 10<sup>-3</sup>. Each dilution was spread onto a separate BA plate supplemented with kanamycin and grown for up to seven days. Kanamycin-resistant colonies were screened for positive transformants as previously described (see Section 2.6.3.4) using gene specific primers and the Tkan forward-out primer (see Table 2.2).

#### **2.6.5 Complementation**

The 11168 *m1aA* complement strain was kindly provided by Professor David Kelly and Dr Aidan Taylor at the University of Sheffield. Briefly, complementation of the 11168 *m1aA* mutant was performed using the pRRA system to generate a complementation vector as previously described (Taylor *et al.*, 2017). The 11168 *m1aA* mutant was transformed with the complementation vector by electroporation and clones selected for apramycin resistance. Correct insertion of the complement gene copy into the genome was confirmed by PCR and DNA sequencing as described in Section 2.6.3.4. In the 11168 *m1aA* complement strain, the inserted *m1aA* gene is under the control of the native promoter.

The 488 *m1aA* and the 488 *Cj0561c* mutants were complemented using the pCJC1 complementation vector as previously described (Gundogdu *et al.*, 2011; Jervis *et al.*, 2015). Briefly, the complete wild-type gene was amplified by PCR to contain the native ribosome binding site, start codon, and stop

codon with primers pCJC1mlaA(F/R) or pCJC1Cj0561c(F/R) (Table 2.2) which contained added restriction sites to introduce a NcoI restriction site at the 5' end and a NheI restriction site at the 3' end. The wild-type gene was amplified using Phusion High-Fidelity DNA Polymerase Master Mix with HF buffer as described in Section 2.6.3.1. PCR products were screened by gel electrophoresis and purified using the QIAquick PCR Purification Kit. The amplified gene was digested with NheI and NcoI using the following double digest reaction:

Reaction set up:

PCR product	1 µg
10X NEBuffer 2.1	5 µl
NheI	1 µl
NcoI	1 µl
DEPC treated water	to 50 µl

Incubated at 37° for 15 minutes, purified using the QIAquick PCR purification kit.

The digested gene amplicon was then ligated into the pCJC1 complementation vector using T4 DNA ligase as described in Section 2.6.3.5. The ligated plasmid was electroporated into the 488 *mlaA* or *Cj0561c* mutants as described in Section 2.6.3.6 to insert the wild-type gene copy into the 488 ortholog of the *C. jejuni* 11168 pseudogene *Cj0223*. Putative clones were selected for on BA plates supplemented with chloramphenicol then verified by PCR and sequencing as described in Section 2.6.3.4 using chloramphenicol cassette specific primers (see Table 2.2). The complemented genes are under the control of a constitutive chloramphenicol promoter.

## 2.6.6 Whole genome sequencing

Whole genome sequencing (WGS) of the 488 wild-type strain was performed by Dr Ozan Gundogdu at the London School of Hygiene and Tropical Medicine as previously described (Ugarte-Ruiz *et al.*, 2015). Briefly, WGS libraries were constructed using the Nextera XT DNA Library Preparation Kit. gDNA sequencing was performed on an Illumina MiSeq System using a MiSeq Reagent kit V3 (600-cycle) with 301 cycle paired end sequencing. Read quality was assessed in FastQC (Andrews, 2010) and reads quality controlled using Trimmomatic (v0.32) ('Leading' and 'trailing' setting of 3 with a 'slidingwindow' setting of 4 : 20, reads less than 36 nucleotides were discarded) (Bolger *et al.*, 2014). Read mapping was performed using BWA-MEM (v0.7.7-r441) (Li and Durbin, 2009) against the WGS of *C. jejuni* NCTC 11168 (AL111168). Genome assembly was performed using VelvetOptimiser (v2.2.5) with n50 optimisation (Zerbino and Birney, 2008; Gladman and Seemann, 2012). Contigs were ordered against *C. jejuni* NCTC 11168 WGS using ABACAS (v1.3.1) (Assefa *et al.*, 2009). Genome annotation was

performed with Prokka (Seemann, 2014). WGS were viewed using Artemis (Carver *et al.*, 2012). WGS comparisons were made between the 488 wild-type and 11168 wild-type WGS using ACT (Artemis Comparison Tool) (Carver *et al.*, 2005), to assist with identification of *mia* and *Cj0561c* orthologs.

## **2.6.7 RNA isolation**

*C. jejuni* Brucella broth cultures were set up as previously described in Section 2.2.1 and grown for eight hours. 10 ml of RNAprotect Bacteria Reagent (Qiagen) was added to a 50 ml falcon tube. 5 ml of the eight hour *C. jejuni* cultures was mixed with the RNAprotect Bacterial Reagent and vortexed. The mixture was incubated at room temperature for five minutes, then centrifuged at 3,000 x g at 4°C for 20 minutes. The supernatant was discarded and pellet stored at -80°C for up to a week. RNA was extracted from *C. jejuni* pellets using the PureLink RNA Mini Kit (Invitrogen) according to manufacturer's protocol. Briefly, *C. jejuni* pellets were thawed on ice for 10 minutes. 0.6 µl of β-mercaptoethanol (14.3 M) was added to 600 µl of Lysis buffer then added to the thawed *C. jejuni* pellet. The pellet was mixed thoroughly by pipetting then vortexed vigorously until the pellet was completely dispersed. 600 µl was transferred to a pre-chilled 1.5 ml microcentrifuge tube. 600 µl of 70% (v/v) ethanol was added and the sample was vortexed thoroughly until any visible precipitate was dispersed. The mixture was added to a PureLink RNA Mini Kit spin column and centrifuged at 13,000 rpm for 15 seconds and flow through discarded. This step was repeated until the total sample volume had been processed. 700 µl of Wash Buffer I was added to the spin column then centrifuged at 17,000 x g for 15 seconds, flow through was discarded and spin column was placed into a new collection tube. 500 µl of Wash Buffer II (prepared with 99% (v/v) ethanol) was added to the spin column then centrifuged at 17,000 x g for 15 seconds and flow through was discarded, this step was repeated once. The spin column was added to a new collection tube and centrifuged at 17,000 x g for two minutes to remove any residual wash buffer. The spin column was added to new collection tube and 40 µl of RNase-free water added directly to the spin column membrane. The spin column was incubated at room temperature for one minute then centrifuged at 17,000 x g for 30 seconds. The eluted RNA was reapplied to the spin column membrane and previous step was repeated. Eluted RNA was added to a pre-chilled 1.5 ml microcentrifuge tube, the concentration was quantified using a NanoDrop ND-1000 spectrophotometer and RNA was stored at -80°C.

## **2.6.8 qRT-PCR**

### **2.6.8.1 cDNA synthesis**

RNA was isolated as described in Section 2.6.7. DNA contamination was removed using the TURBO DNA-free kit (Invitrogen) as follows:

10X TURBO DNase buffer	5 $\mu$ l
Turbo DNase (2 U/ $\mu$ l)	1 $\mu$ l
RNA	2,000 ng
RNase-free water	to 50 $\mu$ l

The mixture was gently vortexed and incubated at 37°C for 45 minutes. 5  $\mu$ l of DNase inactivation reagent was added, the mixture was vortexed then incubated at room temperature for five minutes with occasional mixing. The mixture was centrifuged at 9,600 x g for 90 seconds to pellet inactivation reagent and 40  $\mu$ l of supernatant was transferred to a 1.5 ml microcentrifuge tube.

cDNA was synthesised using the SuperScript III First-Strand Synthesis System for RT-PCR (Invitrogen) using the following reaction:

Random hexamers (50 ng/ $\mu$ l)	2 $\mu$ l
dNTP mix (10 mM)	2 $\mu$ l
RNA	200 ng
RNase-free water	to 20 $\mu$ l

The primer reaction was incubated at 65°C for five minutes, placed immediately onto ice then separated into 10  $\mu$ l aliquots. 10  $\mu$ l of the following cDNA synthesis mix was added to one aliquot, and 10  $\mu$ l omitting the SuperScript III RT added to the second aliquot.

10X RT Buffer	2 $\mu$ l
MgCl <sub>2</sub> (25 mM)	4 $\mu$ l
DTT (0.1 M)	2 $\mu$ l
RNaseOUT (40 U/ $\mu$ l)	1 $\mu$ l
SuperScript III RT (200 U/ $\mu$ l)	1 $\mu$ l

SuperScript III RT was replaced with 1  $\mu$ l RNase-free water for the no SuperScript negative control samples. Samples were vortex then briefly centrifuged. The cDNA synthesis reaction was incubated at 25°C for 10 minutes, 50°C for 50 minutes then reaction was terminated at 85°C for five minutes. Samples were incubated on ice for one minute then briefly centrifuged. 0.5  $\mu$ l of RNase H (5 U/ $\mu$ l) was added and samples were incubated at 37°C for 20 minutes. cDNA was stored at -20°C until use.

#### **2.6.8.2 qRT-PCR**

To investigate the expression of selected genes, total RNA from both the 11168H and 488 wild-type strains grown in Brucella broth to mid-log phase either in the presence or absence of 0.2% (w/v) ST, 0.05% (w/v) SDC, 0.7 mM LSB or 0.2% (w/v) taurine was extracted using Invitrogen PureLink RNA kit

as described in Section 2.6.7. cDNA was synthesised as described in Section 2.6.8.1. qRT-PCRs were performed in triplicate using SYBR green master mix (Thermo Fisher Scientific) in the following reaction:

SYBR Green Master Mix (2X)	10 $\mu$ l
Forward primer (100 pmol/ $\mu$ l)	0.4 $\mu$ l
Reverse primer (100 pmol/ $\mu$ l)	0.4 $\mu$ l
cDNA template	0.8 $\mu$ l
DEPC treated water	8.4 $\mu$ l

qRT-PCR primers are listed in Table 2.2. qRT-PCRs were performed using an ABI7500 machine (Applied Biosystems) using the following cycling conditions:

Initial holding stage	- 50°C for 20 seconds
Initial denaturation	- 95°C for 10 minutes
40 cycles of –	
Denaturation	- 95°C for 15 seconds
Annealing and extension	- 60°C for 1 minute
Melt curve:	
95°C for 15 seconds	
60°C for 1 minute	
95°C for 30 seconds	
60°C for 15 seconds	

Relative gene expression comparisons were performed using the  $\Delta\Delta$ CT (cycle threshold) method (Schmittgen and Livak, 2008) and previously published *C. jejuni rpoA* primers (Ritz *et al.*, 2009) for internal controls to normalise the mean CT of each gene to the constitutively expressed housekeeping gene *rpoA*.

## 2.6.9 RNA-Seq

### 2.6.9.1 Experimental design

The strains chosen for RNA-Seq analysis were the 11168H and 488 wild-type strains. 11168H was chosen due to being a well-characterised laboratory strain with a well-annotated genome. The 488 wild-type strain was chosen as a recent clinical isolate. RNA was extracted from mid-log phase cultures to characterise the response of otherwise minimally stressed cells to biologically relevant concentrations of bile salts. The bile salt concentrations selected were 0.2% (w/v) ST and 0.05% (w/v) SDC. The experimental conditions were screened prior to RNA-Seq analysis by qRT-PCR to analyse the

expression of *cmeB*, a gene with a previously well-characterised link to regulation by bile salts (Lin *et al.*, 2003; Lin *et al.*, 2005a; Malik-Kale *et al.*, 2008; Clark *et al.*, 2014). The number of replicates chosen were based on recommendations by a recent study (Schurch *et al.*, 2016) analysing replicate number for RNA-Seq based studies, which suggested a minimum of six biological replicates per condition should be used. Seven biological replicates were selected for this study.

### **2.6.9.2 Preparation of rRNA depleted RNA**

RNA was extracted from mid-log phase cultures as described in Section 2.6.7. DNA contamination was removed using the TURBO DNA-free kit (Invitrogen) as described in Section 2.6.8.1 using 7 µg of RNA for each sample. The RIN (RNA integrity number) (Schroeder *et al.*, 2006) of DNase treated RNA was analysed on an Agilent Technologies 2100 Bioanalyzer system (Agilent) using a RNA 6000 nano chip (Agilent) to ensure only high quality RNA was used for RNA-Seq library preparations.

Agilent chip priming station base plate was set to position C and the lever clip set to the top position. All reagents were warmed to room temperature for 30 minutes before use. The RNA 6000 ladder was denatured at 70°C for two minutes then cooled immediately on ice. The denatured ladder was separated into 1.2 µl aliquots and stored at -80°C until use. The RNA gel matrix was prepared by adding 550 µl of RNA gel matrix to an Agilent spin column provided. The RNA gel matrix was centrifuged at 1,500 g for 10 minutes at room temperature. The filtered gel was separated into 65 µl aliquots and stored at 4°C until use. The gel-dye mix was prepared fresh for each assay. 1 µl of dye was mixed with 65 µl of filtered gel matrix. The mix was vortexed then centrifuged at 13,000 g for 10 minutes at room temperature. An RNA 6000 chip was placed in the Agilent chip priming station and 9 µl of gel-dye mix loaded to the indicated well. The chip priming station plunger was set to 1 ml and the priming station closed. The plunger was pressed down until held in place by the clip and left for 30 seconds. The clip was released, then after five seconds the plunger pulled back to the 1 ml position. 9 µl of gel dye mix was loaded to two further indicated wells. 5 µl of RNA marker was added to each sample and ladder well. 1 µl of sample was pipetted into each sample well and 1 µl of ladder into the ladder well. The chip was then run on an Agilent Technologies 2100 Bioanalyzer system.

Ribosomal RNA (rRNA) was depleted using the RiboMinus Transcriptome Isolation Kit for bacteria (Invitrogen). To prepare RiboMinus Magnetic Beads, the beads were thoroughly vortexed to re-suspend. For each sample, 250 µl of bead suspension was added to a 1.5 ml RNase-free microcentrifuge tube. The tube was placed on a DynaMag-2 Magnet (Invitrogen) stand for one minute. The supernatant was discarded and beads were resuspended in 250 µl of RNase-free water. The tube was placed on a magnetic stand for one minute then the supernatant discarded. This step was repeated once. RiboMinus beads were resuspended in 250 µl of Hybridisation Buffer then placed on a

magnetic stand for one minutes. The supernatant was discarded and beads were resuspended in 100  $\mu$ l of Hybridisation Buffer. Beads were kept at room temperature prior to use.

For each sample 4-5  $\mu$ g of DNAase Treated RNA (Final volume 18  $\mu$ l) was added to a 1.5 ml microcentrifuge tube. To each tube 4  $\mu$ l of RiboMinus Probe (100 pmol/ $\mu$ l) and 100  $\mu$ l of Hybridisation buffer was added then incubated at 37°C for five minutes to denature RNA. Denatured RNA was placed on ice for at least 30 seconds. Samples were collected by brief centrifugation then transferred to a tube containing 100  $\mu$ l of pre-prepared RiboMinus Magnetic beads and vortexed. RNA was incubated with the RiboMinus Magnetic beads for 15 minutes at 37°C with occasional mixing. Contents of tubes was collected by brief centrifugation then placed on a magnetic stand for one minute. The supernatant containing the rRNA depleted RNA was transferred to a 1.5 ml microcentrifuge tube.

rRNA depleted RNA samples were concentrated using the RiboMinus Concentration Module (Invitrogen). To each sample 250  $\mu$ l of Binding buffer (L3) and 125  $\mu$ l of 96-100% (v/v) ethanol was added. The samples were mixed well then loaded to a RiboMinus Concentration Module spin column. Samples were passed through by centrifugation at 14,000 x g for 1 minute and flow through discarded. 200  $\mu$ l of Wash Buffer (W5) prepared with ethanol was added to each column then passed through by centrifugation at 14,000 x g for 1 minute and flow through discarded. The wash step was repeated once. The spin column was transferred to a fresh collection tube then centrifuged at 14,000 x g to remove any residual wash buffer. Spin column was transferred to a fresh collection tube and 12  $\mu$ l of RNase-free water added directly to the spin column membrane. Spin columns were incubated at room temperature for 1 minute then centrifuged at 14,000 x g for one minute to elute RNA. Depletion of rRNA was analysed using a RNA 6000 chip as described previously and concentration measured on a NanoDrop ND-1000 spectrophotometer. RNA was stored at -80°C prior to library preparation.

### **2.6.9.3 Generation of mRNA library**

#### **2.6.9.3.1 First strand cDNA synthesis**

Messenger RNA (mRNA) libraries were prepared using the Illumina TrueSeq Stranded mRNA Library Prep Kit (Illumina, California, USA) according to the manufacturer's low throughput sample preparation protocol replacing the polyA enrichment step with the rRNA depletion as described in Section 2.6.9.2. The protocol was entered at the mRNA fragmentation step as recommended by manufacturer and as detailed in previous publications (Kreuder *et al.*, 2017; Crofts *et al.*, 2018) using the TrueSeq Stranded mRNA Library Prep Kit for preparation of bacterial mRNA libraries.

DNase-treated and rRNA-depleted mRNA was diluted to 200 ng in 5  $\mu$ l of RNase-free water. Each sample was added to a separate well of a 96-well PCR plate. 13  $\mu$ l of Fragment, Prime, Finish Mix

(FPF) was added to each sample well and mixed by pipetting. The FPF mix contained random hexamers for reverse transcription priming and is used as the first strand cDNA reaction buffer. The sample plate was sealed with a Microseal B (Bio-Rad) and incubated at 94°C for eight minutes then cooled to 4°C. The sample plate was briefly centrifuged, the seal was removed and 17 µl transferred to a fresh 96-well PCR plate. Superscript II (Invitrogen) was mixed 1 µl to 9 µl with First Strand Act D Mix and 8 µl of mix added to each sample well. Reaction wells were mixed by pipetting then sealed with a Microseal B. The first strand cDNA was then synthesised with the following program:

Pre-heated lid set to 100°C

25°C for 10 minutes

42°C for 15 minutes

70°C for 15 minutes

Hold at 4°C

#### **2.6.9.3.2 Second strand cDNA synthesis**

The second strand cDNA was synthesised as follows. The 96-well plate containing first strand cDNA was briefly centrifuged and the adhesive seal was removed. 5 µl of resuspension buffer was added to each well. 20 µl of Second Strand Marking Master Mix was added to each well and mixed by pipetting. The 96-well plate was sealed with a Microseal B then incubated at 16°C for one hour. The sample plate was then left to stand at room temperature for five minutes prior to the following wash step.

AMPure XP beads (Beckman Coulter) were warmed to room temperature and thoroughly vortexed. 90 µl of AMPure beads were added to each well containing double stranded cDNA and mixed by pipetting. cDNA was incubated at room temperature with beads for 15 minutes. The ds (double stranded) cDNA plate was then placed on a Magnetic Stand-96 (Invitrogen) for five minutes before discarding supernatant. The cDNA plate was left on the magnetic stand for the following wash steps. 200 µl of freshly prepared 80% (v/v) ethanol was added to each well taking care not to disturb the bead pellet. The bead pellet was incubated at room temperature with 80% (v/v) ethanol for 30 seconds, then ethanol was discarded. The ethanol wash was repeated once. Bead pellets were allowed to dry at room temperature for 15 minutes, then 17.5 µl of Resuspension Buffer was added to each well. The cDNA plate was then removed from the magnetic stand and the pellet resuspended in Resuspension Buffer. The cDNA plate was incubated at room temperature for two minutes, placed back on the magnetic stand for five minutes then 15 µl of supernatant was transferred to a fresh PCR plate. cDNA was stored at -20°C for up to seven days before the 3' A-tailing step.

### 2.6.9.3.3 A-tailing of ds cDNA and index adapter ligation

The cDNA plate was briefly centrifuged and the adhesive seal was removed. 2.5 µl of Resuspension Buffer and 12.5 µl of A-Tailing Mix was added to each sample well then mixed by pipetting. The plate was sealed with a Microseal B and A-Tailed using the following program:

Pre-heated lid set to 100°C

37°C for 30 minutes

70°C for 5 minutes

Hold at 4°C

Adapters were ligated to A-Tailed ds-cDNA fragments as follows using the TruSeq RNA CD Index plate (96 indexes, 96 samples) (Illumina). The index plate was thawed at room temperature for 10 minutes then briefly centrifuged. Each adapter well contained a unique dual index combination of a D5 and D7 indexes. 2.5 µl of Resuspension Buffer and 2.5 µl of Ligation Mix was added to each sample well containing A-tailed ds cDNA. 2.5 µl of Adapter from the TruSeq RNA CD Index plate was added to each sample well and mixed by pipetting. Each well of the index adapter plate was used once so as each sample had a unique adapter combination. Libraries with a higher plexity than 12 are of high enough plexity to not have a colour misbalance and thus adapters may be selected in rows corresponding to location of samples in the A-tailed ds cDNA plate. Libraries with a plexity lower than 12 should use adapter combinations detailed in the Illumina Index Adapter Pooling guide. The sample plate with added Index Adapters was sealed with a Microseal B, briefly centrifuged then incubated at 30°C for 10 minutes. The adhesive seal was removed and 5 µl of Stop Ligation Buffer was added to each well. The Stop Ligation Buffer was mixed by pipetting.

AMPure XP beads were warmed to room temperature and thoroughly vortexed. 42 µl of AMPure XP beads were added to each sample well and mixed by pipetting. The adapter ligation reaction was incubated with AMPure XP beads at room temperature for 15 minutes then placed on a magnetic stand for five minutes. The supernatant was discarded and bead pellet was washed twice with 200 µl of 80% (v/v) ethanol then air dried as described in Section 2.6.9.3.2. The washed bead pellet was resuspended in 52.5 µl of Resuspension Buffer, incubated at room temperature for two minutes then placed back on the magnetic stand for five minutes until liquid was clear. 50 µl of supernatant was transferred to a fresh PCR plate. AMPure XP bead wash was then repeated as described above using 50 µl of AMPure XP beads and washed bead pellet was resuspended in 22.5 µl of Resuspension Buffer. The sample plate was then incubated at room temperature for two minutes and placed on a magnetic stand for five minutes. 20 µl was transferred to a fresh 96-well PCR plate, sealed with a Microseal B and stored at -20°C for up to seven days before enrichment of DNA fragments.

#### **2.6.9.3.4 Enrichment of DNA fragments**

DNA fragments with adapters ligated to both ends were then selectively enriched by PCR using an adapter specific PCR primer cocktail. The 96-well sample plate was thawed on ice then briefly centrifuged. 5 µl of PCR Primer Cocktail and 25 µl of PCR Master Mix was added to each sample well then mixed by pipetting. The sample plate was sealed with a Microseal B adhesive seal and cDNA fragments were enriched using the following program:

Pre-heated lid set to 100°C

98°C for 30 seconds

15 cycles of:

98°C for 10 seconds

60°C for 30 seconds

72°C for 30 seconds

72°C for 5 minutes

Hold at 4°C

The PCR enrichment reaction was purified using 50 µl of AMPure XP beads as described in Section 2.6.9.3.2, with 32.5 µl of Resuspension buffer used to resuspend the air-dried bead pellet. The bead pellet was resuspended and was incubated at room temperature for two minutes, placed on a magnetic stand for five minutes until liquid was clear then 30 µl of supernatant was transferred to a fresh 96-well PCR plate. 5 µl of purified enrichment reaction was transferred to a second 96-well PCR plate to be used for library validation and quantification leaving 25 µl to be used for library normalisation and pooling. Both plates were stored at -20°C for up to seven days.

#### **2.6.9.3.5 Library validation and quantification**

To achieve high quality data, libraries need to be standardised to achieve optimum cluster densities across the flow cell. This was performed by quantifying fragment sizes and sample concentrations. The library fragment size distribution of each sample preparation was analysed on an Agilent DNA 1000 chip using an Agilent Technologies 2100 Bioanalyzer system. Agilent chip priming station base plate was set to position C and the lever clip set to the lowest position. All reagents were warmed to room temperature for 30 minutes before use. 25 µl of DNA dye concentrate was added to one vial of DNA gel matrix then loaded onto an Agilent spin column. This gel-dye mix was centrifuged at 2,240 g for 15 minutes at room temperature. A DNA 1000 chip was placed in the Agilent chip priming station and 9 µl of gel-dye mix loaded to the indicated well. The chip priming station plunger was set to 1 ml and the priming station closed. The plunger was pressed down until held in place by the clip and left for 60 seconds. The clip was released, then after five seconds the plunger pulled back to the 1 ml

position. 9 µl of gel dye mix was loaded to two further indicated wells. 5 µl of DNA marker was added to each sample and ladder well. 1 µl of sample was pipetted into each sample well and 1µl of ladder into the ladder well. The chip was then run on an Agilent Technologies 2100 Bioanalyzer system. The average band size for each preparation should be around 260 bp. Additional smaller or larger bands indicate contamination. If the baseline of the Bioanalyzer graph was not flat this indicated bead contamination causing interference with the electric charge passed through the chip. If bead contamination was present, the sample plate was equilibrated to room temperature and placed on a magnetic stand for five minutes prior to pipetting for library pooling.

Library preparations were quantified on a Qubit 2.0 Fluorometer (Thermo Fisher Scientific) using the dsDNA high-sensitivity (HS) assay kit (Thermo Fisher Scientific). All reagents were warmed to room temperature for 30 minutes before use. Working solution was prepared by mixing the Qubit reagent 1 in 2000 with Qubit buffer. Two DNA standard tubes were set up containing 190 µl of working solution. One assay tube per sample containing 198 µl of working solution was set up. 10 µl of each of the DNA standard was added to a DNA standard tube, vortexed then incubated at room temperature for two minutes. Standard tubes were placed into the Qubit 2.0 Fluorometer and readings taken to calibrate the assay. 2 µl of each library preparation was added to an assay tube containing 198 µl of working solution, vortexed and incubated at room temperature for two minutes. Readings were taken and ng/µl recorded.

#### **2.6.9.4 mRNA library normalisation and pooling**

The concentration of each sample library was normalised to 10 nM in a fresh 96-well PCR plate using Tris-HCl 10 mM, pH 8.5 with 0.1% (v/v) Tween 20. Library nM concentrations were calculated from the Qubit concentration readings and Bioanalyzer average band size for each library using the following equation:

$$\frac{\text{concentration (ng/}\mu\text{l)}}{660 \text{ g/mol} \times \text{average library fragment size (bp)}} \times 10^6 = \text{concentration in nM}$$

\*660 g/mol is the average molecular mass of one base pair.

\*The value is multiplied by  $10^6$  to convert units from M/ml to nM/µl

The volume required to dilute 10 µl of library preparation sample to 10 nM was calculated using the following calculation:

$$\frac{V_s}{D_c \text{ nM} / S_c \text{ nM}} - V_s = T_v$$

$V_s$  = Volume of sample (10 µl)

$D_c$  = Desired concentration (10 nM)

$S_c$  = Sample concentration (nM)

$T_v$  = Volume of Tris-HCl required

10 µl of each sample was pooled into a 1.5 ml microcentrifuge tube. 30 µl of pool library sample was treated using the Illumina Free Adapter Blocking Reagent. 30 µl of Free Adapter Blocking reagent was mixed with 30 µl of pooled library sample then incubated on the following program:

Pre-heated lid set to 100°C

38°C for 20 minutes

60°C for 20 minutes

Hold at 4°C

AMPure XP beads were warmed to room temperature and 60 µl of beads were used to purify the Free Adapter Blocking reaction as described in Section 2.6.9.3.2 using 22.5 µl of Resuspension Buffer to resuspend ethanol-washed, air-dried bead pellet. 20 µl of supernatant was transferred to a 0.6 ml microcentrifuge tube. The concentration and average band size were reanalysed as described in Section 2.6.9.3.5 using the Qubit dsDNA high-sensitivity (HS) assay kit and Agilent DNA 1000 chip assay kit. The pooled library sample was re-diluted in Tris-HCl 10 mM, pH 8.5 with 0.1% (v/v) Tween 20 to 10 nM using the calculations detailed above. Pooled library sample was stored at -20°C for up to seven days prior to DNA sequencing.

#### **2.6.9.5 Sequencing of mRNA library**

mRNA libraries were sequenced using a MiSeq Reagent kit V3 (150-cycle) on a MiSeq System (Illumina) according to manufacturer's protocol. The MiSeq System was cleaned using a maintenance wash prior to sequencing run with three wash cycles using 0.5% (v/v) Tween 20. The reagent cartridge was thawed in a water bath at room temperature for 90 minutes until all wells were fully thawed. Cartridge reagents wells were then mixed by inversion and cartridge gently tapped to remove bubbles. The cartridge was stored at 4°C for up to six hours.

The pooled library preparation was thawed on ice then diluted to 4 nM in Tris-HCl 10 mM, pH 8.5 with 0.1% (v/v) Tween 20. A fresh dilution of 0.2 N NaOH was prepared by mixing 800 µl of DEPC treated water with 200 µl of 1.0 N NaOH. 5 µl of 4 nM pooled library preparation was mixed with 5 µl of 0.2 N

NaOH and incubated at room temperature for five minutes to denature the library then 990  $\mu$ l of HT1 hybridisation buffer was added to the denatured library. The resultant library concentration was 20 pM. The library was then further diluted to 12 pM in HT1 hybridisation buffer and stored on ice. The PhiX control was diluted 4 nM in Tris-HCl 10 mM, pH 8.5 with 0.1% (v/v) Tween 20 then 5  $\mu$ l denatured and diluted to 20 pM as described for the mRNA library. A 1% spike-in of the PhiX control was added to the mRNA library.

600  $\mu$ l of 12 pM mRNA library with 1% PhiX spike in was loaded into the 'Load Samples' reservoir of the sequencing reagent cartridge. The flow cell was cleaned using Milli-Q water to remove storage buffer salts, then dried with lint-free cleaning tissue. The flow cell was wiped with ethanol to remove streaks or tissue fibres. The flow cell was loaded into the flow cell clamp in the MiSeq system. The 500 ml PR2 incorporation buffer bottle and empty waste bottle were loaded into the reagent compartment. The reagent cartridge with library samples was loaded into the reagent cartridge chiller.

The sample information sheet, created in 'Illumina Experiment Manager', was loaded to the MiSeq System and sequencing run started. The sample information sheet contained sample metadata and MiSeq run parameters. The parameters selected were:

- Workflow – Generate FASTQ
- Index adapters - Truseq RNA CD Index plate
- Indexing scheme – Dual-index
- Read type – Paired end (read 1 and read 2)
- Number of cycles – 76 each for read 1 and read 2.

The libraries were demultiplexed and FASTQ files were downloaded from the MiSeq System and analysed as follows in Section 2.6.9.6. A post-run wash was performed as described for the pre-run wash in Section 2.6.9.2.

## **2.6.9.6 Data analysis**

### **2.6.9.6.1 Read mapping and counting**

RNA sequencing data analysis was performed by Dr Umer Ijaz at the University of Glasgow. The paired-end reads were trimmed and filtered using Sickle v1.200 (Joshi and Fass, 2011) by using a sliding window approach and trimming the reads where the average base quality drops below Q20. Only the reads that were above 10 bp length were kept after trimming. The 11168H genome sequence (FASTA format) and annotation (GFF format) were downloaded. Bowtie2 (Langmead and Salzberg, 2012) was used to map the reads against the reference sequence. This generated the mapping in SAM format which were later converted to BAM format using Samtools (Li *et al.*, 2009) and were index sorted. gffread from cufflinks suite (Trapnell *et al.*, 2010) was used to convert annotations from GFF to GTF

format. These were then used in Bedtools (with multicov- bams option) (Quinlan and Hall, 2010) with the mapped reads to generate transcript counts per samples. A script written by Dr Umer Ijaz [<http://userweb.eng.gla.ac.uk/umer.ijaz/bioinformatics/GENERATEtable.sh>] was then used to collate all these transcripts into a n=21 samples x p=1,667 transcripts abundance tables. Statistical analysis on these abundance tables were performed in R.

Ordination of abundance tables in reduced space (beta diversity) was performed using Principal Coordinate Analysis (PCoA) plots of transcripts Bray-Curtis distance in Vegan's cmdscale() function (Oksanen *et al.*, 2007). Analysis of variance for explanatory variables (or sources of variation) was performed using Vegan's adonis() against distance matrix (Bray-Curtis). This function referred to as PERMANOVA, fits linear models to distance matrices and uses a permutation test with pseudo-F ratios to give an R squared value, which if significant, tells you the % variability in transcriptome structure to find transcripts that are significantly different between multiple categories considered in this study.

#### **2.6.9.6.2 DESeq**

The DESeqDataSetFromMatrix() function from DESeq2 (Love *et al.*, 2014) package was used with the adjusted p-value significance cut-off of 0.05 and log-fold change cut-off of 1. This function uses negative binomial GLM (generalised linear model) to obtain maximum likelihood estimates for the transcripts log-fold change between the two conditions. Then Bayesian shrinkage was applied to obtain shrunken log-fold changes subsequently employing the Wald test for obtaining significances. The abundances for significant transcriptomes were then visualised using RPKM (Reads per kilo million) representations.

#### **2.6.9.6.3 sPLS-DA – sparse Partial Least Squares Discriminant Analysis**

Abundance tables generated in Section 2.6.9.6.1 and metadata tables containing treatment group information were normalised prior to analysis by TSS (Total Sum Scaling) and CLR (Centred Log Ratio) transformation to project TSS data (which resides in a simplex space) to the Euclidian space. sPLS-DA analysis was performed separately both with and without a prefiltering step which removed the bottom 1% of low abundance read counts. PLS-DA analysis was performed in R following the steps detailed in (Kim-Anh Le Cao *et al.*, 2016). Briefly the 'perf' function was run with no variable selection to generate a plot of the overall classification error rate and the balanced error rate (BER). The optimal number of components to include was determined using the 'tune.splsda' function with either M-fold or 'leave one out' (LOO) cross validation repeated 14 times prior to running sPLS-DA analysis. sPLS-DA multilevel analysis was then performed. The most discriminative features that characterise each group identified by the sPLS-DA analysis were displayed in contribution plots which display the abundance

of each discriminative feature, and for which group the features were most abundant. Heatmaps using Euclidian distance with Ward linkage were also generated.

#### **2.6.10 Primers used in this study**

All primers used in this study were ordered from Integrated DNA Technologies (ITD). Primers designed during this study were designed using the ITD OligoAnalyzer tool to determine primer characteristics (Table 2.2). Primer dimer  $\Delta G$  values stronger than -9 kcal/mole were avoided when possible. Only primers with a hairpin melting temperatures lower than the primer melting temperature were used. Specificity was assessed by either Primer-Blast, presence of non-specific bands on agarose gel electrophoresis, or presence of multiple peaks on qPCR melt-curve graphs. qRT-PCR primer names begin with 'qRT'. All other primers were used for mutant or complement strain construction (Table 2.2).

**Table 2.2.** Primers used in this study.

Name	Sequence	GC Content	T <sub>m</sub>	Hairpin ΔG	Hairpin T <sub>m</sub>	Self-Dimer ΔG	Source
GSmlaA(F)	TAG GAG TTT TTG CTG AG	41.2	45.8	0.17	22.7	-3.14	This study
GSmlaA(R)	GCT AAG TTC ATT GCG TC	47.1	48.3	0.52	16.1	-3.61	This study
ISAmIaA(F1)	GAG CTC GGT ACC CGG GGA TCC TCT AGA GTC TGG CAC TAC AAT AAA TAA GG	52	68.3	-1.8	38.1	-15.89	This study
ISAmIaA(R1)	AAG CTG TCA AAC ATG AGA ACC AAG GAG AAT GTT TTG GTA TTC TTG TTC AA	36	65.2	-2.66	36.3	-8.66	This study
ISAmIaA(F2)	GAA TTG TTT TAG TAC CTA GCC AAG GTG TGC ATT TAT ATC CAT TCT TGC GT	38	65	-3.14	41.8	-7.05	This study
ISAmIaA(R2)	AGA ATA CTC AAG CTT GCA TGC CTG CAG GTC GCC AGT TGT TAT TAT CAT TG	44	67.6	-2.13	41.4	-16.38	This study
pCJC1mlaA(F)	CCC CCA TGG TTT TAG GAG TTT TTG CTG AGA ATA AAA TTT ATA TC	34.1	61.3	0	25	-11.52	This study
pCJC1mlaA(R)	CCC GCT AGC TTA TTT GCT AAG TTC ATT G	42.9	58	-1.61	43	-10.44	This study
pRRAmIaA(F)	ACA CTC TAG ATT TAG GAG TTT TTG CTT G	35.7	55.4	-0.87	35.9	-7.31	This study
pRRAmIaA(R)	ACA CCA ATT GGA TTA AAA ATA TTT TTT TCA TTA A	17.6	53.2	-2.9	39.9	-19.46	This study
Ex-H1Cj0561F	AGT CAC AAT GCT GAT AAT TCA GAC T	36	54.4	-2.48	48.3	-5.36	This study
Int-H1Cj0561R	TTG CTA AGA TCT AAA TAA GCT CTT TCG TAG C	35.5	56.7	-1.01	31.8	-7.82	This study
Int-H2Cj0561F	TTA TTT AGA TCT TAG CAA ATA TGA AGC AGT AGG AAC	30.6	56.9	-0.53	32.3	-7.82	This study
Ex-H2Cj0561R	GAA TTT ATA TCC TAT ACC AGT TAG GAC A	32.1	52.1	-1.45	49.4	-7.2	This study
pCJC1Cj0561c(F)	CCC CCA TGG TTT CAA GGA GAA CAT TTG AAA AAA TAT TTA	33.3	60.6	-1.8	36	-11.69	This study
pCJC1Cj0561c(R)	CCC GCT AGC TTA GAA TTT ATA TCC TAT ACC AGT TAG	38.9	58.7	-0.33	30	-10.44	This study
GScmeB(F)	GTA TTC AAG TGA TGG CTC A	42.1	49.5	0.02	24.7	-3.53	This study
GScmeB(R)	GAA TAT ATG CTA CTC CTG C	42.1	47.1	0.25	21.3	-6.35	This study
TKanR-R-out	TGG GTT TCA AGC ATT AGT CC	45	52.7	0.79	11.8	-3.14	Adapted from (Gundogdu <i>et al.</i> , 2016)
TkanR-F-out	GTG GTA TGA CAT TGC CTT C	47.4	51	0.2	22.4	-3.43	Adapted from (Gundogdu <i>et al.</i> , 2016)
CamR-F-out	CGA TTG ATG ATC GTT GTA	38.9	46.7	-2.09	44.5	-6.66	(Gundogdu <i>et al.</i> , 2016)
CamR-R-out	TAC AGC AGA CTA TAC TG	41.2	44	-0.67	32.5	-3.55	(Gundogdu <i>et al.</i> , 2016)
EryR-F-out	CGA AAT TAC ACC TCT GTA CT	40	49.2	-0.6	33	-5.36	Personal communication with Dr Arnoud van Vliet
EryR-R-out	TGA TAG TAT AGC TGA TGA G	36.8	44.9	-0.1	26.6	-6.34	Personal communication with Dr Arnoud van Vliet

qRTmlaA(F)	GAT CCT ACT TGG GCA AGT ATA GC	47.8	62.2	-3	52.5	-7.8	This study
qRTmlaA(R)	ATG CTT ACG AGC AAA GAC GCA ATG	45.8	65.9	-3.1	58.1	-6.69	This study
qRTmlaC(F)	CCA CTT CTA TGG TAG TAG ATG GG	47.8	61.2	-1.12	33.2	-5.02	This study
qRTmlaC(R)	GTA GGG CAT CAA AGC CTT GGT T	50	65.1	-2.75	55.4	-6.21	This study
qRTcmeA(F)	GCA GCA AAG AAG AAG CAC C	52.6	61.6	-0.87	37.1	-3.14	This study
qRTcmeA(R)	GTC CGT AAG CCG AAT CAA C	52.6	60.5	-1.31	46.4	-3.61	This study
qRTcmeB(F)	TCC TTC TTT AAC CCC TCC TAC	47.6	60.6	1.71	-10.9	-4.85	This study
qRTcmeB(R)	TTG ATT GCA TCT TCG ATA GGA C	40.9	60.5	-0.91	32.4	-7.05	This study
qRTcmeC(F)	ACC ATC TTG CTT CAA CGT C	47.4	60.3	0.73	13.5	-6.3	This study
qRTcmeC(R)	TCT AAA TCC CCG CTT TCA AAT C	40.9	61	0.79	15.2	-3.89	This study
qRTCj0561c(F)	AGC CTC CAT TTT AAC CCA ATC	42.9	60.8	1.55	-5.4	-4.85	This study
qRTCj0561c(R)	GCA CCG ATA AAA GGA ATG AAA G	40.9	60.1	-0.92	38.3	-3.61	This study
qRTCj0561cKO(F)	AGA CAC TAT CGC ACA AAG CTC	47.6	62.3	-1.29	43.8	-6.34	This study
qRTCj0561cKO(R)	GGA TCA GTT CCT ACT GCT TCA TAT T	40	62.4	-2.55	40.7	-4.89	This study
qRTmetB(F)	GTT GCT ACT CCT TTC TTA CTC C	45.5	60.2	0.82	10.4	-3.14	This study
qRTmetB(R)	CTA AGC CAA GTG ATG ATG ACT C	45.5	60.5	-0.66	36.3	-3.14	This study
qRTCj0418(F)	AGA CAA ATC GCA GCA GCA G	52.6	63	-2.01	53.5	-3.61	This study
qRTCj0418(R)	GGC TTC TTC GGC TTT AAG TTT C	45.5	61.9	-0.88	37.6	-4.85	This study
qRTrhoA(F)	CGA GCT TGC TTT GAT GAG TG	50	61.3	-0.52	40.1	-6.34	(Ritz <i>et al.</i> , 2009)
qRTrhoA(R)	AGT TCC CAC AGG AAA ACC TA	45	60.9	-1.85	49	-6.59	(Ritz <i>et al.</i> , 2009)
qRTrrs(F)	AAG GGC CAT GAT GAC TTG AC	50	62.3	0.31	20.3	-9.28	(Ritz <i>et al.</i> , 2009)
qRTrrs(R)	AGC GCA ACC CAC GTA TTT AG	50	62.7	-0.51	31.7	-9.89	(Ritz <i>et al.</i> , 2009)
qRTgyrA(F)	GTT ATT ATA GGT CGT GCT TT	35	55.5	0.49	15.6	-3.61	This study
qRTgyrA(R)	CTA TGA GGT GGG ATG TTT GT	45	59.4	1.36	-11.3	-1.6	This study

GS = gene specific; ISA = isothermal assembly; pRRA = *C. jejuni* complementation vector; pCJC1 = *C. jejuni* complementation vector; Ex-H1 or Ex-H2 = SOE PCR External primers for homology arm 1 (H1) or homology arm 2 (H2); Int-H1 or Int-H2 = SOE PCR Internal primers for homology arm 1 (H1) or homology arm 2 (H2); Tkan = Truncated adaption of kanamycin cassette specific primers from Gundogdu *et al.*, Cam<sup>r</sup> = Chloramphenicol cassette specific primers; Ery<sup>r</sup> = erythromycin cassette specific primers; qRT = quantitative reverse transcription PCR.

## 2.7 Statistical analysis

At least three biological replicates were performed each in triplicate for each experiment. Statistical analyses were performed using Prism software (GraphPad Software, USA). Variables were compared using a student's *t*-test or a one sample *t*-test with \* indicating a  $p < 0.05$ , \*\* indicating a  $p < 0.01$ , \*\*\* indicating a  $p < 0.001$ , and \*\*\*\* indicating a  $p < 0.0001$ . RNA-Seq statistical analysis was performed in R as described in Section 2.6.9.6.

## **Chapter 3: Sodium taurocholate stimulates *Campylobacter jejuni* outer membrane vesicle production via down-regulation of the maintenance of lipid asymmetry pathway**

Contribution of others:

The *Campylobacter jejuni* 11168 *miaA* mutant and 11168H *miaA* complement strains were provided by Dr Aidan Taylor in collaboration with Professor David Kelly at the University of Sheffield.

Whole genome sequencing of *Campylobacter jejuni* strains was performed by Dr Ozan Gundogdu at the London School of Hygiene and Tropical Medicine.

3,3'-Dipropylthiadicarbocyanine Iodide (DiSC3) membrane permeability assay was performed by Dr Aidan Taylor in collaboration with Professor David Kelly at the University of Sheffield.

Nanoparticle tracking analysis was performed by myself and Dr Jody Winter at Nottingham Trent University.

Figure 2 from the Davies *et al.* (2019) publication was produced by Dr Aidan Taylor in collaboration with Professor David Kelly at the University of Sheffield.

### **3.1 Preface**

#### **3.1.1 Aims and objective**

*C. jejuni* OMVs contain numerous virulence-associated proteins including the cytolethal distending toxin (CDT) and three serine proteases (Lindmark *et al.*, 2009; Elmi *et al.*, 2012; Elmi *et al.*, 2016; Elmi *et al.*, 2018). As *C. jejuni* lacks the classical virulence-associated secretion systems of other enteric pathogens that deliver effectors directly into target cells (Parkhill *et al.*, 2000), OMVs may have a particularly important role in virulence. *C. jejuni* OMV production is stimulated by the presence of physiological concentrations of the bile salt ST through an unknown mechanism (Elmi *et al.*, 2018). The MLA pathway has been implicated in a novel mechanism for OMV biogenesis, open to regulation by host signals (Roier *et al.*, 2016).

The aim of the work presented in this chapter was to investigate the role of the MLA pathway in *C. jejuni* OMV biogenesis with ST as a potential regulator. Key datasets are included in the following publication by Davies *et al.* (2019) with additional optimisation data not included in the publication included in this preface. OMV production by the 11168 wild-type strain was quantified by analysing protein and lipid concentrations of OMV preparations and OMV particle counts were produced by NTA. OMV production was also investigated in the presence and absence of ST for a 11168 *miaA* knock-out mutant. The membrane stability of the wild-type and mutant strains was characterised to determine whether changes in OMV production could be due to changes in structural stability of the

OM. The expression of the genes encoding two MLA components in the presence of ST was analysed by qRT-PCR.

### 3.1.2 Assay optimisation data

#### 3.1.2.1 Growth kinetics

Growth kinetics were investigated in the presence and absence of a biologically relevant concentration of ST (0.2% w/v) for the 11168 (Figure 3.1) and 488 (Figure 3.2) wild-type, *mlaA* mutant and *mlaA* complement strains. Growth kinetics were characterised to determine the optimum timepoint for OMV isolation and to detect any obvious defects in growth. The *mlaA* mutant strains had similar rates of growth compared to the respective wild-type strains prior to stationary phase but declined more rapidly during the death phase. With the exception of a single timepoint for the 11168H *mlaA* complement (Figure 3.1G, Table 3.1); there were no significant differences in growth observed for any strain in the presence of 0.2% (w/v) ST prior to stationary phase. Neither the 11168 nor the 488 *mlaA* mutant strains showed any significant differences in growth at any timepoint in the presence of 0.2% (w/v) ST compared to in the absence of ST (Figure 3.1E,F, Figure 3.2E,F, Table 3.1-3.2). The growth of each wild-type strain in the presence of ST appeared similar to that of the respective *mlaA* mutant. The more rapid decline during the death phase exhibited by the *mlaA* mutant strains could be due to the metabolic cost associated with the inability or reduced ability to recycle PLs from the OM to the IM. Additionally, a differential effect in response to the addition of ST was observed between the wild-type and *mlaA* mutant strains. This could also be explained by only the wild-type strains experiencing additional metabolic strain caused by down-regulation of the MLA pathway in the presence of ST.

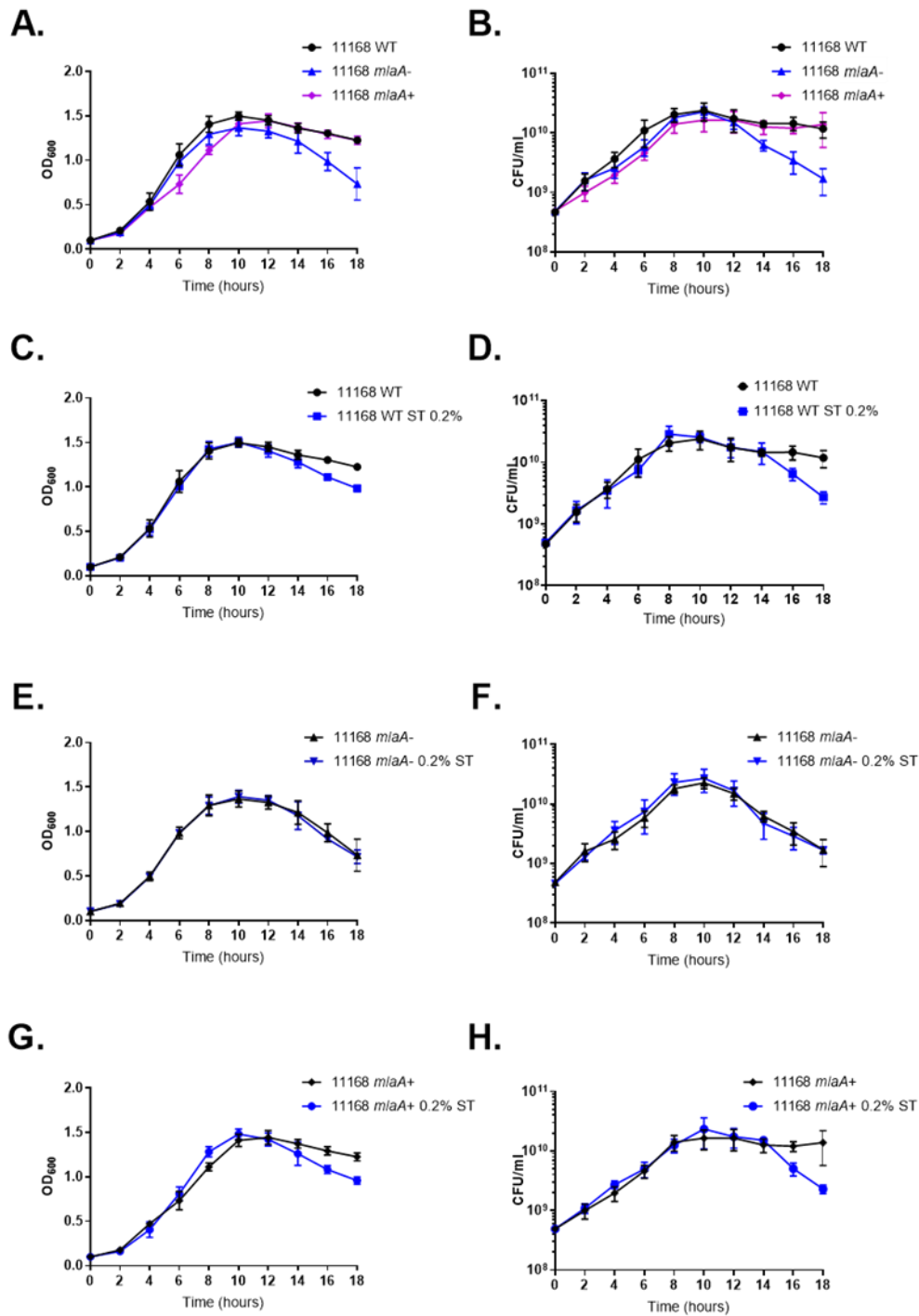


**Figure 3.1.** Growth kinetics of 11168 strains characterised by measuring OD<sub>600</sub> values (A, C, E & G) and colony forming units (CFUs/ml) (B, D, F & H) every two hours for 18 hours. Growth curves of *C. jejuni* 11168 wild-type (C & D), *miaA* mutant (E & F) and *miaA* complement (G & H) strains. Strains were grown in Brucella broth under microaerobic conditions at 37°C either in the presence or absence of 0.2% (w/v) ST.

**Table 3.1.** *P* – values of growth kinetics depicted in Figure 3.1 for 11168 strains grown either in the presence of absence of 0.2% (w/v) ST.

Timepoint (hours)	(A) WT/-	(A) WT/+	(A) -/+	(B) WT/-	(B) WT/+	(B) -/+	(C)	(D)	(E)	(F)	(G)	(H)
2	0.4053	0.1552	0.4703	0.9166	0.1071	0.1023	0.7363	0.8528	0.6507	0.4073	0.44	0.5931
4	0.5626	0.271	0.4926	0.1365	0.0448	0.3308	0.853	0.8416	0.836	0.2956	0.2087	0.1242
6	0.3419	0.0024	0.0149	0.1735	0.0562	0.306	0.4731	0.3099	0.995	0.5886	0.2763	0.6937
8	0.1516	0.0022	0.0543	0.5276	0.1485	0.2497	0.7609	0.2194	0.9501	0.4047	0.0083	0.6355
10	0.0389	0.0977	0.5051	0.8416	0.2635	0.225	0.8857	0.7822	0.6741	0.5831	0.1868	0.4365
12	0.0033	0.8423	0.013	0.5095	0.8005	0.6584	0.2385	0.994	0.5628	0.6304	0.6578	0.8221
14	0.1428	0.7655	0.1145	0.0035	0.4586	0.0328	0.1754	0.9174	0.763	0.3637	0.2368	0.3035
16	0.0019	0.7625	0.0027	0.0082	0.3763	0.0051	0.0005	0.0096	0.2976	0.6342	0.0051	0.0033
18	0.0061	0.9819	0.0006	0.0091	0.7118	0.0619	0.0001	0.0037	0.8461	0.9685	0.0001	0.0701

(A) WT/- = Figure 3.1A comparison of wild-type and *mlaA* mutant; (A) WT/+ = Figure 3.1A comparison of wild-type and *mlaA* complement; (A) -/+ = Figure 3.1A comparison of *mlaA* mutant and *mlaA* complement; (B) WT/- = Figure 3.1B comparison of wild-type and *mlaA* mutant; (B) WT/+ = Figure 3.1B comparison of wild-type and *mlaA* complement; (B) -/+ = Figure 3.1B comparison of *mlaA* mutant and *mlaA* complement; (C) = Figure 3.1C comparison of wild-type with and without ST; (D) Figure 3.1D comparison of wild-type with and without ST; (E) Figure 3.1E comparison of *mlaA* mutant with and without ST; (F) Figure 3.1F comparison of *mlaA* mutant with and without ST; (G) Figure 3.1G comparison of *mlaA* complement with and without ST; (H) Figure 3.1H comparison of *mlaA* mutant with and without ST. Light grey =  $p < 0.05$ ; dark grey with black text =  $p < 0.01$ ; dark grey white text =  $p < 0.001$ .

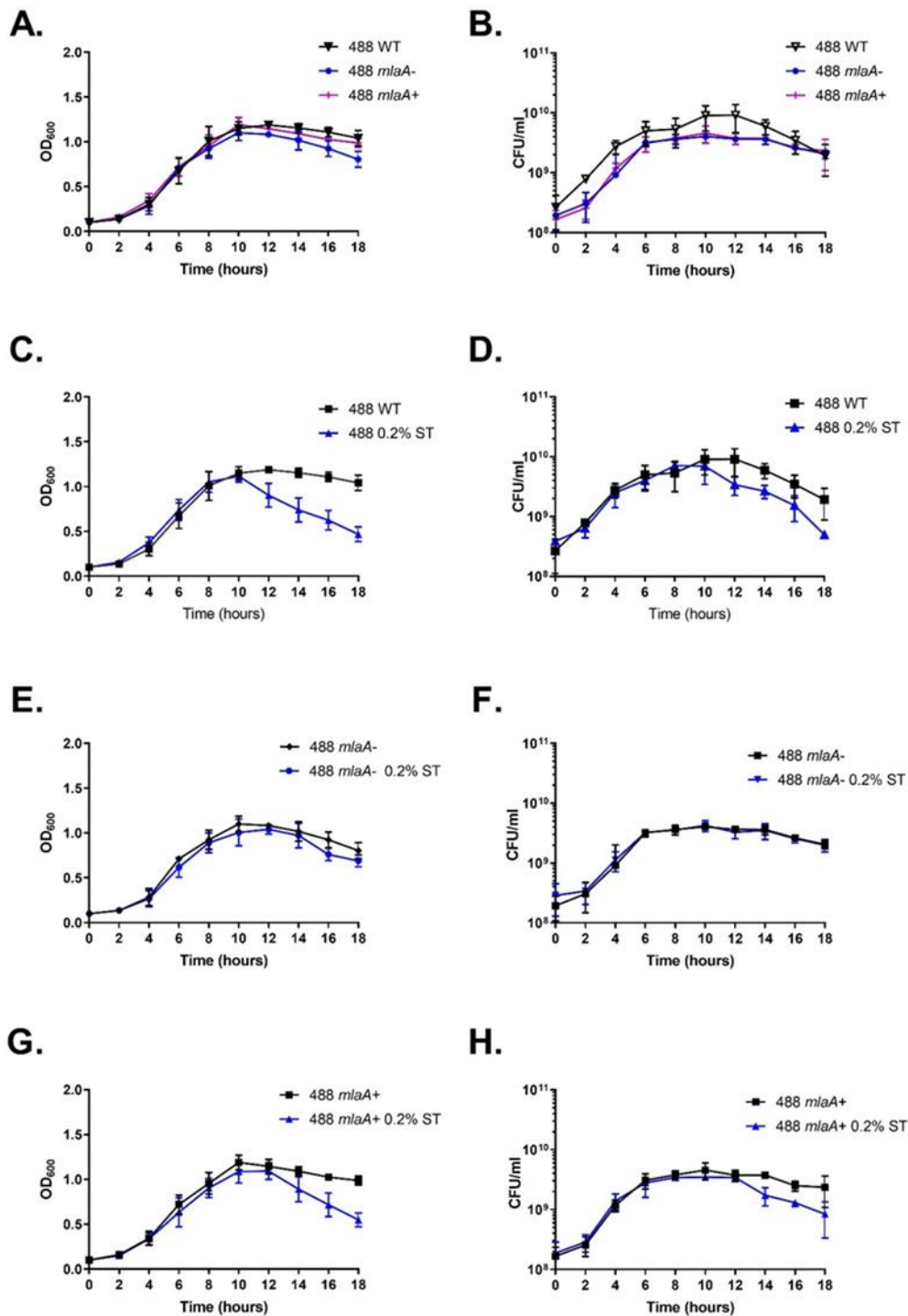


**Figure 3.2.** Growth kinetics of 488 strains characterised by measuring OD<sub>600</sub> values (A, C, E & G) and colony forming units (CFUs/ml) (B, D, F & H) every two hours for 18 hours. Growth curves of *C. jejuni* 488 wild-type (C & D), *mlaA* mutant (E & F) and *mlaA* complement (G & H) strains. Strains were grown in Brucella broth under microaerobic conditions at 37°C either in the presence or absence of 0.2% (w/v) ST.

**Table 3.2.** *P* – values of growth kinetics depicted in Figure 3.2 for 488 strains grown either in the presence of absence of 0.2% (w/v) ST.

Timepoint	(A) WT/-	(A) WT/+	(A) -/+	(B) WT/-	(B) WT/+	(B) -/+	(C)	(D)	(E)	(F)	(G)	(H)
2	0.9297	0.2099	0.3048	0.0003	0.0006	0.0429	0.2447	0.2458	0.8952	0.7965	0.5734	0.7115
4	0.7971	0.5151	0.3728	0.0043	0.0227	0.6622	0.2333	0.7745	0.7996	0.7683	0.8889	0.503
6	0.662	0.6488	0.9181	0.0545	0.1425	0.7049	0.4497	0.3758	0.2066	0.8882	0.4795	0.7333
8	0.4751	0.6701	0.7387	0.2232	0.1998	0.8328	0.6828	0.2176	0.7258	0.92	0.5978	0.4314
10	0.4491	0.529	0.2623	0.0111	0.1463	0.668	0.5705	0.5459	0.4009	0.7451	0.3054	0.2569
12	0.0004	0.3399	0.1801	0.1125	0.0554	0.5701	0.0052	0.088	0.1937	0.4252	0.4659	0.5516
14	0.0722	0.1573	0.3544	0.0775	0.0906	0.8193	0.0007	0.0342	0.6921	0.8838	0.0812	0.0068
16	0.0176	0.0788	0.1333	0.8848	0.314	0.7682	0.0001	0.0502	0.0642	0.7853	0.0174	0.0151
18	0.01	0.3179	0.0168	0.3232	0.6693	0.7271	0.0001	0.078	0.1111	0.868	0.0003	0.1267

(A) WT/- = Figure 3.2A comparison of wild-type and *mlaA* mutant; (A) WT/+ = Figure 3.2A comparison of wild-type and *mlaA* complement; (A) -/+ = Figure 3.2A comparison of *mlaA* mutant and *mlaA* complement; (B) WT/- = Figure 3.2B comparison of wild-type and *mlaA* mutant; (B) WT/+ = Figure 3.2B comparison of wild-type and *mlaA* complement; (B) -/+ = Figure 3.2B comparison of *mlaA* mutant and *mlaA* complement; (C) = Figure 3.2C comparison of wild-type with and without ST; (D) Figure 3.2D comparison of wild-type with and without ST; (E) Figure 3.2E comparison of *mlaA* mutant with and without ST; (F) Figure 3.2F comparison of *mlaA* mutant with and without ST; (G) Figure 3.2G comparison of *mlaA* complement with and without ST; (H) Figure 3.2H comparison of *mlaA* mutant with and without ST. Light grey =  $p < 0.05$ ; dark grey with black text =  $p < 0.01$ ; dark grey white text =  $p < 0.001$ .

### 3.1.2.2 Membrane sensitivity concentration optimisation

The membrane integrity of the *miaA* mutants was investigated to ensure any changes in OMV production were not an artifact of compromised OM integrity. To determine the optimum concentrations to use for membrane stress assays, late log-phase cultures of the 11168 wild-type, *miaA* mutant and *miaA* complement were spotted onto Brucella agar supplemented with ST (Figure 3.3) or LSB (Figure 3.4). Only a slight reduction in growth was observed for any strain when grown on Brucella agar supplemented with 2% (w/v) ST. This result was replicated in Brucella broth supplemented with 2% (w/v) ST (Figure 3 in Davies *et al.*, 2019). Due to concerns about the solubility of higher concentrations of ST in broth or agar and as 2% (w/v) ST is a far higher concentration than accepted as biologically relevant, further concentrations were not investigated. No growth was observed on Brucella agar plates supplemented with LSB at concentrations higher than 2 mM for the 11168 strains. Supplementation with 1 mM LSB caused around a 4-log reduction in growth (Figure 3.4). Therefore, 1.25 mM LSB was selected as a suitable stress concentration.

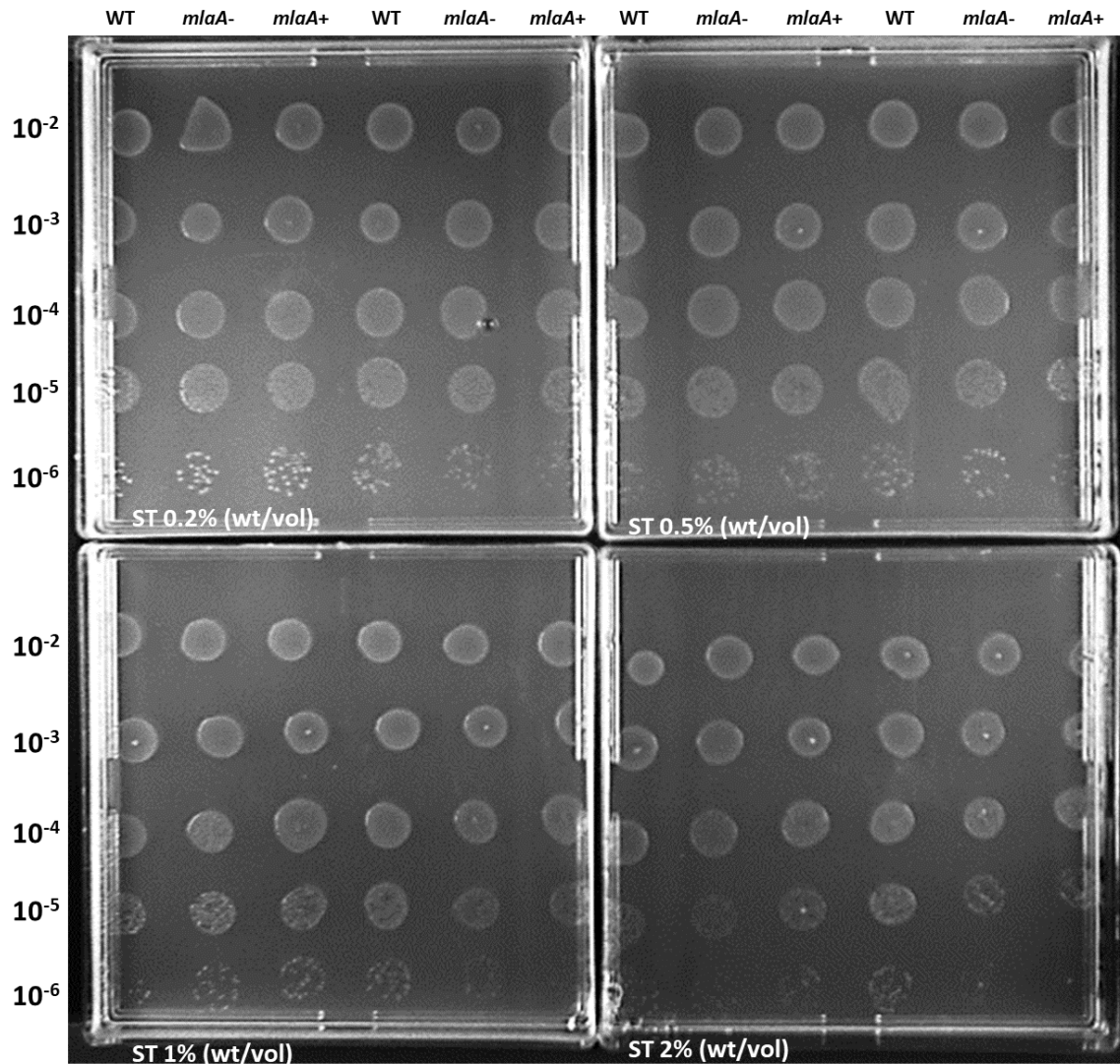


**Figure 3.3.** Optimisation of the ST membrane stress assay. Mid-log phase cultures of *C. jejuni* 11168 wild-type, *mlaA* mutant and *mlaA* complement strains were spotted onto Brucella agar supplemented with 0.2%, 0.5%, 1% or 2% (w/v) ST. Each culture was 10-fold serially diluted to 10<sup>-6</sup> and dilutions 10<sup>-2</sup> – 10<sup>-6</sup> spotted twice per plate onto duplicate assay plates. Assay plates were grown under microaerobic conditions at 37°C for four days.

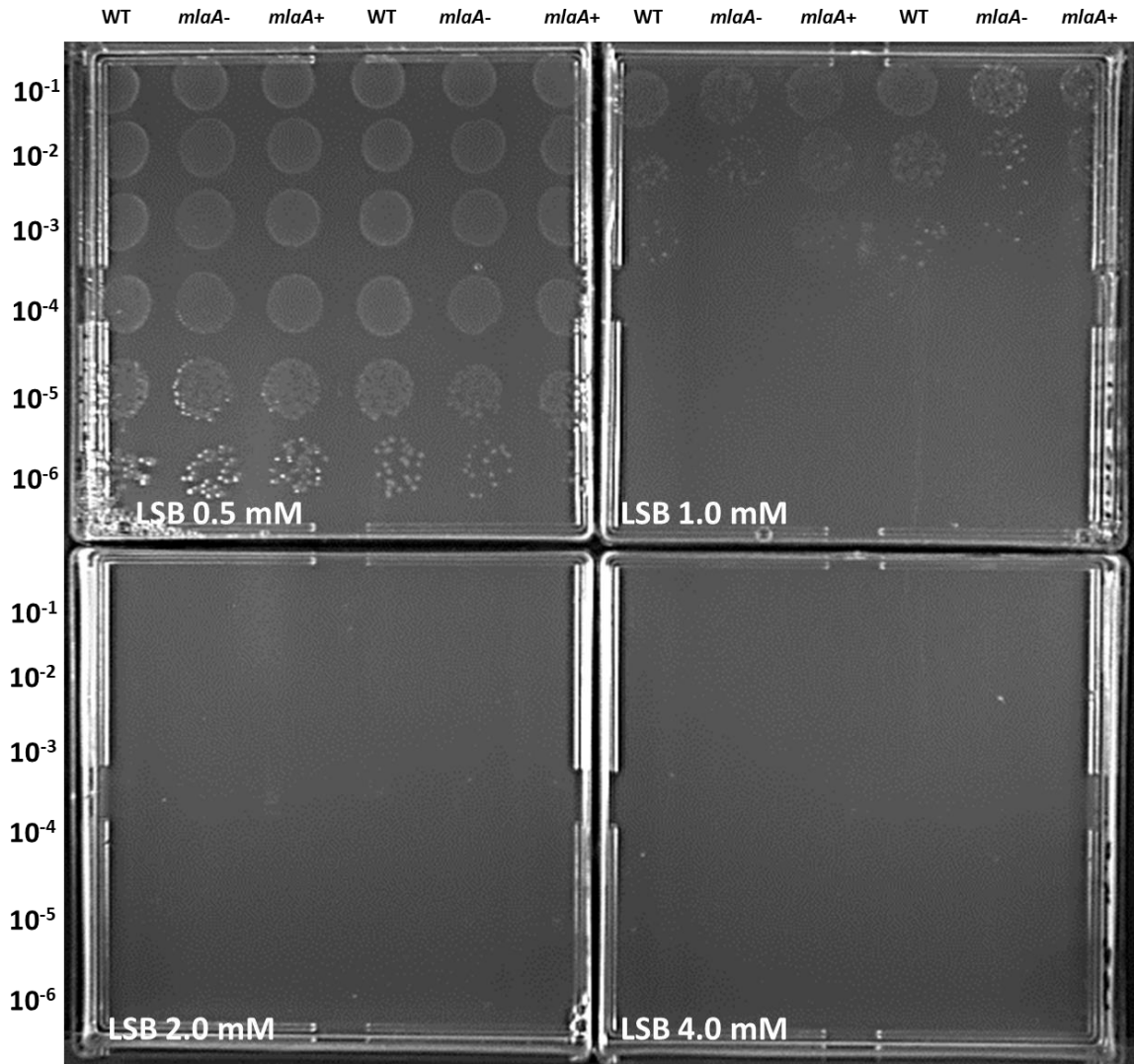


**Figure 3.4.** Optimisation of the lauryl LSB membrane stress assay. Mid-log phase cultures of *C. jejuni* 11168 wild-type, *mlaA* mutant and *mlaA* complement strains were spotted onto Brucella agar supplemented with 0.5 mM, 1.0 mM, 2.0 mM or 4.0 mM LSB. Each culture was 10-fold serially diluted to  $10^{-6}$  and dilutions  $10^{-1}$  –  $10^{-6}$  spotted twice per plate onto duplicate assay plates. Assay plates were grown under microaerobic conditions at 37°C for four days.

### 3.1.2.3 Outer membrane vesicle production - lauryl sulfobetaine

OMVs were isolated in the presence or absence of 0.5 mM LSB. LSB-OMVs were isolated from two biological replicates. As an increase in OMV production was observed for both the 11168 wild-type and the *miaA* mutant (see Figure 3.5BC), it was considered unlikely that the increased OMV production observed in response to LSB was via a regulated mechanism involving the MLA pathway but instead due to detergent-based disruption of the bacterial membrane. As such, further investigation of LSB-OMVs was not continued. Survival of cells in the presence of 0.5 mM LSB (see Figure 3.5A) was not reduced and as cells were isolated from late-log phase cultures, it is unlikely the increased OMV mass was a result of cell lysis debris. This supports the data in the attached publication linking increased OMV production in the presence of ST to changes in regulation of the MLA pathway. Increased OMV production in the presence of 0.2% (w/v) ST was observed for the 11168 wild-type strain, but not the *miaA* mutant (Figure 5 and 6 in Davies *et al.*, 2019).

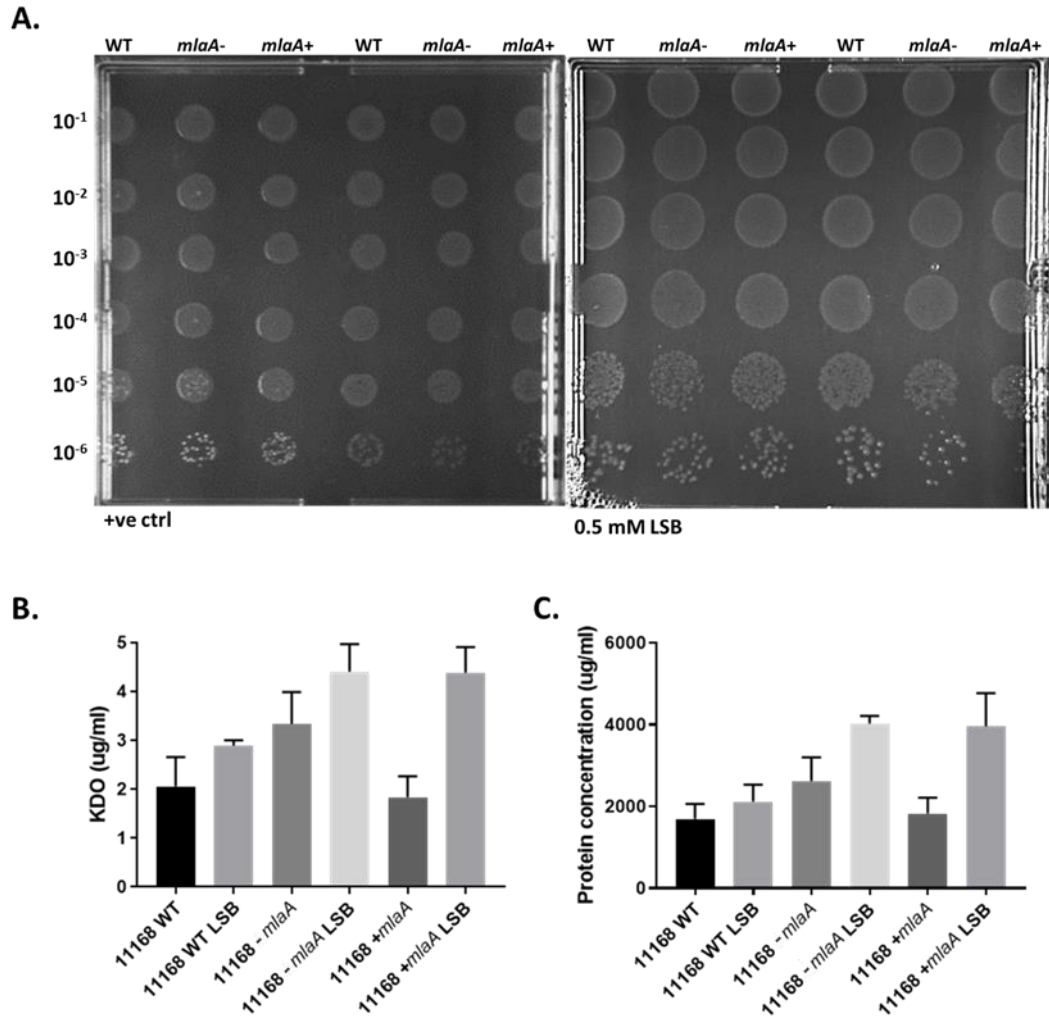


**Figure 3.5.** Sub-inhibitory concentrations of lauryl LSB increases OMV production. **(A)** Mid-log phase cultures of *C. jejuni* 11168 wild-type, *mlaA* mutant and *mlaA* complement strains were spotted onto Brucella agar either with or without 0.5 mM LSB. Each culture was 10-fold serially diluted to  $10^{-6}$  and dilutions  $10^{-1} - 10^{-6}$  spotted twice per plate onto duplicate assay plates. Assay plates were grown under microaerobic conditions at 37°C for four days. **(B & C)** OMVs were isolated from late-log phase *C. jejuni* cultures grown in Brucella broth either in the presence or absence of 0.5 mM LSB. OMV and LSB-OMV preparations from cultures of *C. jejuni* 11168 wild-type, *mlaA* mutant and *mlaA* complement strains of equivalent  $OD_{600}$  values were quantified by analysing total KDO **(B)** as a measurement of LOS and total protein **(C)**. Statistical analysis was not performed for OMV quantification data as results are representative of two biological replicates.

### **3.2 Publication: Sodium Taurocholate Stimulates *Campylobacter jejuni* Outer Membrane Vesicle Production via Down-Regulation of the Maintenance of Lipid Asymmetry Pathway**

Following section contains pre-print Microsoft Word format for the following reference. See Appendix 1 for published PDF format.

#### **Reference:**

DAVIES, C., TAYLOR, A. J., ELMI, A., WINTER, J., LIAW, J., GRABOWSKA, A. D., GUNDOGDU, O., WREN, B. W., KELLY, D. J. & DORRELL, N. 2019. Sodium Taurocholate Stimulates *Campylobacter jejuni* Outer Membrane Vesicle Production via Down-Regulation of the Maintenance of Lipid Asymmetry Pathway. *Frontiers in Cellular and Infection Microbiology*, 9. doi: 10.3389/fcimb.2019.00177

# Sodium taurocholate stimulates *Campylobacter jejuni* outer membrane vesicle production via down-regulation of the maintenance of lipid asymmetry pathway

Cadi Davies<sup>1</sup>, Aidan J Taylor<sup>2</sup>, Abdi Elmi<sup>1</sup>, Jody Winter<sup>3</sup>, Janie Liaw<sup>1</sup>, Anna Grabowska<sup>1</sup>, Ozan Gundogdu<sup>1</sup>, Brendan W Wren<sup>1</sup>, David J Kelly<sup>2\*</sup> & Nick Dorrell<sup>1\*</sup>

<sup>1</sup> Faculty of Infectious & Tropical Diseases, London School of Hygiene & Tropical Medicine, London, United Kingdom

<sup>2</sup> Department of Molecular Biology & Biotechnology, University of Sheffield, Sheffield, United Kingdom

<sup>3</sup> School of Science & Technology, Nottingham Trent University, Nottingham, United Kingdom.

## \* Correspondence:

<sup>1\*</sup> Mailing address: Faculty of Infectious & Tropical Diseases, London School of Hygiene & Tropical Medicine, Keppel Street, London, WC1E 7HT, United Kingdom

Tel: +44 (0)20 7927 2838

E-mail: [nick.dorrell@lshtm.ac.uk](mailto:nick.dorrell@lshtm.ac.uk)

<sup>2\*</sup> Mailing address: Department of Molecular Biology & Biotechnology, University of Sheffield, Western Bank, Sheffield, S10 2TN, United Kingdom.

Tel: +44 (0)114 222 4414

E-mail: [d.kelly@sheffield.ac.uk](mailto:d.kelly@sheffield.ac.uk)

**Keywords:** *Campylobacter*<sub>1</sub>, bile salts<sub>2</sub>, outer membrane vesicles<sub>3</sub>, maintenance of lipid asymmetry pathway<sub>4</sub>, MlaA<sub>5</sub>.

## Abstract

*Campylobacter jejuni* outer membrane vesicles (OMVs) contain numerous virulence-associated proteins including the cytolethal distending toxin and three serine proteases. As *C. jejuni* lacks the classical virulence-associated secretion systems of other enteric pathogens that deliver effectors directly into target cells, OMVs may have a particularly important role in virulence. *C. jejuni* OMV production is stimulated by the presence of physiological concentrations of the bile salt ST through an unknown mechanism. The maintenance of MLA pathway has been implicated in a novel mechanism for OMV biogenesis, open to regulation by host signals. In this study we investigated the role of the MLA pathway in *C. jejuni* OMV biogenesis with ST as a potential regulator. OMV production was quantified by analysing protein and lipid concentrations of OMV preparations and OMV particle counts produced by NTA. Mutation of *mlaA* which encodes the outer membrane component of the MLA pathway significantly increased OMV production compared to the wild-type strain. Detergent sensitivity and membrane permeability assays confirmed the increased OMV production was not due to changes in membrane stability. The presence of 0.2% (w/v) ST increased wild-type OMV production and reduced OMV size, but did not further stimulate *mlaA* mutant OMV production or significantly alter *mlaA* mutant OMV size. qRT-PCR analysis demonstrated that the presence of ST decreased expression of both *mlaA* and *mlaC* in *C. jejuni* wild-type strains 11168 and 488. Collectively the data in this study suggests *C. jejuni* can regulate OMV production in response to host gut signals through changes in expression of the MLA pathway. As the gut bile composition is dependent on both diet and the microbiota, this study highlights the potential importance of diet and lifestyle factors on the varying disease presentations associated with gut pathogen infection.

## Introduction

*Campylobacter jejuni* is a microaerophilic Gram-negative bacterium that is the leading cause of foodborne bacterial gastroenteritis worldwide (Silva *et al.*, 2011; Kaakoush *et al.*, 2015). Whilst *C. jejuni* has a number of potential virulence factors, including a cytolethal distending toxin (Lindmark *et al.*, 2009; Elmi *et al.*, 2012) and multiple proteases (Karlyshev *et al.*, 2014; Elmi *et al.*, 2016; Elmi *et al.*, 2018), *C. jejuni* lacks the classical virulence associated secretion systems of other enteric pathogens that deliver effectors directly to target cells (Parkhill *et al.*, 2000). A T6SS has been identified in a proportion of strains, however the function and variability of T6SSs among *C. jejuni* strains is still poorly understood (Bleumink-Pluym *et al.*, 2013; Ugarte-Ruiz *et al.*, 2015). An alternative machinery to deliver potential virulence determinants are OMVs, which can act as a general secretion pathway among Gram-negative bacteria and maybe are of particular importance for *C. jejuni* virulence and survival.

OMVs are small spherical membrane-bound structures ranging in size from 10-500 nm in diameter formed from the OM of Gram-negative bacteria and released into the extracellular environment (Kuehn and Kesty, 2005; Schwechheimer and Kuehn, 2015). OMVs provide a mechanism to deliver cargo in concentrated, selectively packaged parcels, protected from the extracellular environment with the potential for site specific targeting to receptors on cells (Kuehn and Kesty, 2005; Bomberger *et al.*, 2009; Bonnington and Kuehn, 2014; Bitto *et al.*, 2017). OMV production appears evolutionarily conserved in Gram-negative bacteria despite being metabolically energy consuming, suggesting OMVs have vital roles (Kulp and Kuehn, 2010; Roier *et al.*, 2016). OMV production has been observed under a range of conditions in both pathogenic and non-pathogenic Gram-negative bacteria (Mashburn-Warren *et al.*, 2008; Elmi *et al.*, 2012; Altindis *et al.*, 2014; Zakharzhevskaya *et al.*, 2017); both on solid and in liquid media (Schooling and Beveridge, 2006; Schwechheimer and Kuehn, 2015) and in the presence or absence of stress (Schwechheimer and Kuehn, 2015). Conditions or gene mutations resulting in the absence of OMVs have not been identified. OMVs have been suggested to have a variety of functions important in survival and virulence via processes such as competition for growth (Manning and Kuehn, 2011; Kulkarni *et al.*, 2015), immunomodulation (Koeppen *et al.*, 2016; Tsatsaronis *et al.*, 2018), biofilm formation (Schooling and Beveridge, 2006), bacterial communication (Mashburn and Whiteley, 2005; Mashburn-Warren *et al.*, 2008) and the delivery of biomolecules such as toxins (Bielaszewska *et al.*, 2017; Elmi *et al.*, 2018).

Until recently there has been no general regulatory model for OMV biogenesis that could be widely applicable to Gram-negative bacteria. The three main OMV biogenesis models proposed previously have been based on either changes in cell wall to OM linkages, stress or a species-specific mechanism. One previously proposed model suggests that the build-up of cellular components (such as misfolded

proteins due to heat shock, or peptidoglycan fragments due to cell wall remodelling defects) at the OM result in bulging and subsequent blebbing (Zhou *et al.*, 1998; McBroom and Kuehn, 2007). OMVs have since been demonstrated to contain biologically active cargo and not just cell waste (Mashburn and Whiteley, 2005; Bielaszewska *et al.*, 2017; Elmi *et al.*, 2018). A second mechanism proposed that the reduction in cell wall to OM interactions can cause areas prone to blebbing. This has been demonstrated by OMVs being released at cell division sites with high frequency (Kulp and Kuehn, 2010), however OMV release is not restricted to cell division sites (Elhenawy *et al.*, 2016). Deatherage *et al.* (2009) studied the effect of removing cell wall to OM linkages on OMV production and found removal of OmpA linkages did not compromise the cell membrane. However removal of other linkages (*lpp*, *tolA*, *tolB* and *pal*) did cause membrane defects. Additional studies have found that the down-regulation of *ompA* is dependent on the membrane stress sigma factor,  $\sigma^E$  (Song *et al.*, 2008). A further mechanism has been identified in the OM of *Pseudomonas aeruginosa*, which has increased fluidity compared to the OM of other Gram-negative bacteria. *P. aeruginosa* produces a quorum sensing molecule PQS which induces membrane curvature through interactions with lipid A to stabilise and reduce fluidity of the OM. Without PQS, *P. aeruginosa* struggles to reach the membrane curvature necessary to form OMVs. However this proposed mechanism appears specific to *P. aeruginosa* cells (Mashburn and Whiteley, 2005; Mashburn-Warren *et al.*, 2008).

More recently, Roier *et al.* (2016) have proposed a new general regulatory model based on the MLA pathway that could be widely applicable to Gram-negative bacteria. The MLA pathway has been shown to play a role in the retrograde trafficking of PLs from the outer leaflet of the OM to the IM. The core components of this pathway are highly conserved in Gram-negative bacteria (Malinverni and Silhavy, 2009). The pathway consists of an IM ABC (ATP binding cassette) transporter consisting of MlaBDEF (MlaB is absent in  $\alpha$  and  $\epsilon$  *proteobacteria*), a periplasmic chaperone MlaC and the OM lipoprotein MlaA. The components of the MLA pathway are homologous to YrbCDEF and VacJ in *Haemophilus influenzae*. Roier *et al.* proposed that down-regulation or mutation of the MLA pathway or components of this pathway will lead to an accumulation of PLs in the outer leaflet of the OM. This accumulation leads to an asymmetric expansion which eventually results in the formation of an OMV. Roier *et al.* demonstrated increased OMV production in *mia* mutants, as well as reduced *mia* gene expression in *H. influenzae* under iron-limiting conditions. The same study suggested that iron limitation signalled entry to the host nasopharynx, and the subsequent increase in OMV production was a potential mechanism to defend against antibody and complement-mediated attack.

A range of virulence factors have been identified within *C. jejuni* OMVs, including the cytolethal distending toxin and putative virulence-associated proteases that contribute to *C. jejuni* invasion into IECs (Lindmark *et al.*, 2009; Elmi *et al.*, 2016; Elmi *et al.*, 2018). *C. jejuni* OMVs isolated at 37°C (human

body temperature) have also been shown to differ in protein abundance compared to 42°C (avian body temperature), suggesting *C. jejuni* can alter cargo in response to host signals (Taheri *et al.*, 2019). An important feature of a pathogen is the ability to sense the environment and to appropriately alter and co-ordinate the regulation of virulence factors. We have previously reported the potential significance of the bile salt ST in the regulation of OMV-mediated virulence in *C. jejuni* (Elmi *et al.*, 2018) and have demonstrated increased OMV production in the presence of physiologically relevant concentrations of ST. In addition, the OMVs isolated from cultures supplemented with ST (ST-OMVs) exhibited increased proteolytic activity, cytotoxicity and immunogenicity to IECs. ST has also been shown to up-regulate virulence gene expression in *Vibrio cholerae* by causing alterations in disulphide bond formation in TcpP (transmembrane transcription factor) (Yang *et al.*, 2013).

This study further investigates the link between the MLA pathway and OMV production in Gram-negative bacteria. Increased OMV production without compromising membrane stability was observed in a *C. jejuni* 11168 *miaA* mutant. This study also builds on previous work linking the bile salt ST to increased OMV production, by identifying a potential mechanism for the ST-OMV phenotype. OMV production was observed to increase in the *C. jejuni* wild-type strain, but not in the *miaA* mutant in the presence of ST. Growth of *C. jejuni* in the presence of ST also resulted in reduced expression of *mia* genes. The data in this study supports the MLA model of OMV production and the link between bile salts and potential virulence regulation in *C. jejuni*.

## Materials and methods

### Bacterial strains and growth conditions

The *C. jejuni* wild-type strains used in this study were NCTC 11168 (the widely studied human clinical isolate) and 488 (a recent Brazilian human isolate obtained from Daiani Teixeira Da Silva). Cultures were grown in a microaerobic chamber (Don Whitley Scientific, United Kingdom) containing 85% (v/v) N<sub>2</sub>, 10% (v/v) CO<sub>2</sub> and 5% (v/v) O<sub>2</sub> at 37°C either on BA plates containing Columbia agar base (Oxoid, United Kingdom), 7% (v/v) horse blood (TCS Microbiology, United Kingdom) and *Campylobacter* Selective Supplement (Oxoid), or in Brucella broth (Oxoid) shaking at 75 rpm unless otherwise stated. *C. jejuni* strains were grown on BA plates for 24 hours prior to experiments unless otherwise stated. *Escherichia coli* XL2-Blue MRF' competent cells (Stratagene, United Kingdom) were used for cloning and were grown at 37°C in aerobic conditions either in LB (Oxoid) shaking at 200 rpm or on LB agar plates (Oxoid). When required, ampicillin (100 µg/ml), kanamycin (50 µg/ml), apramycin (60 µg/ml) or chloramphenicol (50 µg/ml for *E. coli* or 10 µg/ml for *C. jejuni*) were added to cultures.

### Construction of *C. jejuni* mutants

The *C. jejuni* 11168 *miaA* gene was inactivated by deletion of the reading frame by homologous cross-over and replacement with a kanamycin resistance cassette. The mutation vector was created using the Gibson isothermal assembly method as previously described (Taylor *et al.*, 2017). The *C. jejuni* 11168 wild-type strain was transformed by electroporation and mutant clones selected for kanamycin resistance. Correct insertion and orientation of the kanamycin cassette into the genome was confirmed by PCR.

The *C. jejuni* 488 *miaA* mutant was constructed by natural transformation using genomic DNA from the *C. jejuni* 11168 *miaA* mutant spotted onto the *C. jejuni* 488 wild-type strain. Transformations were performed on Mueller-Hinton agar (Oxoid) plates for five hours under microaerobic conditions at 37°C. Transformants were screened on BA plates supplemented with kanamycin, then putative mutants verified by PCR and sequencing.

### Complementation of *C. jejuni* *miaA* mutants

Complementation of the *C. jejuni* 11168 *miaA* mutant was performed using the pRRA system to generate a complementation vector as previously described (Taylor *et al.*, 2017). The 11168 *miaA* mutant was transformed with the complementation vector by electroporation and clones selected for apramycin resistance. Correct insertion of the expression cassette into the genome was confirmed by PCR. In the 11168 *miaA* complement strain, the inserted *miaA* gene is under the control of the native promoter.

The *C. jejuni* 488 *miaA* mutant was complemented using the pCJC1 complementation vector as previously described (Gundogdu *et al.*, 2011; Jervis *et al.*, 2015). Briefly, the complete wild-type gene was amplified by PCR to contain the native ribosome binding site, start codon and stop codon with primers pCJC1miaA(F/R) (Table 1) to introduce a *Nco*I site at the 5' end and a *Nhe*I site at the 3' end. The amplified gene was digested with *Nhe*I and *Nco*I and ligated into the pCJC1 complementation vector which was used to insert the wild-type gene copy into the 488 orthologue of the *C. jejuni* 11168 pseudogene *cj0223*. Putative clones were selected on BA plates supplemented with chloramphenicol then verified by PCR and sequencing. In the 488 *miaA* complement strain, the inserted *miaA* gene is under the control of a constitutive chloramphenicol promoter.

### **3,3'-dipropylthiadicarbocyanine iodide (DiSC3) permeability Assay**

DiSC3 is a potentiometric fluorescent probe which accumulates on, and translocates into, hyperpolarised lipid bilayers and is frequently used to measure membrane permeability. Fluorescence was monitored at Ex/Em wavelength of 622/670 nm in a Cary Eclipse (Agilent, United States) fluorescence spectrophotometer. *C. jejuni* cells were washed in 20 mM sodium phosphate buffer, pH 7.4, containing 10 mM KCl, and set to an optical density at 600 nm of 0.1. DiSC3 was added to 5 µM final concentration and fluorescence emission followed for two minutes to establish the baseline. Polymyxin B was then added (100 µM final concentration) and emission followed for a further one minute, before the addition of SDS (20 mM final concentration) to give the maximum fluorescence value. Percentage incorporation of the dye into the membrane was calculated by:

$$100 - \left( \frac{\text{emission after Polymyxin B (minus baseline)}}{\text{maximum emission after SDS (minus baseline)}} \right) \times 100$$

### **Growth kinetics and membrane sensitivity assays**

The growth of each *C. jejuni* wild-type, mutant and complement strains was characterised by measuring both the OD<sub>600</sub> value and colony forming units (CFUs) of a liquid culture every two hours for 18 hours. Sensitivity to the bile salt sodium ST at biologically relevant concentrations was analysed measuring OD<sub>600</sub> and CFU/ml of liquid cultures supplemented with 0.2% (w/v) ST every two hours for 18 hours. Sensitivity to ST at high concentrations was analysed by comparing the OD<sub>600</sub> and CFU/ml of late-log phase broth cultures in the presence or absence of 2% (w/v) ST. Sensitivity to the zwitterionic detergent lauryl sulfobetain (LSB) was analysed by comparing CFU/ml of mid-log phase cultures serially diluted and spotted onto Brucella agar with or without supplementation of LSB (1.25 mM final concentration). Sensitivity to polymyxin B was analysed by comparing CFU/ml of mid-log phase cultures serially diluted and spotted onto BA plates with and without supplementation with polymyxin B (2.5 µg/ml final concentration).

### **Outer membrane vesicle isolation**

*C. jejuni* OMVs were isolated as previously described (Elmi *et al.*, 2012). Briefly, *C. jejuni* from a 24 hour BA plate were resuspended in Brucella broth and used to inoculate 50 ml of pre-equilibrated Brucella broth to an OD<sub>600</sub> of 0.1. Cultures were grown to late-log phase, timepoints determined by growth kinetics for each strain. OD<sub>600</sub> values were normalised to OD<sub>600</sub> 1.0 and the sterile supernatants obtained by pelleting cells and filter-sterilising supernatants through a 0.22 µm membrane (Millipore, United Kingdom). The supernatants were then concentrated to 2 ml using an Ultra-4 Centrifugal Filter Unit with a nominal 10 kDa cut-off (Millipore). The concentrated filtrate was ultra-centrifuged at 150,000 × g for 3 hours at 4°C using a TLA 100.4 rotor (Beckman Instruments, United States). The resulting OMV pellet was washed by resuspending in PBS and pelleting by ultra-centrifugation as described above. All isolation steps were performed at 4°C and the resulting OMVs pellet was resuspended in PBS and stored at -20°C.

### **Quantification of outer membrane vesicles**

The protein concentration of OMV preparations was quantified using a commercial bicinchoninic-acid (BCA) assay kit according to the manufactures protocol (Thermo Fisher Scientific, United Kingdom), using BSA as the protein standard. The lipo-oligosaccharide of OMV preparations was quantified by measuring (KDO) content as described previously (Lee and Tsai, 1999). Briefly, 50 µl samples were hydrolysed with 50 µl sulphuric acid (0.5 N) at 100°C for 15 minutes, then mixed with 50 µl 0.1 M periodate reagent (H<sub>5</sub>IO<sub>6</sub>) and incubated at room temperature for 10 minutes. 200 µl 4% (w/v) sodium arsenite reagent (NaAsO<sub>2</sub>) then 800 µl 0.6% (w/v) thiobarbituric acid was added and samples heated again to 100°C for 15 minutes. Samples were mixed with 1 ml dimethyl sulfoxide (DMSO) to stabilise the chromophore and OD<sub>548</sub> measurements taken. 2-Keto-3-deoxyoctonate ammonium salt (Sigma-Aldrich, United Kingdom) was used as the KDO standard.

### **Analysis of outer membrane vesicles by nanoparticle tracking analysis**

NTA was conducted using a ZetaView PMX 110 instrument (Particle Metrix GmbH, Germany) following the manufacturer's instructions. The instrument was calibrated against a known concentration of PS100 nanoparticles with 100 nm diameter (Applied Microspheres B.V., The Netherlands). Nanostandards and OMV samples were suspended in particle-free PBS (Sigma-Aldrich) and diluted appropriately before analysis. Each sample was counted and sized across two cycles of 11 frames per cycle with a flow cell sensitivity of 80%.

### **Quantitative real-time polymerase chain reaction (qRT-PCR)**

To investigate the expression of *miaA* and *miaC*, total RNA from both the *C. jejuni* 11168 and 488 wild-type strains, grown in Brucella broth to mid-log phase either in the presence or absence of 0.2% (w/v)

ST was extracted using Invitrogen PureLink RNA kit (Invitrogen, United Kingdom). DNA contamination was removed using the TURBO DNA-free kit (Thermo Fisher Scientific). Purified RNA was quantified using a NanoDrop machine (NanoDrop Technologies, United Kingdom) and used to synthesise complementary DNA (cDNA) using the SuperScript III First-Strand Synthesis kit (Thermo Fisher Scientific). qRT-PCRs were performed in triplicate using SYBR green master mix (Thermo Fisher Scientific) and an ABI7500 machine (Applied Biosystems). Relative gene expression comparisons were performed using the  $\Delta\Delta\text{CT}$  (cycle threshold) method (Schmittgen and Livak, 2008) and previously published *C. jejuni rpoA* primers (Ritz *et al.*, 2009) for internal controls to normalise the mean CT of each gene to the stably expressed housekeeping gene *rpoA*.

### **Statistical analysis**

At least three biological replicates were performed each in triplicate for each experiment. Statistical analyses were performed using Prism software (GraphPad Software). Variables were compared using a student's *t*-test with \* indicating a *p* value < 0.05, \*\* indicating a *p* value < 0.01, and \*\*\* indicating a *p* value < 0.001.

## Results

### Identification of *C. jejuni* orthologues of the MLA pathway in *E. coli*

The genomes of *C. jejuni* 11168 and 488 contain sets of genes encoding proteins homologous to components of the MLA pathway in *E. coli* and the VacJ and YrbCEFD proteins in *H. influenzae*. The MLA pathway consists of MlaA (OM lipoprotein), MlaC (periplasmic chaperone) and MlaEFD (IM ABC transporter). In *C. jejuni* these proteins are encoded in two separate regions of the genome (Figure 1). Cj1371 and Cj1372 in *C. jejuni* 11168 are within the same gene cluster and are homologous to MlaA and MlaC in *E. coli* (amino acid sequence similarity of 29.4% and 21.6% respectively to *E. coli* MG1655 MlaA and MlaC) and VacJ and YrbC in *H. influenzae* (amino acid sequence similarity of 25.8% and 22.2% respectively to *H. influenzae* KW20 VacJ and YrbC). Homologous proteins were also identified in *C. jejuni* 488 with 97.4% and 96.8% amino acid similarity to Cj1371 and Cj1372 respectively. Cj1646, Cj1647 and Cj1648 in *C. jejuni* 11168 are encoded by the same gene cluster and are homologous to MlaEFD in *E. coli* (amino acid sequence similarity of 27.6%, 31.8% and 18.8% respectively to *E. coli* MG1655 MlaEFD) and YrbEFD in *H. influenzae* (amino acid sequence similarity of 27.7%, 36.4% and 22.8% respectively to *H. influenzae* KW20 YrbEFD). Homologous proteins were also identified in *C. jejuni* 488 with 98.1%, 99.2% and 97.6% amino acid similarity to Cj1646, Cj1647 and Cj1648 respectively. *miaB* or *yrbB* were absent in the *C. jejuni* strains used in this study.  $\epsilon$  proteobacteria have previously been reported to lack *miaB* homologs (Roier *et al.*, 2016). The MLA nomenclature will be used for this study. The *C. jejuni* 11168 published annotated whole genome sequence (Sanger database: ID CJ11168 accession number AL111168) has assigned colour qualifiers based on predicted functionality. MlaDEFC are predicted to be functionally linked to cell surfaces (IM, OM, secreted, surface structures). MlaA is predicted to be functionally linked to pathogenicity, adaptation and chaperones (Figure 1).

### No change in sensitivity of *miaA* mutant to detergent compared to wild-type strains

As the MLA pathway is proposed to play a role in the maintenance of the bacterial OM (Malinverni and Silhavy, 2009), the membrane integrity of the *miaA* mutants was investigated to ensure any changes in OMV production were not an artefact of a fragile OM. Membrane permeability of the *C. jejuni* 11168 parent cell membranes in the absence of OMVs was analysed using the DiSC3 assay. *C. jejuni* cells were washed (removing OMVs) then re-suspended in assay buffer. There was no significant difference in percentage incorporation of the dye after membrane stress with 100  $\mu$ M final concentration polymyxin B between the 11168 wild-type, *miaA* mutant or complement strain (Figure 2).

Growth or survival during culture conditions in the presence of detergents (LSB and ST) were used to investigate membrane integrity. No significant difference in growth rates measured by either OD<sub>600</sub> readings or CFU/ml was observed prior to stationary phase for either the *mlaA* mutant or the complemented mutant when compared to the respective wild-type strain. There was also no significant difference observed for any strain when grown in the presence of 0.2% (w/v) ST (biologically relevant concentration) compared to the same strain cultured in Brucella broth alone prior to stationary phase. The *C. jejuni* 11168 strain was able to grow to higher CFU and OD<sub>600</sub> values than the *C. jejuni* 488 strain (Figure S1).

Survival of bacteria in the presence of high concentrations of detergent was investigated either by plating bacteria onto agar supplemented with 1.25 mM LSB or by culturing bacteria in Brucella broth supplemented with 2% (w/v) ST. Survival of both the *mlaA* mutant and complement strains was comparable to the corresponding wild-type strains for both detergents (Figure 3AB). 1.25 mM LSB caused around a 4-log reduction in growth for 11168 strains compared to around a 2-log reduction for 488 strains. Less than a log reduction in growth was observed for bacteria cultured in 2% (w/v) ST (Figure 3B).

#### ***mlaA* mutants exhibit increased resistance to polymyxin B.**

Polymyxin B targets cells through binding to LOS or LPS, meaning OMVs are capable of binding polymyxin B in the extracellular environment (Manning and Kuehn, 2011). Resistance to a low concentration of polymyxin B (2.5 µg/ml) was used as an initial screen for increased OMV production in the *mlaA* mutants compared to the respective wild-type strains. The *C. jejuni* 11168 and 488 *mlaA* mutants were significantly more resistant to polymyxin B compared to their wild-type strains under culture conditions. Complementation of the 11168 *mlaA* mutant with the *mlaA* gene under the control of the native promoter almost completely restored wild-type polymyxin B sensitivity, however complementation of the 488 *mlaA* mutant with the *mlaA* gene under the control of a constitutive chloramphenicol promoter did not. It would appear that the expression of the inserted *mlaA* gene in the 488 *mlaA* complement is not sufficient to restore the wild-type phenotype under these stress conditions (Figure 3C).

#### ***mlaA* mutation results in increased OMV production.**

Total protein and KDO concentration were used to quantify OMV preparations. KDO is a component of LOS and can be used to indicate the amount of OM present. As protein and KDO concentrations are unable to determine if OMV preparations contain more OMVs or larger OMVs, NTA was used to verify any changes in production. OMV preparations were from bacterial cultures of equivalent volume and OD<sub>600</sub> readings. OMV preparations isolated from the *C. jejuni* 11168 *mlaA* mutant had significantly

higher concentrations of both protein and KDO compared to the wild-type and complement strains (Figure 4). The OMV preparations of the *mlaA* mutant strains were also confirmed to contain more OMVs by NTA particle counts (Figure S2).

### **Co-culture with sodium taurocholate increases lipid and protein concentration of *C. jejuni* OMVs.**

To investigate the link between ST and OMV production proposed by Elmi *et al.* (Elmi *et al.*, 2018), OMVs were isolated from *C. jejuni* 11168 wild-type, *mlaA* mutant and complement strains co-cultured with 0.2% (w/v) ST. OMV preparations isolated from ST supplemented cultures had significantly higher concentrations of KDO for the wild-type and complement strains (Figure 5). ST did not increase the KDO concentration of the *mlaA* mutant OMV preparations. Protein concentrations were significantly higher for the wild-type strain in the presence of ST and higher, but not significantly so for the *mlaA* complement strain. The protein concentration did not increase in the presence of ST for the *mlaA* mutant (Figure 5). The increase in OMVs based on KDO and protein concentrations in the presence of ST for the wild-type and complement strain also correlated to an increase in particle number for NTA (Figure S2).

### **Changes in lipid and protein concentration of OMVs are inversely proportional to OMV size.**

In addition to quantifying OMV production levels, the size of the OMVs produced were also investigated by NTA. OMV preparations from all strains and all conditions contained one main size cluster which contained 92-99% of the population. An increase in protein, KDO and particle number either in the presence of ST or in the absence of a complete MLA pathway correlated to a reduction in OMV size. OMVs isolated from the *C. jejuni* 11168 wild-type, *mlaA* mutant and *mlaA* complement strain had a mode diameter of 177, 140 and 184 nm respectively, when isolated from cultures grown in Brucella broth. When co-cultured with 0.2% (w/v) ST, ST-OMV mode diameters were 137, 133 and 159 for the 11168 wild-type, *mlaA* mutant and *mlaA* complement strains respectively (Figure 6). A similar inverse correlation between OMV quantity and size was also observed for mean OMV diameters (Figure S2).

### **Co-culture of *C. jejuni* with sodium taurocholate results in reduced gene expression of *mlaA* and *mlaC***

As the *C. jejuni* 11168 *mlaA* mutant was not observed to increase OMV production in the presence of 0.2% (w/v) ST in contrast to the wild-type strain, the effect of 0.2% (w/v) ST on the relative expression of genes encoding components of the MLA pathway was investigated. *mlaA* and *mlaC* were selected for investigation. RNA was isolated from mid-log phase cultures of the *C. jejuni* 11168 and 488 wild-

type strains. An approximate 2-fold down-regulation of gene expression of both *miaA* and *miaC* in both wild-type strains (11168 and 488) in the presence of ST compared to the absence of ST, was observed relative to the *rpoA* internal control (Figure 7).

## Discussion

Previous characterisations of the cargo of *C. jejuni* OMVs have identified biologically active compounds that contribute to immunogenicity, cytotoxicity and the breakdown of the gut barrier mediated by bacterial proteases (Jang *et al.*, 2014; Elmi *et al.*, 2016b; Elmi *et al.*, 2018). The mechanisms regulating OMV production in *C. jejuni* however are still poorly understood. In this study, we have characterised both the role of the MLA pathway in *C. jejuni* OMV production, as well as the role of ST in regulating the MLA pathway. OMV production in *C. jejuni* was increased either in the presence of a biologically relevant concentration of ST or in the absence of a complete MLA pathway, linking the model proposed by Roier *et al.* (2016) with the ST phenotype observed by Elmi *et al.* (2018).

Despite the bacteriostatic effect of bile salts (Begley *et al.*, 2005), in this study *C. jejuni* was shown to be highly tolerant to ST stress, showing less than a log-reduction in growth at 2% (w/v) ST, a concentration higher than is considered to be biologically relevant (Elmi *et al.*, 2018). This then suggests that much lower and biologically relevant concentrations of ST could act as stimuli without compromising bacterial growth or membrane integrity. This is in agreement with a previous study (Elmi *et al.*, 2018), which did not observe any defect in growth of *C. jejuni* associated with a biologically relevant concentration of ST (0.2% w/v). The effect of a combination of bile salts similar to that expected to be found in the human gut was not investigated in this study, however the resistance to ST demonstrated here highlights the exquisite adaptation of *C. jejuni* to the gut environment where localised signals co-ordinate bacterial behaviour.

There is conflicting evidence in the literature regarding the impact of *mfa* mutations on membrane integrity. Malinverni and Silhavy (2009) observed increased sensitivity of *E. coli mfa* mutants to SDS in combination with EDTA, but not to SDS alone. EDTA is a chelating compound that is thought to destabilise LPS to increase membrane permeability (Finnegan and Percival, 2015). The metabolic cost, rather than the membrane integrity of the *E. coli mfa* mutants unable to down-regulate OMV production as well as patching areas effected by EDTA, could be the more likely cause of the increased mutant sensitivity. Abellon-Ruiz *et al.* (2017a) observed growth defects in an *E. coli mfaA* mutant compared to the wild-type strain in the presence of both doxycycline and chlorpromazine. This suggested that the PL accumulation at the OM created transient patches of PL bilayer creating windows of opportunity for small molecules that are readily able to diffuse through PL bilayers to enter the cell. However, as an *mfa* mutant is unable to down-regulate the creation of these PL bilayer patches, this membrane defect phenotype would be less applicable to a wild-type strain which would be able to up-regulate OMV production without compromising integrity in favourable conditions and down-regulate production reducing the creation of these patches in unfavourable conditions. Roier *et*

*al.* (2016) also did not observe any obvious membrane defects for the *mfa* mutants in response to detergent stress, supporting the model that increased OMV production is due to a regulated process and is not an artefact of an unstable membrane.

As the membrane of an OMV contains either LOS or LPS, it has been suggested OMVs can confer protection against compounds that target or bind to this component of the bacterial membrane, such as bacteriophage or polymyxin B. This was demonstrated by a study that examined the ability of OMVs to protect against low concentrations of polymyxin B (Manning and Kuehn, 2011). Resistance to this antibiotic is normally achieved through modifications of LOS or LPS preventing the antibiotic binding to the bacterial OM. Manning and Kuehn (2011) observed that only OMVs from polymyxin B sensitive strains conferred protection against polymyxin B when added to a culture of a polymyxin B sensitive bacteria, as polymyxin B was unable to bind to OMVs produced by a polymyxin B resistant strain. Here we demonstrated that there was no significant difference in resistance to polymyxin B between the 11168 wild-type strain and the *mfaA* mutant when cells were washed and supernatant discarded to remove OMVs. The fluorescent probe DiSC3 accumulates on, and translocates into, hyperpolarised lipid bilayers, so the DiSC3 assay was used to investigate changes in bacterial membrane permeability. After the addition of polymyxin B, there was no difference in the change in bacterial membrane permeability of the *mfaA* mutant compared to the 11168 wild-type strain. Based on these results, resistance to a low concentration of polymyxin B (2.5 µg/ml) under culture conditions was investigated as an initial screen for increased OMV production by *mfaA* mutants. A positive correlation between increased OMV production and polymyxin B resistance was observed. As OMV isolation is laborious, this could provide a quick and easy initial screen for OMV production levels.

Both in this study and in a previous study (Elmi *et al.*, 2018), a biologically relevant concentration of ST was shown to stimulate OMV production. 0.2% (w/v) ST was observed to almost double OMV production by the *C. jejuni* 11168 wild-type strain. Mutation of *mfaA* increased OMV production by the same magnitude in the absence of ST, whilst ST did not significantly further stimulate OMV production by the *mfaA* mutant. This increase was also shown by NTA to be due to the presence of increased numbers of OMVs rather than larger OMVs. The increase in OMV production was also associated with a small reduction in OMV size. It is possible that this is due to an increase in PLs in the membrane of the OMVs, based on the model proposed by Roier *et al.*, altering the membrane curvature during the formation of the OMV. The reduced size of wild-type ST-OMVs was also similar to that of the *mfaA* mutant OMVs. Both the *mfaA* mutant OMVs and wild-type ST-OMVs had comparable diameters. This is in contrast to data from a recent study (Taheri *et al.*, 2018) which did not observe increased OMV production in response to ox bile. Ox bile was used to represent a mixture of bile salts, similar to what would be found in the gut, whereas ST alone was used in this study, a

single component of human bile. Bile composition not only varies between species but also between individuals of the same species, as well as depending on the location in the gut (Sjövall, 1959; Falany *et al.*, 1994; Nagana Gowda *et al.*, 2009; Chiang, 2017). For example, in humans the proportion of taurine to glycine conjugated bile salts is diet determined. Humans with a taurine rich diet (animal-based products) will have a higher proportion of taurine conjugated bile salts compared to low taurine diet (Sjövall, 1959; Wojcik *et al.*, 2010; Ridlon *et al.*, 2016). As oxes are herbivores, the bile pool composition maybe low in taurine conjugated bile salts, such as ST. Previous work by Elmi *et al.* found the effect of ST on OMV production to be dose-dependent (Elmi *et al.*, 2018). The low dose of ox bile used in this other study, along with the potentially low proportion of taurine conjugates within the ox bile, could explain the different results observed between these studies.

Roier *et al.* (2016) proposed that iron limitation regulates the MLA pathway in *H. influenzae*, *V. cholerae* and *E. coli* in a Fur dependent manner. However, a RNA sequencing study did not highlight a link between Fur and the MLA pathway in *C. jejuni* (Butcher *et al.*, 2015). As ST has previously been linked to *C. jejuni* virulence and OMV production, ST was investigated as a potential regulator of the *C. jejuni* MLA pathway. The differential effect ST had on OMV production in the *C. jejuni* 11168 wild-type strain compared to the *m1aA* mutant suggests a direct interaction between ST and the MLA pathway in *C. jejuni*. These are the first data suggesting a role for bile salts in regulating the MLA pathway. The qRT-PCR results in this study showed around a 2-fold down-regulation of *m1aA* and *m1aC* in response to ST exposure, further strengthening the hypothesised interaction between ST and the MLA pathway in *C. jejuni*. As previous studies have suggested removing one component of the MLA pathway prevents functionality (Malinverni and Silhavy, 2009; Roier *et al.*, 2016), this could explain why ST appeared to have no effect on OMV production in a single *m1a* mutant.

In summary, the data in this study suggests *C. jejuni* can regulate OMV production in response to host gut signals through changes in expression of the MLA pathway. Increased OMV production without compromising membrane stability was observed in a *m1aA* mutant and a potential mechanism for the ST-OMV phenotype was identified. In the presence of ST, OMV production was shown to increase in the wild-type strain, but not in a *m1aA* mutant. Growth of *C. jejuni* in the presence of ST also resulted in reduced expression of both *m1aA* and *m1aC*. Our data supports the MLA model of OMV production and the link between bile salts and potential virulence regulation in *C. jejuni*. As the gut bile composition is dependent on both diet and the microbiota, this study highlights the potential importance of diet and lifestyle factors on the varying disease presentations associated with gut pathogen infection.

## **Acknowledgements**

The author(s) gratefully acknowledge the support of the Biotechnology and Biological Sciences Research Council Institute Strategic Programme BB/R012504/1 constituent project BBS/E/F/000PR10349.

## Figures

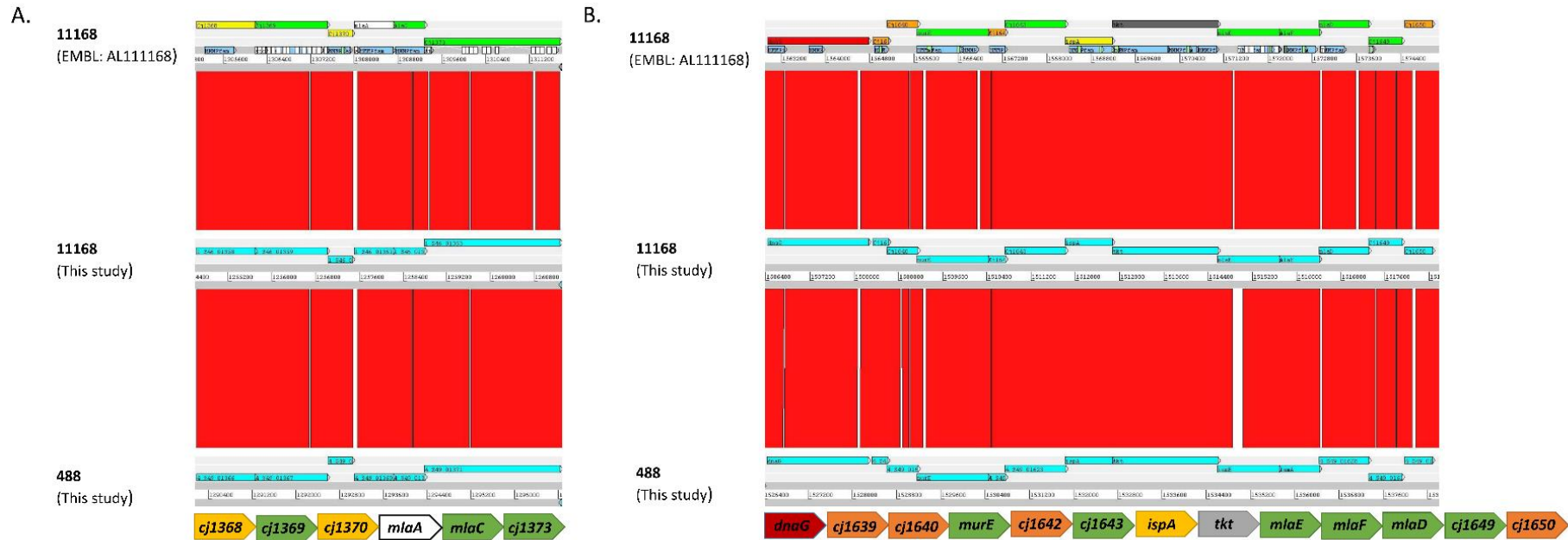


**Figure 1.** Comparison using the Artemis Comparison Tool (ACT) (Carver *et al.*, 2005) software of the gene clusters containing **(A)** *miaAC* and **(B)** *miaEDF* using the *C. jejuni* 11168 original genome sequenced strain from the Sanger public database (ID CJ11168 accession number AL111168) and the new sequences of the 11168 and 488 wild-type strains produced here. Below each ACT window is the conserved organisation of the *mia* gene clusters for the strains used in this study based on synteny between the annotated AL111168 genome sequence and the newly sequenced strains in this study. The colour qualifier for annotated gene sequences was based on gene function following the scheme adopted by the Wellcome Trust Sanger institute Pathogen Genomic Department. Functional colours included in this figure are: yellow (central/intermediary/miscellaneous metabolism); dark green (surface - IM, OM, secreted, surface structures); white (pathogenicity/Adaptation/Chaperones); red (information transfer - transcription/translation + DNA/RNA modification); orange (conserved hypothetical) and dark grey (energy metabolism).

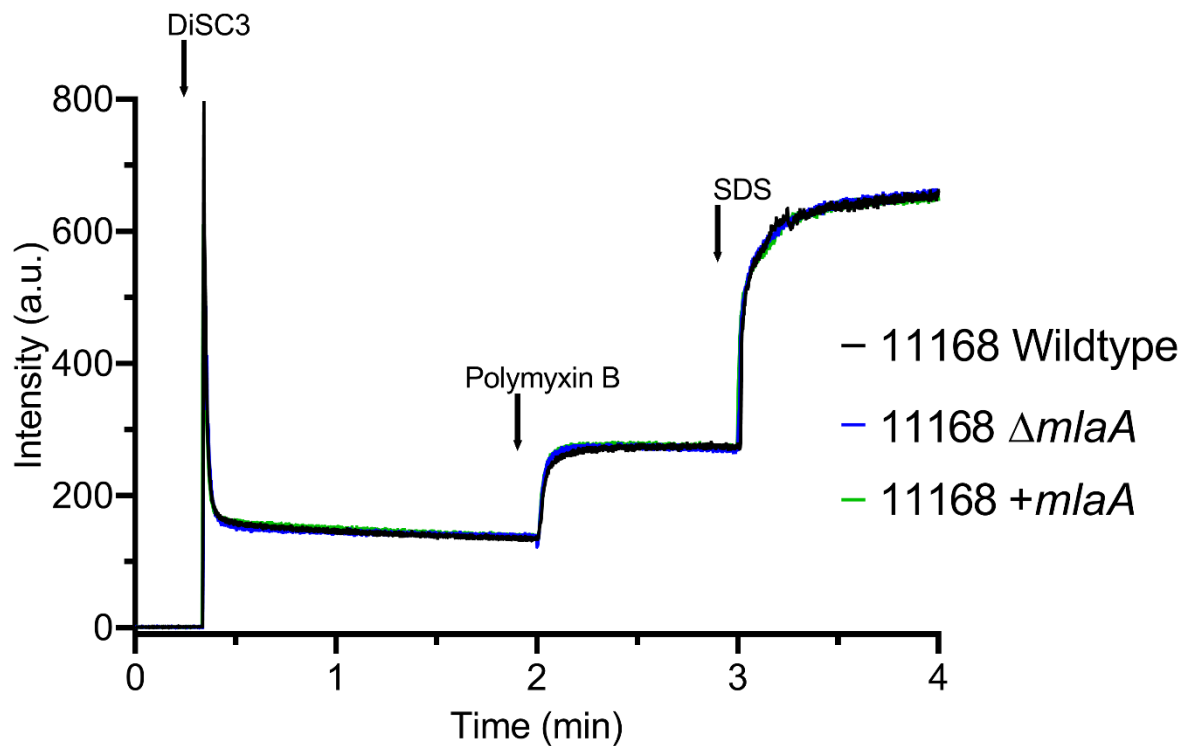


**Figure 2.** Membrane permeability of the *C. jejuni* 11168 wild-type strain, isogenic *m laA* deletion mutant ( $\Delta m laA$ ) and complemented (+*m laA*) strain. Permeability of intact cells was measured using the fluorescent probe 3,3'-Dipropylthiadicarbocyanine Iodide (DiSC3) which accumulates on, and translocates into, hyperpolarised lipid bilayers. Cells were washed prior to the assay, removing OMVs, to measure parent cell membrane permeability. Polymyxin B was added to the cells at a final concentration of 100  $\mu$ M and release of DiSC3 from the membrane was measured. SDS was added at a final concentration of 20 mM to measure maximum fluorescence.

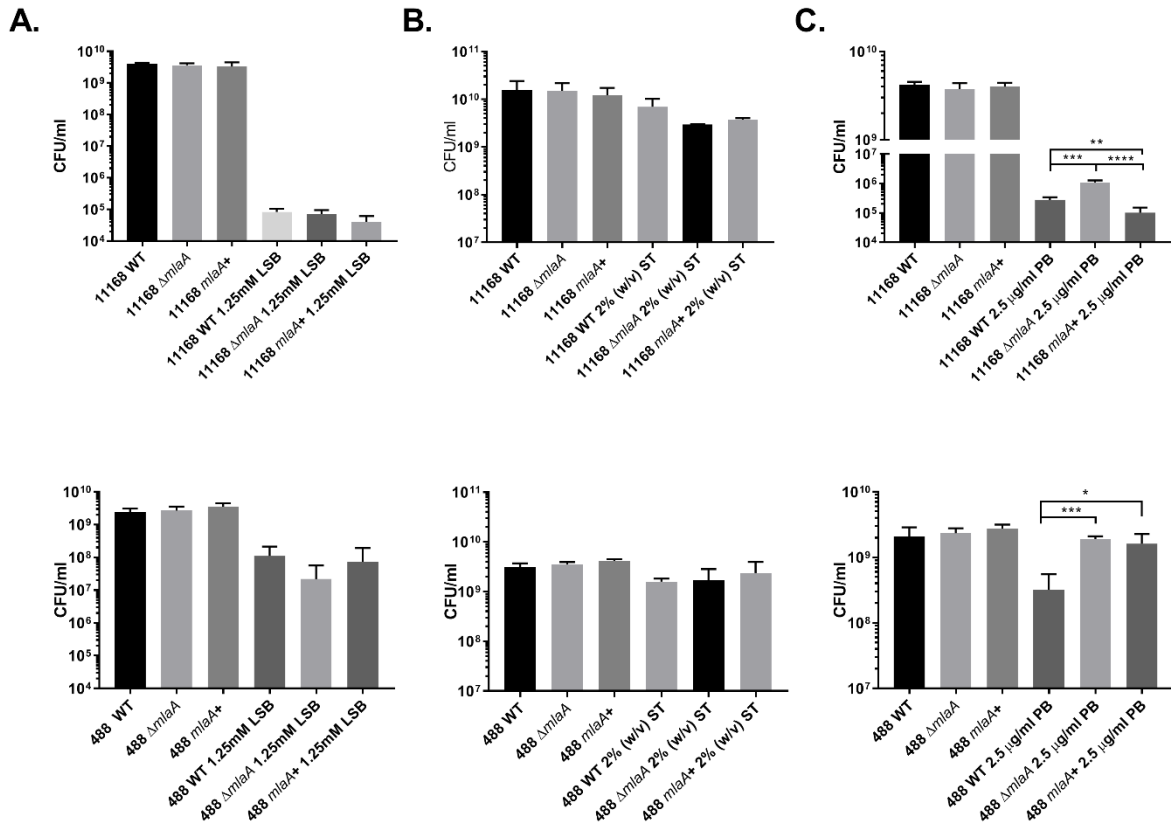


**Figure 3.** Survival of *C. jejuni* strains exposed to detergent stress or detergent-like stress. **(A)** Mid-log phase cultures spotted onto Brucella agar in the presence or absence of 1.25 mM LSB. **(B)** Late-log phase cultures grown in Brucella broth in the presence or absence of 2% (w/v) ST. **(C)** Mid-log phase cultures spotted onto BA in the presence or absence of 2.5  $\mu$ g/ml polymyxin B. \* =  $p < 0.05$ ; \*\* =  $p < 0.01$ ; \*\*\* =  $p < 0.001$ ; \*\*\*\* =  $p < 0.0001$ .

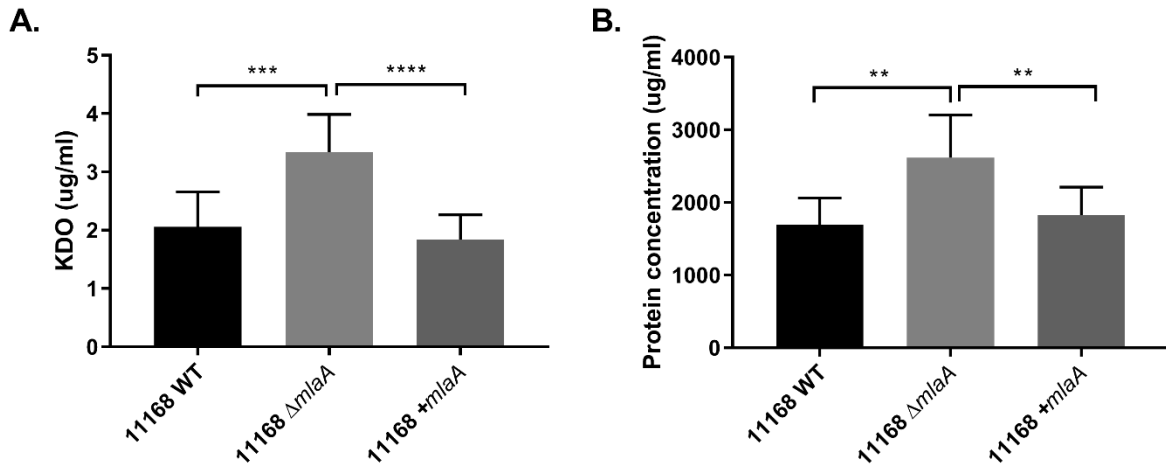


**Figure 4.** Mutation of *m laA* increases OMV production. OMVs were isolated from late-log phase *C. jejuni* 11168 cultures grown in Brucella broth. OMV preparations from cultures of *C. jejuni* 11168 wild-type, *m laA* mutant and complement strains of equivalent OD<sub>600</sub> values were quantified by analysing (A) total KDO as a measurement of LOS and (B) total protein. \*\* =  $p < 0.01$ ; \*\*\* =  $p < 0.001$ ; \*\*\*\* =  $p < 0.0001$ .

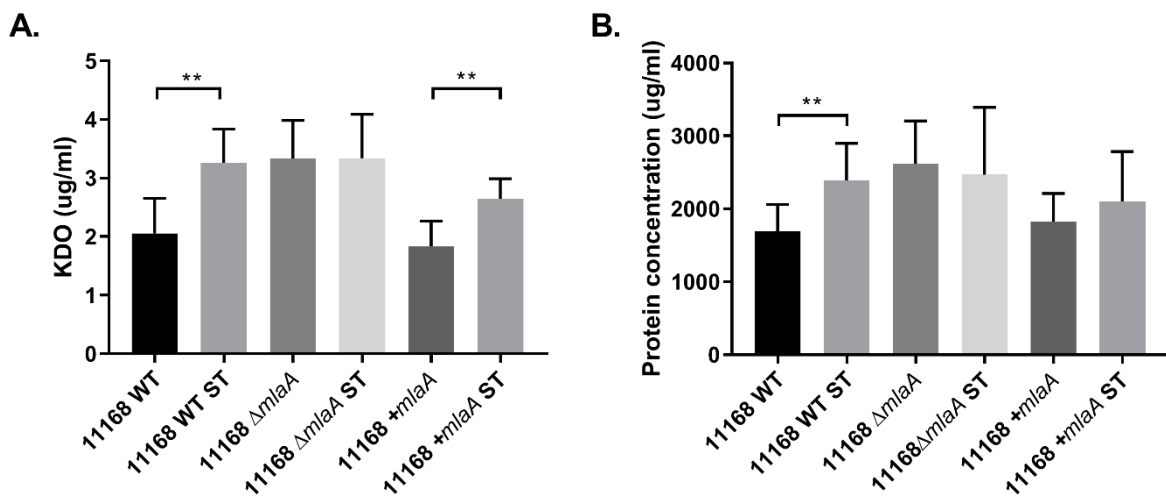


**Figure 5.** The presence of a biologically relevant concentration of ST increases OMV production in *C. jejuni* wild-type strain but not in the *m laA* mutant. OMVs were isolated from late-log phase *C. jejuni* cultures grown in Brucella broth either in the presence or absence of 0.2% (w/v) ST. OMV and ST-OMV preparations from cultures of *C. jejuni* wild-type, *m laA* and mutant and complement strains of equivalent OD<sub>600</sub> values were quantified by analysing (A) total KDO as a measurement of LOS and (B) total protein. \*\* =  $p < 0.01$ .

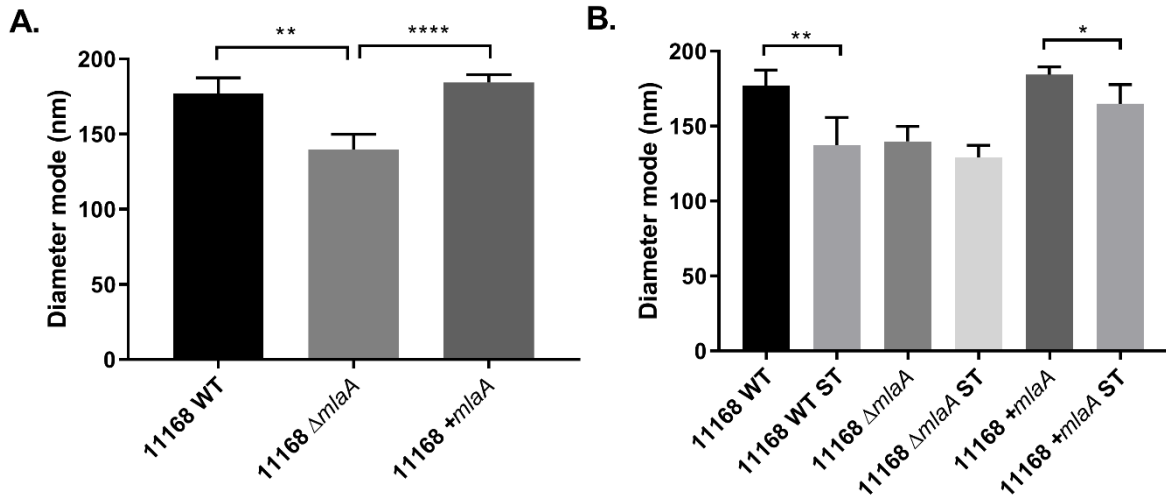


**Figure 6.** Mutation of *mlaA* or ST exposure increase OMV particle numbers not OMV size. OMVs were isolated from late-log phase *C. jejuni* cultures grown in Brucella broth either in the presence or absence of 0.2% (w/v) ST. OMV preparations from cultures of *C. jejuni* wild-type, *mlaA* mutant and complement strains of equivalent OD<sub>600</sub> values were sized by NTA using a PMX 110 ZetaView instrument. **(A)** OMV mode diameter, **(B)** OMV compared to ST-OMV mode diameter. \* =  $p < 0.05$ ; \*\* =  $p < 0.01$ ; \*\*\*\* =  $p < 0.0001$ .

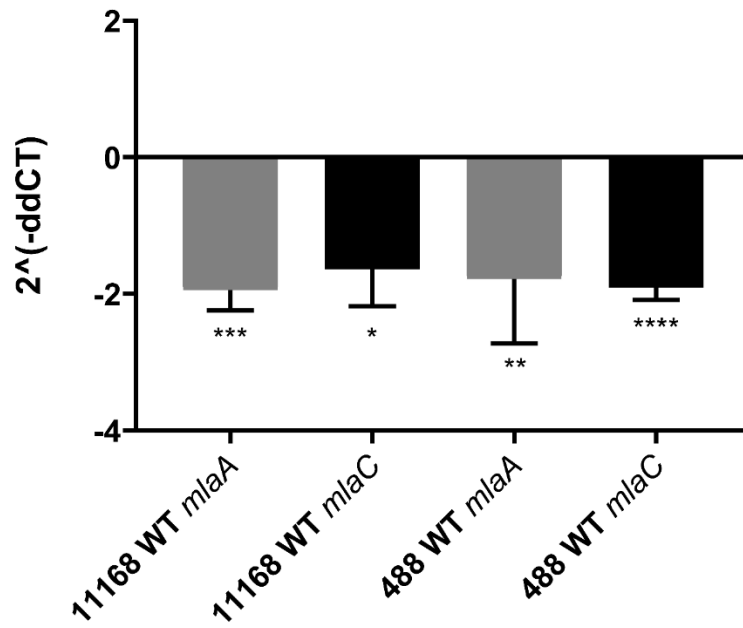


**Figure 7.** qRT-PCR analysis of *mlaA* and *mlaC* transcription in *C. jejuni* 11168 and 488 wild-type strains co-incubated with 0.2% (w/v) ST. Analysis was performed using *mlaA*, *mlaC* and *rpoA* gene specific primers. *rpoA* was used as an internal control.  $2^{(-ddCT)}$  = fold change in gene expression compared to *C. jejuni* grown in the absence of ST.

Note: Error in publication figure, axis is absolute fold change and the value 0 should read 1 on the Y-axis.

## Supplementary data

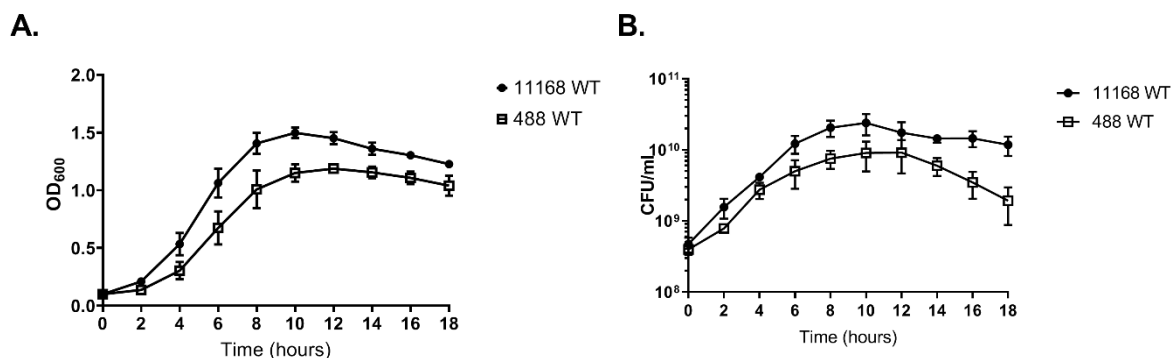


**Figure S1.** Growth curves of *C. jejuni* 11168 wild-type strain compared to the 488 wild-type strain. Strains were grown in Brucella broth under microaerobic conditions at 37°C. Growth was characterised by measuring **(A)** OD<sub>600</sub> values and **(B)** colony forming units (CFUs) every two hours for 18 hours.

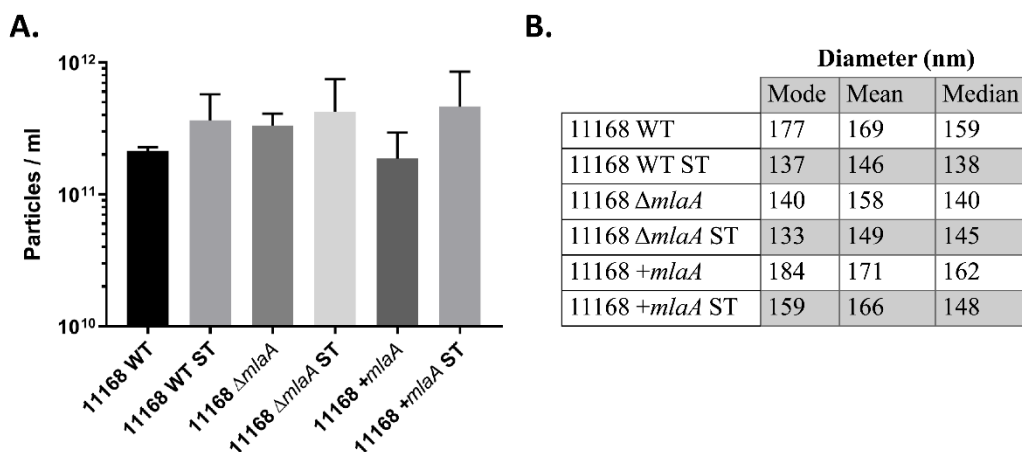


**Figure S2.** Mutation of *mlaA* or ST exposure increase OMV particle numbers not OMV size. OMVs were isolated from late-log phase *C. jejuni* cultures grown in Brucella broth either in the presence or absence of 0.2% (w/v) ST. OMV preparations from cultures of *C. jejuni* wild-type, *mlaA* mutant and complement strains of equivalent OD<sub>600</sub> values were sized by NTA using a PMX 110 ZetaView instrument. **(A)** Particle counts per ml and **(B)** OMV mode diameter, mean and median diameters (nm).

## Tables

**Table 1.** Primers used in this study. GS = gene specific; ISA = isothermal assembly; pRRA = *C. jejuni* complementation vector; pCJC1 = *C. jejuni* complementation vector; qRT = quantitative reverse transcription PCR.

Primer name	Primer sequence 5'-3'	Source
GSmlaA(F)	TAGGAGTTTTTGCTGAG	This study
GSmlaA(R)	GCTAAGTTCATTGCGTC	This study
ISAmIaA(F1)	GAGCTCGGTACCCGGGGATCCTCTAGAGTCTGGCACTACAATAAATAAGG	This study
ISAmIaA(R1)	AAGCTGTCAAACATGAGAACCAAGGAGAATGTTTTGGTATTCTTGTTCAA	This study
ISAmIaA(F2)	GAATTGTTTTAGTACCTAGCCAAGGTGTGCATTTATATCCATTCTTGCGT	This study
ISAmIaA(R2)	AGAATACTCAAGCTTGCATGCCTGCAGGTCGCCAGTTGTTATTATCATG	This study
pCJC1mlaA(F)	CCCCCATGGTTTTAGGAGTTTTTGCTGAGAATAAAATTTATATC	This study
pCJC1mlaA(R)	CCCGCTAGCTTATTGCTAAGTTCATTG	This study
pRRAmIaA(F)	ACACTCTAGATTTAGGAGTTTTTGCTTG	This study
pRRAmIaA(R)	ACACCAATTGGATTAATAAATATTTTTTTCATTAA	This study
qRTmlaA(F)	GATCCTACTTGGGCAAGTATAGC	This study
qRTmlaA(R)	ATGCTTACGAGCAAAGACGCAATG	This study
qRTmlaC(F)	CCACTTCTATGGTAGTAGATGGG	This study
qRTmlaC(R)	GTAGGGCATCAAAGCCTTGGTT	This study
rpoA(F)	CGAGCTTGCTTTGATGAGTG	Ritz <i>et al.</i> 2009
rpoA(R)	AGTCCCACAGGAAAACCTA	Ritz <i>et al.</i> 2009

## Chapter Four: RNA-Seq analysis of the transcriptional response of *C. jejuni* to the bile salts sodium taurocholate and sodium deoxycholate

Contribution of others:

RNAs-Seq bioinformatic analysis was performed by Dr Umer Zeeshan Ijaz at the University of Glasgow.

Figure 4.3 and Figures 4.5-4.10 were produced by Dr Umer Zeeshan Ijaz during bioinformatic analysis

### 4.1 Introduction

An important feature of a pathogen is the ability to sense the environment and appropriately alter and co-ordinate the regulation of virulence or survival factors. In other enteric pathogens, compounds present in the gut such as bile salts and mucin have been shown to play a role in the upregulation of virulence factors. For example *V. cholerae* AcfC (Accessory Colonisation Factor C) is thought to be a sulphate binding protein that senses mucin in the gut and plays a role in co-ordinating chemotaxis towards intestinal mucin (Valiente *et al.*, 2018). ST, which is a bile salt found in the human gut, has been shown to cause upregulation of virulence factors in *V. cholerae* by instigating alterations in disulphide bond formation in the regulatory protein TcpP (transmembrane transcription factor) (Yang *et al.*, 2013). *Vibrio parahaemolyticus* has been shown to upregulate expression of VPI (*Vibrio* Pathogenicity Island) genes, which include a T3SS, in response to crude bile (Gotoh *et al.*, 2010). Crude bile was also demonstrated to cause altered expression of 61 genes in enterotoxigenic *E. coli* (ETEC), including the putative virulence factor CexE which is thought to play a role in colonisation (Joffre *et al.*, 2019; Rivas *et al.*, 2020).

SDC has been shown to play a role in virulence of *C. jejuni*. Malik-Kale *et al.* (2008) observed upregulation of virulence genes such as *ciaB*, *cmeABC*, *dccR* and *tlyA* for *C. jejuni* grown in the presence of SDC. SDC has also been previously shown to increase the promoter activity of *flaA* (Allen and Griffiths, 2001) which encodes a component of the flagella filament and plays a role in chick colonisation (Wassenaar *et al.*, 1993; Jones *et al.*, 2004). Previous work by our group has demonstrated a link between the bile salt ST and the upregulation of OMV production, which have been shown to contain virulence associated cargo such as the cytolethal distending toxin (CDT) and virulence associated proteases (Elmi *et al.*, 2018; Davies *et al.*, 2019).

The aim of this chapter was to further characterise the interaction of *C. jejuni* with bile salts and identify key genes as a starting point for further hypothesis driven research. The transcriptional response of the wild-type 11168H and 488 strains to biologically relevant concentrations of the bile

salts ST and SDC was investigated by RNA-Seq. Bile salts can cause cell stress, such as oxidative stress and membrane damage (Negretti *et al.*, 2017). The transcriptional response of mid-log phase cultures was analysed to avoid inclusion of stress response pathways induced due to the accumulative effect of stresses encountered during late stages of growth. To improve identification of differentially expressed genes, RNA-Seq data was analysed using a combination of unsupervised (DESeq) (Love *et al.*, 2014) and supervised (sPLS-DA) (Kim-Anh Le Cao *et al.*, 2016) analysis methods.

## 4.2 Results

### 4.2.1 Experimental design

To determine the optimal timepoint to sample for mid-log growth phase, growth kinetics of each strain were characterised (Figure 4.1). Previous studies have demonstrated that 0.2% (w/v) ST and 0.05% (w/v) SDC are sufficient to cause transcriptional changes (Malik-Kale *et al.*, 2008; Negretti *et al.*, 2017; Elmi *et al.*, 2018; Davies *et al.*, 2019). However, the transcriptional response to growth in the presence of bile salts has been shown to be both dose dependent and time dependent, with the magnitude of fold change increasing with time and concentration up until a break-point is reached (Malik-Kale *et al.*, 2008; Elmi *et al.*, 2018). Prior to RNA-Seq analysis, the selected timepoint and treatment concentrations were screened by qRT-PCR. The upregulation of *cmeB* in *C. jejuni* is a well characterised transcriptional response to the presence of bile salts (Lin *et al.*, 2005a; Malik-Kale *et al.*, 2008; Clark *et al.*, 2014). Expression of *cmeB* at mid-log phase growth, in the presence or absence of either 0.2% (w/v) ST or 0.05% (w/v) SDC was analysed. Six hours was selected as the mid-log timepoint for both strains as this was approximately half the time taken to reach peak growth. *cmeB* was significantly upregulated in both wild-type strains when grown in the presence of either bile salt. In the presence of 0.2% (w/v) ST, there was greater than 2-fold upregulation of *cmeB* in both 11168H and 488 strains. In the presence of 0.05% (w/v) SDC, there was 2.7 and 1.6-fold upregulation in 11168H and 488 strains respectively (Figure 4.2).

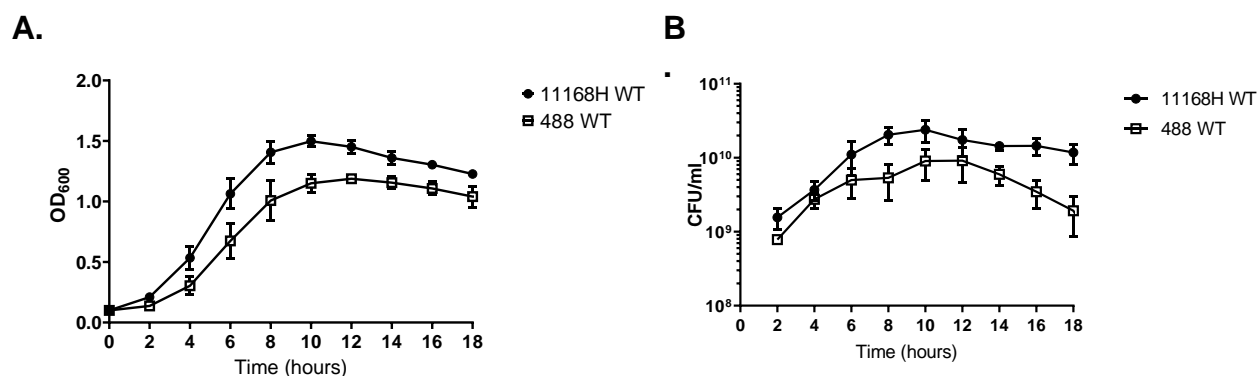


**Figure 4.1.** Growth curves of *C. jejuni* 11168H wild-type strain compared to the 488 wild-type strain. Strains were grown in Brucella broth under microaerobic conditions at 37°C. Growth was characterised by measuring OD<sub>600</sub> values (**A**) and colony forming units (CFU/ml) (**B**) every two hours for 18 hours.

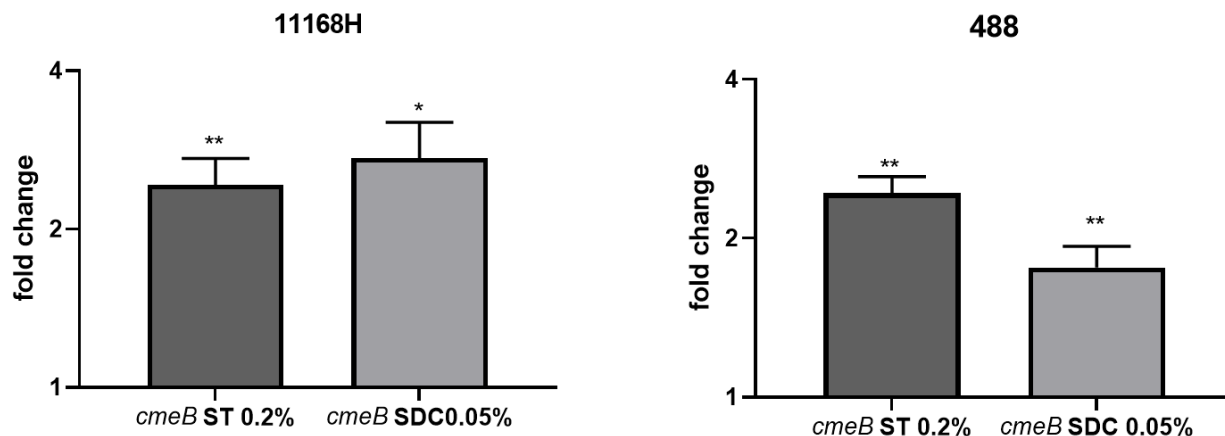


**Figure 4.2.** qRT-PCR analysis of *cmeB* transcription in *C. jejuni* 11168H and 488 wild-type strains co-incubated with 0.2% (w/v) ST or 0.05% (w/v) SDC. *rpoA* was used as an internal control. \*  $p < 0.05$ ; \*\*  $p < 0.01$ .

#### 4.2.2 Biologically relevant concentrations of sodium taurocholate or sodium deoxycholate did not cause significant changes to the overall transcriptional profile of wild-type strains.

RNA was extracted from mid-log phase cultures of the 11168H wild-type and 488 wild-type strains grown in Brucella broth or Brucella broth supplemented with either 0.2% (w/v) ST or 0.05% (w/v) SDC. mRNA libraries from seven biological replicates were constructed using the TruSeq Stranded mRNA Library Preparation Kit from rRNA depleted RNA as described in Section 2.5.9.3. Comparisons of transcriptional profiles were made between *C. jejuni* grown in Brucella broth without supplementation (the reference group) and *C. jejuni* grown in the presence of either 0.2% (w/v) ST or 0.05% (w/v) SDC (the treatment groups). Beta diversity of the reference group compared to each of the treatment groups was visualised with ordination plots generated by Principal Coordinates Analysis (PCoA). PCoA ordered individual samples based on the global transcriptional profiles of each sample. The significance of differences in transcription profiles was analysed by permutational multivariate analysis of variance (PERMANOVA) which gives the percentage variability explained in the transcript structure in terms of metadata provided, such as treatment condition. The clustering of treatment groups overlapped with that of the reference groups (Figure 4.3) and there was no significant difference in transcriptional profiles between the reference condition and each of the treatment conditions for both *C. jejuni* 11168H and 488 strains. For the 11168H wild-type reference condition compared to ST 0.2% (w/v) and SDC 0.05% (w/v),  $p = 0.575$  and  $p = 0.833$  respectively. For the 488

wild-type reference compared to ST 0.2% (w/v) and SDC 0.05% (w/v),  $p = 0.496$  and  $p = 0.821$  respectively.

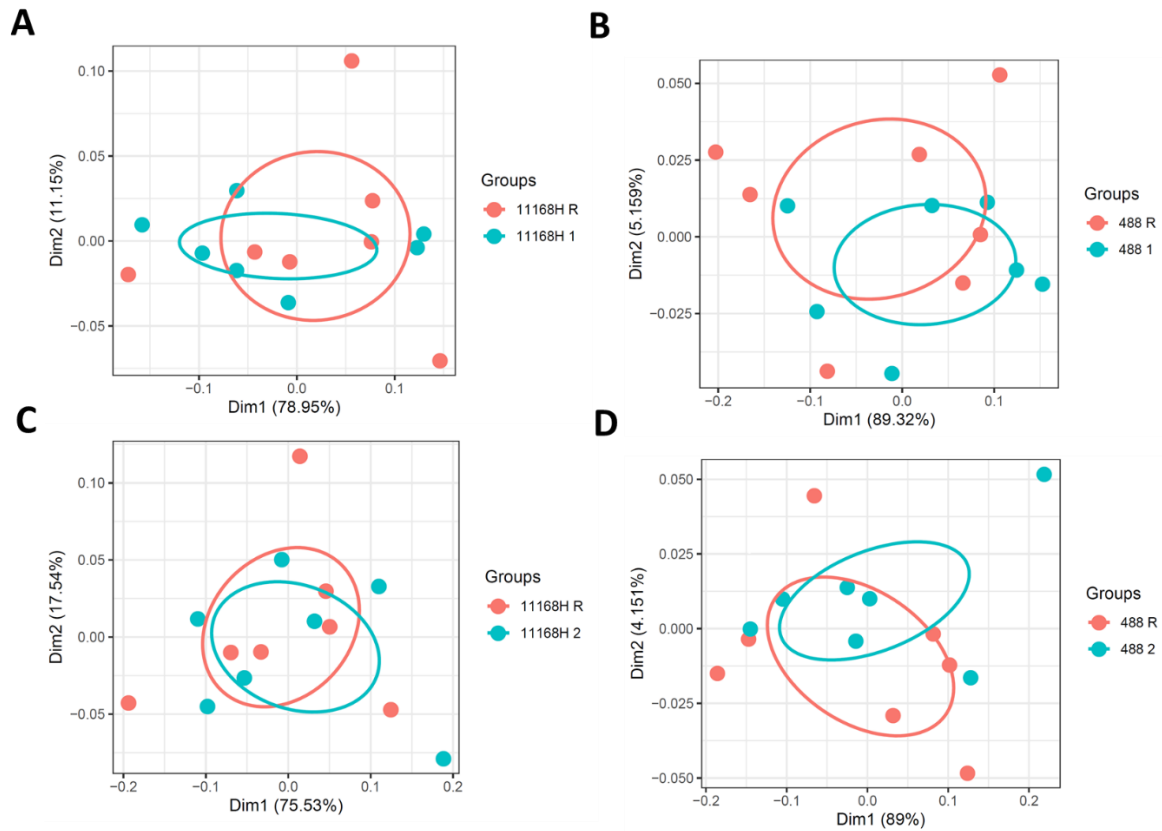


**Figure 4.3.** PCoA analysis of the transcriptional profiles of *C. jejuni* wild-type strains in the presence or absence of biologically relevant concentrations of bile salts. **(A)** 11168H wild-type reference condition compared to treatment with 0.2% (w/v) ST. **(B)** 488 wild-type reference condition compared to treatment with 0.2% (w/v) ST. **(C)** 11168H wild-type reference condition compared to treatment with 0.05% (w/v) SDC. **(D)** 488 wild-type reference condition compared to treatment with 0.05% (w/v) SDC. The X axis represents the variation explained by principal component 1 and the Y axis represents the variation explained by principal component 2. R refers to reference condition. 1 refers to treatment condition 1, 0.2% (w/v) ST. 2 refers to treatment condition 2, 0.05% (w/v) SDC.

#### 4.2.3 Differentially expressed genes identified by DESeq analysis.

Surprisingly there were no significant differences in the global transcriptional profile of the treatment groups (Section 4.2.2), however there was a significant upregulation of *cmeB* under treatment conditions as shown in Figure 4.2. Differential expression of individual genes was analysed by DESeq in R using the DESeq2 package (Love *et al.*, 2014). Changes in expression were considered significant when  $p < 0.05$  and the log-fold change was greater than 1. Each DESeq comparison included seven

reference samples and seven test samples, either ST or SDC treated, totalling 14 samples. No biological replicates were excluded as outliers and the final analysis was run using a LOO cross validation step where for 14 samples, the model was trained by excluding one sample at a time to improve the reliability of genes identified as differentially expressed and to account for between replicate variability that could mask some differentially expressed genes. The frequency of each gene appearing as differentially expressed was recorded as percent stability (Table 4.1). The MA plot for each replicate can be found in Appendix 2-5. Genes identified as differentially expressed by DESeq are shown in Table 4.1. *cmeABC* and *Cj0561c* were identified as significantly upregulated under both test conditions for both strains. *cmeB* was also identified as differentially expressed by qRT-PCR during the pre-RNASeq condition screen (Figure 4.2). *cmeABC* had similar levels of upregulation in response to both bile salts, however *Cj0561c* appeared to show a stronger transcriptional response to ST compared to SDC for both wild-type strains (Figure 4.4).

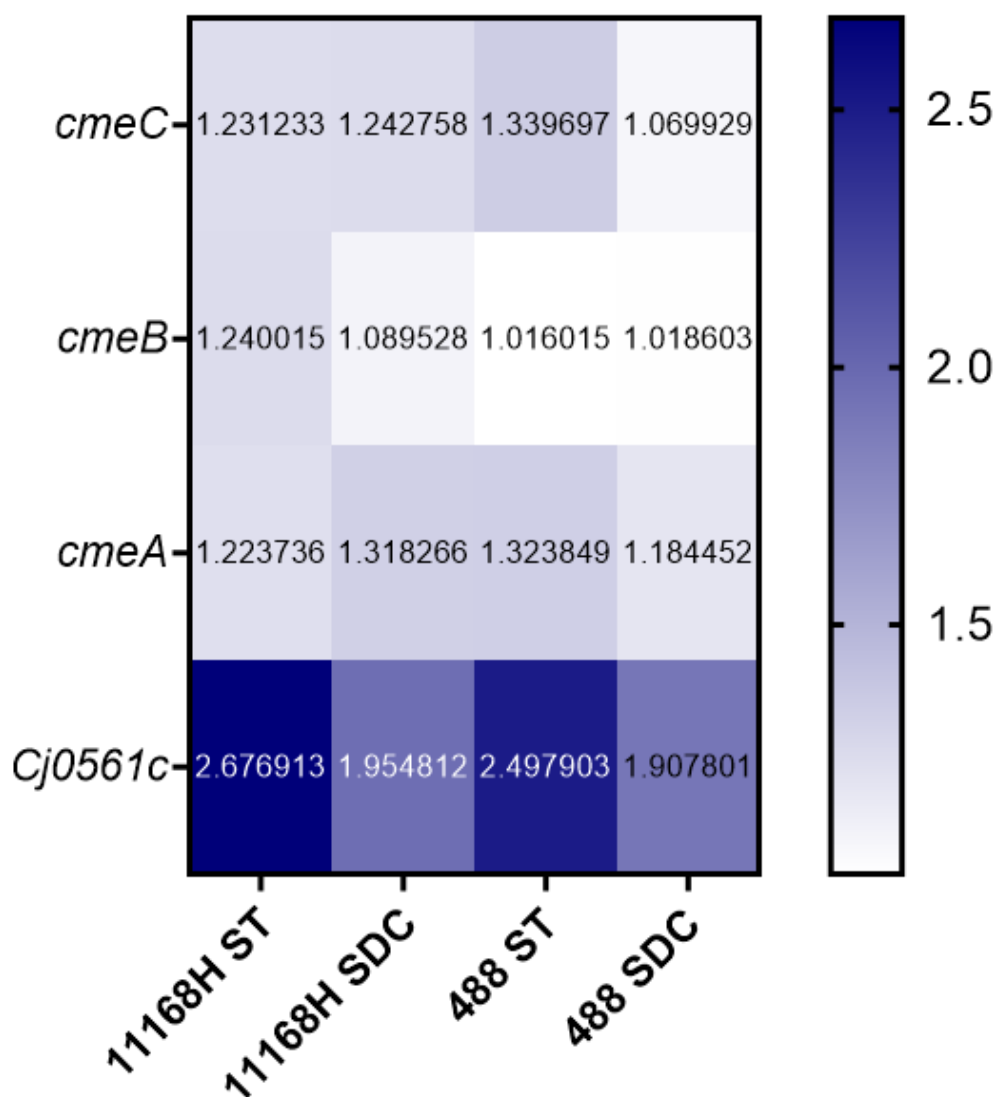


**Figure 4.4.** Heat map showing the mean fold change in expression of *cmeABC* and *Cj0561c* for the 11168H and 488 wild-type strains when grown in the presence of either 0.2% (w/v) ST or 0.05% (w/v) SDC to mid-log phase growth. Figures are based on DESeq analysis results.

A cut-off value of 85% stability was set for differentially expressed genes. This percentage cut-off value requires a gene to be identified in a minimum of 12 out of 14 combinations. After exclusion of differentially expressed genes with stability values less than 85%, the number of total genes identified were one gene (*Cj0561c*) for 11168H reference compared to ST; three genes (*Cj0561c*, *cmeA* and *cmeC*) for 488 reference compared to ST; one gene (*cmeA*) for 11168H reference compared to SDC and one gene (*Cj0561c*) for 488 reference compared to SDC. Certain genes, such as those encoding components of the *cmeABC* transporter, that were excluded due to low stability do have biological

significance (Lin *et al.*, 2005a; Malik-Kale *et al.*, 2008; Clark *et al.*, 2014). This indicated that not all genes with biological significance had been identified by DESeq.

**Table 4.1.** Genes identified by DESeq analysis of RNA-Seq data as being differentially expressed in 11168H or 488 wild-type strains grown in the presence of 0.2% (w/v) ST or 0.05% (w/v) SDC compared to cells grown in the absence of bile salt treatment.

Strain	Treatment	Gene	Locus	Product	Regulation	Stability %	Fold change	padj
11168H	0.2% ST	<i>Cj0561c</i>	Cj0561c	Putative periplasmic protein	+	100.00	2.68	3.21E-07
		<i>cmeA</i>	Cj0367c	Multidrug efflux pump protein CmeA	+	64.29	1.22	0.037
		<i>cmeC</i>	Cj0365c	Multidrug efflux pump protein CmeC	+	14.29	1.24	0.335
		<i>cmeB</i>	Cj0366c	Multidrug efflux pump protein CmeB	+	7.14	1.21	0.465
488	0.2% ST	<i>Cj0561c</i>	Cj0561c	Putative periplasmic protein	+	100.00	2.50	2.71E-08
		<i>cmeC</i>	Cj0365c	Multidrug efflux pump protein CmeC	+	100.00	1.34	0.001
		<i>cmeA</i>	Cj0367c	Multidrug efflux pump protein CmeA	+	100.00	1.32	0.009
		<i>Cj1687</i>	Cj1687	Putative efflux protein	+	21.43	1.48	0.173
		<i>cmeB</i>	Cj0366c	Multidrug efflux pump protein CmeB	+	7.14	1.02	0.063
11168H	0.05% SDC	<i>cmeA</i>	Cj0367c	Multidrug efflux pump protein CmeA	+	100.00	1.32	0.002
		<i>metB</i>	Cj1727c	Putative O-acetylhomoserine (Thiol)-lyase	-	57.14	-1.75	0.044
		<i>Cj0561c</i>	Cj0561c	Putative periplasmic protein	+	35.71	1.48	0.173
		<i>metA</i>	Cj1726c	Homoserine O-acetyltransferase	-	28.57	-1.32	0.181
		<i>cmeC</i>	Cj0365c	Multidrug efflux pump protein CmeC	+	14.29	1.24	0.200
		<i>cmeB</i>	Cj0366c	Multidrug efflux pump protein CmeB	+	7.14	1.09	0.425
		<i>Cj1199</i>	Cj1199	Putative iron/ascorbate-dependent oxidoreductase	-	7.14	-1.67	0.888
		<i>metE</i>	Cj1202	Methylenetetrahydrofolate reductase	-	7.14	-1.11	0.875
488	0.05% SDC	<i>Cj0561c</i>	Cj0561c	Putative periplasmic protein	+	92.86	1.91	4.91E-06
		<i>cmeB</i>	Cj0366c	Multidrug efflux pump protein CmeB	+	42.86	1.00	0.081
		<i>cmeC</i>	Cj0365c	Multidrug efflux pump protein CmeC	+	35.71	1.05	0.085
		<i>cmeA</i>	Cj0367c	Multidrug efflux pump protein CmeA	+	35.71	1.17	0.094
		<i>Cj1308</i>	Cj1308	Putative acyl carrier protein	-	7.14	-1.14	0.586

Genes were identified as significant when the log-fold change was greater than 1 and  $p < 0.05$ . Analysis was performed with a LOO cross validation repeated 14 times. Stability represents the frequency that a gene was identified as significant during the cross validation. + or – represents up or down regulation in response to treatment. Fold change values and adjusted p-values (padj) presented represent the mean obtained from all 14 cross validation repeats.

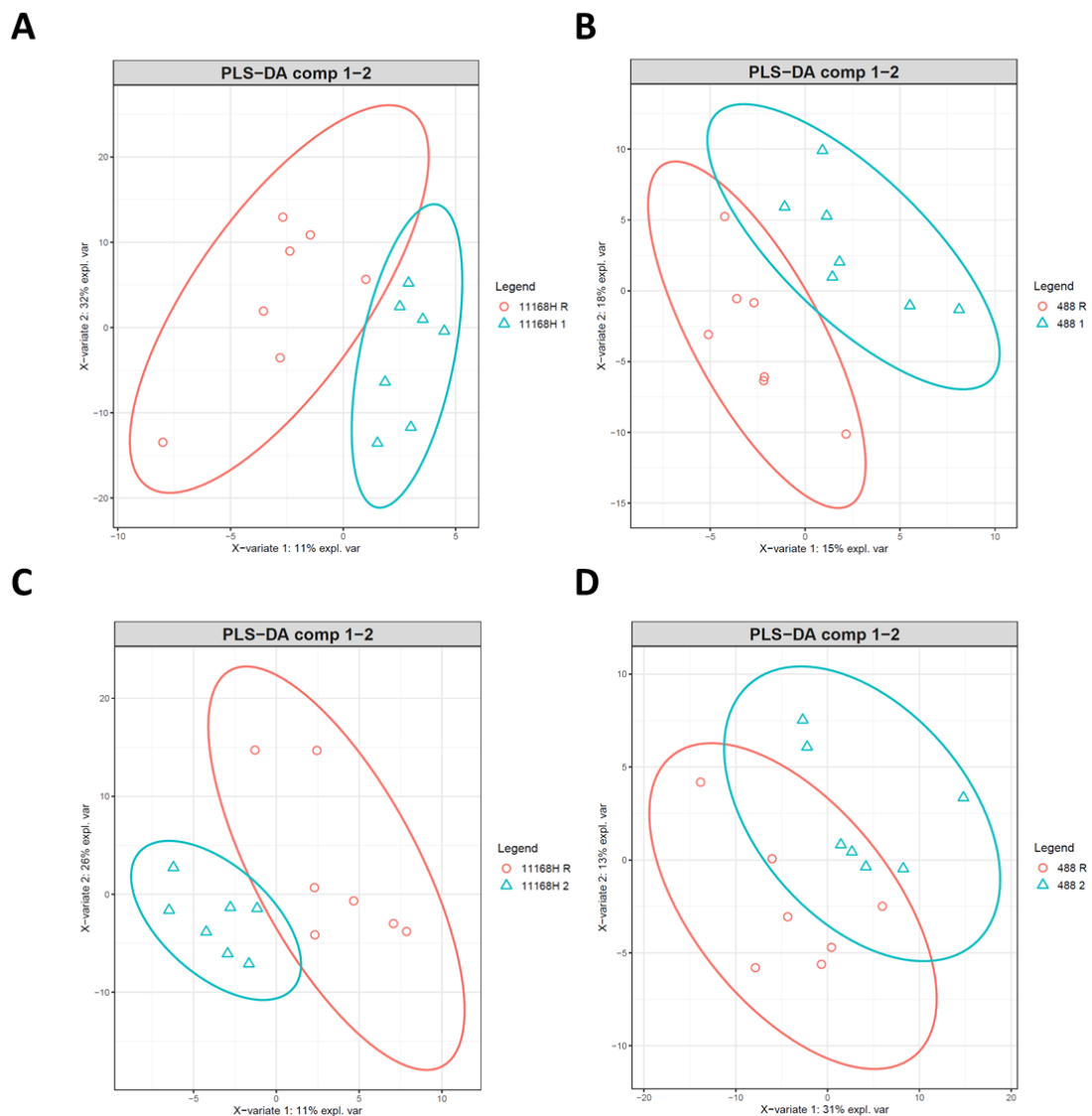
#### 4.2.4 Differentially expressed genes identified by SPLS-DA

As genes with biological significance failed to meet the criteria for identification by DESeq analysis, an alternative discriminatory approach was used. We employed Sparse Partial Least Square-Discriminant Analysis (sPLS-DA) from the mixOmics package for R (Kim-Anh Le Cao *et al.*, 2016; Rohart *et al.*, 2017). This was performed with the intention of removing analytical biases associated with the method. sPLS-DA is a supervised analysis of the RNA-Seq dataset to identify key discriminating factors (genes) between conditions by fitting principal components in both data space as well as by their labelling (reference or treatment) which is simplified as a present/absence matrix to be utilised in the mathematical formulation. The analysis optimises the covariance between scores (data and label), with scores being the distance on principal axis on centred data. Next, sPLS-DA has an L1 penalty constraint built in the optimisation function via LASSO (Least Absolute Shrinkage and Selection Operator) regression to enforce some of the components of the principal axis to go to zero (these are the weights for each gene), thus creating a sparse dataset (Lê Cao *et al.*, 2011). The discriminant factors were then visualised as loading plots which depict the loading weight of each remaining discriminant gene in the sparse dataset and indicating the sample group where the expression was highest.

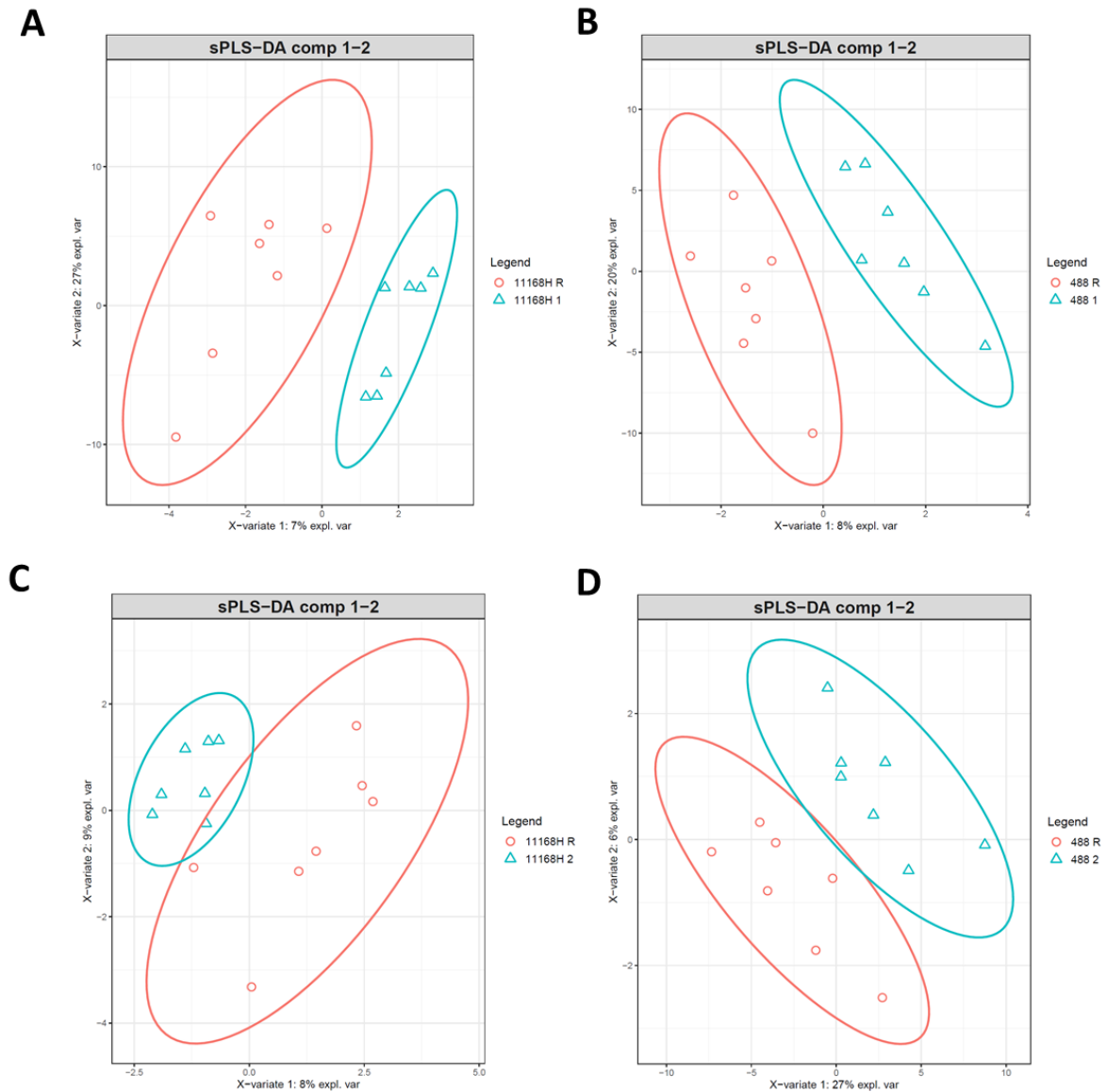
The mixOmics package requires the samples to be pre-normalised and recommends a pre-filtering step to remove consistently low read counts to reduce the computational time. Initially, analysis was performed with a prefiltering step which removed the lowest 1% of read counts. This resulted in sample group clusters that overlapped for both Partial Least Square-Discriminant Analysis (PLS-DA) and sPLS-DA (Figures 4.5-4.6) and there were no common genes identified by both sPLS-DA and DESeq. Genes identified by DESeq had low read counts in comparison to the genes identified by sPLS-DA with the prefiltering step. As the differentially expressed genes identified by DESeq analysis were lowly expressed genes relative to the genes identified by sPLS-DA, the analysis was repeated without the prefiltering step to remove low read counts. This resulted in better separation of sample groups by both PLS-DA and sPLS-DA (Figure 4.7-4.8) and correlated with genes identified previously by DESeq (Tables 4.2-4.5 and Figures 4.9-4.10).

sPLS-DA was run using a LOO cross validation to be consistent with DESeq analysis. The frequency of each gene appearing as differentially expressed was recorded as percent stability. A cut-off value of 85% stability was set for differentially expressed genes. Only genes that met either the frequency stability cut-off, or genes identified by both analysis methods were included in the final list of differentially expressed genes (Table 4.6). Prior to filtering differentially expressed genes based on the stability of identification, sPLS-DA identified a total of 25 genes for the 11168H wild-type in the

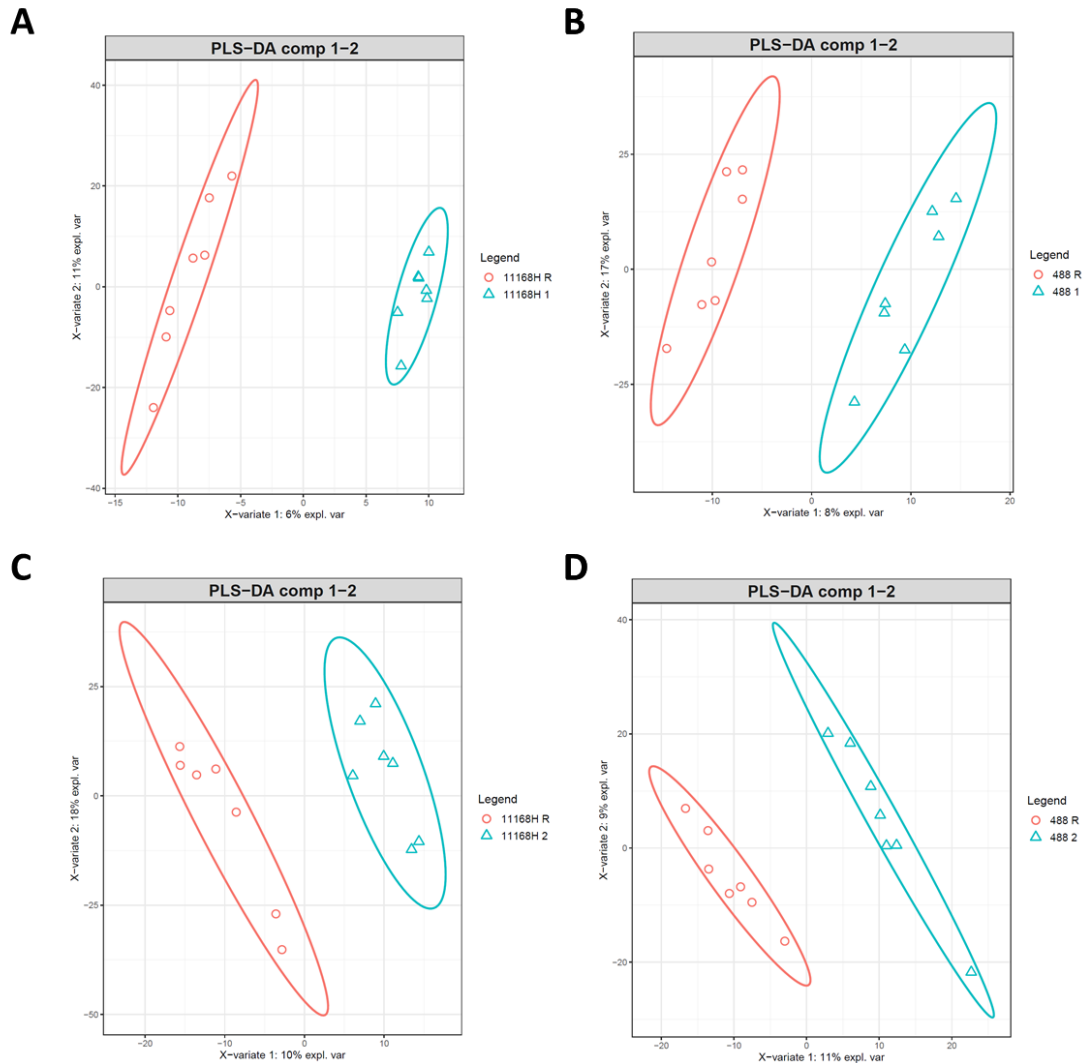
presence of ST and 10 genes in the presence of SDC, of which three genes and one gene were common to both analysis methods for ST and SDC respectively. sPLS-DA identified a total of 15 genes for the 488 wild-type in the presence of ST and 10 genes in the presence of SDC, of which four genes and two genes were common to both analysis methods for ST and SDC respectively.



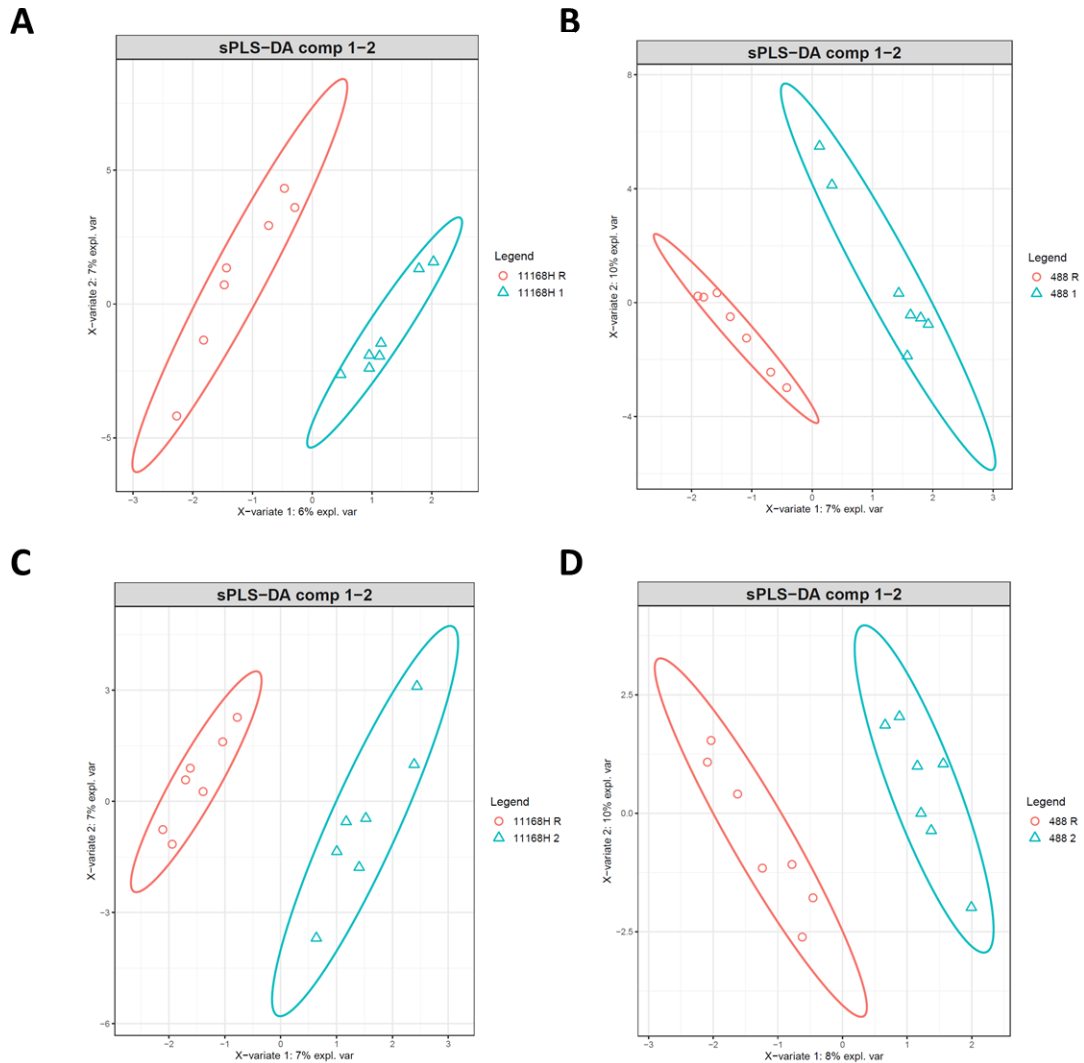
**Figure 4.5.** Clustering of reference and treatment groups by supervised analysis with PLS-DA, showing sample plots with confidence ellipse plots. Analysis was performed with a prefiltering step to remove low read counts. **(A)** 11168H wild-type reference condition compared to treatment with 0.2% (w/v) ST. **(B)** 488 wild-type reference condition compared to treatment with 0.2% (w/v) ST. **(C)** 11168H wild-type reference condition compared to treatment with 0.05% (w/v) SDC. **(D)** 488 wild-type reference condition compared to treatment with 0.05% (w/v) SDC. A prefiltering step to remove the bottom 1% of read counts was performed prior to analysis. R refers to reference condition. 1 refers to treatment condition 1, 0.2% (w/v) ST. 2 refers to treatment condition 2, 0.05% (w/v) SDC.



**Figure 4.6.** Clustering of reference and treatment groups by supervised analysis with discriminant feature selection by sPLS-DA, showing sample plots with confidence ellipse plots. Analysis was performed with a prefiltering step to remove low read counts. **(A)** 11168H wild-type reference condition compared to treatment with 0.2% (w/v) ST. **(B)** 488 wild-type reference condition compared to treatment with 0.2% (w/v) ST. **(C)** 11168H wild-type reference condition compared to treatment with 0.05% (w/v) SDC. **(D)** 488 wild-type reference condition compared to treatment with 0.05% (w/v) SDC. A prefiltering step to remove the bottom 1% of read counts was performed prior to analysis. R refers to reference condition. 1 refers to treatment condition 1, 0.2% (w/v) ST. 2 refers to treatment condition 2, 0.05% (w/v) SDC.



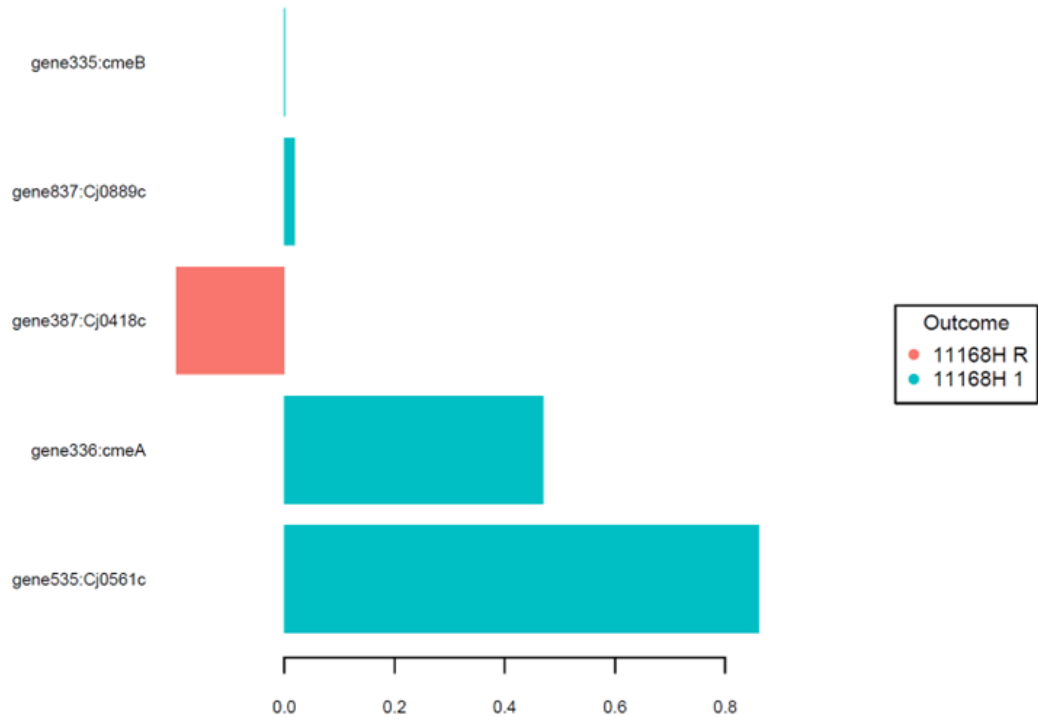
**Figure 4.7.** Clustering of reference and treatment groups by supervised analysis with PLS-DA, showing sample plots with confidence ellipse plots. Analysis was performed without a prefiltering step to remove low read counts **(A)** 11168H wild-type reference condition compared to treatment with 0.2% (w/v) ST. **(B)** 488 wild-type reference condition compared to treatment with 0.2% (w/v) ST. **(C)** 11168H wild-type reference condition compared to treatment with 0.05% (w/v) SDC. **(D)** 488 wild-type reference condition compared to treatment with 0.05% (w/v) SDC. R refers to reference condition. 1 refers to treatment condition 1, 0.2% (w/v) ST. 2 refers to treatment condition 2, 0.05% (w/v) SDC.

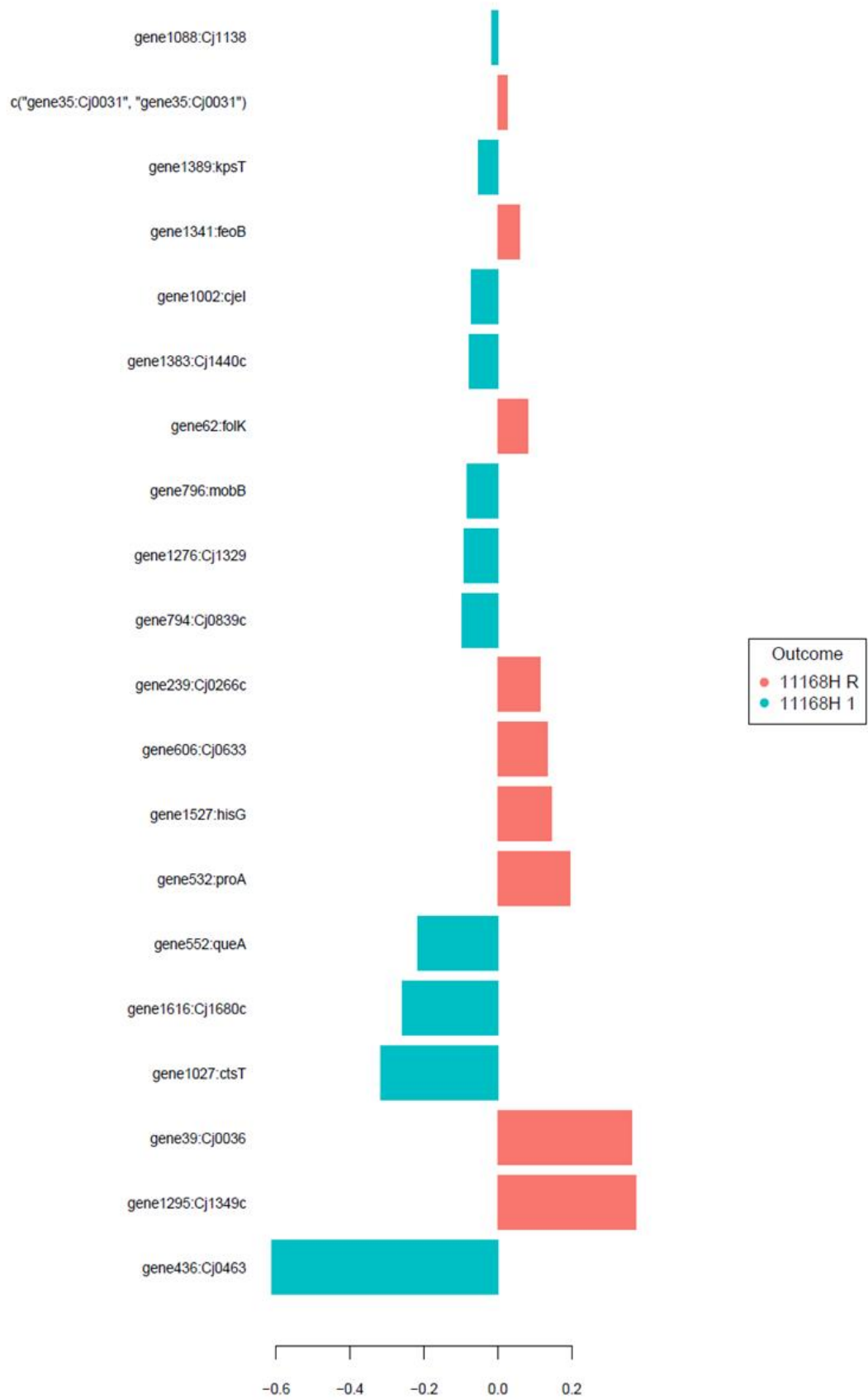


**Figure 4.8** Clustering of reference and treatment groups by supervised analysis with discriminant feature selection by sPLS-DA, showing sample plots with confidence ellipse plots. Analysis was performed without a prefiltering step to remove low read counts. **(A)** 11168H wild-type reference condition compared to treatment with 0.2% (w/v) ST. **(B)** 488 wild-type reference condition compared to treatment with 0.2% (w/v) ST. **(C)** 11168H wild-type reference condition compared to treatment with 0.05% (w/v) SDC. **(D)** 488 wild-type reference condition compared to treatment with 0.05% (w/v) SDC. R refers to reference condition. 1 refers to treatment condition 1, 0.2% (w/v) ST. 2 refers to treatment condition 2, 0.05% (w/v) SDC.

A

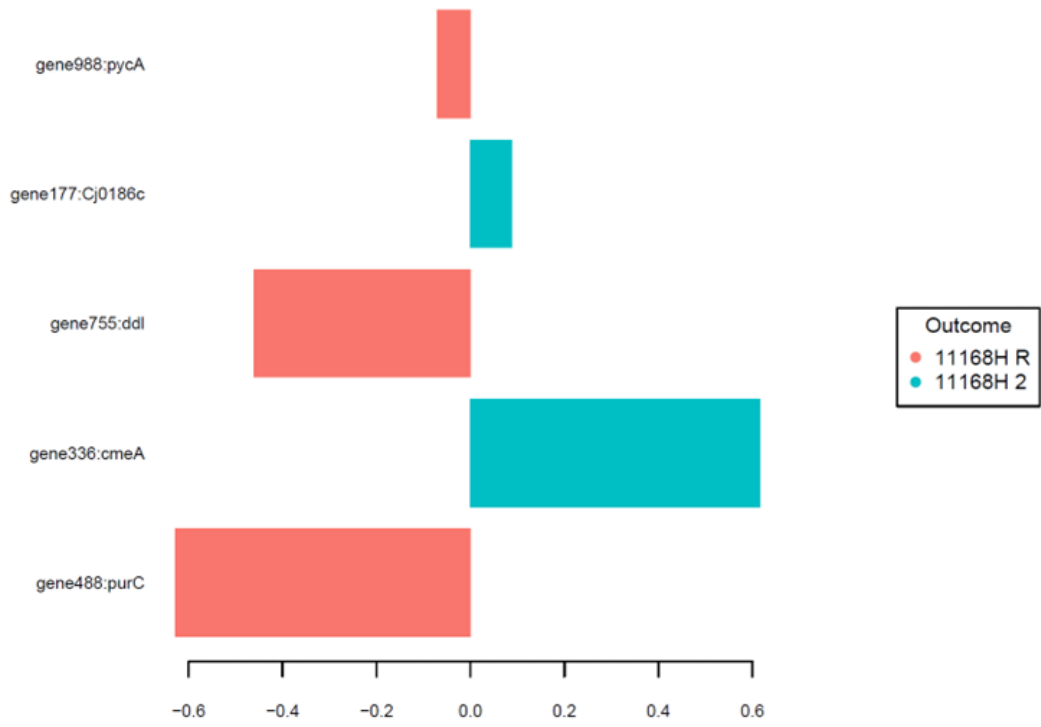
### sPLS-DA Loadings (comp1)

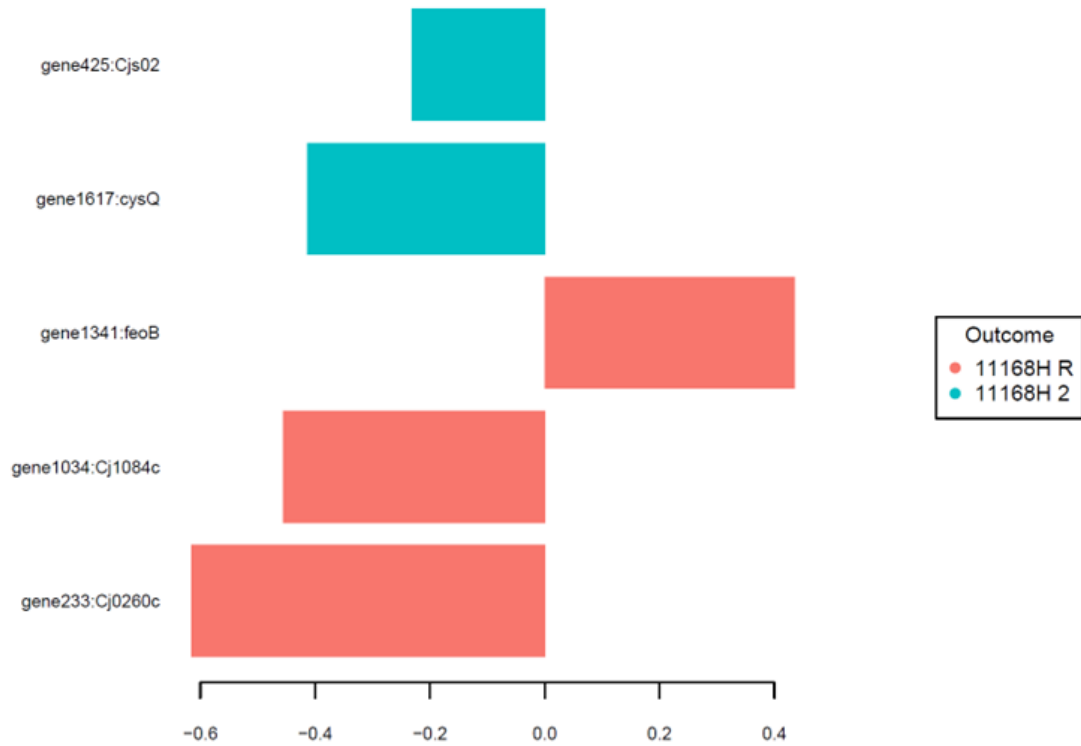


**B****sPLS-DA Loading (comp2)**

C

### sPLS-DA Loadings (comp1)

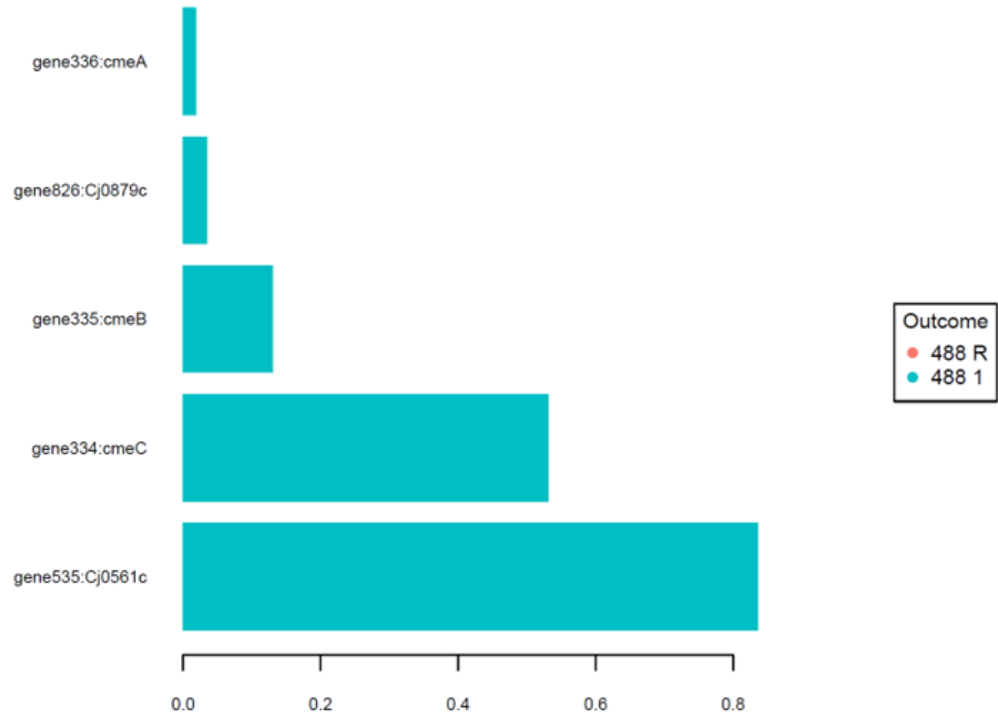


**D****sPLS-DA Loadings (comp2)**

**Figure 4.9.** Loading plot of key discriminant genes identified by sPLS-DA for the 11168H wild-type strain grown in the presence or absence of bile salts. **(A & C)** Loading plot of discriminant genes on the first component, accounting for the largest amount of variance in the dataset. **(B & D)** Loading plot of discriminant genes on the second component accounting for the second largest amount of variance in the data set. **(A & B)** Differential gene expression of the 11168H wild-type strain when grown in the presence of 0.2% (w/v) ST. **(C & D)** Differential gene expression of the 11168H wild-type strain when grown in the presence of 0.05% SDC. The colour of the bar indicates which condition the mean gene expression was greatest, red indicates a downregulation in response to bile salt treatment and blue indicates an increase in expression in response to bile salt treatment. The direction of the bar does not indicate up or downregulation, the length of the bar is an indication of magnitude of variation. The importance of each gene increases from top to bottom. Importance is determined by the loading weight of each gene, genes of greater importance have a greater influence on variation. R refers to reference condition. 1 refers to treatment condition 1, 0.2% (w/v) ST. 2 refers to treatment condition 2, 0.05% (w/v) SDC.

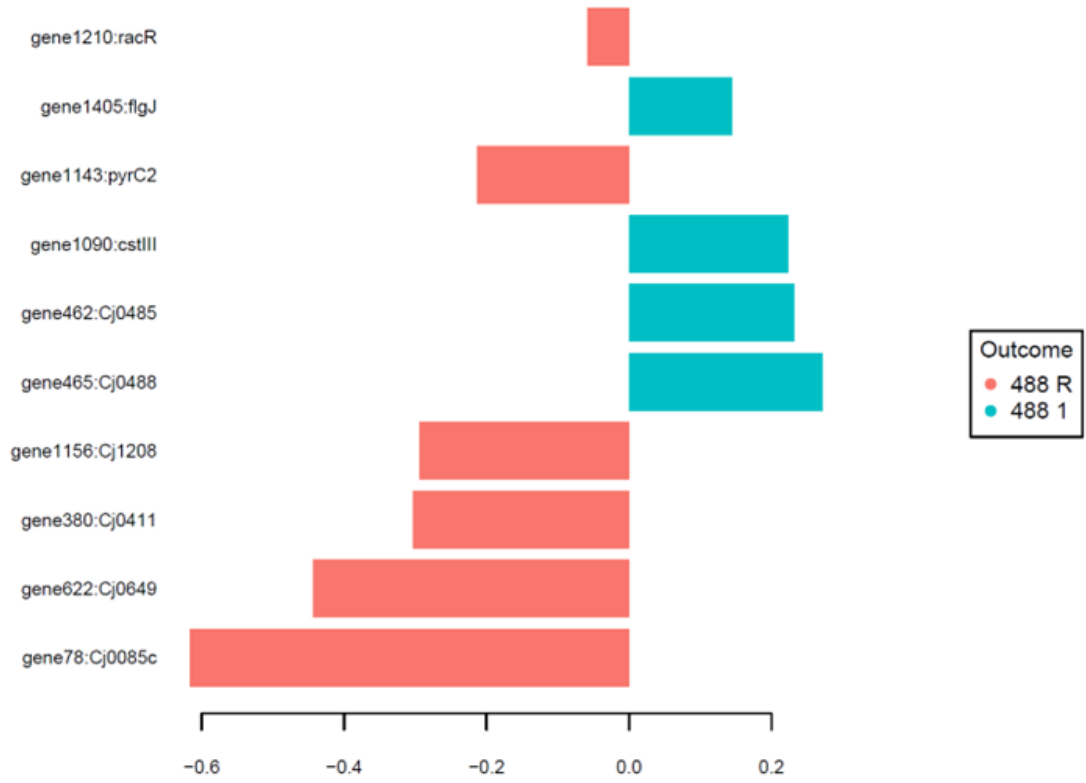
**A**

### sPLS-DA Loadings (comp1)



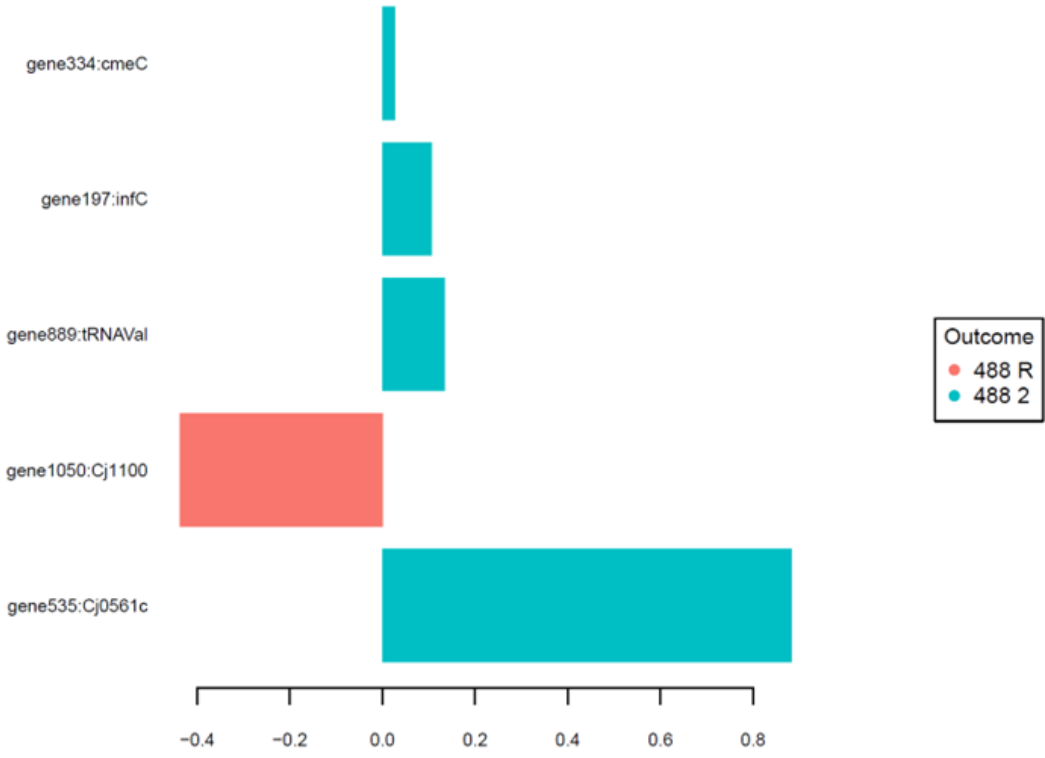
**B**

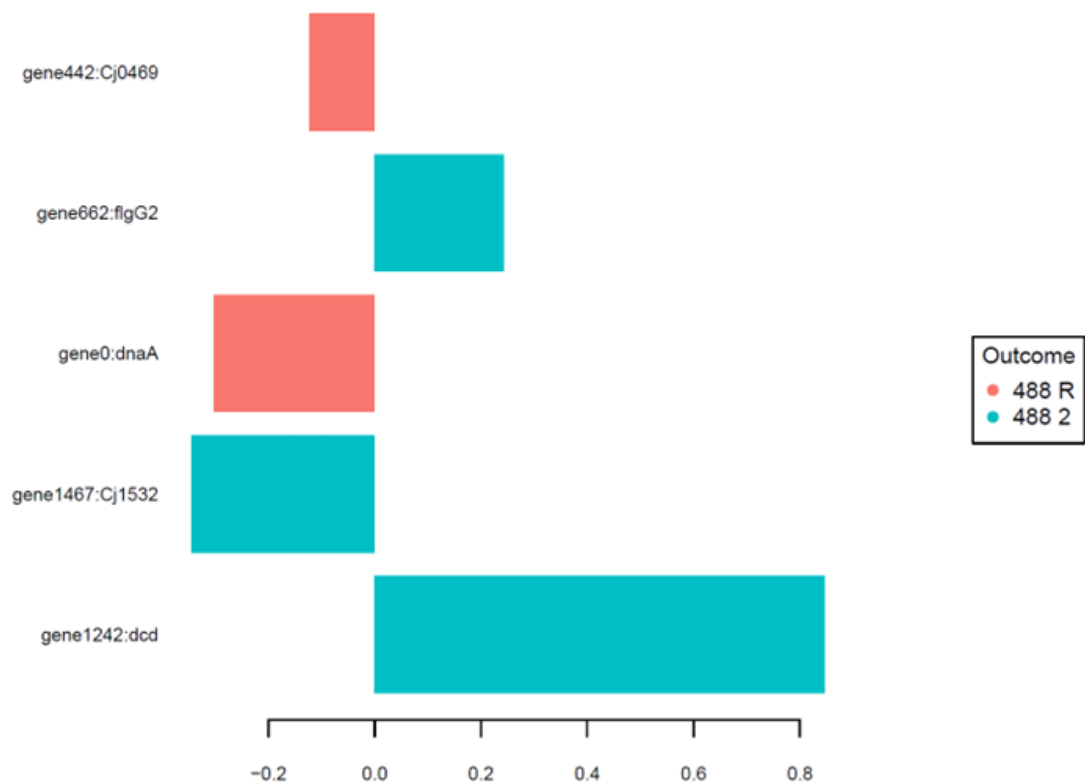
### sPLS-DA Loadings (comp2)



C

### sPLS-DA Loadings (comp1)



**D****sPLS-DA Loadings (comp2)**

**Figure 4.10.** Loading plot of key discriminant genes identified by sPLS-DA for the 488 wild-type strain grown in the presence or absence of bile salts. **(A & C)** Loading plot of discriminant genes on the first component, accounting for the largest amount of variance in the dataset. **(B & D)** Loading plot of discriminant genes on the second component accounting for the second largest amount of variance in the data set. **(A & B)** Differential gene expression of the 488 wild-type strain when grown in the presence of 0.2% (w/v) ST. **(C & D)** Differential gene expression of the 488 wild-type strain when grown in the presence of 0.05% SDC. The colour of the bar indicates which condition the mean gene expression was greatest, red indicates a downregulation in response to treatment and blue indicates an increase in expression in response to treatment. The direction of the bar does not indicate up or downregulation, the length of the bar is an indication of magnitude of variation. The importance of each gene increases from top to bottom. Importance is determined by the loading weight of each gene, genes of greater importance have a greater influence on variation. R refers to reference condition. 1 refers to treatment condition 1, 0.2% (w/v) ST. 2 refers to treatment condition 2, 0.05% (w/v) SDC.

**Table 4.2.** Genes identified by DESeq and sPLS-DA analysis of RNA-Seq data as being differentially expressed for the 11168H wild-type strain grown in the presence of 0.2% (w/v) ST compared to cells grown in the absence of bile salt treatment.

Gene	Locus	Product	DESeq		sPLS-DA		
			Regulation	Stability %	Component	Regulation	Stability %
<i>Cj0561c</i>	Cj0561c	Putative periplasmic protein	+	100.00	1	+	100.00
<i>cmeA</i>	Cj0367c	Multidrug efflux pump protein CmeA	+	64.29	1	+	100.00
<i>cmeB</i>	Cj0366c	Multidrug efflux pump protein CmeB	+	7.14	1	+	21.43
<i>cmeC</i>	Cj0365c	Multidrug efflux pump protein CmeC	+	14.29			
<i>Cj0418c</i>	Cj0418c	Hypothetical protein			1	-	85.71
<i>Cj0889c</i>	Cj0889c	Putative sensory transduction histidine kinase			1	+	42.86
<i>Cj0463</i>	Cj0463	Zinc protease-like protein			2	+	85.71
<i>Cj1349c</i>	Cj1349c	Putative fibronectin/fibrinogen-binding protein			2	-	85.71
<i>Cj1680c</i>	Cj1680c	Putative periplasmic protein			2	+	71.43
<i>Cj0036</i>	Cj0036	Hypothetical protein			2	-	64.29
<i>ctsT</i>	Cj1077	Putative periplasmic protein			2	+	64.29
<i>hisG</i>	Cj1597	ATP phosphoribosyltransferase			2	-	64.29
<i>queA</i>	Cj0577c	S-adenosylmethionine:tRNA ribosyltransferase-isomerase			2	+	57.14
<i>proA</i>	Cj0558c	Gamma-glutamyl phosphate reductase			2	-	57.14
<i>Cj0633</i>	Cj0633	Putative periplasmic protein			2	-	57.14
<i>Cj0266c</i>	Cj0266c	Putative integral membrane protein			2	-	57.14
<i>Cj1329</i>	Cj1329	Putative sugar-phosphate nucleotide transferase			2	+	57.14
<i>Cj0839c</i>	Cj0839c	Uncharacterised protein			2	+	42.86
<i>folK</i>	Cj0065c	2-amino-4-hydroxy-6-hydroxymethyldihydropteridine pyrophosphokinase			2	-	42.86
<i>Cj1440c</i>	Cj1440c	Putative sugar transferase			2	+	42.86

<i>feoB</i>	Cj1398	Ferrous iron transport protein		2	-	42.86
<i>mobB</i>	Cj0841c	Putative molybdopterin-guanine dinucleotide biosynthesis protein		2	+	35.71
<i>Cj1138</i>	Cj1138	Putative galactosyltransferase		2	+	35.71
<i>cjel</i>	Cj1051c	Restriction modification enzyme		2	+	28.57
<i>Cj0031</i>	Cj0031	Putative type IIS restriction/modification enzyme		2	-	21.43
<i>kpsT</i>	Cj1447c	Capsule polysaccharide export ATP-binding protein		2	+	14.29

Genes were identified as significant when the log-fold change was greater than 1 and  $p < 0.05$  for DESeq. Both analysis methods were performed with a LOO cross validation repeated 14 times. Stability represents the frequency that a gene was identified as significant during the cross validation. + indicates upregulation in response to ST; - indicates downregulation in response to ST. Component indicates whether a gene was identified as a key discriminant factor in the first or second component for the sPLS-DA analysis. + or – represents up or down regulation in response to treatment.

**Table 4.3.** Genes identified by DESeq and sPLS-DA analysis of RNA-Seq data as being differentially expressed for the 488 wild-type strain grown in the presence of 0.2% (w/v) ST compared to cells grown in the absence of bile salt treatment.

Gene	Locus	Product	DESeq		Component	sPLS-DA	
			Regulation	Stability %		Regulation	Stability %
<i>Cj0561c</i>	Cj0561c	Putative periplasmic protein	+	100.00	1	+	100.00
<i>cmeC</i>	Cj0365c	Multidrug efflux pump protein CmeC	+	100.00	1	+	100.00
<i>cmeA</i>	Cj0367c	Multidrug efflux pump protein CmeA	+	100.00	1	+	57.14
<i>Cj1687</i>	Cj1687	Putative efflux protein	+	21.43			
<i>cmeB</i>	Cj0366c	Multidrug efflux pump protein CmeB	+	7.14	1	+	78.57
<i>Cj0879c</i>	Cj0879c	Putative periplasmic protein			1	+	50.00
<i>Cj0488</i>	Cj0488	Hypothetical protein			2	+	71.43
<i>Cj0485</i>	Cj0485	Putative oxidoreductase			2	+	71.43
<i>cstIII</i>	Cj1140	Alpha-2,3 sialyltransferase			2	+	71.43
<i>Cj0085c</i>	Cj0085c	Putative amino acid recemase			2	-	57.14
<i>Cj1208</i>	Cj1208	Hypothetical protein			2	-	57.14
<i>flgJ</i>	Cj1463	Flagella biosynthesis protein FlgJ			2	+	50.00
<i>racR</i>	Cj1261	Two-component regulator			2	-	50.00
<i>Cj0649</i>	Cj0649	Putative OstA family protein			2	-	42.86
<i>pyrC2</i>	Cj1195c	Putative dihydroorotase			2	-	42.86
<i>Cj0411</i>	Cj0411	Putative ATP/GTP binding protein			2	-	28.57

Genes were identified as significant when the log-fold change was greater than 1 and  $p < 0.05$  for DESeq. Both analysis methods were performed with a LOO cross validation repeated 14 times. Stability represents the frequency that a gene was identified as significant during the cross validation. + indicates upregulation in response to ST; - indicates downregulation in response to ST. Component indicates whether a gene was identified as a key discriminant factor in the first or second component for the sPLS-DA analysis. + or - represents up or down regulation in response to treatment.

**Table 4.4.** Genes identified by DESeq and sPLS-DA analysis of RNA-Seq data as being differentially expressed for the 11168H wild-type strain grown in the presence of 0.05% (w/v) SDC compared to cells grown in the absence of bile salt treatment.

Gene	Locus	Product	DESeq		sPLS-DA		
			Regulation	Stability %	Component	Regulation	Stability %
<i>cmeA</i>	Cj0367c	Multidrug efflux pump protein CmeA	+	100.00	1	+	100.00
<i>metB</i>	Cj1727c	Putative O-acetylhomoserine (Thiol)-lyase	-	57.14			
<i>Cj0561c</i>	Cj0561c	Putative periplasmic protein	+	35.71			
<i>metA</i>	Cj1726c	Homoserine O-acetyltransferase	-	28.57			
<i>cmeC</i>	Cj0365c	Multidrug efflux pump protein CmeC	+	14.29			
<i>cmeB</i>	Cj0366c	Multidrug efflux pump protein CmeB	+	7.14			
<i>Cj1199</i>	Cj1199	Putative iron/ascorbate-dependent oxidoreductase	-	7.14			
<i>metE</i>	Cj1202	Methylenetetrahydrofolate reductase	-	7.14			
<i>purC</i>	Cj0512	Phosphoribosylaminoimidazole-succinocarboxamide synthase			1	-	100.00
<i>ddl</i>	Cj0798c	D-alanine--D-alanine ligase			1	-	100.00
<i>Cj0186c</i>	Cj0186c	Putative TerC family integral membrane protein			1	+	35.71
<i>pycA</i>	Cj1037c	Biotin carboxylase			1	-	21.43
<i>Cj1084c</i>	Cj1084c	Putative ATP/GTP-binding protein			2	-	57.14
<i>cysQ</i>	Cj1681c	3'(2'),5'-bisphosphate nucleotidase			2	+	42.86
<i>feoB</i>	Cj1398	Ferrous iron transport protein			2	-	35.71
<i>Cj0260c</i>	Cj0260c	Small hydrophobic protein			2	-	28.57

Genes were identified as significant when the log-fold change was greater than 1 and  $p < 0.05$  for DESeq. Both analysis methods were performed with a LOO cross validation repeated 14 times. Stability represents the frequency that a gene was identified as significant during the cross validation. + indicates upregulation in response to SDC; - indicates downregulation in response to SDC. Component indicates whether a gene was identified as a key discriminant factor in the first or second component for the sPLS-DA analysis. + or - represents up or down regulation in response to treatment.

**Table 4.5.** Genes identified by DESeq and sPLS-DA analysis of RNA-Seq data as being differentially expressed for the 488 wild-type strain grown in the presence of 0.05% (w/v) SDC compared to cells grown in the absence of bile salt treatment.

Gene	Locus	Product	DESeq		sPLS-DA		
			Regulation	Stability %	Component	Regulation	Stability %
<i>Cj0561c</i>	Cj0561c	Putative periplasmic protein	+	92.86	1	+	100.00
<i>cmeC</i>	Cj0365c	Multidrug efflux pump protein CmeC	+	35.71	1	+	42.86
<i>cmeB</i>	Cj0366c	Multidrug efflux pump protein CmeB	+	42.86			
<i>cmeA</i>	Cj0367c	Multidrug efflux pump protein CmeA	+	35.71			
<i>Cj1308</i>	Cj1308	Putative acyl carrier protein	-	7.14			
<i>Cj1100</i>	Cj1100	Hypothetical protein			1	-	100.00
<i>infC</i>	Cj0207	Translation initiation factor IF-3			1	+	50.00
<i>dcd</i>	Cj1292	Deoxycytidine triphosphate deaminase			2	+	71.43
<i>flgG2</i>	Cj0697	Flagella basal body protein			2	+	64.29
<i>dnaA</i>	Cj0001	Chromosomal replication initiator protein			2	-	21.43
<i>Cj0469</i>	Cj0469	Amino-acid ABC transporter ATP-binding protein			2	-	21.43
<i>Cj1532</i>	Cj1532	Putative periplasmic protein			2	+	14.29

Genes were identified as significant when the log-fold change was greater than 1 and  $p < 0.05$  for DESeq. Both analysis methods were performed with a LOO cross validation repeated 14 times. Stability represents the frequency that a gene was identified as significant during the cross validation. + indicates upregulation in response to SDC; - indicates downregulation in response to SDC. Component indicates whether a gene was identified as a key discriminant factor in the first or second component for the sPLS-DA analysis. + or - represents up or down regulation in response to treatment.

#### **4.2.5 Final gene list of differentially expressed genes**

A total of six, four, three and three genes identified for 11168H ST, 488 ST, 11168H SDC and 488 SDC respectively which were identified by either both analysis methods, or had a stability value higher than 85% in one of the analysis methods (Table 4.6). Genes such as those that encode for components of the *cmeABC* efflux pump were present in the initial gene lists but were excluded from the final gene lists due to low stability of identification. The *cmeABC* efflux pump genes are transcriptionally linked in an operon and have previous well-characterised links to bile salts, therefore genes present in the initial gene lists should also be considered for further investigation.

**Table 4.6.** Genes differentially expressed in response to bile salts that were either identified by both supervised (DESeq) and unsupervised (sPLS-DA) analysis of RNA-Seq data or appeared in one analysis method with a stability frequency greater than 85% for LOO cross-validation.

Strain/Condition	Gene	Regulation	DESeq			Component	sPLS-DA	
			Stability %	Fold change	padj		Regulation	Stability %
11168H 0.2% ST	<i>Cj0561c</i>	+	100.00	2.68	3.21E-07	1	+	100.00
	<i>cmeA</i>	+	64.29	1.22	0.037	1	+	100.00
	<i>cmeB</i>	+	7.14	1.24	0.335	1	+	21.43
	<i>Cj0418c</i>					1	-	85.71
	<i>Cj0463</i>					2	+	85.71
	<i>Cj1349c</i>					2	-	85.71
488 0.2% ST	<i>Cj0561c</i>	+	100.00	2.50	2.71E-08	1	+	100.00
	<i>cmeC</i>	+	100.00	1.34	0.001	1	+	100.00
	<i>cmeA</i>	+	100.00	1.32	0.009	1	+	57.14
	<i>cmeB</i>	+	7.14	1.02	0.063	1	+	78.57
11168H 0.05% SDC	<i>cmeA</i>	+	100.00	1.32	1.3E-06	1	+	100.00
	<i>purC</i>					1	-	100.00
	<i>ddl</i>					1	-	100.00
488 0.05% SDC	<i>Cj0561c</i>	+	92.86	1.91	4.91E-06	1	+	100.00
	<i>cmeC</i>	+	35.71	1.05	0.085	1	+	42.86

+ or – represents up or down regulation in response to treatment. Fold change values and adjusted p-values (padj) presented represent the mean obtained from all 14 cross validation repeats.

#### 4.2.6 Verification of differentially expressed genes by qRT-PCR

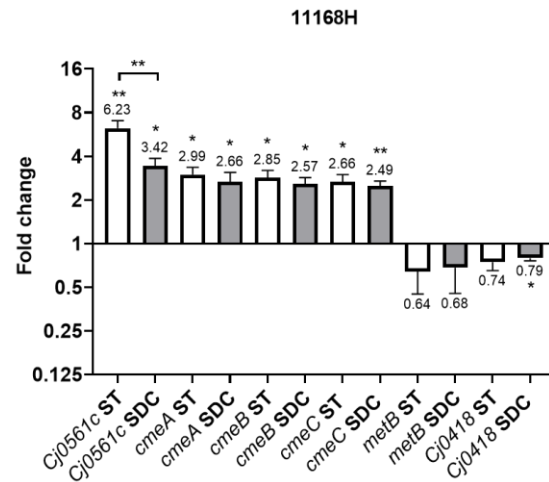
Further investigation of differentially expressed genes by qRT-PCR was performed. *cmeA*, *cmeB*, *cmeC* and *Cj0561c* were all identified as differentially expressed in both wild-type strains for both ST and SDC by at least one of the cross validation runs from at least one of the analysis methods. However, not all of these genes were consistently identified by both analysis methods, with high enough stability to be included in the final gene list (Table 4.6). As such *cmeA*, *cmeB*, *cmeC* and *Cj0561c* were selected for further qRT-PCR investigation. *cmeB* was verified by qRT-PCR prior to RNA-Seq analysis in the treatment pre-screen (Figure 4.2). Analysis of *cmeB* transcription was repeated using additional RNA samples isolated for post RNA-Seq qRT-PCR screening. Two additional genes with varied confidence of identification were selected. *Cj0418* was included in the final gene list (Table 4.6) as differentially expressed for the 11168H wild-type strain grown in the presence of ST due to its high stability of identification by sPLS-DA. *Cj0418* was not identified in any other treatment group or by DESeq analysis. *metB* was identified as differentially expressed by the 11168H wild-type strain grown in the presence of SDC by DESeq analysis, but did not meet the stability criteria to be included in the final gene list. *metB* was not identified in any other treatment group or by sPLS-DA analysis.

RNA was extracted from mid-log phase cultures as described previously for RNA-Seq analysis (Section 2.6.9). *rpoA* was selected as the internal control. *Cj0561c*, *cmeA*, *cmeB* and *cmeC* all had greater than a 2-fold increase in expression for both the 11168H and 488 wild-type strains for both 0.2% (w/v) ST and 0.05% (w/v) SDC. This increase was not statistically significant for 488 *cmeA* and *cmeB* with ST, however only three biological replicates were used for this qRT-PCR data set. RNA-Seq identified *metB* as being differentially expressed for the 11168H wild-type strain grown in the presence of SDC. qRT-PCR confirmed a downregulation of *metB* for 11168H in the presence of SDC, however it was not statistically significant. *metB* was however significantly downregulated for the 488 and 11168H wild-type strains grown in the presence of 0.2% (w/v) ST, and the 488 wild-type strain grown in the presence of 0.05% (w/v) SDC. *Cj0418* was identified as significantly downregulated for the 11168H wild-type strain grown in the presence of ST. This was confirmed by qRT-PCR. Additionally, *Cj0418* was significantly downregulated for the 11168H strain grown in the presence of SDC, and the 488 wild-type strain grown in the presence of ST (Figure 4.11).

**A**

Gene	Strain	DESeq						sPLS-DA			
		ST			SDC			ST		SDC	
		Regulation	Stability	Fold change	Regulation	Stability	Fold change	Regulation	Stability	Regulation	Stability
<i>cj0561c</i>	11168H	+	100	2.68	+	35.71	1.95	+	100		
	488	+	100	2.50	+	92.86	1.91	+	100	+	100
<i>cmeA</i>	11168H	+	64.29	1.22	+	100	1.32	+	100	+	100
	488	+	100	1.32	+	35.71	1.71	+	57.14		
<i>cmeB</i>	11168H	+	7.14	1.24	+	7.14	1.09	+	21.43		
	488	+	7.14	1.02	+	42.86	1.00	+	78.57		
<i>cmeC</i>	11168H	+	14.29	1.21	+	14.29	1.24				
	488	+	100	1.34	+	35.71	1.05	+	100	+	42.86
<i>metB</i>	11168H				-	57.14	-1.75				
	488										
<i>cj0418c</i>	11168H							-	85.71		
	488										

**B**



**C**

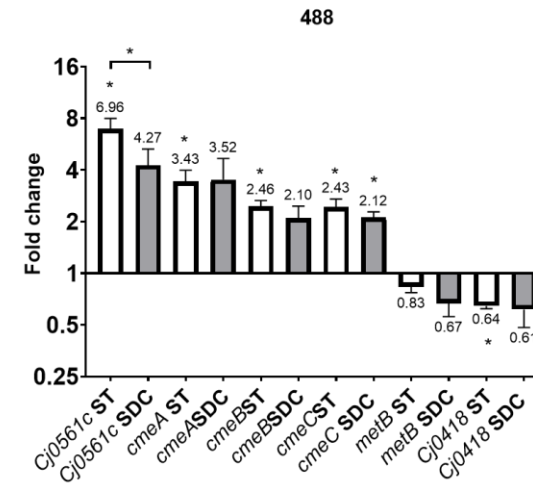


**Figure 4.11.** qRT-PCR analysis of *Cj0561c*, *cmeA*, *cmeB*, *cmeC*, *metB* and *Cj0418* transcription. **(A)** Summary of each genes identification by either DESeq or sPLS-DA and identification stability. Analysis of transcription in *C. jejuni* **(B)** 488 and **(C)** 11168H wild-type strains co-incubated with 0.2% (w/v) ST or 0.05% (w/v) SDC. *rpoA* was used as an internal control. \*  $p < 0.05$ ; \*\*  $p < 0.01$ .

## 4.3 Discussion

### 4.3.1 Sampling conditions

Bile salts are important molecules for signalling and metabolism for both the host and the gut microbiota (Lorenzo-Zúñiga *et al.*, 2003). *C. jejuni* is considered to have a high bile salt tolerance as demonstrated in Figure 3 (Chapter 3). Bile salt tolerance can vary between *C. jejuni* isolates and it has been suggested that a higher tolerance is associated with strains causing human infection (Van Deun *et al.*, 2007). Additionally bile salts have been linked to the regulation of virulence in *C. jejuni* (Malik-Kale *et al.*, 2008; Elmi *et al.*, 2018; Taheri *et al.*, 2018; Davies *et al.*, 2019; Man *et al.*, 2020), however the mechanisms behind the response of *C. jejuni* to bile is still not well understood.

As bile salts can cause cell stress, sampling was carried out at the mid-log phase of growth to avoid characterising the accumulative stress of bile salts with the stresses of later stages of growth. Negretti *et al.* (2017) described the response of *C. jejuni* to the bile salt SDC over time with the initial response being transcription of bile resistance proteins such as the components of the CmeABC efflux system, and putative virulence responses such as increased *flaA* promoter activity and chemotactic responses. The later response is that to the cumulative toxic effects of SDC caused by ROS and DNA damage leading to increased transcription of genes such as *aphC*, *kata*, *sodB*, *trxB* and *tpx*. Validating our selected timepoint as an early response to bile salts, upregulation of *cmeA*, *cmeB* and *cmeC* was observed, but upregulation of oxidative stress related genes were not.

### 4.3.2 Differentially expressed genes identified by DESeq

DESeq identified a total of four genes for the 11168H reference compared to ST; five genes for the 488 reference compared to ST; eight genes for 11168H reference compared to SDC and five genes for 488 reference compared to SDC, in at least one cross validation run for each comparison. However, a cut off value of 85% stability was set for reliably identified genes, and after this exclusion the total number of genes identified was one gene for the 11168H reference compared to ST; three genes for the 488 reference compared to ST; one gene for the 11168H reference compared to SDC and one gene for the 488 reference compared to SDC.

As shown in Appendix 2-5, the transcriptional changes observed were moderate for all comparisons during individual cross validation runs. A maximum of 61 genes and a minimum of 17 genes in any single comparison exhibited greater than a 1 log fold change in expression (Appendix 6), the majority of which possessed a near 1 log fold change and failed to meet statistical significance. However, despite inconsistently meeting the stability criteria, *cmeA*, *cmeB*, *cmeC* and *Cj0561c* were identified

for all DESeq comparisons and are well characterised bile salt response genes. This provides confidence in the genes identified by DESeq, however the statistical analysis method used is not sensitive enough to identify all true differentially expressed genes. As such, any gene identified during a single cross validation DESeq run should be considered for further investigation, providing differential gene expression is confirmed by qRT-PCR. This also indicates that the genes identified by DESeq, in particular *Cj0561c* which was identified with greater than 85% stability for three out of four comparisons, should be considered as key genes in the homeostatic response of *C. jejuni* to bile in the absence of additional stressors.

### **4.3.3 Differentially expressed genes identified by sPLS-DA**

To detect additional differentially expressed genes missed by DESeq analysis, sPLS-DA (a supervised analysis method) was used in order to search for key discriminant factors between comparison sample groups. This method was able to identify a larger population of differentially expressed genes (Tables 4.2-4.5). However, as was previously observed for DESeq analysis many of the identified genes failed to meet the identification stability criteria. sPLS-DA analysis did however validate some genes identified by DESeq. For example, *cmeA* was identified by DESeq as upregulated for 11168H grown in the presence of 0.2% (w/v) ST but was only identified with 64.29% stability, however sPLS-DA identified *cmeA* with 100% stability (Table 4.1). *cmeA*, *cmeB*, *cmeC* and *Cj0561c* were also frequently identified with high stability for multiple comparisons by sPLS-DA, validating the ability of this method to identify differentially expressed genes with high confidence, with the potential for higher sensitivity detection than DESeq. As was suggested for DESeq, given the mild nature of the treatment conditions used for this study, and the absence of additional variables, such as changes in media or incubation conditions between baseline and test samples, all genes identified by at least one cross validation run should be considered for further investigation if verified as differentially expressed by qRT-PCR.

### **4.3.4 Final list of differentially expressed genes**

Initial transcriptional studies of *C. jejuni* utilised microarray technology, which was made possible by the completion of the 11168H whole genome sequence in 2000 (Parkhill *et al.*, 2000). Early work by Stintzi (2003), who characterised the transcriptional changes of *C. jejuni* grown at 42°C compared to 37°C, observed approximately 20% (336 genes) of the genome having significant differential expression. Other microarray transcriptomic work included Carrillo *et al.* (2004) who characterised the role of *flhA* in coordination of flagella genes and virulence factors; Palyada *et al.* (2004) who observed 208 differentially expressed genes between iron rich and iron limiting conditions; Holmes *et al.* (2005) who observed 147 genes differentially expressed in response to iron limitation; Andersen *et al.* (2005)

who observed 30 differentially expressed genes in a *hspR* knock-out mutant compared to the wild type strain; and Kamal *et al.* (2007) who observed 462 genes differentially expressed in a *fliK* knock out compared to its wild-type strain. Following on from this was the adaptation of RNA-Seq based methods for studying bacterial transcriptomics. RNA-Seq offered improved sensitivity along with removing the dependence on gene specific probes, allowing a more comprehensive and less biased approach to studying the bacterial transcriptome and enabling identification of additional transcriptional components such as non-coding RNAs (Marioni *et al.*, 2008; Croucher and Thomson, 2010; van Vliet, 2010). Early bacterial RNA-Seq studies were led by Yoder-Himes *et al.* (2009) studying *Burkholderia cenocepacia*, with early *C. jejuni* RNA-Seq based studies soon following with Chaudhuri *et al.* (2011) characterising the differential gene expression between a 11168H *rpoN* mutant and its wild-type strain; and Dugar *et al.* (2013) who described differential RNA-Seq (dRNA-Seq) for annotation of transcriptional start sites, identification of sRNA and identification of a CRISPR-system in *C. jejuni*.

This study identified a total of eight and four differentially expressed genes for 11168H wild-type and 488 wild-type strains grown in the presence of 0.2% (w/v) ST respectively, and three and two genes for the 11168H and 488 wild-type strains grown in the presence of 0.05% (w/v) SDC respectively. Excluding the identification stability parameter imposed, 26 and 16 genes for 11168H and 488 respectively were identified for growth in ST. For growth in SDC, 16 and 12 genes were identified for 11168H and 488 respectively. From here on, comparisons will be made to the full lists of genes identified irrespective of identification stability. To date, there are no other transcriptional studies characterising the response of *C. jejuni* to ST, however there is a proteomics based study which did observe both ST and SDC upregulating *Cj0561c* and *cmeABC* (Masanta *et al.*, 2019). Several studies have characterised the response of *C. jejuni* to SDC or bile. Malik-Kale *et al.* (2008), in conjunction with  $\beta$ -galactosidase reporter assays, qRT-PCR and phenotypic characterisation of selected genes, investigated the transcriptional response of *C. jejuni* to SDC using microarray analysis. Malik-Kale *et al.* (2008) identified 156 genes to be significantly upregulated and 46 genes significantly downregulated, with significance defined as  $\geq 1.5$ -fold change and  $p < 0.05$  using two biological replicates for RNA isolated from *C. jejuni* F38011 wild-type MH agar plate cultures supplemented with 0.1% (w/v) SDC grown for 12 hours. Of the genes identified by DESeq in this study, four out of eight genes identified for 11168H, and four out of five genes identified for 488 grown in the presence of SDC (*Cj0561c*, *cmeA*, *cmeB* and *cmeC*) were in common with Malik-Kale *et al.* (2008). Of the genes identified by sPLS-DA the only additional gene in common with Malik-Kale *et al.* (2008) was *infC*, a translation initiation factor. As described in Malik-Kale *et al.* (2008), the transcriptional response

observed in qRT-PCR experiments in the same study were time dependent. For example, *ciaB* showed very little transcriptional change prior to nine hours. However, a 1.8-fold change was seen at 12 hours. This, along with the lower concentration of bile salts used in our study, could contribute to the smaller list of differentially expressed genes identified.

Negretti *et al.* (2017) compared the transcriptional response of *C. jejuni* 81-176, 11168H and F38011 wild-type *C. jejuni* strains to SDC using RNA-Seq. MH cultures were supplemented with 0.05% (w/v) SDC and 12 hour MH broth cultures were used as the baseline transcription for comparisons to 16 and 18 hour MH broth cultures supplemented with SDC. A significance value of  $p < 0.1$  and two biological replicates were used for each strain. There were 90 upregulated and 80 downregulated genes common to all three strains. 81-176 saw a total of 355 genes upregulated and 329 genes down regulated at either 16 or 18 hours. 11168 had a total of 565 upregulated and 403 downregulated. F38011 had a total of 580 upregulated and 340 downregulated. Our study did not identify any of the genes that were listed as differentially expressed genes common to all three strains investigated by Negretti *et al.* (2017), however, there were genes common to individual wild-type strains. *Cj0561c* was identified as upregulated in both 11168H and 488 in this study, and upregulated in 81-176, but down regulated in 11168 and F38011 by Negretti *et al.* (2017). Genes encoding the CmeABC efflux system were upregulated by both 11168H and 488 in this study. Negretti *et al.* (2017) did not identify *cmeA*, however, *cmeB* and *cmeC* were upregulated in 81-176 and downregulated in 11168. Other genes common between studies include *Cj1726c*, *Cj0512*, *Cj1037*, *Cj0207* and *Cj1308*.

There have been several *in vivo* RNA-Seq based studies relating to *C. jejuni* bile transcriptomics. Taveirne *et al.* (2013) compared the differential gene expression of either mid-log or stationary phase MH broth cultures of *C. jejuni* 81-176 to that of the caecal content of chicks infected for seven days. A total of 15 chicks comprising three biological replicates were used. A total of 151 and 123 genes were differentially expressed between mid-log and stationary phase cultures compared to *in vivo* respectively. A fold change cut-off of 4-fold with a significance cut off of  $p < 0.05$  was used. *cmeABC* and *Cj0561c* were not identified in this study. Kreuder *et al.* (2017) did identify *Cj0561c* and *cmeABC* during comparisons of *C. jejuni* IA3902 in ovine bile either *in vivo* or *in vitro*. Kreuder *et al.* (2017) made comparisons to the gene expression of the culture inoculum and that of *C. jejuni* in ovine bile both *in vivo* and *in vitro*. Between 123-405 differentially expressed genes were observed in various bile to inoculum comparisons. However, based on a fold-cut of value of 1.5 and significance cut-of value of  $p < 0.05$ , there were 67 upregulated and 10 downregulated genes common to bile exposure *in vivo* and *in vitro*, and it was suggested that these are core genes required for the *C. jejuni* bile response. Interestingly these core genes included upregulation of *cmeABC*, and *Cj0561c*, in addition to

downregulation of *metF*, which is functionally linked to *metB* and *metE*, the latter two of which were identified as significantly down regulated for *C. jejuni* 11168H grown in the presence of 0.05% (w/v) SDC by DESeq analysis (Table 4.4). Liu *et al.* (2018), using RNA-Seq, analysed transcriptional changes between *C. jejuni* 81-176 grown in either MH broth alone or MH broth supplemented with either 30% (w/v) caecal extract, or human faecal extract, incubated for 20 minutes to assess transient transcriptional changes or five hours to assess homeostatic transcriptional changes. Accumulatively for all test conditions compared to broth control a total of 23 genes had a greater than 2-fold upregulated and a total of 17 genes had a greater than 2-fold downregulation. This study demonstrates that when baseline conditions and test condition variables are minimal, fewer genes maybe expected. Differentially expressed genes listed by Liu *et al.* (2018) did not overlap with the differentially expressed genes identified in this study.

#### 4.4 Conclusion

In the absence of additional, often unavoidable variables between transcriptional baseline and test samples, such as variations in timepoint, culture media, and other host factors implicated in host infection compared to *in vitro*, this study has identified potentially key genes in the homeostatic transcriptional response of *C. jejuni* to bile salts in the absence of other stressors. Leading on from this work, future work should aim to validate both genes of high- and low-stability identified in this study. As an initial proof of principle, a selection of high, mid- and low stability genes were verified by qRT-PCR (Figure 4.11). In reality *C. jejuni* will not be facing the isolated stress of a single bile salt, but a greater understanding of the core bile salt response pathways could help to provide a more comprehensive understanding of the vast populations of differentially expressed genes obtained from *in vivo* transcriptomic studies.

In agreement with previous work, this study demonstrated that even in mild conditions, *cmeABC* is readily activated by bile salts, which likely functions to prime *C. jejuni* for passage through the hostile environments encountered within the human gastrointestinal tract. Also in agreement with previous studies, *Cj0561c* appears to have a strong transcriptional link with the presence of bile salts. An interesting observation was the differential response of *Cj0561c* to SDC and ST. *Cj0561c* and *cmeABC* are transcriptionally linked through CmeR. *cmeABC*, with the concentrations of bile salts used in this study, showed comparable transcriptional responses to both bile salts, however *Cj0561c* was significantly upregulated by ST compared to SDC. As peak concentrations of ST and SDC are spatially distinct in the human gut, *Cj0561c* could be a key gene in niche specific behaviour within the human gut. As the function of *Cj0561c* is yet to be characterised, this gene will be the first point of focus for future work.

## Chapter Five: Phenotypic characterisation of bile salt response gene *Cj0561c*

### 5.1 Introduction

*C. jejuni* has evolved to survive in the gastrointestinal tract of avian hosts, overcoming harsh conditions such as the toxicity of bile and its components (Hermans *et al.*, 2012; Urdaneta and Casadesús, 2017). Bile salts are organic detergents that can cause disruption to the bacterial cell membrane, and on reaching the cytoplasm can cause DNA and protein damage (Kandell and Bernstein, 1991; Prieto *et al.*, 2004; Cremers *et al.*, 2014; Negretti *et al.*, 2017). *C. jejuni* possesses the CmeABC multidrug efflux pump which plays a key role in bile resistance and is therefore required for host gut colonisation (Lin *et al.*, 2002; Lin *et al.*, 2003). As with other Gram-negative bacteria, *C. jejuni* has a number of OM proteins (OMPs) which function to create a selective barrier between the extracellular and intracellular environment, preventing entry of harmful compounds but permitting entry of beneficial compounds (Savage, 2001; Nikaido, 2003). These proteins may be lipid anchored lipoproteins or integral OMPs (Koebnik *et al.*, 2000).

OMPs, unlike proteins from other cellular membranes, are embedded in the membrane via  $\beta$ -barrels rather than  $\alpha$ -helices. These OMPs typically contain an even number of  $\beta$ -strands arranged in an antiparallel configuration (Koebnik *et al.*, 2000; Rollauer *et al.*, 2015).  $\beta$ -barrel proteins are also found in the mitochondrial OM and the OM of chloroplasts (Wimley, 2003; Doyle and Bernstein, 2019). The OMPs of Gram-negative bacteria serve a variety of functions including uptake of nutrients, secretion, adhesion, and insertion of proteins into the OM (Beketskaia *et al.*, 2014; Aunkham *et al.*, 2018; Choi and Lee, 2019; Doyle and Bernstein, 2019). Due to the location of OMPs in the Gram-negative OM, OMPs can often be highly antigenic proteins and can be considered as potential vaccine target candidates (Li *et al.*, 2017; Leow *et al.*, 2020). This makes furthering the understanding of these proteins of great clinical and public health importance.

As a large proportion of the *C. jejuni* genome remains uncharacterised (Truccollo *et al.*, 2021), the composition and function of the components of the OM are not yet fully understood. It is thought that *C. jejuni* has more than 60 OMPs (Shoaf-Sweeney *et al.*, 2008; Watson *et al.*, 2014) comprising >3.5% of the *C. jejuni* proteome (Watson *et al.*, 2014). A large proportion of the *C. jejuni* OMP mass is formed by PorA, which is also referred to as MOMP (major OM protein) (Cordwell *et al.*, 2008; Sulaeman *et al.*, 2012). The attributed functions of other characterised *C. jejuni* OMPs and OM lipoproteins include adhesion (CadF, PorA, PEB1, JlpA, FlpA, CapA) (Konkel *et al.*, 1997; Cordwell *et al.*, 2008; Rubinchik *et al.*, 2012), amino acid and nutrient transport (CjaA, PorA, PEB1) (Leon-Kempis Mdel *et al.*, 2006;

Wyszyńska *et al.*, 2008), iron acquisition (ChuA, CfrA, CfrB) (Stintzi *et al.*, 2008), OM maintenance (MlaA) (Malinverni and Silhavy, 2009; Davies *et al.*, 2019) and efflux (CmeC, CmeD) (Lin *et al.*, 2002; Akiba *et al.*, 2006; Su *et al.*, 2014).

This chapter aimed to further characterise the bile salt regulated protein Cj0561c, which has previously been shown to aid colonisation, and despite the link with CmeABC through CmeR, does not appear to play a role in stress resistance (Guo *et al.*, 2008). This study demonstrates that Cj0561c is an OMP rather than a periplasmic protein with some structural and phenotypic similarities to the *E. coli* lipid transport protein FadL (Black, 1988) and the pH sensitive oligosaccharides transporting porin OmpG (Pham *et al.*, 2021). This study, in agreement with the work by Guo *et al.* (2008), has shown that Cj0561c does not appear to be functionally linked to OM integrity.

## 5.2 Results

### 5.2.1 Cj0561c is an outer membrane $\beta$ -barrel protein with a DUF2860 domain

The gene encoding Cj0561c does not appear to form part of an operon. The closest ORFs up and downstream of *Cj0561c* on the same DNA strand are *proA* (*Cj0558c*) and *queA* (*Cj0577c*) which are located 2.5 kb and 13 kb away respectively. The adjacent genes *Cj0560* and *dnaB* (*Cj0562*) are encoded on the opposite DNA strand (see Figure 5.1A).

National Center for Biotechnology Information (NCBI) describes Cj0561c as a periplasmic protein. Cj0561c is 309 amino acids in length with a predicted molecular weight of 34.9 kDa (ProtParam). SignalP-5.0 (Almagro Armenteros *et al.*, 2019) predicts Cj0561c to have a Sec signal sequence with a cleavage site at amino acid position 20-21 with 99.71% probability (Figure 5.1B). Sec signal sequences are typical of OMPs (Oliver and Beckwith, 1982; Cranford-Smith and Huber, 2018). Following on from the cleavage site, Cj0561c is annotated as containing a DUF2860 domain from amino acid 21-309. DUF2860 is an uncharacterised domain with no known function (Roumia *et al.*, 2021). InterPro (Blum *et al.*, 2020) describes DUF2860 proteins as currently having no experimental data or exhibiting features indicative of functions. As of 14.12.2021, InterPro documents 1281 proteins containing DUF2860 domains which are divided into 16 architectural groups. Cj0561c belongs to the most common architectural group which contains a single DUF2860 domain linked to a signal sequence. Of the 1281 listed proteins 1240 belong to this group. The DUF2860 domain modelled by the Baker lab using RoseTTAFold predicts the domain to form a  $\beta$ -barrel structure (Figure 5.2). Furthering the evidence for Cj0561c having OM rather than periplasmic subcellular location, PRED-TMBB2 (Tsirigos *et al.*, 2016) predicts Cj0561c to have 14 transmembrane domains, with larger extracellular loops, and smaller periplasmic turns linking transmembrane domains (see Figure 5.1C,D).





A BLASTP search was performed on the Cj0561c nucleotide sequence against the non-redundant protein sequence database using protein-protein BLAST (blastp) with default parameters. BLASTP search results match to DUF2860 domain containing proteins within the *C. jejuni* species, with the top 100 hits matching with >99% identity with 100% coverage (E = 0 for all 100 hits). The Same BLASTP search applying the filter to excluding *C. jejuni* sequences matched Cj0561c to DUF2860 domain containing proteins in *Campylobacter coli*, *Campylobacter lari*, *Campylobacter fetus* and *Campylobacter* sp. CFSAN093238 with 100% coverage >98% identity. BLASTN search results matched the *Cj0561c* coding sequence to *Campylobacter* genes only, with highest confidence matches correlating to genes present in *C. jejuni* (100% coverage, >99% identity, E = 0) followed by coding sequences present in other *Campylobacter* species such as *Campylobacter* sp. CFSAN093226, *Campylobacter* sp. CFSAN093227, *Campylobacter* sp. CFSAN093238, *Campylobacter* sp. CFSAN093260 and *Campylobacter* sp. CFSAN093259 all with 100% coverage and more than 99% identity. BLASTP search described amino acids 26-309 to contain a DUF2860 domain with the region also predicted to belong to OM Porin protein superfamily (Altschul *et al.*, 1990).

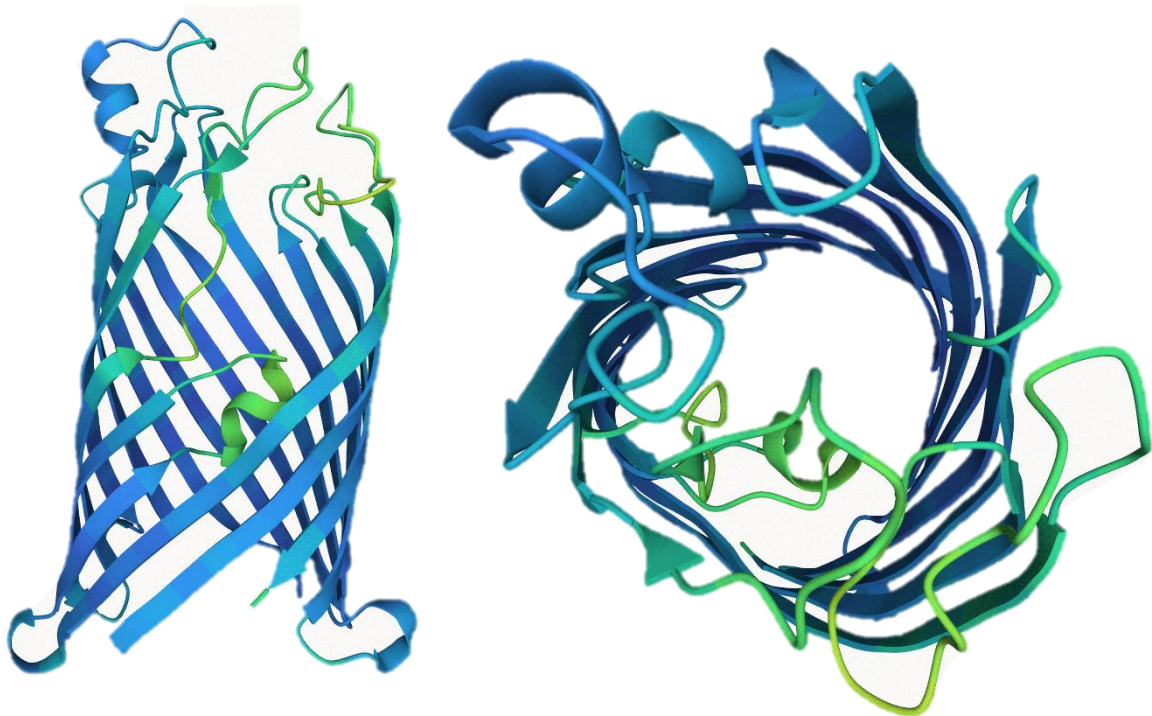
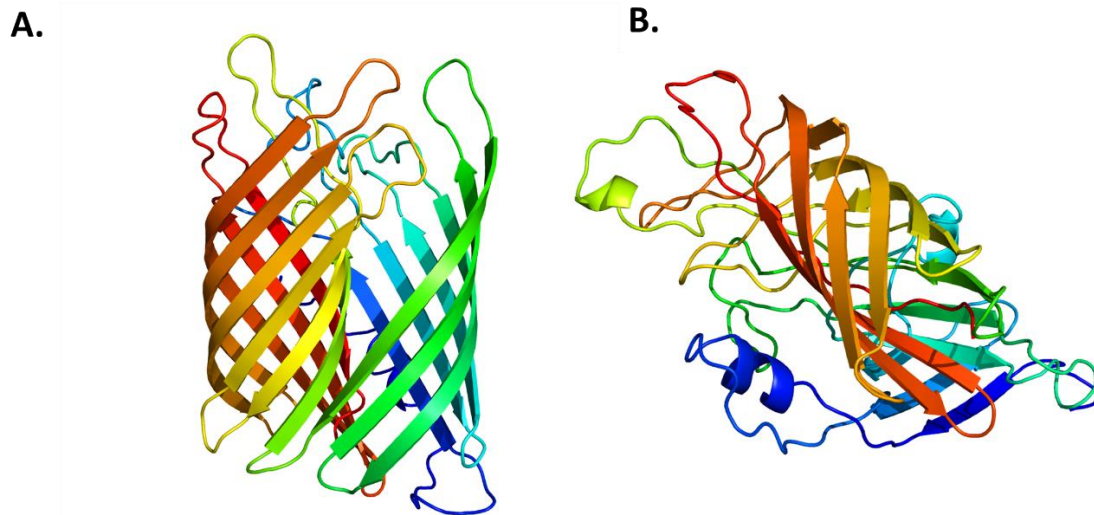


**Figure 5.2.** Structural prediction of DUF2860 domain by the Baker lab using RoseTTAFold obtained from InterPro (Baek *et al.*, 2021).

Based on the BLASTP link to porins, an OMPdb (Roumia *et al.*, 2021) search was performed. OMPdb, a database of  $\beta$ -barrel OMPs, lists Cj0561c as a probable membrane protein with a role in intestinal colonisation, functional category adhesion, and lists Cj0561c as the only characterised member of DUF2860 protein family. The TCDB (Transporter Classification Database) (Saier *et al.*, 2006; Saier *et al.*, 2021) describes DUF2860 family proteins as putative  $\beta$ -barrel proteins ranging between 300-350 amino acids, with an N-terminal signal sequence, mainly possessing 14  $\beta$  transmembrane segments and are predominantly found in proteobacteria. The PRED-TMBB2 tool which predicts the topology of  $\beta$ -barrel OMPs predicts Cj0561c to have 14  $\beta$  strands.

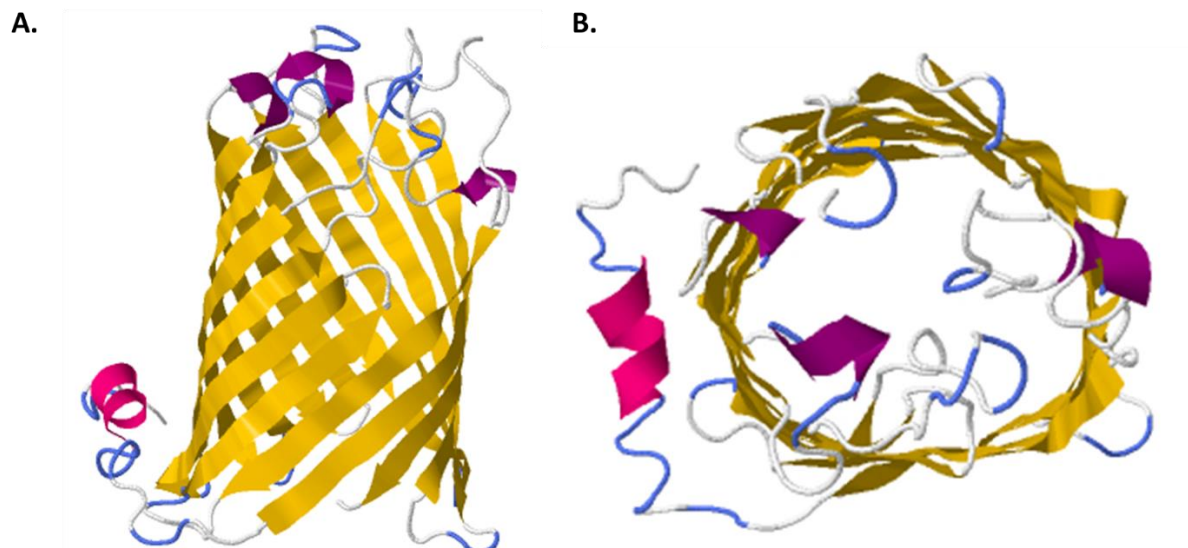
SWISS-MODEL (Waterhouse *et al.*, 2018) top sequence matches were to OprE (*P. aeruginosa* OM porin), Fiu (*E. coli* ferric-catecholate import receptor), OmpC28 (*E. coli* OM porin C) and Omp35 (*Enterobacter aerogenes* phosphoporin). All matches however had QMEAN Z-scores of less than -4 indicating low quality model predictions.

Due to a lack of nucleotide or amino acid sequence similarity to any functionally characterised gene, protein or protein domain, structural predictions were created using Phyre2 (Kelley *et al.*, 2015), RaptorX (Källberg *et al.*, 2012), trRosetta (Du *et al.*, 2021) and RoseTTAFold (Baek *et al.*, 2021). Phyre2, using intensive modelling mode, predicted 92% of residues to be modelled at >90% confidence as shown in Figure 5.3A. 99% of residues were modelled with >90% confidence when intensive modelling was run with initial 20 amino acid signal sequence removed (Figure 5.3B). The Cj0561c sequence is predicted to contain a number of  $\beta$ -strand regions (64%) to form a  $\beta$ -barrel protein. When modelled in Phyre2 Cj0561 only produced high confidence but low percentage identity matches. Of the sequences matched with high confidence (>90%), no sequence had greater than 16% sequence identity. The highest ranked match was to OmpA from of *E. coli* (98.1% confidence, 10% identity).



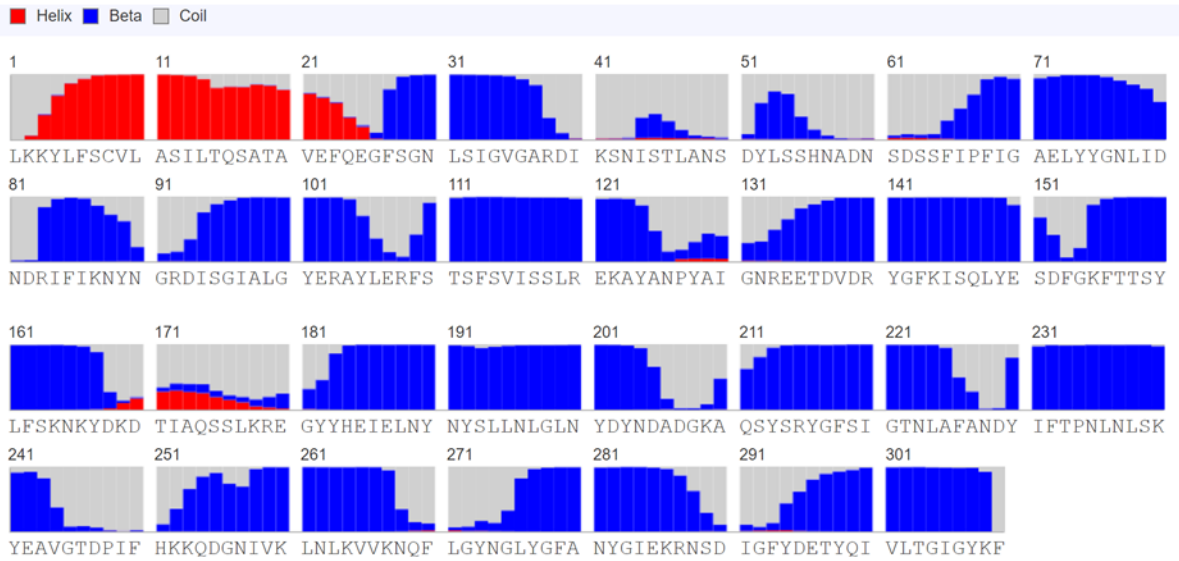
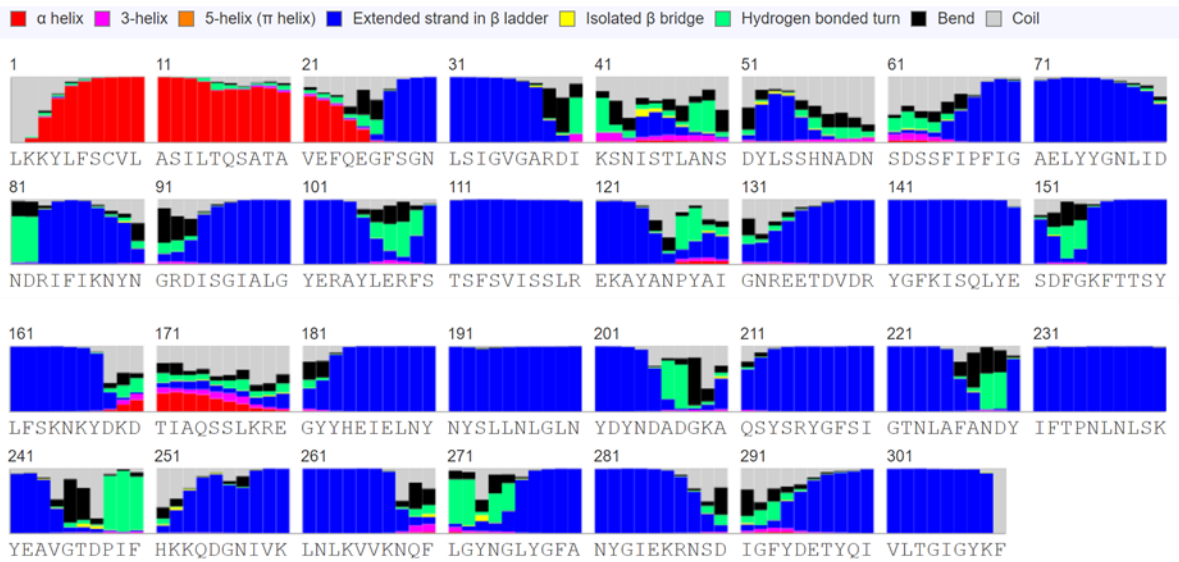
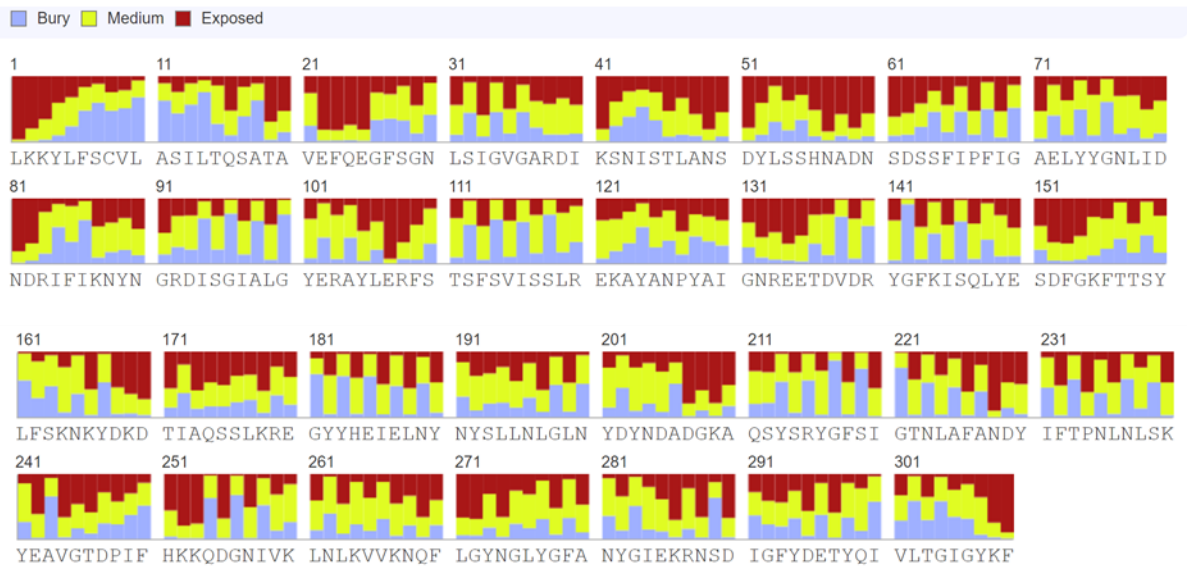
**Figure 5.3** Cj0561c structural prediction produced by Phyre2 using **(A)** Full amino acid sequence, **(B)** Amino acid sequence with the 20 amino acid predicted signal sequence removed. Rainbow colour scheme is used depicting N (blue) to C (red) terminus of the protein (Kelley *et al.*, 2015).

As Phyre2 did not identify any reliable structural matches and did not produce a model resembling the structural prediction for DUF2860 domains (Figure 5.2 and 5.3), RaptorX and trRosetta structural predictions were generated. The RaptorX software is adapted to produce high quality predictions of proteins with no close homologs in PDB (the Protein Data Bank). Both RaptorX and trRosetta produced similar structural models, which resembled the structural prediction for DUF2860 domains produced by Baek *et al.* (2021) (Figures 5.2, 5.4, 5.6).

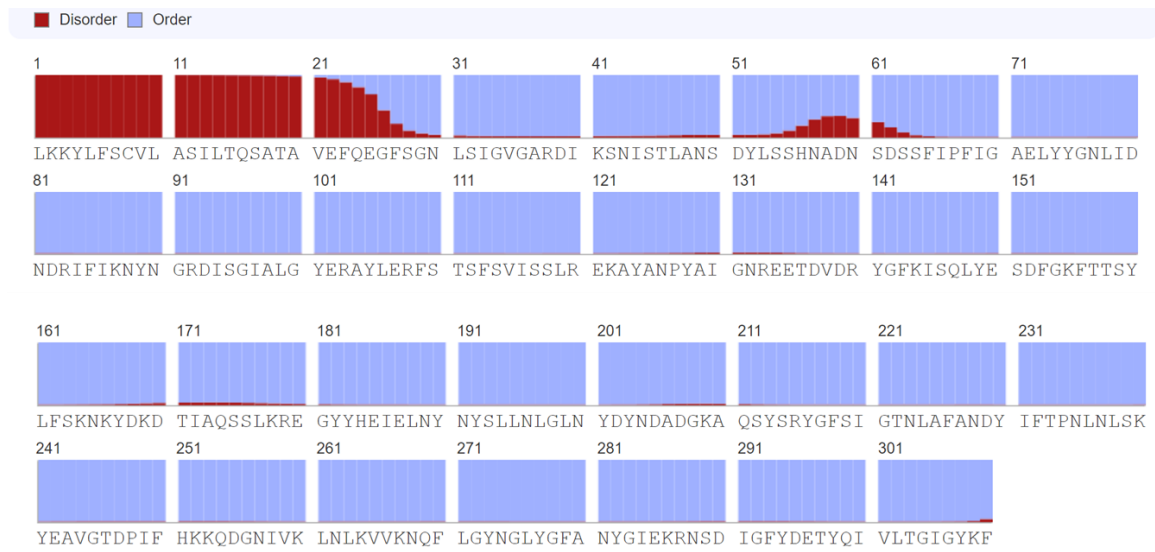


**Figure 5.4** Structural prediction of Cj0561c using RaptorX. **(A)** Side view of Cj0561c. **(B)** Protein channel viewed from extracellular side. Structure is coloured according to predicted secondary structure.  $\alpha$ -helices = magenta;  $\beta$ -sheet = yellow; turn = blue; 3-helix = purple; no structure assigned = white (Källberg *et al.*, 2012; Wang *et al.*, 2016; Wang *et al.*, 2017).

RaptorX property prediction analysis using the complete Cj0561c amino acid sequence, including signal sequence, described Cj0561c as containing 6%  $\alpha$ -helix, 60%  $\beta$ -sheet and 33% coil. The majority of the  $\alpha$ -helix structure was present in the signal sequence region (Figure 5.5 A-B, E). The predicted solvent accessibility of Cj0561c was 33% of the structure exposed, 21% of the structure is buried and the remaining being intermediate (Figure 5.5 C, E). RaptorX predicted 25 amino acids (8%) to be disordered, 21 of which are located in the predicted signal sequence. Although not significant, a small spike in disorder was predicted in extracellular loop 1 with amino acids S55-D62 showing greater than 10% disorder (Figure 5.5D-E).

**A.****B.****C.**

D.



E.

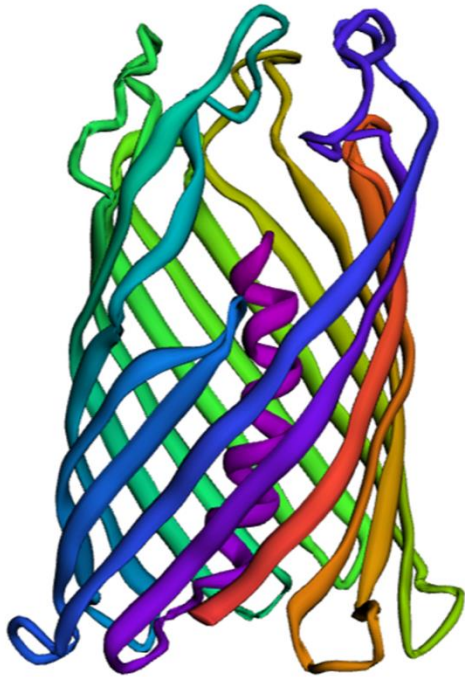


**Figure 5.5** Results of property prediction produced using RaptorX Property Prediction. **(A)** 3-class secondary structure prediction. **(B)** 8-class secondary structure prediction. **(C)** Solvent accessibility prediction. **(D)** Disorder prediction. **(E)** Results summary aligning all the previous predicted properties of each amino acid (Wang *et al.*, 2016)



A further model was produced using RoseTTAFold (Baek *et al.*, 2021). RoseTTAFold uses deep learning to produce predictions of protein structure using limited information, or through alignment to homologues. The software simultaneously factors in patterns in protein sequences, how amino acids within the protein will interact with each other, and the protein's possible three-dimensional structure. RoseTTAFold produced a high confidence model (confidence score of 0.73 out of 1) for Cj0561c using the complete Cj0561c amino acid sequence including predicted signal sequence (Figure 5.7). The model produced is highly similar to those predicted by rtRosetta and RaptorX. RaptorX, rtRosetta and RoseTTAFold all predict a  $\beta$ -barrel possessing a truncated wall region located in the vicinity of extracellular loop 2. Loop 2 happens to be the smallest extracellular loop and is located between the two largest extracellular loops; loop 1 and loop 2. Transmembrane strand 5 in the DUF2860 structural prediction (Figure 5.2) appears to form a kink within the barrel wall. Of note loop 1 and loop 3 appear to block the extracellular entrance to the channel to some degree. Also of note, excluding the predicted signal sequence, loop 1 is the region of the protein with the lowest confidence protein structure prediction or the region with the highest predicted disorder.

A.



B.

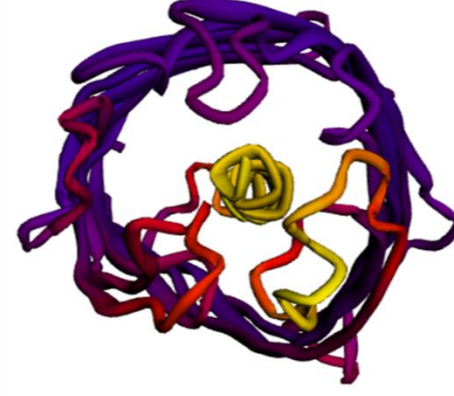
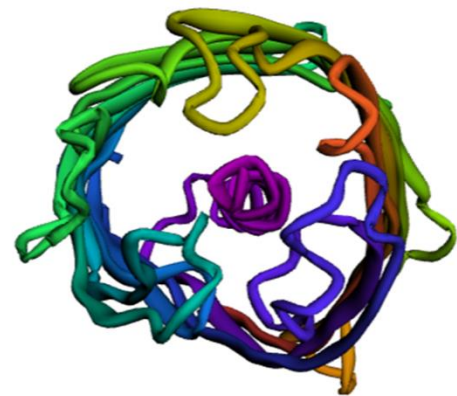
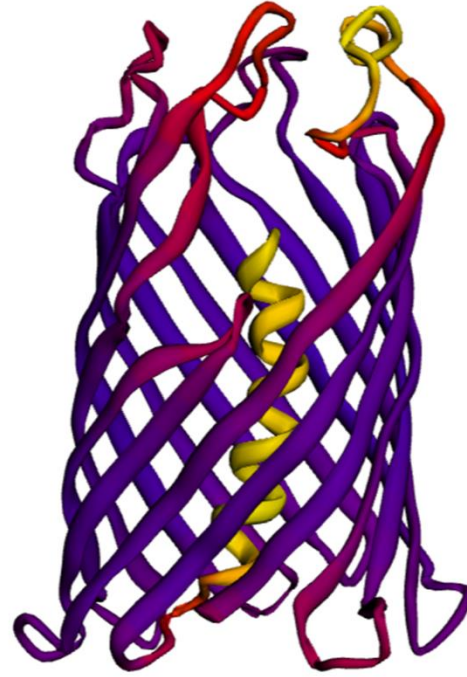


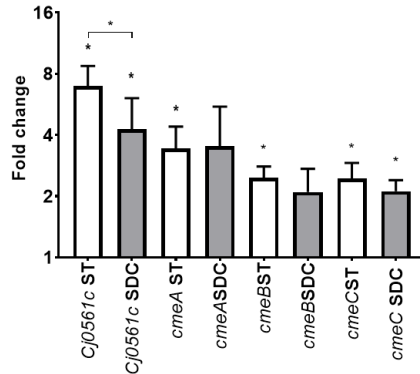
**Figure 5.7** Protein structure prediction produced by RoseTTAFold. **(A)** Protein model prediction coloured using spectrum colour scheme depicting N (purple) to C (red) terminus of the protein. **(B)** Protein model prediction coloured according to confidence, high confidence (purple) – low confidence (yellow). The protein model depicts a side-on view (top) and a protein channel view from the extracellular side (bottom).

### 5.2.2 The regulation of *Cj0561c* by sodium taurocholate and sodium deoxycholate

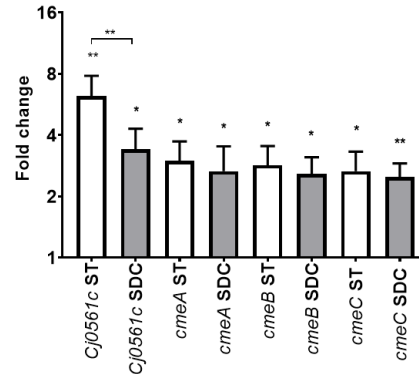
As shown in Chapter 4 (Table 4.6, Figure 4.11), *Cj0561c* and *cmeABC* were upregulated in the presence of both 0.2% (w/v) ST and 0.05% (w/v) SDC. Both *Cj0561c* and *cmeABC* are under the control of the transcriptional regulator CmeR (Guo *et al.*, 2008). CmeR binds to an inverted repeat of TGTAAT. The promoter region of *cmeABC* contains one binding site for CmeR whereas the promoter of *Cj0561c* has two binding sites (Guo *et al.*, 2008). Under the biologically relevant conditions investigated in this study (0.2% (w/v) ST and 0.05% (w/v) SDC), the transcriptional changes of *cmeABC* expression between bile salts was comparable, however, *Cj0561c* demonstrated a significantly greater increase in expression in the presence of ST compared to the response to SDC (Figure 5.8 E-H). Both 11168H and 488 wild-type strains demonstrated this phenotype (Figure 5.8).

To investigate if the absence of *Cj0561c* impacted transcriptional feedback loops of either *Cj0561c* or *cmeABC*, *Cj0561c* knock-out mutants were constructed for both wild-type strains. The *Cj0561c* gene in each strain was inactivated by replacing the central 0.5 kb of coding sequence with a kanamycin resistance cassette (see Section 2.5.3). qRT-PCR primers (qRTCj0561cKO[F/R]) were then designed upstream of the mutation site to measure transcriptional activity. Comparable transcriptional changes in response to ST and SDC were seen for *cmeABC* and *Cj0561c* in the *Cj0561c* mutant strains compared to each respective wild-type strain (Figure 5.8). The *Cj0561c* qRT-PCR primers qRTCj0561c(F/R) used to generate the data in Chapter 4 (Table 4.6, Figure 4.11) are located within the 0.5 kb of coding sequence removed. These primers were included as a negative control for the *Cj0561c* mutant qPCR experiments. There was no detectable transcription seen for these negative control primers (data not shown).

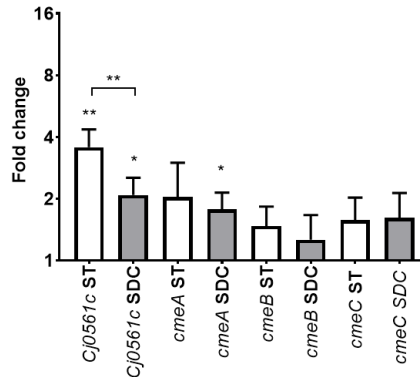
**A. 488 wild-type**



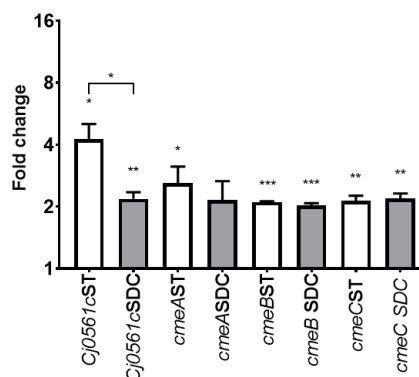
**B. 11168H wild-type**



**C. 488 Cj0561c mutant**



**D. 11168H Cj0561c mutant**



**E.**

	488		p - value
	Fold change		
	0.2% ST	0.05% SDC	
<i>Cj0561c</i>	6.96	4.27	0.0132
<i>cmeA</i>	3.43	3.52	0.9263
<i>cmeB</i>	2.46	2.1	0.4813
<i>cmeC</i>	2.43	2.12	0.3295

**F.**

	488 <i>Cj0561c</i> mutant		p - value
	Fold change		
	0.2% ST	0.05% SDC	
<i>Cj0561c</i>	3.56	2.08	0.004
<i>cmeA</i>	2.03	1.77	0.4921
<i>cmeB</i>	1.47	1.26	0.0627
<i>cmeC</i>	1.57	1.61	0.7873

**G.**

	11168H		p - value
	Fold change		
	0.2% ST	0.05% SDC	
<i>Cj0561c</i>	6.23	3.42	0.0088
<i>cmeA</i>	2.99	2.66	0.2725
<i>cmeB</i>	2.85	2.57	0.2345
<i>cmeC</i>	2.66	2.49	0.6588

**H.**

	11168H <i>Cj0561c</i> mutant		p - value
	Fold change		
	0.2% ST	0.05% SDC	
<i>Cj0561c</i>	4.27	2.18	0.0286
<i>cmeA</i>	2.61	2.16	0.3427
<i>cmeB</i>	2.11	2.03	0.1117
<i>cmeC</i>	2.14	2.19	0.7032

**Figure 5.8** qRT-PCR analysis of *Cj0561c*, *cmeA*, *cmeB* and *cmeC* transcription in *C. jejuni* strains **(A)** 488 wild-type, **(B)** 11168H wild-type, **(C)** 488 *Cj0561c* mutant and **(D)** 11168H *Cj0561c* mutant strains co-incubated with either 0.2% (w/v) ST or 0.05% (w/v) SDC. Analysis was performed using gene specific primers. Two sets of *Cj0561c* primers were used which had amplification regions located either within the gene mutation site for wild-type strains **(A & B)** or as a negative control for *Cj0561c* mutant strains, or upstream of gene mutation side **(C & D)**. Significance of the difference in transcription of each gene between treatment conditions **(E-H)**. *rpoA* was used as an internal control. \* $p < 0.05$ ; \*\* $p < 0.01$ ; \*\*\* $p < 0.001$ .

### 5.2.3 *Cj0561c* does not have a major role in resistance to heat shock or osmotic stress.

To investigate if mutation of *Cj0561c* caused a notable change in fitness, motility, resistance to heat shock and resistance to osmotic stress were characterised for each *Cj0561c* mutant strain. Motility was analysed on semi-solid brucella agar (see Section 2.2.2). Sensitivity to osmotic stress was analysed by comparing growth of each strain on Brucella agar with or without supplementation of NaCl (0.5% (w/v) final concentration). This was performed by preparing a suspension of each strain to an OD<sub>600</sub> of 1.0 and spotting a serial dilution of this suspension onto the osmotic stress assay plates. Sensitivity to heat shock was analysed by comparing CFUs which remained after a bacterial suspension of OD<sub>600</sub> 1.0 was incubated at 55°C for three minutes.

There was no significant difference in motility between each wild-type and respective knock-out mutant strain prior to 48 hours. The 11168H *Cj0561c* mutant had a significant reduction in motility after 72 hours ( $p = 0.0083$ ), however this was not observed for the 488 *Cj0561c* mutant. The 488 *Cj0561c* complement strain was significantly less motile at all timepoints (24 hour  $p = 0.001$ , 48 hour  $p < 0.0001$ , 72 hour  $p < 0.0001$ ) (Figure 5.9). *C. jejuni* 488 strains, excluding the 488 *Cj0561c* complement, were more motile than 11168H strains. There was no significant difference in sensitivity to osmotic stress between wild-type and mutant strains. 11168H strains were more resistant to osmotic stress compared to 488 strains (Figure 5.10). The 11168H *Cj0561c* mutant demonstrated a slight but statistically significant ( $p = 0.0412$ ) increase in survival of heat shock compared to the 11168H wild-type strain. There were no significant differences in heat shock sensitivity between 488 strains. 11168H strains were more resistant to heat shock compared to 488 strains (Figure 5.11).

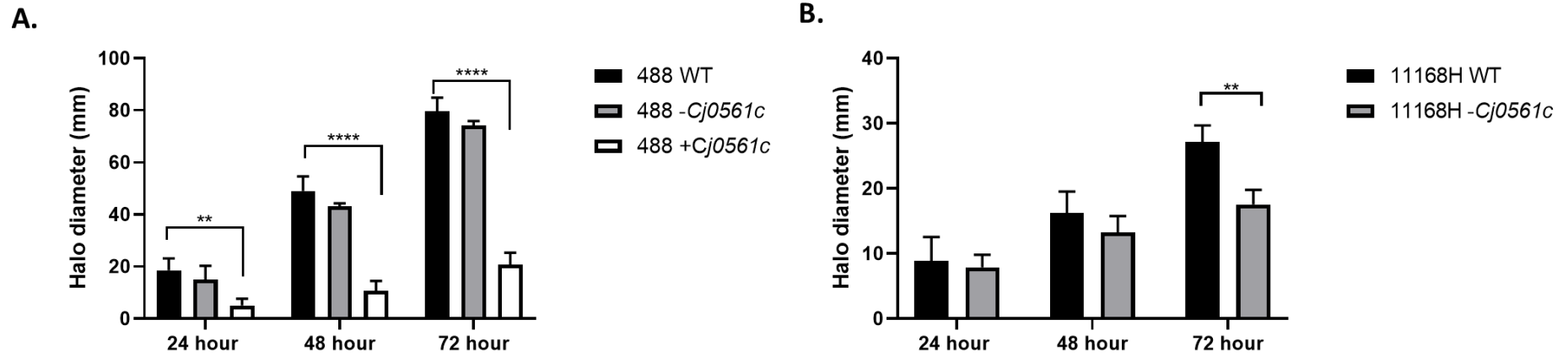


**Figure 5.9.** Motility assay results for **(A)** *C. jejuni* 488 wild-type, 488 *Cj0561c* mutant, 488 *Cj0561c* complement, **(B)** 11168H wild-type and 11168H *Cj0561c* mutant strains. \* $p < 0.05$ ; \*\* $p < 0.01$ ; \*\*\* $p < 0.001$ ; \*\*\*\* $p < 0.0001$ .

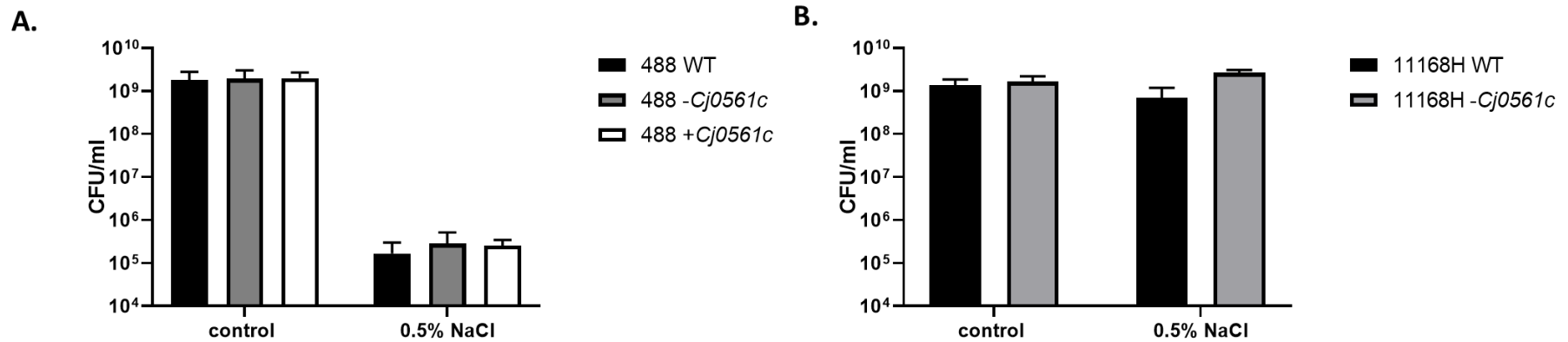
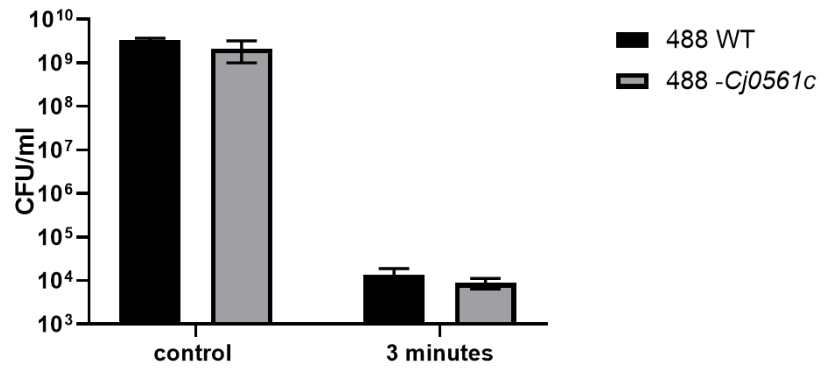


**Figure 5.10.** Osmotic stress assay results for **(A)** *C. jejuni* 488 wild-type, 488 *Cj0561c* mutant, 488 *Cj0561c* complement, **(B)** 11168H wild-type and 11168H *Cj0561c* mutant strains.

**A.**



**B.**

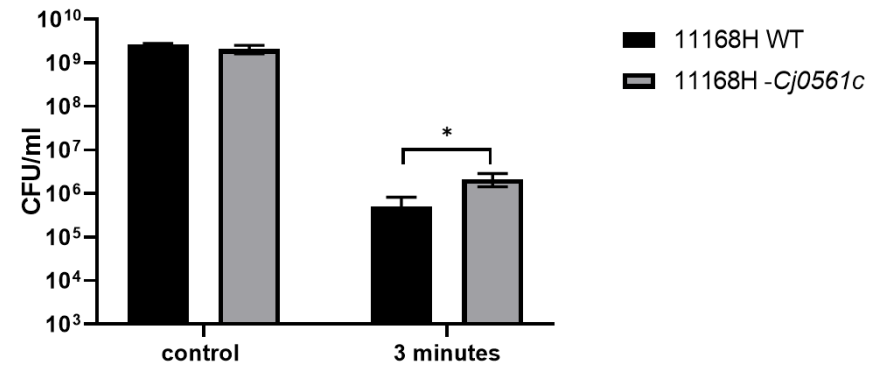


**Figure 5.11** Heat shock assay results for **(A)** *C. jejuni* 488 wild-type, 488 *Cj0561c* mutant, **(B)** 11168H wild-type and 11168H *Cj0561c* mutant strains. Heat treatment was carried out at 55°C for three minutes. \* $p < 0.05$ .

#### **5.2.4 Cj0561c does not appear to play a role in antibiotic resistance**

Due to the transcriptional link with the CmeABC multidrug efflux pump, and as Cj0561c is predicted to form an OM channel (Figures 5.1-5.7), the sensitivity to a range of antibiotics was investigated (Guo *et al.*, 2008). Wild-type and *Cj0561c* mutant strains were tested for sensitivity to amoxicillin/clavulanic acid (3 µg), tetracycline (30 µg), polymyxin B (300 U), ampicillin (10 and 100 µg) and erythromycin (2 µg) by the disk diffusion method (see Section 2.2.4). There was no significant difference in susceptibility to any of the antibiotics tested between each wild-type and respective mutant strain. Of note the 488 strains were significantly more resistant to ampicillin and erythromycin compared to the 11168H strains. 488 wild-type compared to 11168H wild-type, ampicillin 100 µg  $p < 0.0001$ . 488 wild-type compared to 11168H wild-type, erythromycin 2 µg  $p < 0.0001$  (Figure 5.12).

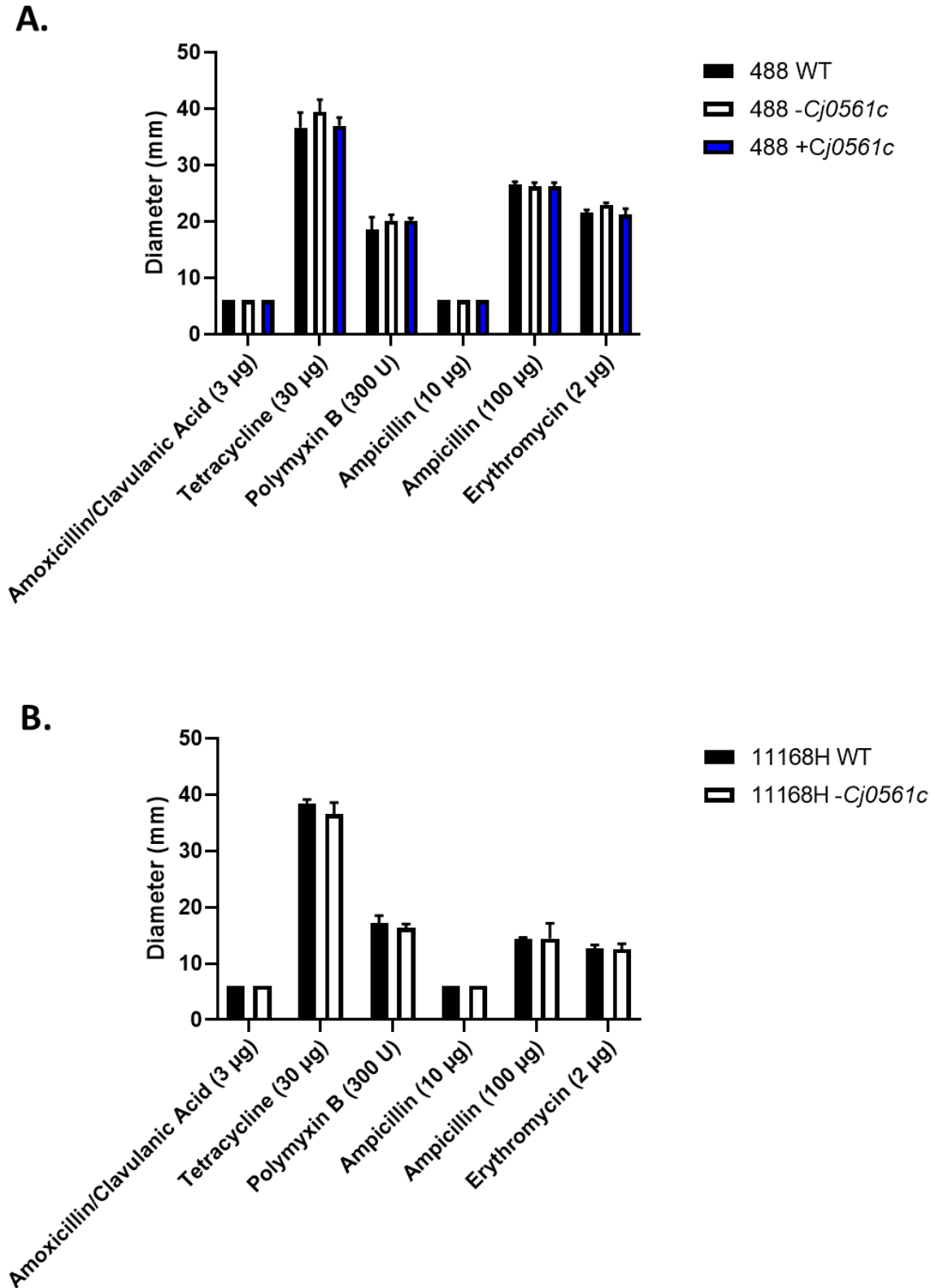


**Figure 5.12** Antibiotic sensitivity results for *C. jejuni* (A) 488 wild-type, 488 *Cj0561c* mutant, 488 *Cj0561c* complement, (B) 11168H wild-type and 11168H *Cj0561c* mutant strains. Antibiotic sensitivity was assayed using the disk diffusion method.

### **5.2.5 Cj0561c is not involved with bile salt sensitivity or active transport**

To further investigate the link between Cj0561c and bile salts, the sensitivity of *Cj0561c* mutant strains to stress level concentrations of either ST or SDC was investigated. The concentration of each bile salt used was 10-fold higher than the biologically relevant concentrations used for transcriptional work during this study. There was no significant difference in sensitivity to either bile salt between each wild-type and respective mutant strain. 11168H strains were more resistant to SDC stress compared to 488 strains. All strains demonstrated a high tolerance to ST stress (Figure 5.13).

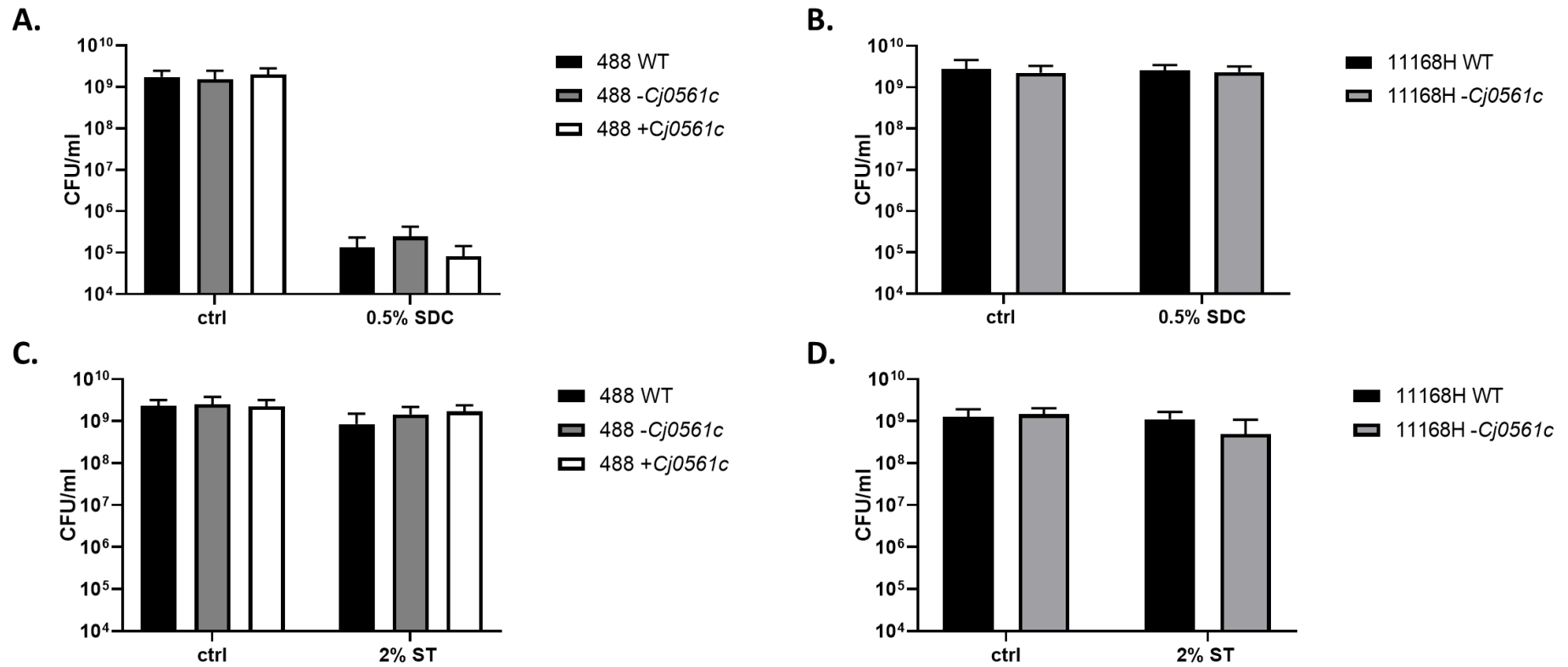


**Figure 5.13.** Sensitivity of *C. jejuni* (A & C) 488 wild-type, 488 *Cj0561c* mutant, 488 *Cj0561c* complement, (B & D) 11168H wild-type and 11168H *Cj0561c* mutant strains to either (C & D) 2% (w/v) ST or (A & B) 0.5% (w/v) SDC. CFU/ml were obtained from a 10-fold serial dilution of each strain spotted onto Brucella agar either with or without bile salts.

Cj0561c is predicted to form a channel in the OM (Figures 5.1-5.7). To further investigate any potential membrane defects caused by removal of the functional protein, sensitivity to 1.5 mM LSB, a zwitterionic detergent, was investigated. The *Cj0561c* mutant strain for both 488 and 11168H were significantly more resistant to LSB stress. The 488 wild-type strain showed around a 12-fold reduction in growth compared to the 488 *Cj0561c* mutant. The 11168H wild-type showed around a 2.5-fold reduction in growth compared to the 11168H *Cj0561c* mutant. The 488 *Cj0561c* complement strain phenotype was comparable to the 488 *Cj0561c* mutant phenotype. The 488 *Cj0561c* complement is not under control of the native promotor (Figure 5.14).

Carbonyl cyanide m-chlorophenyl hydrazone (CCCP) is an uncoupler of oxidative phosphorylation. It is an ionophore that disrupts the proton gradient which impacts protein complexes on the bacterial IM using active transport (Ghoul *et al.*, 1989). It has previously been used in the study of efflux pumps in Gram-negative bacteria including *C. jejuni* (Yan *et al.*, 2006; Ngernsombat *et al.*, 2017). To investigate if Cj0561c could form the OM component of a transport system requiring active transport, sensitivity to 1.5 mM LSB in the presence of CCCP was investigated. Should CCCP inhibit a Cj0561c associated complex, a *Cj0561c* mutant-like phenotype would be expected for the wild-type strain. Both wild-type strains and both *Cj0561c* mutant strains grown in the presence of LSB showed an additional dose-dependent reduction in growth caused by the presence of CCCP. The magnitude of growth reduction caused by CCCP was comparable between wild-type and respective mutant strains. The increased resistance to LSB observed in *Cj0561c* mutant strains was maintained in the presence of CCCP (Figure 5.14).

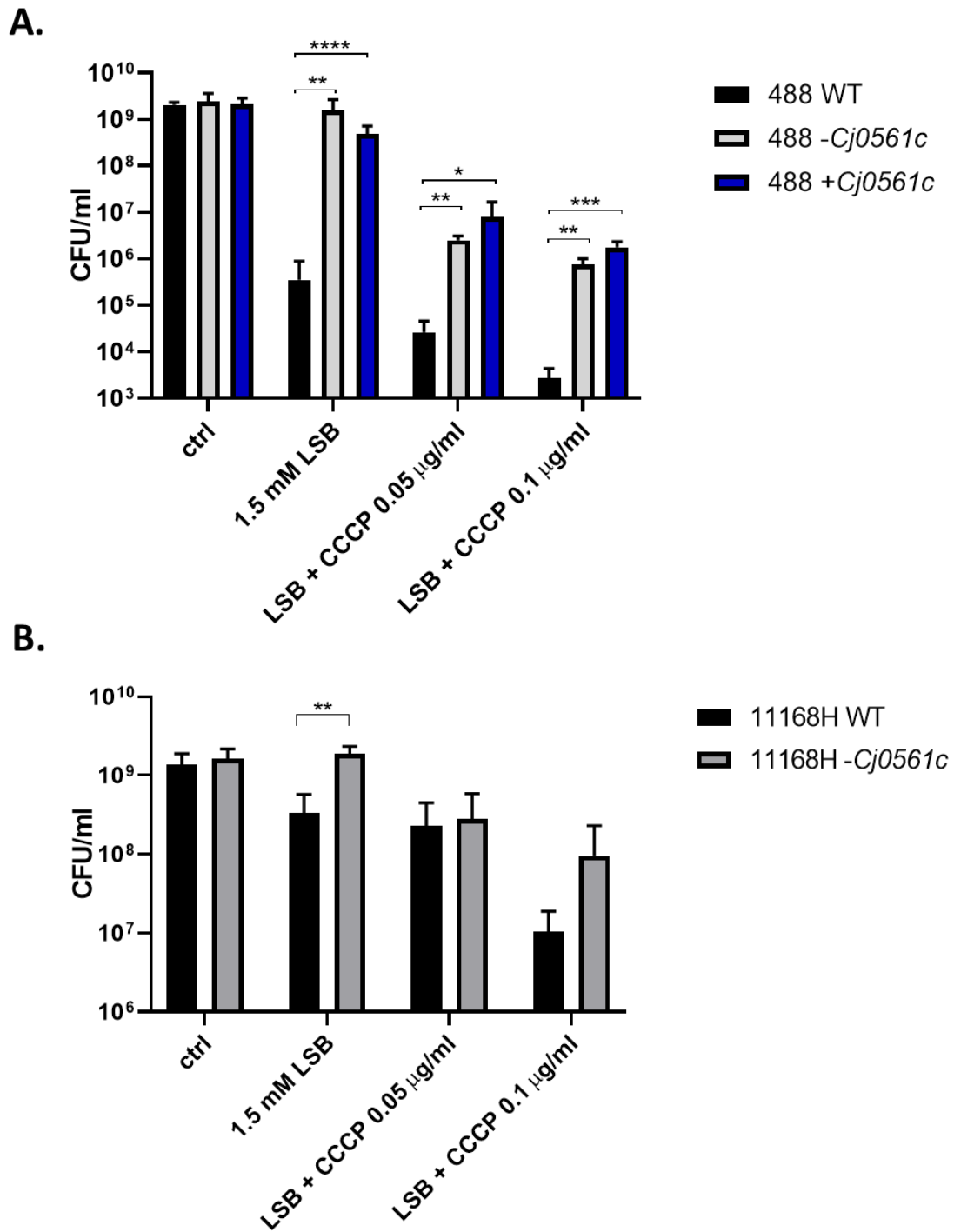
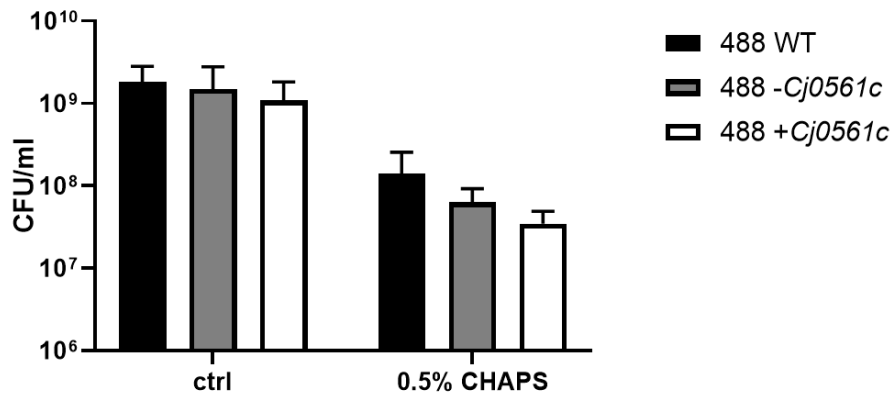


**Figure 5.14.** Sensitivity of *C. jejuni* (A) 488 wild-type, 488 *Cj0561c* mutant, 488 *Cj0561c* complement, (B) 11168H wild-type and 11168H *Cj0561c* mutant strains to either 1.5 mM LSB or 1.5 mM LSB with CCCP (0.05 or 0.1 µg/ml). CFU/ml were obtained from a 10-fold serial dilution of each strain spotted onto Brucella agar either with or without LSB or CCCP. \* $p < 0.05$ ; \*\* $p < 0.01$ .

### 5.2.6 Cj0561c does not have a general role in detergent sensitivity.

To better understand the specificity of the LSB *Cj0561c* phenotype observed in Section 5.2.5, sensitivity to similar detergents was investigated. The zwitterionic detergent LSB is a ammonium betaine in which the nitrogen is attached to dodecyl, 3-sulfatopropyl and two methyl groups (NCBI, 2022b) (Appendix 7). Similar compounds selected were ST, 3-((3-Cholamidopropyl)dimethylammonium)-1-propanesulfonate (CHAPS) and SDS (Appendix 7). ST has been shown to upregulate transcription of *Cj0561c* and contains terminal sulphate group similar to LSB (NCBI, 2022e). SDC does not contain this terminal sulphate group (NCBI, 2022a). CHAPS is a zwitterionic detergent that contains the 3-sulfatopropyl and two methyl groups present in LSB but in place of the dodecyl group is a CA structure similar to ST and SDC (NCBI, 2022c). SDS contains a dodecyl group attached to a sulphate group similar to LSB but lacks the ammonium central group (NCBI, 2022d). Bile salts and SDS are anionic detergents. Sensitivity to ST and SDC have previously been investigated and showed no significant differences between wild-type and mutant strains (Section 5.2.5). There was also no significant difference seen between wild-type and mutant strains for either CHAPS (Figure 5.15) or SDS (Figure 5.16). The presence of ST at biologically relevant concentrations increased resistance to SDS for all strains (Figure 5.16B).

**A.**



**B.**

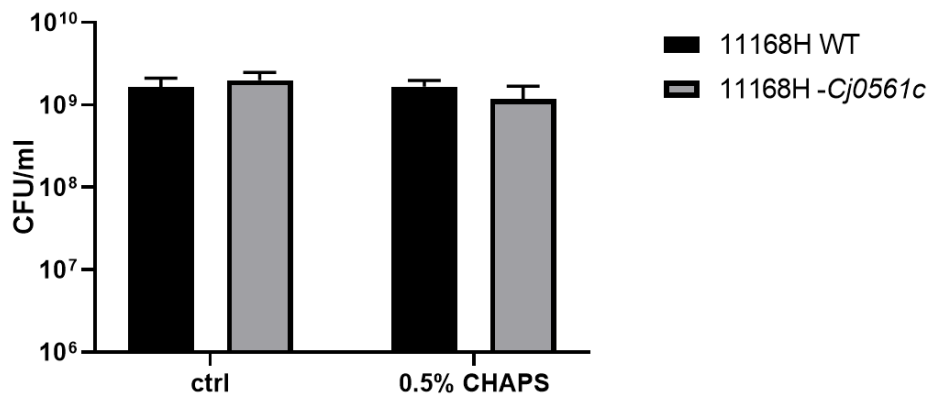


**Figure 5.15.** Sensitivity of *C. jejuni* (A) 488 wild-type, 488 *Cj0561c* mutant, 488 *Cj0561c* complement, (B) 11168H wild-type and 11168H *Cj0561c* mutant strains to 0.5% (w/v) CHAPS. CFU/ml were obtained from a 10-fold serial dilution of each strain was spotted onto Brucella agar either with or without CHAPS.

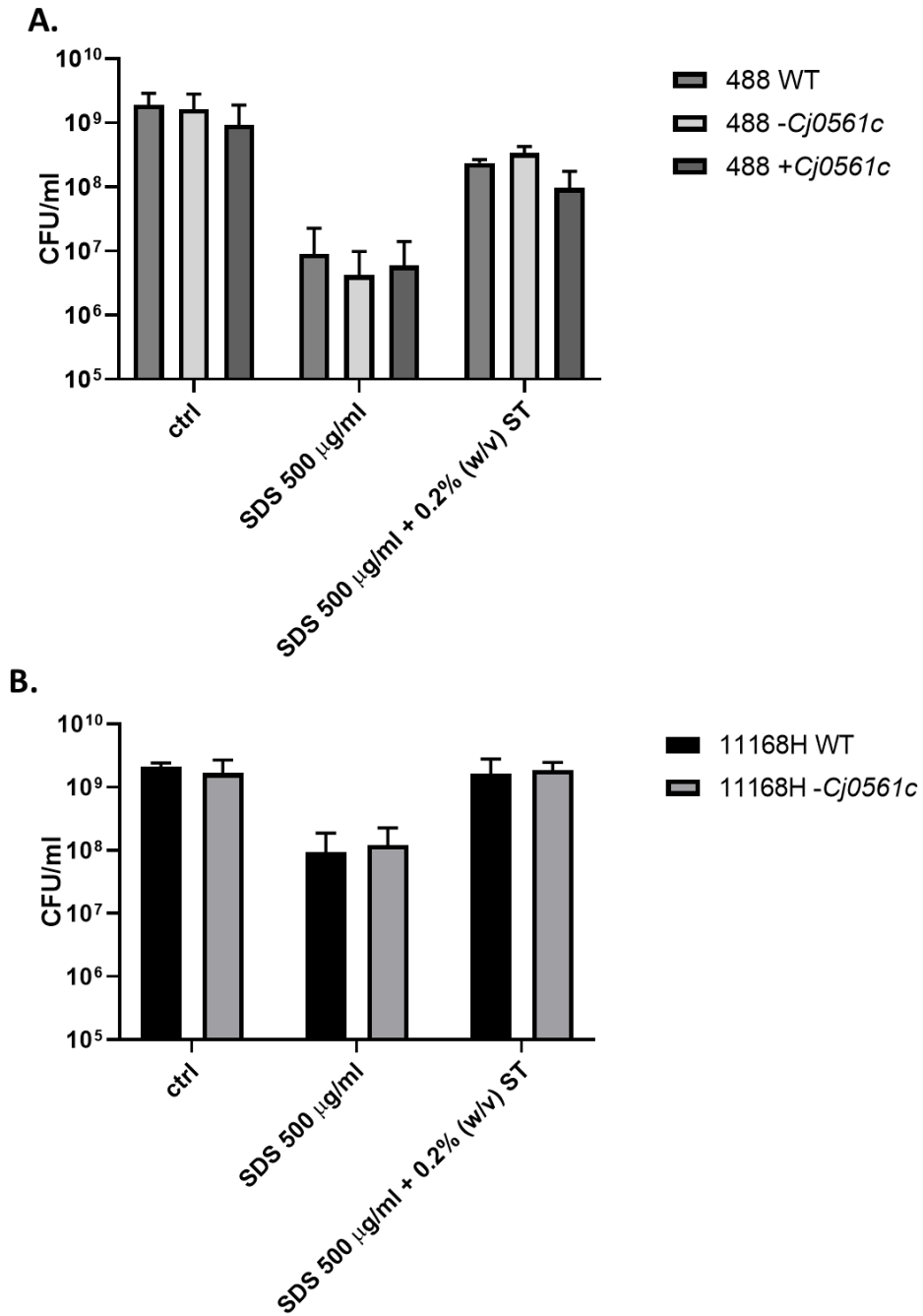
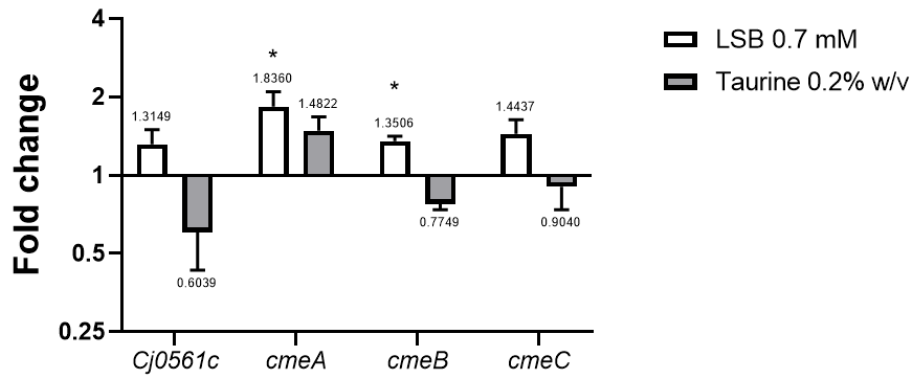


**Figure 5.16** Sensitivity of *C. jejuni* (A) 488 wild-type, 488 *Cj0561c* mutant, 488 *Cj0561c* complement, (B) 11168H wild-type and 11168H *Cj0561c* mutant strains to either 500 µg/ml SDS or 500 µg/ml SDS with 0.2% (w/v) ST. CFU/ml were obtained from a 10-fold serial dilution of each strain was spotted onto Brucella agar either with or without detergents.

### 5.2.7 Transcriptional response of *Cj0561c* and *cmeABC* to LSB and taurine.

In an attempt to better understand the link between *Cj0561c* and the detergents ST and LSB, further qRT-PCR experiments were performed. ST caused a greater transcriptional response compared to SDC. Key structural differences between ST and SDC are that SDC is an unconjugated bile salt whereas ST is conjugated to taurine. SDC also has a hydroxy group from the CA structure removed by 7- $\alpha$  dehydroxylation. To investigate if the presence of taurine could influence the difference in transcriptional response seen between SDC and ST, qRT-PCR was performed on RNA extracted from 488 wild-type and 11168H wild-type mid-log phase cultures grown as previously described (see Section 2.5.7) in the presence of 0.2% (w/v) taurine. Minimal transcriptional changes were seen for cultures supplemented with low concentrations of taurine. The transcription of *cmeABC* was slightly reduced in the presence of 0.2% (w/v) taurine, with the exception of *cmeA* for the 488 wild-type strain. A greater reduction in transcription for *Cj0561c* compared to *cmeABC* was observed for both strains in the presence of taurine (Figure 5.17). RNA was extracted from mid-log phase cultures as described above but with the addition of 0.7 mM LSB. Two preliminary qRT-PCR biological replicates were performed with the 488 wild-type strain using the subinhibitory concentration 0.5 mM LSB (Figure 3.4). Minimal transcriptional changes were observed using 0.5 mM LSB (Appendix 9). 1.0 mM LSB caused around a 4-log reduction in growth (Figure 3.4). As all previous work in this study has utilised subinhibitory detergent concentrations, 1.0 mM LSB would not produce results that are comparable to the other datasets this study. 0.7 mM LSB was selected as an intermediate concentration. 0.7 mM LSB caused moderate transcriptional changes, however, further increases in concentration would be unsuitable for this dataset. Cultures grown in the presence of LSB showed comparable increases in transcription of *Cj0561c* and *cmeABC* (Figure 5.17).

**A.**



**B.**

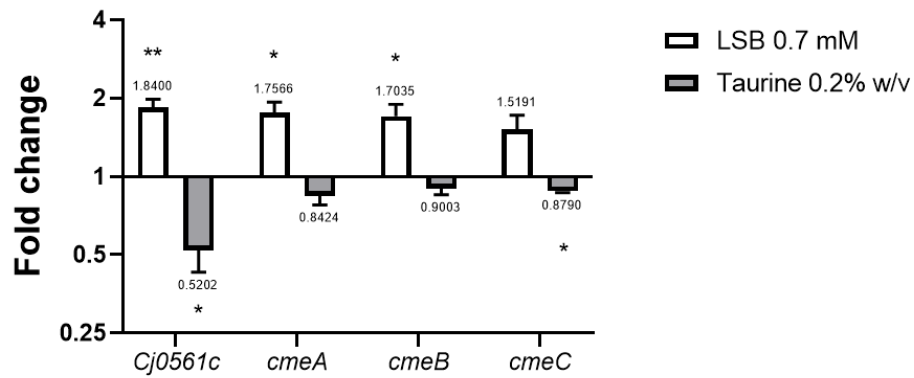


**Figure 5.17** qRT-PCR analysis of *Cj0561c*, *cmeA*, *cmeB* and *cmeC* transcription in *C. jejuni* strains **(A)** 488 wild-type, **(B)** 11168H wild-type, strains co-incubated with either 0.7 mM LSB or 0.2% (w/v) taurine. Analysis was performed using gene specific primers. *rpoA* was used as an internal control. Fold change in gene expression compared to *C. jejuni* grown in the absence of LSB or taurine. \* $p < 0.05$ ; \*\* $p < 0.01$ .

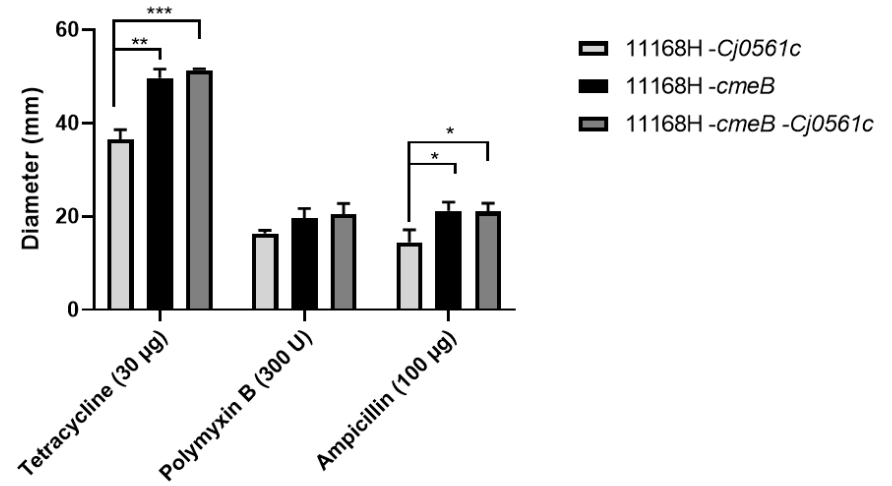
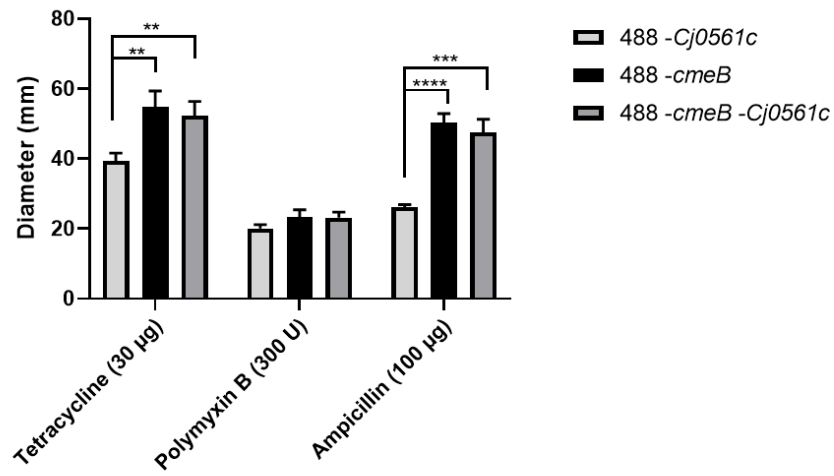
### 5.2.8 CmeABC does not mask a Cj0561c detergent stress phenotype.

To investigate whether the CmeABC efflux pump could compensate or mask antibiotic or detergent stress phenotypes of *Cj0561c* mutant strains, antibiotic and detergent assays were repeated with 488 and 11168H *cmeB* single and *cmeB Cj0561c* double mutants. *Cj0561c* single mutants were constructed using a kanamycin resistance cassette, the *cmeB* mutants were constructed using an erythromycin resistance cassette (see Section 2.5.3). Antibiotic sensitivity was performed as previously described (see Section 2.2.4) using the disk diffusion method for tetracycline (30 µg), polymyxin B (300 U), ampicillin (100 µg). Mutation of *cmeB* did not cause a significant difference in sensitivity to polymyxin B but did significantly increase sensitivity to tetracycline ( $p = 0.0061$  or  $p = 0.0082$  for the 488 *Cj0561c* mutant compared to *cmeB* single or double mutant respectively.  $P = 0.0012$  or  $p = 0.0002$  for the 11168H *Cj0561c* mutant compared to *cmeB* single or double mutant respectively) and ampicillin ( $p < 0.0001$  or  $p = 0.0007$  for the 488 *Cj0561c* mutant compared to *cmeB* single or double mutant respectively.  $P = 0.0241$  or  $p = 0.0248$  for the 11168H *Cj0561c* mutant compared to *cmeB* single or double mutant respectively) compared to the *Cj0561c* single mutant. There was no significant difference in sensitivity to any of the antibiotics observed between the *cmeB* single and *cmeB Cj0561c* double mutants (Figure 5.18A).

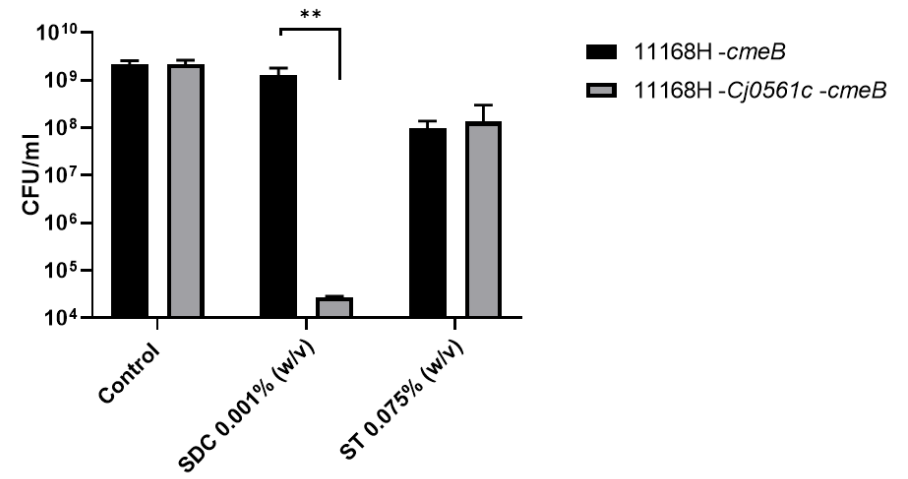
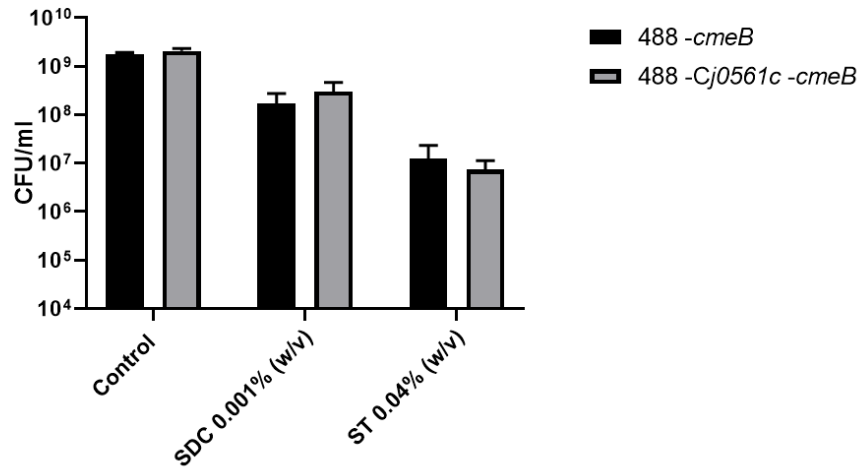
Sensitivity to ST (2% w/v) and SDC (0.5% w/v) was analysed as described previously (see Section 5.2.5) however no growth was observed for either the *cmeB* single or *cmeB Cj0561c* double mutants. Bile salt sensitivity assays were repeated with reduced bile salt concentrations. ST was reduced to 0.04% (w/v) for 488 strains, and 0.075% (w/v) for 11168H strains. SDC was reduced to 0.001% (w/v) for both 488 and 11168H strains. There was no significant difference in sensitivity to either bile salt seen between *cmeB* single or *cmeB Cj0561c* double mutants for 488 strains. For 11168H strains there was no significant difference in sensitivity observed between *cmeB* single or *cmeB Cj0561c* double mutants for ST, however the *cmeB Cj0561c* double mutant demonstrated a significant ( $p = 0.0067$ ) increase in sensitivity to SDC compared to the *cmeB* single mutant (Figure 5.18B).

Sensitivity to either 1.5 mM LSB or 1.5 mM LSB with CCCP (0.05 or 0.1 µg/ml) was analysed as previously described (Section 5.2.5) however no growth was observed for either the *cmeB* single or *cmeB Cj0561c* double mutants. As CCCP sensitivity should not be affected by loss of *cmeB* function, CCCP assays were repeated with reduced LSB concentrations (0.2 mM) only. As seen previously in comparison to wild-type strains (Figure 5.14) mutation of *Cj0561c* did again increase resistance to LSB in *cmeB* mutant strains (Figure 5.18C).

## A. Antibiotic sensitivity



## B. Bile salt sensitivity



### C. Lauryl sulfobetaine and Carbonyl cyanide m-chlorophenyl hydrazone sensitivity

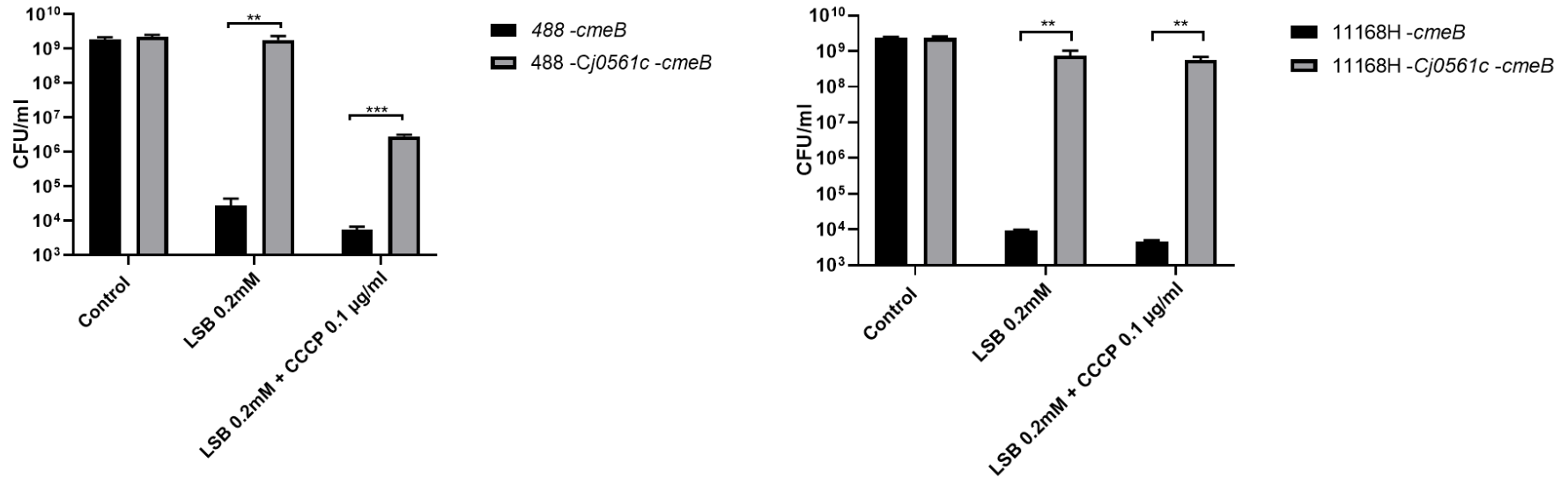


**Figure 5.18.** *cmeB* *Cj0561c* double or *cmeB* single mutant assays. **(A)** Antibiotic sensitivity results for *C. jejuni* 488 and 11168H *cmeB* single and *cmeB* *Cj0561c* double mutant strains. Antibiotic sensitivity was assayed using the disk diffusion method. **(B)** Sensitivity of *C. jejuni* 488 and 11168H *cmeB* single and *cmeB* *Cj0561c* double mutant strains to either 2% (w/v) ST or 0.5% (w/v) SDC. CFU/ml were obtained from a 10-fold serial dilution of each strain was spotted onto Brucella agar either with or without bile salts. **(C)** Sensitivity of *C. jejuni* 488 and 11168H *cmeB* single and *cmeB* *Cj0561c* double mutant strains to 0.2 mM LSB either with or without CCCP 0.1 µg/ml. CFU/ml were obtained from a 10-fold serial dilution of each strain was spotted onto Brucella agar either with or without LSB or CCCP. \* $p < 0.05$ ; \*\* $p < 0.01$ ; \*\*\* $p < 0.001$ ; \*\*\*\* $p < 0.0001$ .

### 5.2.9 Cj0561c has no clear role during bacterial interactions with host cells

OMPs can play a role in adhesion and invasion of host cells (Schmidt *et al.*, 2019). Cj0561c has previously been demonstrated to be required for optimal chick colonisation through an unknown mechanism (Guo *et al.*, 2008). To investigate if Cj0561c could play a role in IEC adhesion or invasion, tissue culture assays were performed using Caco-2 and T84 human IECs. The 488 and 11168H wild-type and *Cj0561c* mutant strains were included in tissue culture assays. The 488 *Cj0561c* complement strain was not included due to the reduced motility phenotype (Figure 5.9). Tissue culture infection assays were carried out as described previously (see Section 2.4.2). For interaction assays, cells were infected for either 3 or 24 hours prior to IEC lysis and CFU enumeration. For invasion assays, cells were infected for either 3 or 24 hours prior to gentamicin treatment followed by IEC lysis and CFU enumeration. For survival assays, IECs were infected for 3 hours followed by gentamicin treatment to remove extracellular bacteria. IECs were then incubated overnight with gentamicin for 24 hours prior to IEC lysis and CFU enumeration. As a control, CFU/ml of bacterial growth in tissue culture media under tissue culture incubation conditions were investigated. There was no significant difference in growth under tissue culture infection condition (Figure 5.19).

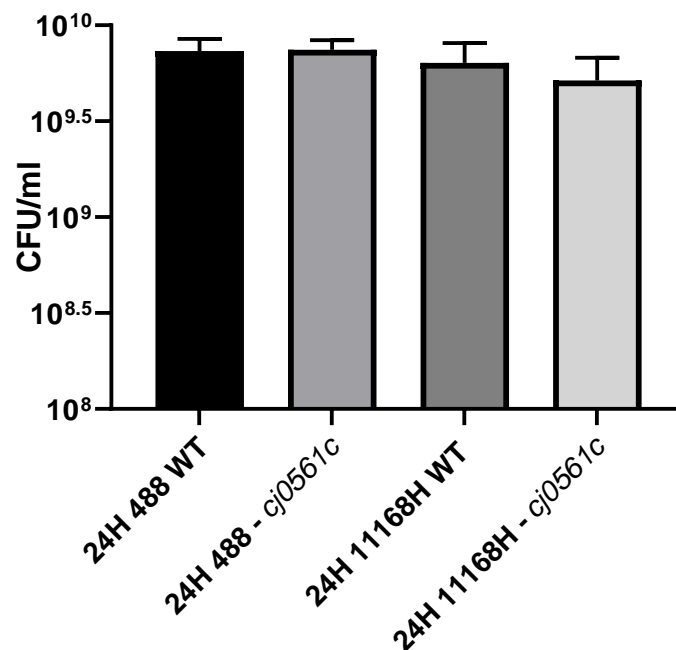


**Figure 5.19.** Growth of *C. jejuni* strains under tissue culture conditions. *C. jejuni* 488 wild-type, 488 *Cj0561c* mutant, 11168H wild-type and 11168H *Cj0561c* mutant strains were incubated in tissue culture medium under anaerobic conditions for 24 hours then plated for CFUs.

When compared to wild-type interaction with either T84 or Caco-2 IECs, at both 3 and 24 hours, the 488 *Cj0561c* mutant showed increased interaction. However, the 11168H *Cj0561c* mutant showed reduced interaction (Figure 5.20 A,B,E). When compared to wild-type invasion, both the 488 and 11168H *Cj0561c* mutants showed reduced invasion of Caco-2 cells at both 3 and 24 hours (Figure 5.20D,E). The 488 *Cj0561c* mutant showed increased invasion of T84 cells at 3 hours, but no difference at 24 hours. The 11168H *Cj0561c* mutant showed no difference in invasion of T84 cells after 3 hours but showed reduced invasion after 24 hours (Figure 5.20C,E).

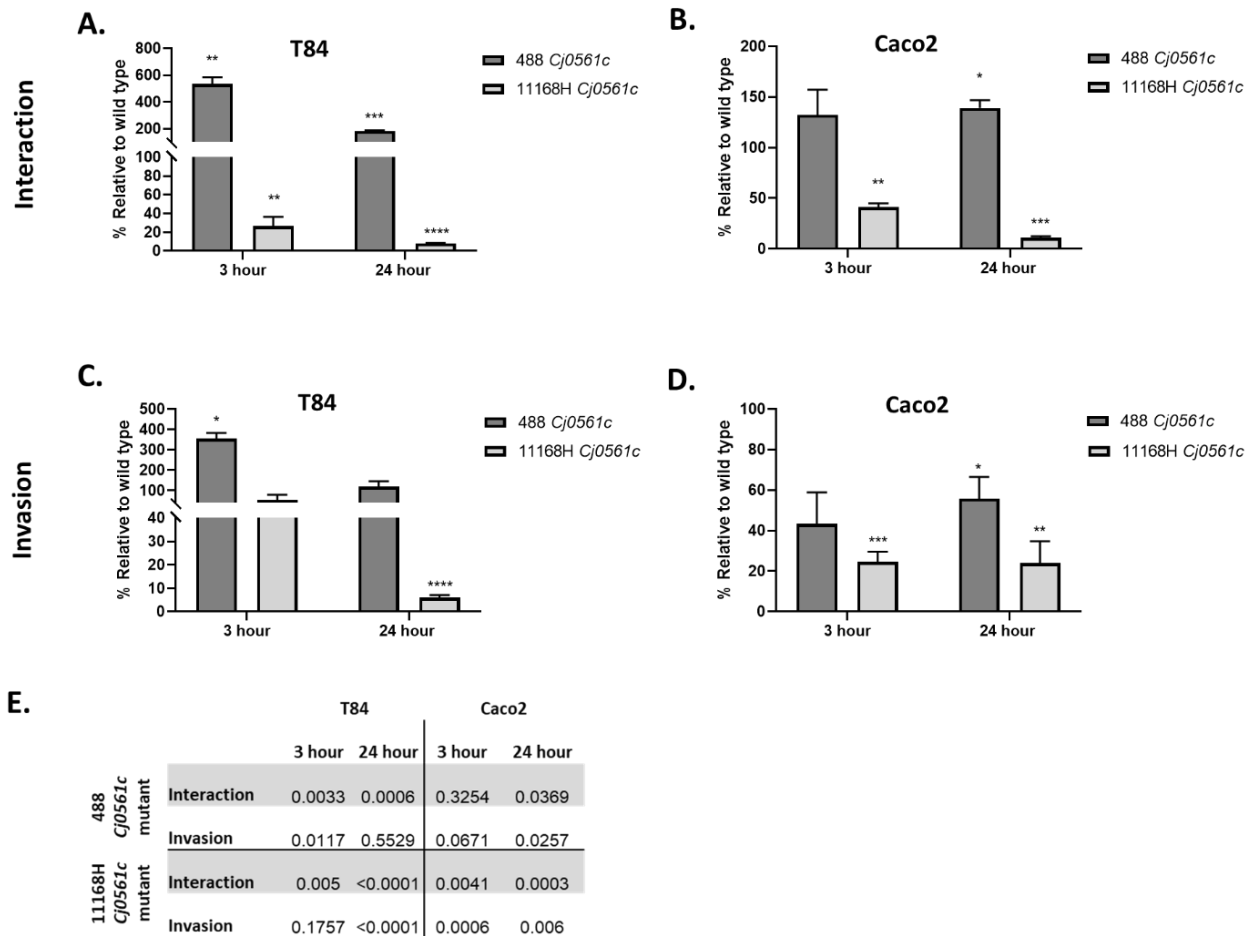


**Figure 5.20.** Interactions with, and invasion of, T84 and Caco-2 human IECs with *C. jejuni* 488 wild-type, 488 *Cj0561c* mutant, 11168H wild-type and 11168H *Cj0561c* mutant strains. **(A & C)** T84 or **(B & D)** Caco-2 cells were infected with *C. jejuni* strains to an MOI of 200:1. **(A & B)** For interaction assays, IECs were infected for either 3 or 24 hours, cells were then washed, lysed, and plated for CFUs. **(C & D)** For invasion assays, IECs were infected for either 3 or 24 hours, cells were then washed, treated with gentamicin for two hours, washed, lysed and plated for CFUs. Results are recorded as a percentage of mutant CFUs/ml relative to respective wild-type CFUs/ml. **(E)** *p*-values for graphs **A-D**. \**p* < 0.05; \*\**p* < 0.01; \*\*\**p* < 0.001; \*\*\*\**p* < 0.0001.

To investigate further, intracellular survival assays were performed. Survival was calculated as percentage survival compared to wild-type CFU (Figure 5.21A), or as percentage survival of invading bacteria (Figure 5.21 B,C). When calculated as percentage of wild-type survival, the 488 *Cj0561c* mutant showed moderately increased survival for both T84 ( $p = 0.0222$ ) and Caco-2 cells ( $p = 0.4863$ ). The 11168H *Cj0561c* mutant showed a significant reduction in survival for both cells lines ( $p < 0.0001$  or  $p = 0.003$  for T84 and Caco2 respectively). When calculated as percentage survival of invading bacteria, there was no significant difference in survival for either cell lines for the 488 *Cj0561c* mutant. The 11168H *Cj0561c* mutant showed no significant difference in survival in Caco-2 cells but shown a small but significant reduction in survival in T84 cells ( $p = 0.0007$ ).

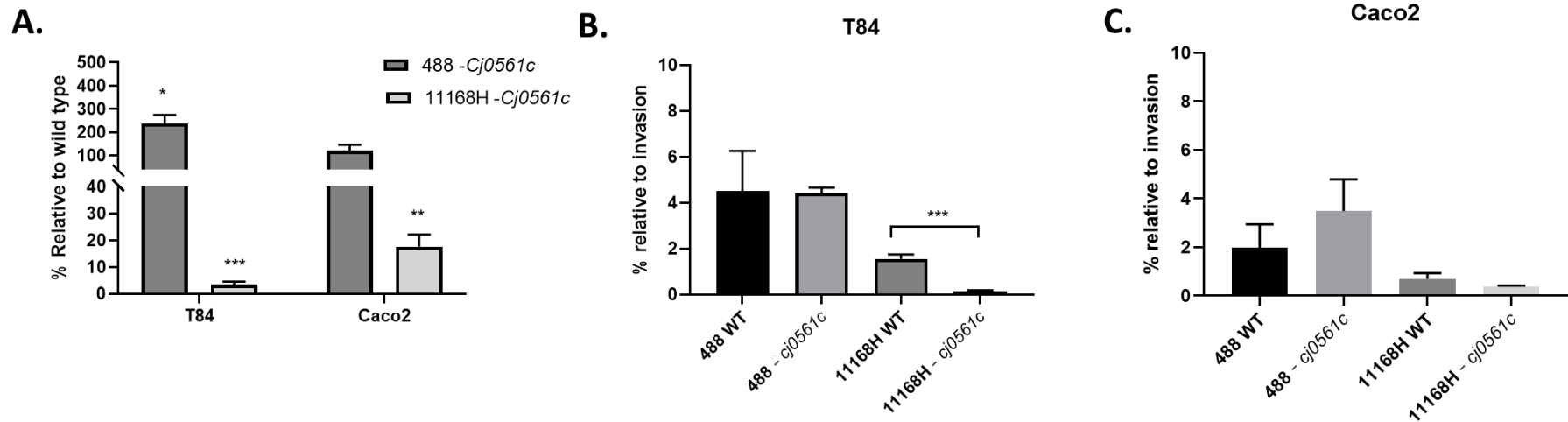


**Figure 5.21.** Survival of *C. jejuni* 488 wild-type, 488 *Cj0561c* mutant, 11168H wild-type and 11168H *Cj0561c* mutant strains with T84 or Caco-2 human IECs. Caco-2 or T84 cells were infected with *C. jejuni* to an MOI of 200:1. Cells were then washed and treated with gentamicin (150  $\mu\text{g/ml}$ ) for two hours, followed by incubation with gentamicin (10  $\mu\text{g/ml}$ ) for 18 hours. Cells were then washed, lysed and plated for CFUs. **(A)** Percentage survival of *C. jejuni* 488 *Cj0561c* mutant or 11168H *Cj0561c* mutant strains in T84 or Caco-2 cells relative to respective wild-type strains. **(B)** Percentage survival of *C. jejuni* 488 wild-type, 488 *Cj0561c* mutant, 11168H wild-type or 11168H *Cj0561c* mutant strains in T84 cells compared to invasion CFUs/ml of each strain. **(C)** Percentage survival of *C. jejuni* 488 wild-type, 488 *Cj0561c* mutant, 11168H wild-type or 11168H *Cj0561c* mutant strains in Caco-2 cells compared to invasion CFU/ml of each strain. \* $p < 0.05$ ; \*\* $p < 0.01$ ; \*\*\* $p < 0.001$ .

Both *C. jejuni* bacterial cells and *C. jejuni* culture supernatant can trigger the secretion of the proinflammatory chemokine IL-8 (Zheng *et al.*, 2008). As OMPs can be potent immunogenic proteins and as Cj0561c has been identified in OMVs secreted by *C. jejuni* (Elmi *et al.*, 2018), the ability of Cj0561c to contribute to the stimulation of IL-8 production was investigated. This was done using either live *C. jejuni* Cj0561c mutant strains or OMVs produced by Cj0561c mutant strains. IL-8 production was quantified using the Invitrogen Human IL-8 Uncoated ELISA kit according to manufacturer's protocol. ELISA input samples were the supernatant of T84 IECs infected for 24 hours with either the 11168H or 488 wild-type or Cj0561c mutant strains, or the OMVs produced by these strains. OMVs were quantified based on total protein concentration then 100 µg of OMVs in 1 ml of infection media was used per well of T84 cells in 24 well tissue culture plates. OMVs were isolated from bacterial cultures (see Section 2.3.1) grown in the presence or absence of 0.2% (w/v) ST.

The 488 Cj0561c mutant triggered significantly higher IL-8 secretion. There was no significant difference in IL-8 secretion from cells infected with either of the 11168H strains (Figure 5.22). There was no significant difference in IL-8 secretion from T84 cells infected with any of the OMV preparations (Figure 5.23). However, all live bacterial cells and OMV preparations did further stimulate IL-8 production in comparison to the uninfected controls.

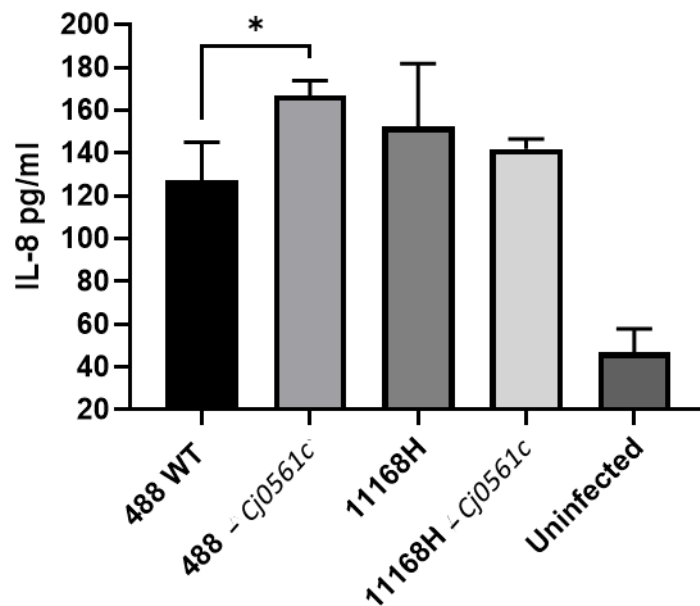


**Figure 5.22.** IL-8 secretion of T84 cells infected with *C. jejuni* 488 wild-type, 488 Cj0561c mutant, 11168H wild-type or 11168H Cj0561c mutant strains. T84 cells were infected with *C. jejuni* strains for 24 hours. IL-8 secreted into infection media was then quantified using the Invitrogen Human IL-8 Uncoated ELISA Kit. \* $p < 0.05$ .

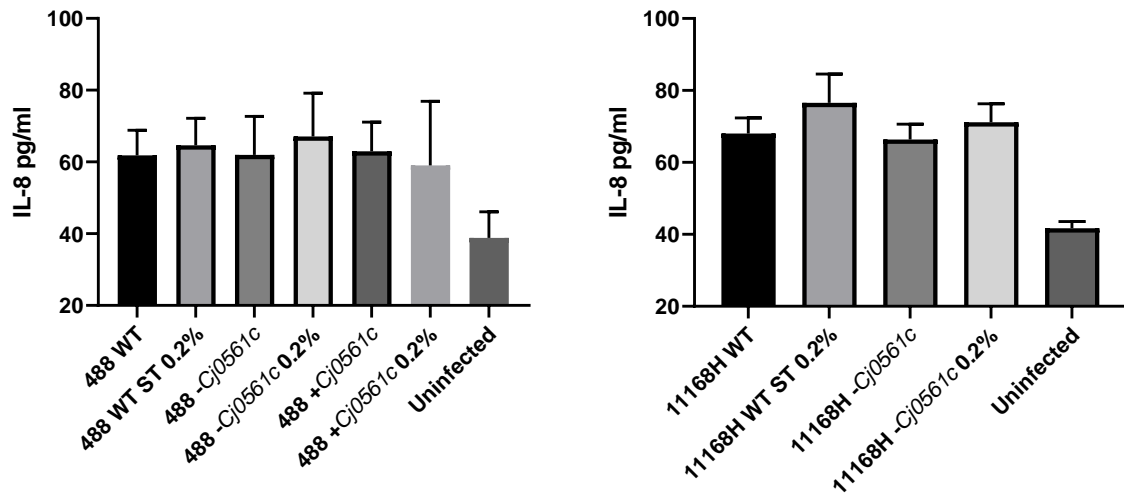


**Figure 5.23** IL-8 secretion of T84 cells inoculated with *C. jejuni* 488 wild-type, 488 *Cj0561c* mutant, 488 *Cj0561c* complement, 11168H wild-type or 11168H *Cj0561c* mutant strain OMVs produced either in the presence or absence of 0.2% (w/v) ST. T84 cells were incubated with *C. jejuni* OMVs for 24 hours. IL-8 secreted into infection media was then quantified using the Human IL-8 Uncoated ELISA Kit.

### 5.2.10 *Cj0561c* plays a role in OMV related cytotoxicity in the *Galleria mellonella* larvae model of infection.

*Galleria mellonella* (Greater wax moth) larvae are susceptible to infection with *C. jejuni* and can provide an alternative to animal models for screening of virulence genes. *G. mellonella* larvae are able to survive at 37°C while also possessing hemocytes, specialised phagocytic cells which form part of the larvae's innate immune response. Hemocytes kill bacteria using antimicrobial peptides and ROS, resembling the mechanisms used by mammalian phagocytes. Growth at 37°C also allows for the incubation of *C. jejuni* at temperatures resembling human infection, which can allow for the expression of temperature sensitive virulence factors (Senior *et al.*, 2011; Askoura and Stintzi, 2017). In addition to infection of live bacteria, *G. mellonella* may also allow for the screening of secreted virulence factors found in culture cell free supernatants (Kay *et al.*, 2019b).

*G. mellonella* larvae were infected with live *C. jejuni* 488 and 11168H wild-type and *Cj0561c* mutant strains (see Section 2.5.1). Larvae were incubated at 37°C under aerobic conditions. Survival and health were recorded every 24 hours for five days. Larvae were recorded as unhealthy once melanisation was visible (Figure 5.24). Larvae that did not move in response to touch were recorded as deceased. Deceased larvae exhibit complete melanisation.

The *C. jejuni* 488 wild-type strain was more virulent than the 11168H wild-type in the *G. mellonella* model of infection, causing around 50% mortality and 100% loss of health after five days, compared to 20% and 60% mortality and health respectively for 11168H (Figure 5.25). The 488 wild-type strain also caused significantly greater mortality and loss of health in comparison to the 488 *Cj0561c* mutant (Figure 5.25 A,B), which reached around 20% and 80% mortality and health respectively after five days. The 11168H wild-type caused similar mortality rates as the 11168H *Cj0561c* mutant (around 15-20% mortality after 5 days), however, the 11168H *Cj0561c* mutant caused a significantly greater reduction in health reaching around 60% and 80% reduction in health for the 11168H wild-type and *Cj0561c* mutant respectively (Figure 5.25 C,D).



**Figure 5.24.** Classification of *G. mellonella* health. **(1)** Healthy larvae with no visible melanisation. **(2)** Unhealthy larvae with melanisation viable in the lateral line. **(3)** Unhealthy larvae with melanisation viable in the lateral line and minor systemic melanisation. **(4)** Unhealthy larvae with major systemic melanisation. **(5)** Deceased larvae with total melanisation.

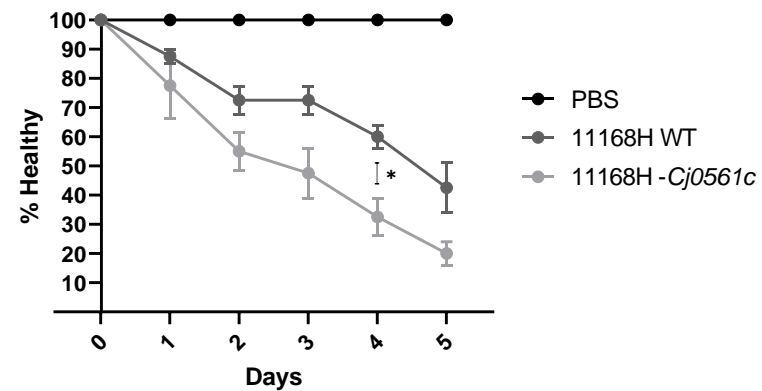
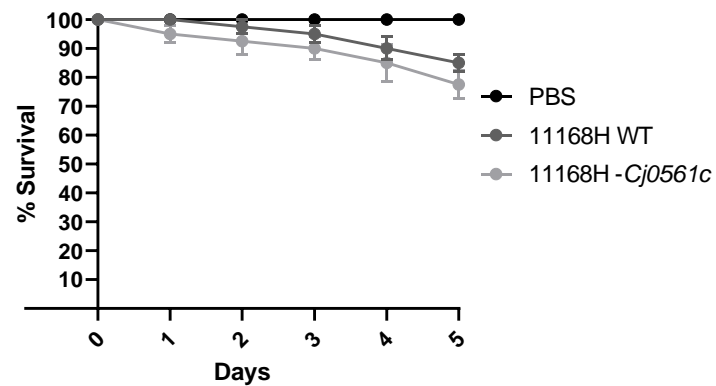
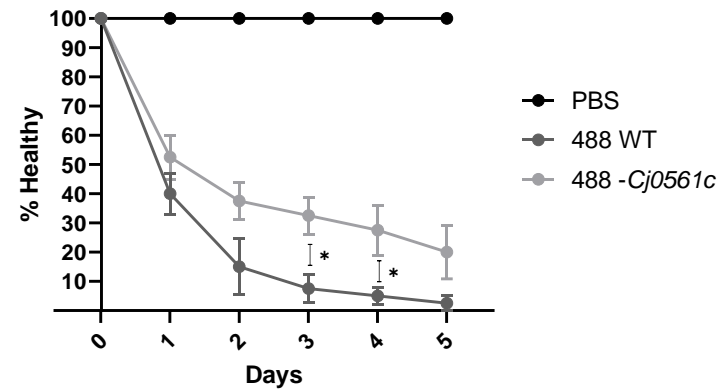
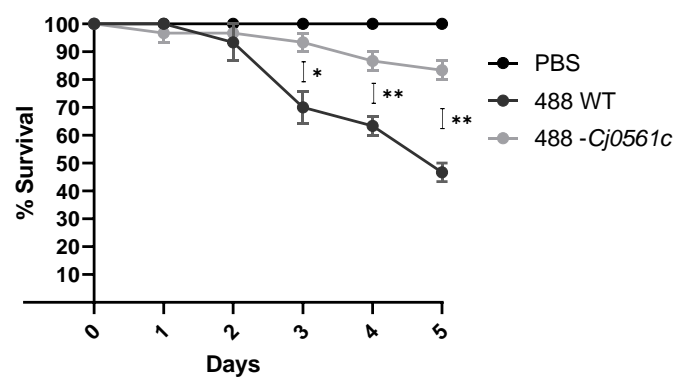


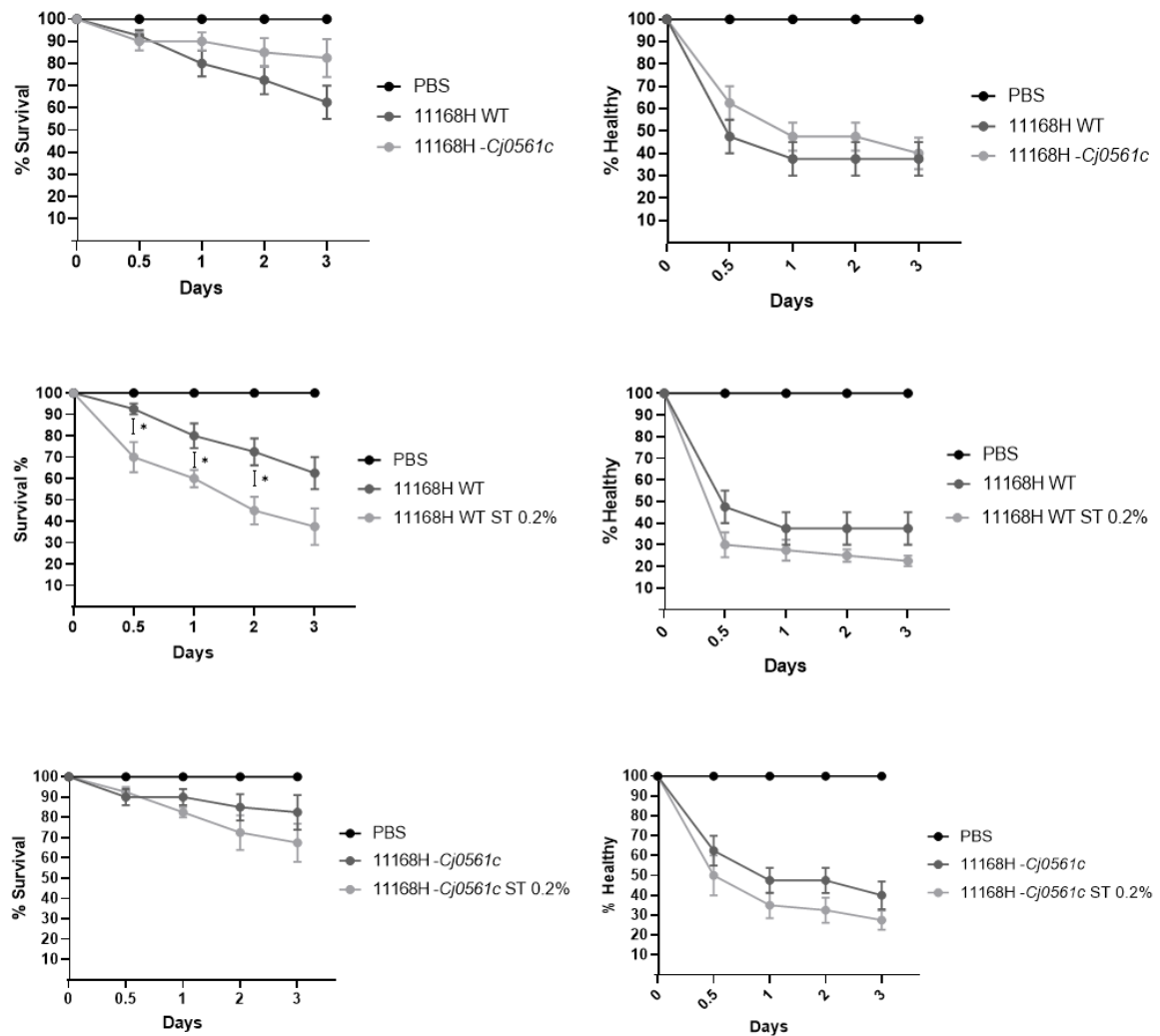
**Figure 5.25.** Infection of *Galleria mellonella* larvae with *C. jejuni* 488 wild-type, 488 *Cj0561c* mutant, 11168H wild-type or 11168H *Cj0561c* mutant strains. For each strain ten larvae were injected per replicate in the right foremost leg with 10  $\mu$ l of bacterial suspension. Additional *G. mellonella* were injected with 10  $\mu$ l sterile PBS as controls. Larvae were incubated at 37°C under aerobic conditions for five days. Health and survival of larvae was recorded every 24 hours. \* $p < 0.05$ ; \*\* $p < 0.01$ .

*C. jejuni* 11168H OMVs have previously been reported to cause mortality of *G. mellonella* larvae. It has also previously been reported that Cj0561c is present in *C. jejuni* OMVs produced during co-culture with ST (Elmi *et al.*, 2018). To further investigate the potential link between Cj0561c and OMV cytotoxicity, *G. mellonella* larvae were injected with 15 µg of OMVs suspended in 10 µl of sterile PBS. OMVs were isolated from *C. jejuni* cultures grown to late log phase either in the presence or absence of 0.2% (w/v) ST. OMVs were isolated from the 488 wild-type, Cj0561c mutant and Cj0561c complement, as well as the 11168H wild-type and Cj0561c mutant. Survival and health were recorded after 12, 24, 48 and 72 hours.

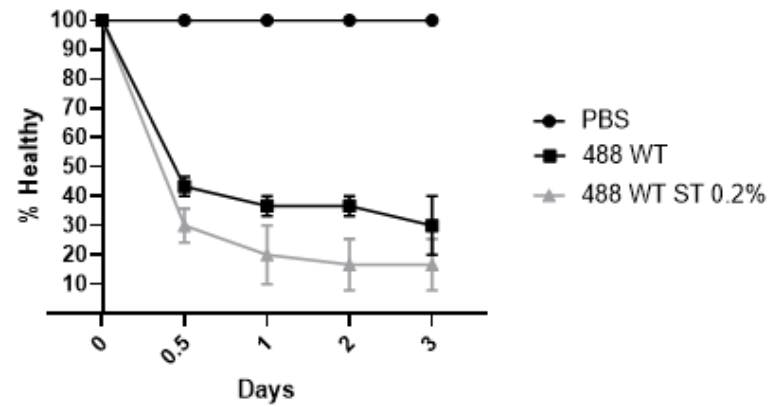
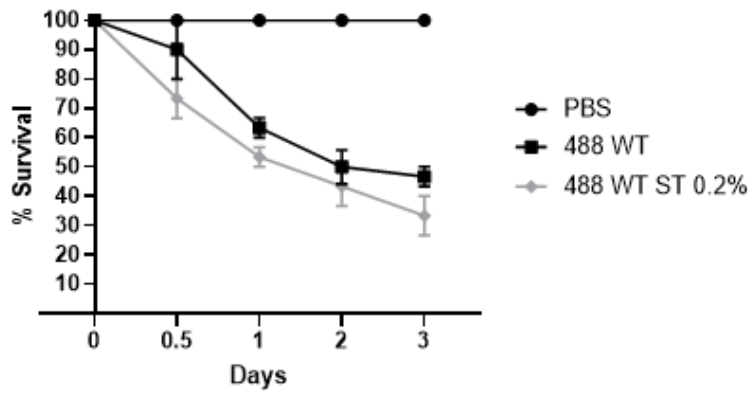
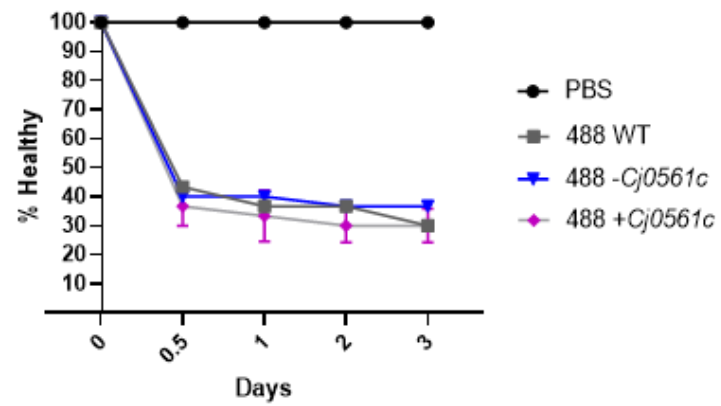
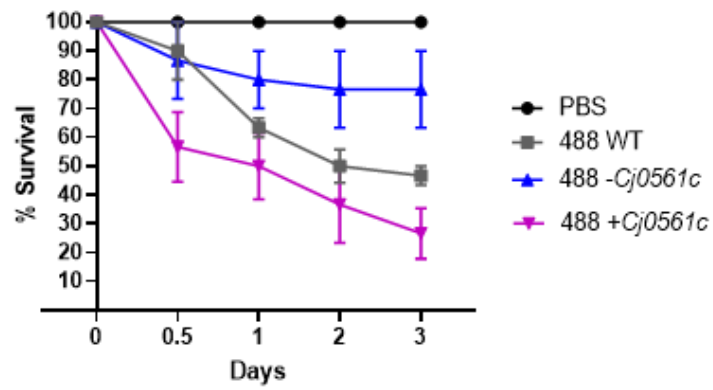
The 488 wild-type OMVs isolated in the absence of ST were more cytotoxic than the 11168H OMVs, reaching around 50% and 40% mortality respectively after three days (Figures 5.26 and 5.27). The reduction in health was comparable between the two wild-type strains (around 60-70% reduction in health reached after three days). 11168H wild-type OMVs were more cytotoxic than the 11168H Cj0561c mutant OMVs, with respect to mortality, (40% and 20% reduction reach after three days for wild-type and Cj0561c mutant respectively) but comparable for health (around a 60% reduction reached after three days) (Figure 5.26). The 488 wild-type OMVs also caused greater mortality when compared to the 488 Cj0561c mutant OMVs (50% and 20% respectively), however reduction in health was comparable reaching around 70% after three days (Figure 5.27).

OMVs produced during co-culture with ST (stOMVs) caused greater mortality for all strains investigated. The cytotoxicity increase observed for 11168H wild-type stOMVs was greater than that of the Cj0561c mutant stOMVs (Figure 5.26). The 11168H Cj0561c mutant stOMVs, despite being more cytotoxic than the 11168H Cj0561c mutant OMVs, did not reach the same level of cytotoxicity as the 11168H wild-type OMVs after three days causing 30% and 40% mortality for the 11168H Cj0561c mutant stOMVs and 11168H wild-type OMVs respectively (Figure 5.26).

The 488 Cj0561c complement strain OMVs showed the greatest cytotoxicity reaching around 70% mortality after three days. The 488 Cj0561c mutant OMVs had the lowest cytotoxicity reaching around 20% mortality after three days. Replicating the phenotype observed for 11168H, the 488 Cj0561c mutant stOMVs, despite having increased cytotoxicity, did not reach the same degree of cytotoxicity as the 488 wild-type OMVs after three days causing around 40% and 50% cytotoxicity respectively (Figure 5.27).



**Figure 5.26** Inoculation of *Galleria mellonella* larvae with 11168H wild-type or 11168H *Cj0561c* mutant strain OMVs produced either in the presence of absence of 0.2% (w/v) ST. For each OMV preparation ten larvae were injected in the right foremost leg with 15  $\mu\text{g}$  of OMVs suspended in 10  $\mu\text{l}$  of PBS. *G. mellonella* were injected with 10  $\mu\text{l}$  sterile PBS as controls. Larvae were incubated at 37°C under aerobic conditions for three days. Health and survival of larvae was recorded after 12, 24, 48 and 72 hours. \* $p < 0.05$ .



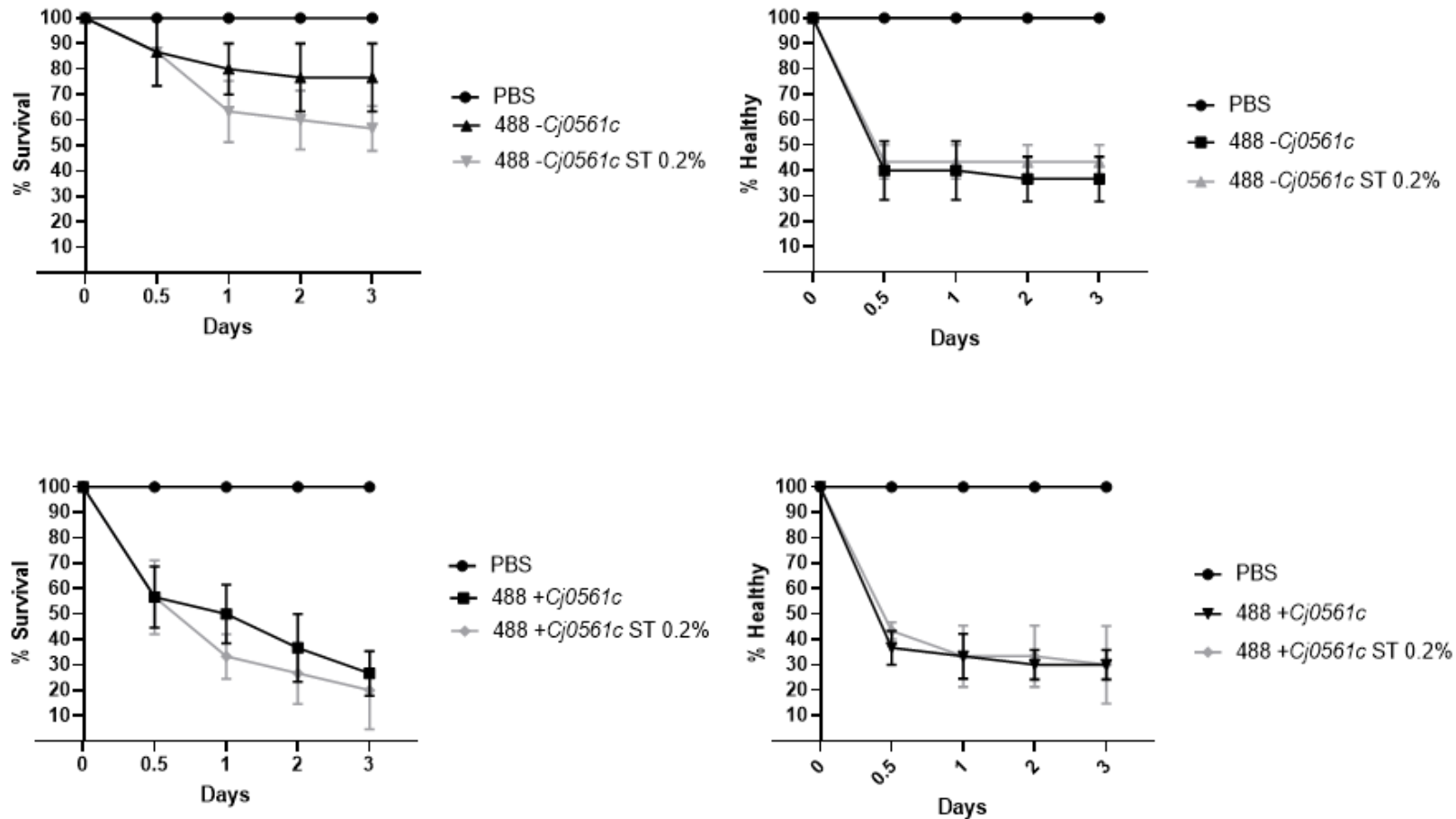


**Figure 5.27** Inoculation of *Galleria mellonella* larvae with 488 wild-type, 488 *Cj0561c* mutant or 488 *Cj0561c* complement strain OMVs produced either in the presence of absence of 0.2% (w/v) ST. For each OMV preparation ten larvae were injected in the right foremost leg with 15  $\mu$ g of OMVs suspended in 10  $\mu$ l of PBS. *G. mellonella* were injected with 10  $\mu$ l sterile PBS as controls. Larvae were incubated at 37°C under aerobic conditions for three days. Health and survival of larvae was recorded after 12, 24, 48 and 72 hours.

### 5.3 Discussion

Cj0561c is a putative protein which has previously been linked to regulation by bile salts through CmeR. Despite a link with CmeABC through CmeR, previous studies did not associate Cj0561c with antimicrobial resistance. To date, the only well-characterised phenotype associated with mutation of *Cj0561c* is a reduced ability to colonise chickens (Guo *et al.*, 2008). This study was not able to identify the function of Cj0561c, however a hypothetical function in lipid transport was suggested.

Cj0561c is currently annotated as a putative periplasmic protein in the UniProt database (Entry ID Q0PAV5) and NCBI database (Gene ID: 905206). Publications have also described Cj0561c as a putative periplasmic fusion protein functioning in transport across membranes (Guo *et al.*, 2008; Roumia *et al.*, 2021); putative membrane transporter (Dzieciol *et al.*, 2011); and periplasmic protein (Zhang *et al.*, 2009; Masanta *et al.*, 2019). Using both template guided and template free modelling programs, this study presents compelling evidence for the true location and structure of Cj0561c as a  $\beta$ -barrel OMP with 14 transmembrane domains. However, this should be verified in future work by crystallography. Further functional predictions of Cj0561c are limited due to the lack of a template with both high sequence coverage and identity obtained from database searches (see Section 5.2.1), as well as the absence of a protein structure deposited in PDB, a limitation which is common for  $\beta$ -barrel proteins (Tian *et al.*, 2018). Sequence level similarities of *C. jejuni* proteins to well-characterised proteins in other organisms such as *E. coli* are often low, and so the availability of a crystal structure and PDB entry would enable further functional predictions, for example using 3D-BLAST protein structure search. Other 14 transmembrane domain proteins include *E. coli* FadL; *Staphylococcus aureus* and *V. cholerae* hemolysins; *E. coli* OmpG; *Ralstonia pickettii* TbuX; *Aeromonas hydrophila* aerolysin; *Xenorhabdus nematophila* NilB; *Cytophaga hutchinsonii* SprP; *Haemophilus influenzae* Hap SAAT; and *Pseudomonas putida* TodX (Fairman *et al.*, 2011; Roumia *et al.*, 2021). When the structure of Cj0561c is confirmed, key structural features that should be targeted by point-mutations for more detailed phenotypic studies are extracellular loops 1-3. Loops 1 and 3 are the largest predicted extracellular loops and were also modelled with lower confidence and higher predicted disorder compared to other regions of Cj0561c (Figure 5.1 and 5.4). This is maybe an indication of high flexibility in these regions which could be key for function. Extracellular loops are the most flexible regions of  $\beta$ -barrel proteins and can form multiple conformations important for function (Koebnik, 1999; Tian *et al.*, 2018). Loop 2 was the smallest predicted loop and appears within a truncated region of the barrel wall, appearing to be orientated within the channel lumen, so could be important for selectivity of passage (see Figures 5.1-5.7).

In agreement with work by Dzieciol *et al.* (2011), the transcriptional response of *Cj0561c* to ST was significantly greater than that to SDC, despite comparable transcriptional changes observed for the *cmeABC* operon for both ST and SDC (Figure 5.8). This suggests that *Cj0561c* is subject to additional regulation independent of CmeR. Guo *et al.* (2008) constructed a transcriptional fusion of the promoter region of *Cj0561c* and a promoterless *lacZ* gene to investigate transcription of *Cj0561c* using  $\beta$ -galactosidase assays. Induction of the construct by CA or taurocholic acid (TCA) was then measured in a *cmeR* wild-type and a *cmeR* knockout mutant background. A 17-fold and 28-fold increase in response to CA and TCA respectively in the *cmeR* wild-type, and a 1.5-fold and 2-fold increase for CA and TCA respectively in the *cmeR* mutant strain were observed for the transcriptional fusion constructs. The low-level transcriptional activation maintained in the absence of *cmeR* in the study by Guo *et al.* (2008) is consistent with the presence of additional, transcription level, CmeR-independent regulation of *Cj0561c*. The transcriptional regulation of *Cj0561c* was further investigated using *Cj0561c* mutant strains. qRT-PCR primers targeting upstream of the *Cj0561c* mutation site were designed to analyse the native promoter activity in the absence of the intact coding sequence. *Cj0561c* and the *cmeABC* operon had lower, but still significant, fold change values in response to both bile salts for both strains. The significant difference between the transcriptional response of *Cj0561c* to ST and SDC was also maintained. As there was no increase in the transcriptional requirement of *Cj0561c* or the *cmeABC* operon in the absence of a functional copy of *Cj0561c* and presence of bile salts, it is unlikely that *Cj0561c* functions in a bile salt stress response. It is also unlikely that *Cj0561c* transcription is dependent on a feedback loop influenced by the activity of *Cj0561c* in respect to bile salts. In agreement with previous studies (Guo *et al.*, 2008), there was no increase in detergent or antibiotic sensitivity of *Cj0561c* mutant strains (Figures 5.12-5.16), further supporting the notion that *Cj0561c* does not have a role in membrane defence.

The profile of bile salts will vary along the length of the human gut, with the small intestine containing a higher proportion of primary conjugated bile salts, compared to the large intestine which has a higher proportion of secondary unconjugated bile salts (Northfield and McColl, 1973; Perez de la Cruz Moreno *et al.*, 2006). As discussed in Section 1.4.2, ST is representative of the small intestine bile salt profile, SDC is more representative of the large intestine profile. The decrease in proportion of taurine conjugated bile salts in the human large intestine, the preferred gut niche of *C. jejuni*, compared to the small intestine, is also true for the bile pool composition in the chicken gut (Beery *et al.*, 1988; Yin *et al.*, 2021). Yin *et al.* (2021) observed a prevalence of over 80% taurine conjugated bile salts in chicken ileum contents, compared to less than 25% in the caeca. The differing transcriptional response

of *Cj0561c* to SDC and the taurine conjugated bile salt ST could represent a response specific for different regions within the host gut.

Mutation of *Cj0561c* did confer increased resistance to the zwitterionic detergent LSB. Sulfobetaines are a group of zwitterionic detergents that are effective antibacterial agents with the activity of a specific sulfobetaine strongly dependent on its alkyl chain length. LSB has a 12 carbon alkyl chain (Wieczorek *et al.*, 2016). LSB is known to inhibit the carnitine/acyl-carnitine transporter in mitochondria by functioning as a substrate analogue. However, inhibition by sulfobetaines is reduced as alkyl chain length is reduced (Indiveri *et al.*, 1998). The increased resistance observed for both the 11168H and 488 *Cj0561c* mutant strains is an interesting phenotype given the structural similarity of the *Cj0561c* predicted structure to FadL, a long chain fatty acid transporter in *E. coli* (Black, 1988). Both *Cj0561c* and FadL are 14-transmembrane domain OMPs with a truncation or opening in the barrel wall (van den Berg *et al.*, 2004).

Previous studies with *E. coli* have observed LSB phenotypes associated with MCE domain proteins. MCE proteins obtained their name from an initial characterisation study which observed a non-pathogenic *E. coli* strain being able to enter and survive within mammalian cells when expressing *Mycobacterium tuberculosis mce1A* gene (Arruda *et al.*, 1993). Later research investigating the role of MCE domain proteins have characterised their role in lipid transport (Marjanovic *et al.*, 2011). One study observed disruptions in sulfolipid transport in *M. tuberculosis* with a *mce2* mutation (Marjanovic *et al.*, 2011). *C. jejuni* possesses MlaD, a MCE domain protein containing a single MCE domain forming part of the IM complex of the MLA pathway which is involved in the retrograde trafficking of PLs from the OM to the IM (Roier *et al.*, 2016; Davies *et al.*, 2019). MlaD is likely the only MCE domain protein possessed by *C. jejuni* (Isom *et al.*, 2017). Isom *et al.* (2017) observed growth inhibition in response to mutation of MCE domain proteins in *E. coli*, with a triple mutant, which had all three *E. coli* MCE domain proteins (MlaD, PqiB and YebT) disrupted, showing the most severe LSB sensitivity phenotype, indicating a role for the lipid transporting MCE domain proteins in LSB resistance. MlaD, PqiB and YebT all bind PLs and are thought to function in pathways contributing to maintenance of the OM (Isom *et al.*, 2017). Isom *et al.* (2017) hypothesised that the LSB phenotype observed for MCE domain proteins could be due to LSB inhibiting a lipid transport pathway with overlap to the function of the MCE protein pathways, or that MCE proteins are able to traffic LSB away from its target. There was a variability in phenotype observed by Isom *et al.* (2017) for sulfobetaines of different alkyl chain length, indicating substrate specificity of the MCE/sulfobetaine phenotype similar to that observed by Indiveri *et al.* (1998) for the carnitine/acyl-carnitine transporter in mitochondria. In contrast to the results observed by Isom *et al.* (2017), mutation of *Cj0561c* increased resistance to LSB. The link between LSB

and lipid transporting pathways, along with the predicted structure of *Cj0561c* showing some structural similarities to FadL, could indicate a lipid-linked functional role for *Cj0561c*. Given the increased LSB resistance observed for the *Cj0561c* mutant it would be tempting to speculate a potential role in lipid import for *Cj0561c*, with LSB functioning as a substrate analogue, similar to the inhibition of the carnitine/acyl-carnitine transporter in mitochondria (Indiveri *et al.*, 1998). This hypothesis could be further investigated with sulfobetaines of varied alkyl chain length to investigate potential substrate specificity.

Interestingly, carnitine has been linked to bile salt tolerance. *Listeria monocytogenes* possesses the OpuC carnitine transport system, which is regulated by bile salts and has expression co-related with the bile efflux system BilE. There is an interesting resemblance to the co-expression of *cmeABC* with *Cj0561c* through bile salt regulation. *L. monocytogenes* imports carnitine as a mechanism of stress defence (Watson *et al.*, 2009). Carnitine is also utilised by *Listeria* and *Bacillus* species as a means of protection against both hot and cold stress (Hoffmann and Bremer, 2011). Carnitine also functions in a range of stress defence mechanisms in other bacteria including *P. aeruginosa* (Lucchesi *et al.*, 1995), *E. coli* (Verheul *et al.*, 1998), and *Bacillus subtilis* (Kappes and Bremer, 1998). Carnitine can also function in bacterial metabolism and respiration as a final electron acceptor (Angelidis *et al.*, 2002; Meadows and Wargo, 2015). However, *Cj0561c* has no structural resemblance to OpuC (Figures 5.1-5.7) based on the UniProt (accession number UniProtKB - G2JZ41) structural prediction of OpuC produced by AlphaFold (Jumper *et al.*, 2021), or to the crystal structure of the *E. coli* CaiT carnitine transporter (Tang *et al.*, 2010), all of which are alpha helical transmembrane proteins. Nevertheless, given the link to bile salts and LSB, further work could investigate if *Cj0561c* plays a role in a carnitine stress response pathway, which may not be evident under standard culture conditions, using carnitine supplemented bile salt stress assays.

The increased resistance of *Cj0561c* mutant strains to LSB has provided the ability to screen for inhibition of *Cj0561c*. CCCP is a compound that disrupts the proton gradient, impacting protein complexes on the bacterial IM utilising active transport (Ghoul *et al.*, 1989). CCCP has previously been used to investigate the activity of *CmeABC* in *C. jejuni* (Lin *et al.*, 2002; Yan *et al.*, 2006; Su *et al.*, 2017). Addition of CCCP to LSB stress assays did not cause either the 488 or 11168H wild-type strains to display a *Cj0561c* mutant-like phenotype. As such, it is unlikely that *Cj0561c* functions in conjunction with an inner-membrane component requiring energy from the proton motive force. Therefore, it is unlikely that *Cj0561c* is a membrane fusion protein as described previously (Guo *et al.*, 2008; Roumia *et al.*, 2021), as this is often a characteristic of membrane fusion proteins (Zgurskaya *et al.*, 2009).

LSB caused a comparable increase in transcription of *Cj0561c* and the *cmeABC* operon in both the 11168H and 488 wild-type strains, similar to the transcriptional response observed for SDC. Given that there were different levels of expression of *Cj0561c* and the *cmeABC* operon in response to ST, it could be reasoned that the transcriptional change of *Cj0561c* in response to SDC and LSB is related to the transcriptional requirement of the *cmeABC* operon via CmeR. The specificity of the response to ST was further investigated. There are two key distinguishing features between ST and SDC. Both possess a CA structure, however in ST this is conjugated to a taurine molecule. SDC is unconjugated but has a hydroxy group from the CA structure removed by 7- $\alpha$  dehydroxylation. Abundance of taurine or taurine containing compounds in the gut has been linked to medical conditions associated with a change in gut microbial communities. Jacobs *et al.* (2016) characterised the faecal microbiome of patients with inflammatory bowel disease (IBD) and observed characteristic microbial composition shifts and an increase in bile acids, taurine and tryptophan present in the faeces of IBD patients. Yu *et al.* (2016) studied the effects taurine supplementation had on the microbiome and metabolism of mice and concluded that taurine has the potential to regulate the micro-ecology of the gut, and increase production of short chain fatty acids which could provide health benefits by inhibiting the growth of pathogenic bacteria. However, Sasaki *et al.* (2017), using a batch fermentation model and the bacteria cultured from human faecal samples did not observe any changes in the microbiome or production of short chain fatty acids. Later, Stacy *et al.* (2021), using a mouse model of infection, described that increases in host taurine production caused an increase of taurine utilisers in the host gut microbiota. The taurine utilisers are able to convert taurine to sulphide, which can impact aerobic respiration and survival of subsequent pathogenic species entering the gut. *C. jejuni* is however able to utilise an array of molecules as electron donor and acceptors, including the anaerobic electron acceptor DMSO (van der Stel and Wösten, 2019). The differential transcriptional response of *Cj0561c* to ST and SDC may represent a fitness adaption within different microbial communities. To assess if the taurine component could cause the transcriptional differences between ST and SDC, qRT-PCR experiments were repeated in the presence of taurine. Overall, at 0.2% (w/v) taurine the transcription of *Cj0561c* and the *cmeABC* operon was slightly but not significantly reduced compared to the control condition. There was also a slight, but not significant difference in the transcriptional response of *Cj0561c* in comparison to the *cmeABC* operon, indicating taurine could play a minor role in the regulation of *Cj0561c*.

Mutation of *cmeB* increased the sensitivity of *C. jejuni* to LSB, with LSB sensitivity assays requiring a reduction in LSB concentration from 1.5 mM to 0.2 mM to allow CFU growth. This demonstrates that the CmeABC efflux pump is critical for LSB tolerance, validating the qRT-PCR data that revealed an

increased transcriptional requirement of the *cmeABC* operon in the presence of LSB. Of note the differences in sensitivity to LSB between wild-type and *Cj0561c* mutant strains increased with the addition of a mutation in *cmeB*. There was a greater transcriptional difference between the *cmeB* single mutant and *cmeB Cj0561c* double mutant than there was between the *Cj0561c* single mutant and wild-type strain for both 11168H and 488. It would be tempting to speculate that this could be an indication that LSB is able to enter the cell through interaction with Cj0561c, as the stress associated with LSB when Cj0561c is functional becomes more pronounced in the absence of a functional CmeABC efflux system to compensate. If this is true, this would be an indication that passage through interaction with Cj0561c is relatively specific as mutation of *Cj0561c* did not alter sensitivity to tetracycline or ampicillin in a *cmeB* mutant background.

As previous work has shown reduced fitness of a *Cj0561c* mutant in chicken colonisation (Guo *et al.*, 2008), the role of Cj0561c in host cell interactions was investigated. There was no clear phenotype observed during tissue culture assays. The 488 strains tended to produce conflicting phenotypes to that of 11168H strains. The 488 *Cj0561c* mutant strain had significantly higher interaction with cell lines whereas the 11168H *Cj0561c* mutant had significantly lower interaction. Invasion was also significantly lower for the 11168H *Cj0561c* mutant strain. The invasion of the 488 *Cj0561c* mutant strain was increased compared to the 488 wild-type for T84 cells but was reduced for Caco-2 cells. The scale of the difference in interaction with T84 cells between the 488 wild-type and 488 *Cj0561c* mutant strain was greater than the difference in invasion of these strains (Appendix 9). The scale of the difference in invasion of T84 cells at both timepoints for the 488 wild-type and *Cj0561c* mutant strain was around 40% less than the difference in interaction between these strains. The difference in Caco-2 cell invasion had reduced by around 60% for both timepoints relative to the difference observed for interaction. This indicates that a smaller proportion of the adhered 488 *Cj0561c* mutant cells were able to invade compared to the 488 wild-type. This reduction does agree with the 11168H data sets showing the 11168H *Cj0561c* mutant to be less invasive. Further work is needed to confirm this phenotype. There was a slight but significant increase in IL-8 secretion for T84 cells infected with the 488 *Cj0561c* mutant strain compared to the wild-type, but no significant differences observed for IL-8 induction by the 11168H strains. The ability to survive within invaded cells was comparable for the 488 strains, but was reduced for the 11168H *Cj0561c* mutant strain compared to the 11168H wild-type. All strains were able to adhere, invade and survive within both cell lines, demonstrating Cj0561c is not essential for host cell interactions. Cj0561c has previously been shown to produce large transcriptional changes in response to host conditions. Kreuder *et al.* (2017) observed between a 15.8 to 29.3-fold increase in expression of *Cj0561c* in *C. jejuni* SA (sheep abortion) clone IA3902 in response

to growth in ovine bile either *in vivo* or *in vitro* after 3 or 24 hours. It is possible that under the assay conditions used in this study, transcription of *Cj0561c* in wild-type strains was not high enough to produce a clear phenotype. There were also differences in invasion ability of the 488 *Cj0561c* mutant strain between cell lines, therefore the choice of cell line could also play a role in the results produced in this study. Kovács *et al.* (2020) investigated the transcriptional changes of *C. jejuni* strain CjTD-119 after three hours invasion of ATCC INT 407 human embryonic intestine (jejunum and ileum) cell line. Kovács *et al.* (2020) observed large transcriptional changes throughout the genome and observed a significant upregulation of *Cj0561c* after three hours of infection. Future work should investigate transcription levels of *Cj0561c* under the tissue culture conditions used prior to further host cell interaction assays. The contrasting results between 11168H strains and 488 strains observed during tissue culture assays was also observed for the *G. mellonella* model of infection. The 11168H *Cj0561c* mutant showed reductions in interaction, invasion and survival in tissue culture assays (Figure 5.20 and 5.21), but had increased cytotoxicity in *G. mellonella*. The 488 *Cj0561c* mutant had reduced cytotoxicity.

OMVs have previously been shown to harbour secreted virulence factors capable of cytotoxic effects in the *G. mellonella* model of infection (McMahon *et al.*, 2012; Elmi *et al.*, 2018). Unlike the observations for live whole-cell, infection of *G. mellonella*, larvae inoculated with OMVs produced similar results for both the 11168H and 488 strains. Both the 488 and 11168H *Cj0561c* mutant OMVs were less cytotoxic compared to the wild-type OMVs. This may indicate that *Cj0561c* has a role in the biogenesis or virulence of OMVs. The cytotoxicity of OMVs produced in the presence of 0.2% (w/v) ST demonstrated a comparable increase in cytotoxicity by both wild-type and mutant strains when compared to the OMVs of each strain produced in the absence of ST. *Cj0561c* mutant stOMVs were unable to reach the same level of cytotoxicity as wild-type OMVs for either strain. This demonstrates that *Cj0561c* is not essential for OMV mediated cytotoxicity but does play a significant role.

As previously discussed, OMPs play a key role in the maintenance and dynamics of the OM, playing vital roles in the addition and removal of lipids and proteins from the OM. OMPs are therefore important in the production and properties of OMVs. *V. cholerae* exhibits an adaptive response to sensing the host gut environment, during which increased production of OMVs through a down-regulation of the MLA pathway accelerate the transient adaptation of the OM to become more suitable for the host gut environment (Zingl *et al.*, 2020). The increased removal of the OM in the form of OMVs increases the speed of accumulation of glycine-modified LPS and removal of porins which are permissive to entry of harmful compounds (Zingl *et al.*, 2020). The membrane lipid composition of OMVs can impact the efficiency of OMVs binding to, and entry into, host cells.

O'Donoghue *et al.* (2017) observed reduced efficiency of uptake of *E. coli* O-antigen deficient OMVs into HeLa epithelial cells. Previous work with *Klebsiella pneumoniae* has shown O-antigen mutants also have altered OMV cargo selection (Cahill *et al.*, 2015), which could play a role in adhesion and internalisation of O-antigen deficient OMVs. OMVs of other gut colonising bacteria have been shown to enrich proteins that enhance invasion potential of the OMV, such as the localisation of invasins (Kesty *et al.*, 2004). Enrichment of specific lipids into OMVs has also been reported, such as the enrichment of OMVs with phosphatidylinositol with unsaturated fatty acid chains which are sparsely found in the parent cell membrane of *Campytophaga ochracea* (Naradasu *et al.*, 2021). Elhenawy *et al.* (2016) observed deacylated lipid A, modified by OMP PagL, exclusively in OMVs produced by *S. enterica* serovar Typhimurium compared to the hexa-acylated lipid A found in the cell OM.

Alternatively, alterations in the surface properties of OMVs have also been linked to OMV uptake efficiency. OMVs produced in the presence of bile salts by *C. jejuni* have been shown to increase the invasion potential of live *C. jejuni* cells co-inoculated with bile-OMVs (Taheri *et al.*, 2018). Taheri *et al.* (2018) observed OMVs produced in the presence of bile were more hydrophobic and speculated this increased hydrophobicity increased adhesion. OMV size has also be speculated to influence the mechanism by which OMVs are endocytosed, and therefore the kinetics of uptake (Kaparakis-Liaskos and Ferrero, 2015). Variations in lipid composition and saturation can impact membrane curvature (Mukhopadhyay *et al.*, 2008; Roier *et al.*, 2016; Elhenawy *et al.*, 2016; Giordano *et al.*, 2020), for example, PLs with long lipid chains are more ridged than those with shorter chain length. This increased rigidity reduces the flexibility of the membrane (Catalá, 2012). Transient changes in lipid profiles at OMV release sites on the parent cell could provide a means for altering the entry dynamics of OMVs response to environmental stimulus.

*C. jejuni* OMVs are documented to utilise lipid rafts for endocytosis (Elmi *et al.*, 2012). Lipid rafts are tightly packed, less fluid regions of the host membrane enriched in protein receptors, sphingolipids and cholesterol, with the composition of lipid rafts causing invaginations of the host membrane which can trigger endocytosis (Amano *et al.*, 2010; Mulcahy *et al.*, 2014). The sub-proteome of lipid rafts can vary from other regions of the membrane (Yurtsever and Lorent, 2020) with proteins such as pathogen recognition receptors being enriched in lipid rafts. As lipid components of OMVs can impact the host immune response, such as the recognition of LPS by toll-like receptor 4 (TLR4) (Lu *et al.*, 2008), it may be that bacterial cells alter the composition of OMVs targeting these regions to allow immune evasion, immunomodulation or stimulate proinflammatory responses which could lead to chronic inflammatory conditions and cell damage (Lu *et al.*, 2008). It has been shown that LPS modifications to prevent recognition by TLR4 facilitates immune evasion. For example, in response to human body

temperature *Yersinia pestis* produce tetra-acylated lipid A, which is poorly recognised by TLR4 (Rebeil *et al.*, 2006).

An example of immunomodulation is demonstrated by *Borrelia burgdorferi*, the causative agent of Lyme disease. *B. burgdorferi* is unable to synthesise long-chain fatty acids and is therefore reliant on lipid scavenging for membrane maintenance. During host infection, *B. burgdorferi* incorporates lipid and cholesterol components of the host lipid-rafts into OMVs to enable the incorporation of bacterial lipids into the cell membrane in a two-way lipid exchange to promote host mediated cell damage (LaRocca *et al.*, 2010; Crowley *et al.*, 2013). Other bacteria, such as *H. pylori*, also incorporate host cholesterol into their membranes (Crowley *et al.*, 2013). Should the previous speculation of Cj0561c playing a role in lipid import be correct, then Cj0561c could provide a means of lipid scavenging, either for host interactions, or to compensate for the metabolic burden associated with replacing lost lipids during periods of increased lipid loss, such as increased OMV production in response to bile salts.

The structural prediction of Cj0561c does bear some structural similarity to the long chain fatty acid transporter FadL (van den Berg *et al.*, 2004). Both Cj0561c and FadL have 14 transmembrane domains. Transmembrane strand 5 of Cj0561c, based on the DUF2860 domain structural prediction (Figure 5.2), contains a slight kink, similar to that in FadL strand 3. The strand 3 kink of FadL is thought to facilitate the lateral movement of long chain fatty acids into the membrane (Dirusso and Black, 2004). This kink was not present in the structural predictions of Cj0561c produced in this study, however, the recently updated UniProt Cj0561c entry now contains a structural prediction of Cj0561c produced by alphafold (Q0PAV5\_CAMJE) which does detail a strand 5 kink. The strands preceding the kink region in both Cj0561c and FadL are short, creating a truncation in the barrel wall. Such truncations have been observed in other OMPs such as *E. coli* Wzi and PagP (Khan and Bishop, 2009; Bushell *et al.*, 2013). Khan and Bishop (2009) produced a model for PagP in which lateral diffusion of lipids is enabled by the truncation region in the barrel wall. Lateral transfer for hydrophobic molecules through an opening in the barrel wall into the OM has been reported for other OMPs, such as the 8 stranded  $\beta$ -barrel proteins OmpW and AlkL (Grant *et al.*, 2014). AlkL from *P. putida* has been studied with regard to a potential use in the biotechnology industry. Expression of *P. putida* AlkL in *E. coli* has been shown to increase the uptake of C<sub>10</sub>-C<sub>16</sub> alkanes to improve alkane oxidation yields (Grant *et al.*, 2014).

Based on the structural prediction of DUF2860 domains (Figure 5.2), the extracellular loop 2 appears to face inwards into the channel pore. A striking difference between Cj0561c and FadL, OmpW and AlkL is the lack of a N-terminal hatch domain in Cj0561c. FadL, OmpW and AlkL all contain a 'hatch' or 'plug' which requires a conformational change to allow access for lateral diffusion of cargo through the lateral opening in the barrel wall (Call *et al.*, 2016). However, the hatch domain of FadL is not

essential for import of fatty acid (Salvador López and Van Bogaert, 2021) and is also not present in PagP (Khan and Bishop, 2009). It is plausible that the inward facing loop 2 and the flexible extracellular loops 1 and 3 provide a mechanism to restrict entry to Cj0561c, enabling substrate specific transport. OmpG, another 14 transmembrane domain  $\beta$ -barrel protein which was utilised as a structurally homologous template by rtRosetta (see Section 5.2.1), is a porin that alternates between open and closed states based on pH-induced conformational changes of extracellular loops. The pH-dependent gating of OmpG represents an example of how OMPs are able to alter membrane permeability in response to external signals (Conlan *et al.*, 2000; Mari *et al.*, 2010; Perez-Rathke *et al.*, 2018). It may be that DUF2860 proteins are fatty acid transporters which encompass structural features of other known fatty acid transporters, such as FadL and PagP, forming a structurally distinct class of transporters.

It has also been observed that the phospholipidome of *C. jejuni* is highly dynamic in response to environmental changes. For example, *C. jejuni* can alter the proportion of lysophospholipids present in the OM in response to oxygen concentration and growth phase (Cao *et al.*, 2020). Cao *et al.* (2020) described *C. jejuni* as having an unusually high proportion of lysophospholipids within the phospholipidome, and that mutation of *pldA* significantly reduced but did not completely remove lysophospholipids from the OM. Cao *et al.* (2020) also noted that not all phospholipidome changes observed at various growth phases could be attributed to transcriptional changes of PL production genes, indicating alternative methods for lipid turnover exist.

In addition to structural similarities, Cj0561c does have phenotypic similarities to FadL. Noteworthy phenotypes of FadL include; removal of FadL in *E. coli* increasing tolerance to alkanes; crystallography studies demonstrating binding of lauryldimethylamine oxide (LDAO) within the channel of FadL; and the lack of requirement of FadL for external energy input. Call *et al.* (2016) observed that removal of FadL increased tolerance to hexane stress, whereas Zhang *et al.* (2011) found no difference in phenol sensitivity associated with FadL removal. Phenol stress causes membrane damage and alterations in membrane permeability (Heipieper *et al.*, 1991). Comparably in this study, mutation of *Cj0561c* caused increased resistance to LSB but did not cause an overall shift in sensitivity to other membrane targeting agents. The crystal structure of FadL produced by Berg *et al.* (2004), contained a single molecule of LDAO bound within the channel of FadL (Berg *et al.*, 2004; Dirusso and Black, 2004). LDAO was used in the membrane protein preparation for crystallography and is a zwitterionic detergent with a C<sub>12</sub> alkyl tail similar to LSB. Release of substrate into the OM by FadL is not dependent on external energy input (Lepore *et al.*, 2011). CCCP assays (Figure 5.14) indicated that Cj0561c is not part of a protein complex dependent on the proton motive force of the IM.



## 5.4 Conclusion

In summary, the data presented in this chapter suggests that Cj0561c is an OMP with a potential role in lipid transport and OMV associated virulence. Mutation of *Cj0561c* increased resistance to the zwitterionic detergent LSB, a compound previously utilised in the study of lipid transport systems in both eukaryotic and prokaryotic cells. There was no increased sensitivity to membrane targeting compounds associated with loss of function of Cj0561c, therefore if Cj0561c is involved with lipid transport into the OM, it is unlikely that the principal function of Cj0561c is membrane repair and maintenance, but rather in tailoring the lipid composition of the membrane for optimal fitness under specific conditions. The potential role of Cj0561c described in this study is hypothetical, and the production of a crystal structure, in addition to further OMV and lipid focused phenotypic characterisation is required.

## Chapter Six: Final Discussion

### 6.1 Summary

An important feature of a pathogen is the ability to sense the environment and to appropriately alter and co-ordinate the regulation of virulence factors. Bile or bile salts are recognised as important host factors exploited by enteric pathogens as a signal to alter virulence gene regulation (Alam *et al.*, 2010; Sistrunk *et al.*, 2016; Joffre *et al.*, 2019). *C. jejuni* lacks a conserved virulence associated secretion system capable of delivering effectors directly to target cells (Parkhill *et al.*, 2000; Ugarte-Ruiz *et al.*, 2015; Liaw *et al.*, 2019). OMVs have been described as a type 0 secretion system (TOSS) (Thay *et al.*, 2014; Guerrero-Mandujano *et al.*, 2017) and are conserved amongst Gram-negative bacteria. As OMVs are able to deliver cargo in concentrated parcels directly into host cells (Kuehn and Kesty, 2005), OMVs may have a particularly important role for *C. jejuni* virulence and survival.

The MLA pathway has been proposed to play a role in the regulation of OMV production in Gram-negative bacteria (Roier *et al.*, 2016). The *C. jejuni* genome contains genes encoding proteins homologous to the MLA pathway in *E. coli* and the VacJ/YrbCEFD pathway in *H. influenzae*. This study confirmed *C. jejuni* can regulate OMV biogenesis in response to host gut signals through changes in expression of the MLA pathway. It was also demonstrated that the increased OMV production observed for the 11168 *mlaA* mutant strain was not an artifact of a fragile OM. The *C. jejuni* 11168 wild-type strain increased OMV production in the presence of 0.2% (w/v) ST. This ST phenotype was not reproduced by the 11168 *mlaA* mutant strain, indicating that ST regulated OMV production through the MLA pathway. This was verified by qRT-PCR analysis demonstrating that the presence of ST decreased expression of both *mlaA* and *mlaC* in *C. jejuni* wild-type strains 11168 and 488. Collectively the data supports the MLA model of OMV production and the link between bile salts and potential virulence regulation in *C. jejuni*.

RNA was extracted from mid-log phase cultures of the *C. jejuni* 488 wild-type and 11168H wild-type strains in the presence and absence of 0.2% (w/v) ST and 0.05% (w/v) SDC. The transcriptome data was analysed using DESeq and sPLS-DA. Both analysis methods were run using a LOO cross validation to improve reliability of identified genes. Despite the mild conditions used in this study, and the low number of genes identified, *cmeABC* was upregulated by both ST and SDC validating the conditions and analysis methods used. This study has identified potential key genes in the homeostatic transcriptional response of *C. jejuni* to bile salts in the absence of other stressors and variables. *Cj0561c* was frequently identified differentially expressed genes during cross validation. *Cj0561c* also

often exhibited the greatest transcriptional change and therefore Cj0561c is likely to be a key bacterial protein involved in the response of *C. jejuni* to bile salts. Additionally, there was a differential response of Cj0561c to ST and SDC, indicating Cj0561c is not only activated by bile salts, but that expression is tailored in response to different bile salts. To date there is no known function of Cj0561c published.

Cj0561c is annotated by NCBI as a periplasmic protein, however, structural prediction data produced during this study indicates Cj0561c is a  $\beta$ -barrel OMP. Cj0561c has transcriptional links to *cmeABC* through CmeR but has not previously been characterised to play a role in stress resistance (Guo *et al.*, 2008). In agreement with previous work, mutation of Cj0561c did not increase sensitivity to the detergents or antibiotics tested in this study. Additionally, mutation of Cj0561c in *C. jejuni* strains 488 and 11168H did not increase the transcriptional requirement of the Cj0561c native promoter or the *cmeABC* operon in the presence of bile salts. Therefore it is unlikely that expression of Cj0561c is upregulated in the presence of bile salts to assist CmeABC with tolerance to bile salts. Mutation of Cj0561c did increase resistance to LSB, a detergent that has been previously used as a substrate analogue in lipid transport assays (Indiveri *et al.*, 1998; Isom *et al.*, 2017). Mutation of Cj0561c also reduced the cytotoxicity of OMVs in the *G. mellonella* larvae model of infection. This, in addition to the phenotypic and predicted structural similarity of Cj0561c to FadL, suggests a potential role in lipid transport and OMV associated virulence.

## **6.2 Future work**

### **6.2.1 OMV production in the presence of sodium taurocholate at 42°C**

ST has been shown to play a role in OMV mediated virulence at 37°C (human body temperature) during this study and previously by Elmi *et al.* (2018). An enrichment of virulence associated proteins in OMVs produced at 37°C compared to OMVs produced at 42°C (avian body temperature) has been documented by Taheri *et al.* (2019). Given the abundance of taurine conjugated bile salts in the avian gut (Yin *et al.*, 2021), and the differing disease presentations associated with *C. jejuni* infection in chickens compared to humans (Awad *et al.*, 2018), OMV production and virulence at 42°C requires investigation.

### **6.2.2 Further characterisation of the transcriptional response of *C. jejuni* to bile salts using additional timepoints.**

RNA-Seq analysis detected minor, but biologically relevant, transcriptional changes under the conditions investigated. There were a number of genes identified during individual cross validation runs that were not identified with high enough stability to be reliably identified as differentially expressed. Preliminary work analysing several of these genes by qRT-PCR did confirm differential

expression. Using qRT-PCR, a more comprehensive investigation of genes identified with varying identification stabilities during RNA-Seq analysis should be performed. The transcriptional response of *C. jejuni* to bile varies over time, with prolonged culture in bile often producing more pronounced transcriptional changes. This in part may be due to the accumulative stress of bile salts and additional stresses faced during later stages of growth triggering stress response pathways. Negretti *et al.* (2017) described that the initial response of *C. jejuni* to SDC included upregulation of genes encoding virulence factors such as *flaA* and *cmeABC*, but prolonged culture induced stress response pathways associated with the accumulative toxic effects of growth in SDC. An earlier study by Malik-Kale *et al.* (2008) using  $\beta$ -galactosidase assays observed a time dependent increase in expression of *ciaB* between 9 and 15 hours of culture. This increase resembled the dose dependent transcriptional increase of *ciaB* observed between 0.05 to 0.2% (w/v) SDC. This demonstrates that the response of *C. jejuni* to bile salts over time is not fixed and that the timepoint selected for analysis can be as significant as the concentration used. Future work should investigate transcriptional changes during later stages of growth using either RNA-Seq analysis or qRT-PCR analysis of selected genes. This investigation should include both the prolonged culture in the presence of ST and SDC, and the short-term exposure of late growth phase cultures by addition of bile salts 20 minutes prior to RNA isolation. This could provide a greater insight into genes utilised by *C. jejuni* in the initial response to detection of bile and genes associated with the adaptive response to survive in bile.

Given the prevalence of taurine conjugates within the chicken bile pool (Yin *et al.*, 2021), *in vivo* chicken transcriptional studies would further understanding of the response of *C. jejuni* to bile in a host gut environment. *In vitro* transcriptional studies have limited ability to replicate the host environment. *In vivo*, gut pathogens will encounter a complex array of potential transcriptional stimuli. For example, a gut pathogen will need to coordinate genes required for competition with host microflora, such as the upregulation of nutrient scavenging pathways (Coyte and Rakoff-Nahoum, 2019), or activation of the T6SS to deliver toxins to competing bacteria (Li *et al.*, 2022). However, activation of the T6SS under certain host conditions can be harmful, as it is thought bile salts can enter the bacterial cell through the T6SS (Lertpiriyapong *et al.*, 2012). Therefore, transcriptional responses under host conditions can be a negotiation, and produce differing results to the same isolated stimuli *in vitro*. Within the gut, a pathogen will also encounter a wide array or both beneficial and harmful, host and microflora metabolites. Colonisation dynamics can be impacted by the ability of a bacteria to sense these metabolites and appropriately coordinate a response (Luethy *et al.*, 2017). As metabolites can vary based on location within the gut (Ridlon *et al.*, 2006), *in vivo* transcription profiles may also vary based on gut niche. It is therefore important to consider the relevance of experimental

design in regard to both host model and within host location. The cellular architecture will also vary dependent on region of the gut. For example, certain cell receptors required for efficient cell interaction can be restricted to specific cell types or locations. Such as the presence of focal adhesion points on the basolateral surface of IECs (Murphy and Brinkworth, 2021), or the expression of different differing intimin adhesion proteins by different *E. coli* strains influencing the trophism towards different regions of the gut (Fitzhenry *et al.*, 2003; Aktan *et al.*, 2007). Interaction of a pathogen with specific cell receptors can then lead to host bacterial transcriptional cross talk, whereby the transcriptional profile of the host is altered in response to the interaction with the pathogen. The altered host cell transcription may then further alter the transcriptional profile of the pathogen (Baddal *et al.*, 2015).

Given the complex nature of stimuli encountered during host infection, *in vivo* transcriptional studies, despite often providing more representative conditions, can prove difficult to decipher. Parallel *in vitro* transcriptional studies reproducing isolated stimuli can assist in the interpretation of *in vivo* datasets (Moreau *et al.*, 2017; Kreuder *et al.*, 2017; De Lay *et al.*, 2021). For example, Kreuder *et al.* (2017) investigated transcriptional response of *C. jejuni* to ovine bile *in vitro* and *in vivo* compared to standard *in vitro* culture conditions. Between 123-405 differentially expressed genes were observed in the presence of bile either *in vitro* or *in vivo*. 67 genes were common to both *in vivo* and *in vitro* bile exposure. The use of *in vitro* investigation in parallel to *in vivo* enabled the identification of an important subset of bile specific genes from a larger pool of differentially expressed genes. Furthering this, recent advances in RNA-Seq methodology has enabled the development of Dual RNA-Seq. Dual RNA-seq characterises the host transcriptional response to pathogen infection, and the transcriptional response of the pathogen to the host environment simultaneously. This enables the capture of host/pathogen transcriptional cross talk (Baddal *et al.*, 2015; Macho Rendón *et al.*, 2021). Utilisation of this technique using either human or chicken cell lines *in vitro*, then comparing results to the transcriptional response of *C. jejuni* to the chicken gut *in vivo* could further the understanding of the interaction of *C. jejuni* with host cells.

### **6.2.3 Determining the crystal structure of Cj0561c**

To date there is no crystal structure available for any of the DUF2860 domain proteins, however a predicted DUF2860 structure has been produced by Baek *et al.* (2021). More recently the UniProt Cj0561c entry now contains a structural prediction produced by AlphaFold (Q0PAV5\_CAMJE). To enable a more comprehensive understanding of Cj0561c and the DUF2860 family of proteins a crystal structure is required. A crystal structure would enable more reliable predictions of regions potentially crucial to function, which could then be targeted by point mutations. Identification of key residues

would provide a better insight to the function and potentially mechanisms of activity of DUF2860 domain proteins.

#### **6.2.4 Investigation into the specificity of the *Cj0561c* mutant sulfobetaine phenotype**

LSB sensitivity has previously been associated with lipid transport pathways in both eukaryotic and prokaryotic cells (Indiveri *et al.*, 1998; Isom *et al.*, 2017). The LSB phenotype associated with mutation of *Cj0561c* should be further investigated using additional sulfobetaines of varied alkyl chain length. Previous work described sulfobetaine activity to be strongly dependent on alkyl chain length (Wieczorek *et al.*, 2016; Isom *et al.*, 2017). An alkyl chain length specific response could provide further evidence for lipid transport by *Cj0561c* and substrate specificity.

#### **6.2.5 Characterisation of interaction and invasion of *C. jejuni* co-inoculated with *C. jejuni* wild-type and *Cj0561c* mutant outer membrane vesicles**

Assays characterising interaction and invasion of IECs by the *C. jejuni* 488 and 11168H *Cj0561c* mutants did not produce a clear phenotype, however the *Cj0561c* mutants appeared less invasive. Further work is required to verify this phenotype. Similarly, *G. mellonella* infections with live *C. jejuni* cells also produced inconclusive results, with 11168H strains producing contrasting results to 488 strains. Unlike the observations for live whole-cell infection of *G. mellonella*, larvae inoculated with OMVs produced similar results for both the 11168H and 488 strains. OMVs produced by the *Cj0561c* mutants were less cytotoxic than wild-type OMVs. *C. jejuni* OMVs have been shown to enhance parent cell invasion of IECs (Elmi *et al.*, 2016). Elmi *et al.* (2018) described the presence of *Cj0561c* to be exclusive to stOMVs. Future work could incorporate OMVs and stOMVs isolated from *C. jejuni* wild-type and *Cj0561c* mutants into interaction and invasion assays, using the methodology previously described by Elmi *et al.* (2016) to assess if *Cj0561c* is able to enhance parent cell invasion of IECs.

#### **6.2.6 Characterisation of *C. jejuni* wild-type and *Cj0561c* mutant outer membrane vesicles produced in the presence or absence of sodium taurocholate**

Gram-negative bacteria are able to alter the lipid profile of OMVs in response to environmental stimuli (LaRocca *et al.*, 2010; Elhenawy *et al.*, 2016). Taheri *et al.* (2018) observed that *C. jejuni* OMVs produced in the presence of low concentrations of bile were more hydrophobic and were able to increase the invasion potential of parent cells when co-inoculated. Alterations in the OM lipid profile will alter cell surface hydrophobicity (Stolarek *et al.*, 2021). Future work should characterise the hydrophobicity of *C. jejuni* wild-type and *Cj0561c* mutant OMVs and stOMV as an initial investigation into potential lipidome differences associated with mutation of *Cj0561c*. If differences in hydrophobicity are observed this could provide a putative mechanism for the phenotype described by

Taheri *et al.* (2018). Cao *et al.* (2020) characterised the phospholipidome of *C. jejuni* and noted that the composition of PLs in the OM of *C. jejuni* is highly dynamic in response to environmental changes. Similar mass spectrometry-based analysis could be performed to characterise the OM and OMV PL components of *C. jejuni* wild-type and *Cj0561c* mutant strains. Additional follow up experiments could include OMV proteomic analysis or analysis of wild-type and *Cj0561c* OMV and stOMV cell entry dynamics with the aim of producing a model detailing how *Cj0561c* increases fitness of *C. jejuni* in the host gut environment. If a *Cj0561c* OMV interaction or invasion phenotype is determined, entry dynamics could be indirectly monitored by measuring phenotypic differences caused by lipid raft disrupting compounds as described by Elmi *et al.* (2012). Alternatively, a mechanism utilising fluorescent probes, similar to that described by O'Donoghue *et al.* (2017) for *E. coli*, could be adapted for *C. jejuni* to directly monitor entry kinetics of OMVs.

## References

- ABELLON-RUIZ, J., KAPTAN, S. S., BASLE, A., CLAUDI, B., BUMANN, D., KLEINEKATHOFER, U. & VAN DEN BERG, B. 2017a. Structural basis for maintenance of bacterial outer membrane lipid asymmetry. *Nature Microbiology*, 2, 1616-1623.
- ABELLON-RUIZ, J., KAPTAN, S. S., BASLE, A., CLAUDI, B., BUMANN, D., KLEINEKATHOFER, U. & VAN DEN BERG, B. 2017b. Structural basis for maintenance of bacterial outer membrane lipid asymmetry. *Nature Microbiology*, 2, 1616-1623.
- ABOUELHADID, S., NORTH, S. J., HITCHEN, P., VOHRA, P., CHINTOAN-UTA, C., STEVENS, M., DELL, A., CUCCUI, J. & WREN, B. W. 2019a. Quantitative Analyses Reveal Novel Roles for N-Glycosylation in a Major Enteric Bacterial Pathogen. *MBio*, 10.
- ABOUELHADID, S., RAYNES, J., BUI, T., CUCCUI, J. & WREN, B. 2019b. N-linked glycans confer protein stability and modulate multidrug efflux pump assembly in *Campylobacter jejuni*. *BioRxiv* 585463.
- AKIBA, M., LIN, J., BARTON, Y. W. & ZHANG, Q. 2006. Interaction of CmeABC and CmeDEF in conferring antimicrobial resistance and maintaining cell viability in *Campylobacter jejuni*. *Journal of Antimicrobial Chemotherapy*, 57, 52-60.
- AKTAN, İ., LA RAGIONE ROBERTO, M. & WOODWARD MARTIN, J. 2007. Colonization, Persistence, and Tissue Tropism of *Escherichia coli* O26 in Conventionally Reared Weaned Lambs. *Applied and Environmental Microbiology*, 73, 691-698.
- AKTAR, S., OKAMOTO, Y., UENO, S., TAHARA, Y. O., IMAIZUMI, M., SHINTANI, M., MIYATA, M., FUTAMATA, H., NOJIRI, H. & TASHIRO, Y. 2021. Incorporation of Plasmid DNA Into Bacterial Membrane Vesicles by Peptidoglycan Defects in *Escherichia coli*. *Frontiers in Microbiology*, 12, 747606.
- ALAM, A., TAM, V., HAMILTON, E. & DZIEJMAN, M. 2010. vttR A and vttR B encode ToxR family proteins that mediate bile-induced expression of type three secretion system genes in a non-O1/non-O139 *Vibrio cholerae* strain. *Infection and Immunity*, 78, 2554-2570.
- ALEMKA, A., NOTHAFT, H., ZHENG, J. & SZYMANSKI, C. M. 2013. N-glycosylation of *Campylobacter jejuni* surface proteins promotes bacterial fitness. *Infection and Immunity* 81, 1674-1682.
- ALLEN, K. J. & GRIFFITHS, M. W. 2001. Effect of environmental and chemotactic stimuli on the activity of the *Campylobacter jejuni* flaA  $\sigma_{28}$  promoter. *FEMS Microbiology Letters*, 205, 43-48.
- ALLOS, B. M. 1997. Association between *Campylobacter* Infection and Guillain-Barré Syndrome. *The Journal of Infectious Diseases*, 176, S125-S128.
- ALMAGRO ARMENTEROS, J. J., TSIRIGOS, K. D., SØNDERBY, C. K., PETERSEN, T. N., WINTHER, O., BRUNAK, S., VON HEIJNE, G. & NIELSEN, H. 2019. SignalP 5.0 improves signal peptide predictions using deep neural networks. *Nature Biotechnology*, 37, 420-423.
- ALNOUTI, Y., CSANAKY, I. L. & KLAASSEN, C. D. 2008. Quantitative-profiling of bile acids and their conjugates in mouse liver, bile, plasma, and urine using LC-MS/MS. *Journal of Chromatogr B Analytical Technologies in the Biomedical and Life Sciences*, 873, 209-17.
- ALTINDIS, E., FU, Y. & MEKALANOS, J. J. 2014. Proteomic analysis of *Vibrio cholerae* outer membrane vesicles. *Proceedings of the National Academy of Sciences*, 111, E1548-56.
- ALTSCHUL, S. F., GISH, W., MILLER, W., MYERS, E. W. & LIPMAN, D. J. 1990. Basic local alignment search tool. *Journal of Molecular Biology*, 215, 403-10.
- AMANO, A., TAKEUCHI, H. & FURUTA, N. 2010. Outer membrane vesicles function as offensive weapons in host-parasite interactions. *Microbes and Infection*, 12, 791-8.
- AMOUR, C., GRATZ, J., MDUMA, E., SVENSEN, E., ROGAWSKI, E. T., MCGRATH, M., SEIDMAN, J. C., MCCORMICK, B. J., SHRESTHA, S., SAMIE, A., MAHFUZ, M., QURESHI, S., HOTWANI, A., BABJI, S., TRIGOSO, D. R., LIMA, A. A., BODHIDATTA, L., BESSONG, P., AHMED, T., SHAKOOR, S.,

- KANG, G., KOSEK, M., GUERRANT, R. L., LANG, D., GOTTLIEB, M., HOUP, E. R. & PLATTSMILLS, J. A. 2016. Epidemiology and Impact of Campylobacter Infection in Children in 8 Low-Resource Settings: Results From the MAL-ED Study. *Clinical Infectious Diseases*, 63, 1171-1179.
- ANDERSEN, M. T., BRØNDSTED, L., PEARSON, B. M., MULHOLLAND, F., PARKER, M., PIN, C., WELLS, J. M. & INGMER, H. 2005. Diverse roles for HspR in Campylobacter jejuni revealed by the proteome, transcriptome and phenotypic characterization of an hspR mutant. *Microbiology (Reading)*, 151, 905-915.
- ANDREWS, S. 2010. *FastQC, A quality control tool for high throughput sequence data* [Online]. Available: <http://www.bioinformatics.babraham.ac.uk/projects/fastqc/> [Accessed 2020].
- ANGELIDIS, A. S., SMITH, L. T., HOFFMAN, L. M. & SMITH, G. M. 2002. Identification of opuC as a chill-activated and osmotically activated carnitine transporter in Listeria monocytogenes. *Applied and Environmental Microbiology*, 68, 2644-2650.
- ARRUDA, S., BOMFIM, G., KNIGHTS, R., HUIIMA-BYRON, T. & RILEY, L. W. 1993. Cloning of an M. tuberculosis DNA fragment associated with entry and survival inside cells. *Science*, 261, 1454-7.
- ASHGAR, S. S., OLDFIELD, N. J., WOOLDRIDGE, K. G., JONES, M. A., IRVING, G. J., TURNER, D. P. & ALA'ALDEEN, D. A. 2007. CapA, an autotransporter protein of Campylobacter jejuni, mediates association with human epithelial cells and colonization of the chicken gut. *Journal of Bacteriology*, 189, 1856-65.
- ASKOURA, M. & STINTZI, A. 2017. Using Galleria mellonella as an Infection Model for Campylobacter jejuni Pathogenesis. *Methods in Molecular Biology*, 1512, 163-169.
- ASSEFA, S., KEANE, T. M., OTTO, T. D., NEWBOLD, C. & BERRIMAN, M. 2009. ABACAS: algorithm-based automatic contiguation of assembled sequences. *Bioinformatics*, 25, 1968-1969.
- AUNKHAM, A., ZAHN, M., KESIREDDY, A., POTHULA, K. R., SCHULTE, A., BASLÉ, A., KLEINEKATHÖFER, U., SUGINTA, W. & VAN DEN BERG, B. 2018. Structural basis for chitin acquisition by marine Vibrio species. *Nature Communications*, 9, 1-13.
- AWAD, W. A., HESS, C. & HESS, M. 2018. Re-thinking the chicken–Campylobacter jejuni interaction: a review. *Avian Pathology*, 47, 352-363.
- BACHTIAR, B. M., COLOE, P. J. & FRY, B. N. 2007. Knockout mutagenesis of the kpsE gene of Campylobacter jejuni 81116 and its involvement in bacterium–host interactions. *FEMS Immunology & Medical Microbiology*, 49, 149-154.
- BACKERT, S., BERNEGGER, S., SKÓRKO-GLONEK, J. & WESSLER, S. 2018. Extracellular HtrA serine proteases: an emerging new strategy in bacterial pathogenesis. *Cellular Microbiology*, 20, e12845.
- BACON, D. J., SZYMANSKI, C. M., BURR, D. H., SILVER, R. P., ALM, R. A. & GUERRY, P. 2001. A phase-variable capsule is involved in virulence of Campylobacter jejuni 81-176. *Molecular Microbiology*, 40, 769-777.
- BADDAL, B., MUZZI, A., CENSINI, S., CALOGERO, R. A., TORRICELLI, G., GUIDOTTI, S., TADDEI, A. R., COVACCI, A., PIZZA, M., RAPPUOLI, R., SORIANI, M. & PEZZICOLI, A. 2015. Dual RNA-seq of Nontypeable Haemophilus influenzae and Host Cell Transcriptomes Reveals Novel Insights into Host-Pathogen Cross Talk. *MBio*, 6, e01765.
- BAEK, M., DIMAIO, F., ANISHCHENKO, I., DAUPARAS, J., OVCHINNIKOV, S., LEE, G. R., WANG, J., CONG, Q., KINCH, L. N., SCHAEFFER, R. D., MILLÁN, C., PARK, H., ADAMS, C., GLASSMAN, C. R., DEGIOVANNI, A., PEREIRA, J. H., RODRIGUES, A. V., DIJK, A. A. V., EBRECHT, A. C., OPPERMAN, D. J., SAGMEISTER, T., BUHLHELLER, C., PAVKOV-KELLER, T., RATHINASWAMY, M. K., DALWADI, U., YIP, C. K., BURKE, J. E., GARCIA, K. C., GRISHIN, N. V., ADAMS, P. D., READ, R. J. & BAKER, D. 2021. Accurate prediction of protein structures and interactions using a three-track neural network. *Science*, 373, 871-876.

- BALABAN, M. & HENDRIXSON, D. R. 2011. Polar flagellar biosynthesis and a regulator of flagellar number influence spatial parameters of cell division in *Campylobacter jejuni*. *PLOS Pathogens*, 7, e1002420-e1002420.
- BANZHAF, M., YAU, H. C., VERHEUL, J., LODGE, A., KRITIKOS, G., MATEUS, A., CORDIER, B., HOV, A. K., STEIN, F., WARTEL, M., PAZOS, M., SOLOVYOVA, A. S., BREUKINK, E., VAN TEEFFELEN, S., SAVITSKI, M. M., DEN BLAAUWEN, T., TYPAS, A. & VOLLMER, W. 2020. Outer membrane lipoprotein Nlpl scaffolds peptidoglycan hydrolases within multi-enzyme complexes in *Escherichia coli*. *The EMBO Journal*, 39, e102246.
- BARRERO-TOBON, A. M. & HENDRIXSON, D. R. 2012. Identification and analysis of flagellar coexpressed determinants (Feds) of *Campylobacter jejuni* involved in colonization. *Molecular Microbiology*, 84, 352-369.
- BASDEN, E. H., TOURTELLOTTE, M. E., PLASTRIDGE, W. N. & TUCKER, J. S. 1968. Genetic Relationship Among Bacteria Classified as Vibrios. *Journal of Bacteriology*, 95, 439-443.
- BEERY, J. T., HUGDAHL, M. B. & DOYLE, M. P. 1988. Colonization of gastrointestinal tracts of chicks by *Campylobacter jejuni*. *Applied and Environmental Microbiology*, 54, 2365-2370.
- BEGLEY, M., GAHAN, C. G. M. & HILL, C. 2005. The interaction between bacteria and bile. *FEMS Microbiology Reviews*, 29, 625-651.
- BEKETSKAIA, M. S., BAY, D. C. & TURNER, R. J. 2014. Outer membrane protein OmpW participates with small multidrug resistance protein member EmrE in quaternary cationic compound efflux. *Journal of Bacteriology*, 196, 1908-1914.
- BÉLANGER, M., KOZAROV, E., SONG, H., WHITLOCK, J. & PROGULSKE-FOX, A. 2012. Both the unique and repeat regions of the *Porphyromonas gingivalis* hemagglutinin A are involved in adhesion and invasion of host cells. *Anaerobe*, 18, 128-134.
- BERG, B. V. D., BLACK, P. N., CLEMONS, W. M. & RAPOPORT, T. A. 2004. Crystal Structure of the Long-Chain Fatty Acid Transporter FadL. *Science*, 304, 1506-1509.
- BERNARD, A. R., JESSOP, T. C., KUMAR, P. & DICKENSON, N. E. 2017. Deoxycholate-Enhanced *Shigella* Virulence Is Regulated by a Rare  $\pi$ -Helix in the Type Three Secretion System Tip Protein IpaD. *Biochemistry*, 56, 6503-6514.
- BERNIER, S. P., SON, S. & SURETTE, M. G. 2018. The Mla Pathway Plays an Essential Role in the Intrinsic Resistance of *Burkholderia cepacia* Complex Species to Antimicrobials and Host Innate Components. *Journal of Bacteriology*, 200.
- BIELASZEWSKA, M., RÜTER, C., BAUWENS, A., GREUNE, L., JAROSCH, K.-A., STEIL, D., ZHANG, W., HE, X., LLOUBES, R., FRUTH, A., KIM, K. S., SCHMIDT, M. A., DOBRINDT, U., MELLMANN, A. & KARCH, H. 2017. Host cell interactions of outer membrane vesicle-associated virulence factors of enterohemorrhagic *Escherichia coli* O157: Intracellular delivery, trafficking and mechanisms of cell injury. *PLOS Pathogens*, 13, e1006159.
- BITTO, N. J., CHAPMAN, R., PIDOT, S., COSTIN, A., LO, C., CHOI, J., D'CRUZE, T., REYNOLDS, E. C., DASHPER, S. G., TURNBULL, L., WHITCHURCH, C. B., STINEAR, T. P., STACEY, K. J. & FERRERO, R. L. 2017a. Bacterial membrane vesicles transport their DNA cargo into host cells. *Sci Rep*, 7, 7072.
- BLACK, P. N. 1988. The fadL gene product of *Escherichia coli* is an outer membrane protein required for uptake of long-chain fatty acids and involved in sensitivity to bacteriophage T2. *Journal of Bacteriology*, 170, 2850-2854.
- BLACK, R. E., LEVINE, M. M., CLEMENTS, M. L., HUGHES, T. P. & BLASER, M. J. 1988. Experimental *Campylobacter jejuni* Infection in Humans. *The Journal of Infectious Diseases*, 157, 472-479.
- BLASER, M. J. 1997. Epidemiologic and clinical features of *Campylobacter jejuni* infections. *Journal of Infectious Diseases*, 176 Suppl 2, S103-5.
- BLEUMINK-PLUYM, N. M., VAN ALPHEN, L. B., BOUWMAN, L. I., WOSTEN, M. M. & VAN PUTTEN, J. P. 2013b. Identification of a functional type VI secretion system in *Campylobacter jejuni* conferring capsule polysaccharide sensitive cytotoxicity. *PLOS Pathogens*, 9, e1003393.

- BLUM, M., CHANG, H.-Y., CHUGURANSKY, S., GREGO, T., KANDASAAMY, S., MITCHELL, A., NUKA, G., PAYSAN-LAFOSSE, T., QURESHI, M., RAJ, S., RICHARDSON, L., SALAZAR, G. A., WILLIAMS, L., BORK, P., BRIDGE, A., GOUGH, J., HAFT, D. H., LETUNIC, I., MARCHLER-BAUER, A., MI, H., NATALE, D. A., NECCI, M., ORENGO, C. A., PANDURANGAN, A. P., RIVOIRE, C., SIGRIST, C. J. A., SILLITOE, I., THANKI, N., THOMAS, P. D., TOSATTO, S. C. E., WU, C. H., BATEMAN, A. & FINN, R. D. 2020. The InterPro protein families and domains database: 20 years on. *Nucleic Acids Research*, 49, D344-D354.
- BOLGER, A. M., LOHSE, M. & USADEL, B. 2014. Trimmomatic: a flexible trimmer for Illumina sequence data. *Bioinformatics (Oxford, England)*, 30, 2114-2120.
- BOMBERGER, J. M., MACEACHRAN, D. P., COUTERMARSH, B. A., YE, S., O'TOOLE, G. A. & STANTON, B. A. 2009. Long-distance delivery of bacterial virulence factors by *Pseudomonas aeruginosa* outer membrane vesicles. *PLOS Pathogens*, 5, e1000382.
- BONNINGTON, K. E. & KUEHN, M. J. 2014. Protein selection and export via outer membrane vesicles. *Biochimica et Biophysica Acta*, 1843, 1612-9.
- BUSHELL, S. R., MAINPRIZE, I. L., WEAR, M. A., LOU, H., WHITFIELD, C. & NAISMITH, J. H. 2013. Wzi is an outer membrane lectin that underpins group 1 capsule assembly in *Escherichia coli*. *Structure (London, England : 1993)*, 21, 844-853.
- BUTCHER, J., HANDLEY, R. A., VAN VLIET, A. H. & STINTZI, A. 2015. Refined analysis of the *Campylobacter jejuni* iron-dependent/independent Fur- and PerR-transcriptomes. *BMC Genomics*, 16, 498.
- CAHILL, B. K., SEELEY, K. W., GUTEL, D. & ELLIS, T. N. 2015. *Klebsiella pneumoniae* O antigen loss alters the outer membrane protein composition and the selective packaging of proteins into secreted outer membrane vesicles. *Microbiology Research*, 180, 1-10.
- CALL, T. P., AKHTAR, M. K., BAGANZ, F. & GRANT, C. 2016. Modulating the import of medium-chain alkanes in *E. coli* through tuned expression of FadL. *Journal of Biological Engineering*, 10, 5.
- CAO, X., BROUWERS, J. F. H. M., VAN DIJK, L., VAN DE LEST, C. H. A., PARKER, C. T., HUYNH, S., VAN PUTTEN, J. P. M., KELLY, D. J. & WÖSTEN, M. M. S. M. 2020. The Unique Phospholipidome of the Enteric Pathogen *Campylobacter jejuni*: Lysophospholipids Are Required for Motility at Low Oxygen Availability. *Journal of Molecular Biology*, 432, 5244-5258.
- CARPENTER, C. D., COOLEY, B. J., NEEDHAM, B. D., FISHER, C. R., TRENT, M. S., GORDON, V. & PAYNE, S. M. 2014. The Vps/VacJ ABC transporter is required for intercellular spread of *Shigella flexneri*. *Infection and Immunity* 82, 660-9.
- CARRILLO, C. D., TABOADA, E., NASH, J. H., LANTHIER, P., KELLY, J., LAU, P. C., VERHULP, R., MYKYTCZUK, O., SY, J., FINDLAY, W. A., AMOAKO, K., GOMIS, S., WILLSON, P., AUSTIN, J. W., POTTER, A., BABIUK, L., ALLAN, B. & SZYMANSKI, C. M. 2004. Genome-wide expression analyses of *Campylobacter jejuni* NCTC11168 reveals coordinate regulation of motility and virulence by flhA. *Journal of Biological Chemistry*, 279, 20327-38.
- CARVER, T., HARRIS, S. R., BERRIMAN, M., PARKHILL, J. & MCQUILLAN, J. A. 2012. Artemis: an integrated platform for visualization and analysis of high-throughput sequence-based experimental data. *Bioinformatics (Oxford, England)*, 28, 464-469.
- CARVER, T. J., RUTHERFORD, K. M., BERRIMAN, M., RAJANDREAM, M.-A., BARRELL, B. G. & PARKHILL, J. 2005. ACT: the Artemis comparison tool. *Bioinformatics*, 21, 3422-3423.
- CATALÁ, A. 2012. Lipid peroxidation modifies the picture of membranes from the "Fluid Mosaic Model" to the "Lipid Whisker Model". *Biochimie*, 94, 101-109.
- CDC. 2019. *Campylobacter (Campylobacteriosis)* [Online]. Available: <https://www.cdc.gov/campylobacter/technical.html> [Accessed 01.05.202].
- CHABAN, B., COLEMAN, I. & BEEBY, M. 2018. Evolution of higher torque in *Campylobacter*-type bacterial flagellar motors. *Scientific Reports*, 8, 97.
- CHAMPION, O. L., KARLYSHEV, A. V., SENIOR, N. J., WOODWARD, M., LA RAGIONE, R., HOWARD, S. L., WREN, B. W. & TITBALL, R. W. 2010. Insect Infection Model for *Campylobacter jejuni*

- Reveals That O-methyl Phosphoramidate Has Insecticidal Activity. *The Journal of Infectious Diseases*, 201, 776-782.
- CHATTERJEE, D. & CHAUDHURI, K. 2011. Association of cholera toxin with *Vibrio cholerae* outer membrane vesicles which are internalized by human intestinal epithelial cells. *FEBS Letters*, 585, 1357-1362.
- CHAUDHURI, R. R., YU, L., KANJI, A., PERKINS, T. T., GARDNER, P. P., CHOUDHARY, J., MASKELL, D. J. & GRANT, A. J. 2011. Quantitative RNA-seq analysis of the *Campylobacter jejuni* transcriptome. *Microbiology (Reading, England)*, 157, 2922-2932.
- CHIANG, J. Y. 2017. Recent advances in understanding bile acid homeostasis. *F1000Research*, 6, 2029.
- CHOI, D. S., KIM, D. K., CHOI, S. J., LEE, J., CHOI, J. P., RHO, S., PARK, S. H., KIM, Y. K., HWANG, D. & GHO, Y. S. 2011. Proteomic analysis of outer membrane vesicles derived from *Pseudomonas aeruginosa*. *Proteomics*, 11, 3424-3429.
- CHOI, U. & LEE, C.-R. 2019. Distinct Roles of Outer Membrane Porins in Antibiotic Resistance and Membrane Integrity in *Escherichia coli*. *Frontiers in Microbiology*, 10.
- CHONG, Z. S., WOO, W. F. & CHNG, S. S. 2015. Osmoporin OmpC forms a complex with MlaA to maintain outer membrane lipid asymmetry in *Escherichia coli*. *Molecular Microbiology*, 98, 1133-1146.
- CLARK, C. G., CHONG, P. M., MCCORRISTER, S. J., SIMON, P., WALKER, M., LEE, D. M., NGUY, K., CHENG, K., GILMOUR, M. W. & WESTMACOTT, G. R. 2014. The CJIE1 prophage of *Campylobacter jejuni* affects protein expression in growth media with and without bile salts. *BMC Microbiology*, 14, 70.
- COKER, A. O., ISOKPEHI, R. D., THOMAS, B. N., AMISU, K. O. & OBI, C. L. 2002. Human campylobacteriosis in developing countries. *Emerging infectious diseases*, 8, 237-244.
- CONLAN, S., ZHANG, Y., CHELEY, S. & BAYLEY, H. 2000. Biochemical and biophysical characterization of OmpG: a monomeric porin. *Biochemistry*, 39, 11845-11854.
- CORDWELL, S. J., LEN, A. C. L., TOUMA, R. G., SCOTT, N. E., FALCONER, L., JONES, D., CONNOLLY, A., CROSSETT, B. & DJORDJEVIC, S. P. 2008. Identification of membrane-associated proteins from *Campylobacter jejuni* strains using complementary proteomics technologies. *PROTEOMICS*, 8, 122-139.
- COYTE, K. Z. & RAKOFF-NAHOUM, S. 2019. Understanding Competition and Cooperation within the Mammalian Gut Microbiome. *Current biology : CB*, 29, R538-R544.
- CRANFORD-SMITH, T. & HUBER, D. 2018. The way is the goal: how SecA transports proteins across the cytoplasmic membrane in bacteria. *FEMS microbiology letters*, 365, fny093.
- CREMERS, C. M., KNOEFLER, D., VITVITSKY, V., BANERJEE, R. & JAKOB, U. 2014. Bile salts act as effective protein-unfolding agents and instigators of disulfide stress in vivo. *Proceedings of the National Academy of Sciences*, 111, E1610-E1619.
- CROFTS, A. A., POLY, F. M., EWING, C. P., KUROIWA, J. M., RIMMER, J. E., HARRO, C., SACK, D., TALAAT, K. R., PORTER, C. K., GUTIERREZ, R. L., DENEARING, B., BRUBAKER, J., LAIRD, R. M., MAUE, A. C., JAEP, K., ALCALA, A., TRIBBLE, D. R., RIDDLE, M. S., RAMAKRISHNAN, A., MCCOY, A. J., DAVIES, B. W., GUERRY, P. & TRENT, M. S. 2018. *Campylobacter jejuni* transcriptional and genetic adaptation during human infection. *Nature Microbiology*, 3, 494-502.
- CROUCHER, N. J. & THOMSON, N. R. 2010. Studying bacterial transcriptomes using RNA-seq. *Current Opinion in Microbiology*, 13, 619-24.
- CROWLEY, J. T., TOLEDO, A. M., LAROCCA, T. J., COLEMAN, J. L., LONDON, E. & BENACH, J. L. 2013. Lipid exchange between *Borrelia burgdorferi* and host cells. *PLOS pathogens*, 9, e1003109-e1003109.
- CUCCUI, J., EASTON, A., CHU, K., BANCROFT, G., OYSTON, P., TITBALL, R. & WREN, B. 2007. Development of signature-tagged mutagenesis in *Burkholderia pseudomallei* to identify genes important in survival and pathogenesis. *Infection and Immunity* 75, 1186-1195.

- DAVIES, C., TAYLOR, A. J., ELMI, A., WINTER, J., LIAW, J., GRABOWSKA, A. D., GUNDOGDU, O., WREN, B. W., KELLY, D. J. & DORRELL, N. 2019. Sodium Taurocholate Stimulates Campylobacter jejuni Outer Membrane Vesicle Production via Down-Regulation of the Maintenance of Lipid Asymmetry Pathway. *Frontiers in Cellular and Infection Microbiology*, 9.
- DAVIS, L. M., KAKUDA, T. & DIRITA, V. J. 2009. A Campylobacter jejuni znuA orthologue is essential for growth in low-zinc environments and chick colonization. *Journal of Bacteriology*, 191, 1631-40.
- DAWSON, P. A. 2016. Bile Secretion and the Enterohepatic Circulation. In: FELDMAN, M., FRIEDMAN, L. S. & BRANDT, L. J. (eds.) *Sleisenger and Fordtran's Gastrointestinal and Liver Disease*. 10th ed.: Elsevier.
- DE LAY, B. D., CAMERON, T. A., DE LAY, N. R., NORRIS, S. J. & EDMONDSON, D. G. 2021. Comparison of transcriptional profiles of Treponema pallidum during experimental infection of rabbits and in vitro culture: Highly similar, yet different. *PLOS Pathogens*, 17, e1009949.
- DEATHERAGE, B. L., LARA, J. C., BERGSBAKEN, T., RASSOULIAN BARRETT, S. L., LARA, S. & COOKSON, B. T. 2009. Biogenesis of bacterial membrane vesicles. *Molecular Microbiology*, 72, 1395-407.
- DHITAL, S., DEO, P., STUART, I. & NADERER, T. 2021. Bacterial outer membrane vesicles and host cell death signaling. *Trends Microbiol*, 29, 1106-1116.
- DIRUSSO, C. C. & BLACK, P. N. 2004. Bacterial long chain fatty acid transport: gateway to a fatty acid-responsive signaling system. *Journal of Biological Chemistry*, 279, 49563-6.
- DJENNAD, A., LO IACONO, G., SARRAN, C., LANE, C., ELSON, R., HÖSER, C., LAKE, I. R., COLÓN-GONZÁLEZ, F. J., KOVATS, S., SEMENZA, J. C., BAILEY, T. C., KESSEL, A., FLEMING, L. E. & NICHOLS, G. L. 2019. Seasonality and the effects of weather on Campylobacter infections. *BMC Infectious Diseases*, 19, 255.
- DOIG, P., YAO, R., BURR, D. H., GUERRY, P. & TRUST, T. J. 1996. An environmentally regulated pilus-like appendage involved in Campylobacter pathogenesis. *Molecular Microbiology*, 20, 885-894.
- DORRELL, N., MANGAN, J. A., LAING, K. G., HINDS, J., LINTON, D., AL-GHUSEIN, H., BARRELL, B. G., PARKHILL, J., STOKER, N. G. & KARLYSHEV, A. V. 2001. Whole genome comparison of Campylobacter jejuni human isolates using a low-cost microarray reveals extensive genetic diversity. *Genome Research*, 11, 1706-1715.
- DOYLE, M. T. & BERNSTEIN, H. D. 2019. Bacterial outer membrane proteins assemble via asymmetric interactions with the BamA  $\beta$ -barrel. *Nature Communications*, 10, 3358.
- DU, Z., SU, H., WANG, W., YE, L., WEI, H., PENG, Z., ANISHCHENKO, I., BAKER, D. & YANG, J. 2021. The trRosetta server for fast and accurate protein structure prediction. *Nature Protocols*, 16, 5634-5651.
- DUBB, R. K., NOTHAFT, H., BEADLE, B., RICHARDS, M. R. & SZYMANSKI, C. M. 2019. N-glycosylation of the CmeABC multidrug efflux pump is needed for optimal function in Campylobacter jejuni. *Glycobiology*, 30, 105-119.
- DUGAR, G., HERBIG, A., FÖRSTNER, K. U., HEIDRICH, N., REINHARDT, R., NIESELT, K. & SHARMA, C. M. 2013. High-Resolution Transcriptome Maps Reveal Strain-Specific Regulatory Features of Multiple Campylobacter jejuni Isolates. *PLOS Genetics*, 9, e1003495.
- DZIECIOL, M., WAGNER, M. & HEIN, I. 2011. CmeR-dependent gene Cj0561c is induced more effectively by bile salts than the CmeABC efflux pump in both human and poultry Campylobacter jejuni strains. *Research in Microbiology*, 162, 991-998.
- EKIERT, D. C., BHABHA, G., ISOM, G. L., GREENAN, G., OVCHINNIKOV, S., HENDERSON, I. R., COX, J. S. & VALE, R. D. 2017. Architectures of Lipid Transport Systems for the Bacterial Outer Membrane. *Cell*, 169, 273-285.e17.
- ELHENAWY, W., BORDING-JORGENSEN, M., VALGUARNERA, E., HAURAT, M. F., WINE, E. & FELDMAN, M. F. 2016. LPS Remodeling Triggers Formation of Outer Membrane Vesicles in Salmonella. *MBio*, 7.

- ELLEN, R. P. & GROVE, D. A. 1989. Bacteroides gingivalis vesicles bind to and aggregate Actinomyces viscosus. *Infection and Immunity* 57, 1618-1620.
- ELLIS, T. N. & KUEHN, M. J. 2010. Virulence and Immunomodulatory Roles of Bacterial Outer Membrane Vesicles. *Microbiology and Molecular Biology Reviews*, 74, 81-94.
- ELMI, A., DOREY, A., WATSON, E., JAGATIA, H., INGLIS, N. F., GUNDOGDU, O., BAJAJ-ELLIOTT, M., WREN, B. W., SMITH, D. G. E. & DORRELL, N. 2018. The bile salt sodium taurocholate induces Campylobacter jejuni outer membrane vesicle production and increases OMV-associated proteolytic activity. *Cellular Microbiology*, 20.
- ELMI, A., NASHER, F., JAGATIA, H., GUNDOGDU, O., BAJAJ-ELLIOTT, M., WREN, B. & DORRELL, N. 2016. Campylobacter jejuni outer membrane vesicle-associated proteolytic activity promotes bacterial invasion by mediating cleavage of intestinal epithelial cell E-cadherin and occludin. *Cellular Microbiology*, 18, 561-72.
- ELMI, A., WATSON, E., SANDU, P., GUNDOGDU, O., MILLS, D. C., INGLIS, N. F., MANSON, E., IMRIE, L., BAJAJ-ELLIOTT, M., WREN, B. W., SMITH, D. G. & DORRELL, N. 2012. Campylobacter jejuni outer membrane vesicles play an important role in bacterial interactions with human intestinal epithelial cells. *Infection and Immunity* 80, 4089-98.
- FAHERTY, C. S., REDMAN, J. C., RASKO, D. A., BARRY, E. M. & NATARO, J. P. 2012. Shigella flexneri effectors OspE1 and OspE2 mediate induced adherence to the colonic epithelium following bile salts exposure. *Molecular Microbiology*, 85, 107-121.
- FAIRMAN, J. W., NOINAJ, N. & BUCHANAN, S. K. 2011. The structural biology of  $\beta$ -barrel membrane proteins: a summary of recent reports. *Current opinion in structural biology*, 21, 523-531.
- FALANY, C. N., JOHNSON, M. R., BARNES, S. & DIASIO, R. B. 1994. Glycine and taurine conjugation of bile acids by a single enzyme. Molecular cloning and expression of human liver bile acid CoA:amino acid N-acyltransferase. *Journal of Biological Chemistry*, 269, 19375-19379.
- FERRERO, R. L. & LEE, A. 1988. Motility of Campylobacter jejuni in a Viscous Environment: Comparison with Conventional Rod-shaped Bacteria. *Microbiology*, 134, 53-59.
- FIGUEROA, G., GALENO, H., TRONCOSO, M., TOLEDO, S. & SOTO, V. 1989. Prospective study of Campylobacter jejuni infection in Chilean infants evaluated by culture and serology. *Journal of Clinical Microbiology*, 27, 1040-1044.
- FINLAYSON-TRICK, E., CONNORS, J., STADNYK, A. & VAN LIMBERGEN, J. 2019. Regulation of Antimicrobial Pathways by Endogenous Heat Shock Proteins in Gastrointestinal Disorders. *Gastrointestinal Disorders*, 1.
- FINNEGAN, S. & PERCIVAL, S. L. 2015. EDTA: An Antimicrobial and Antibiofilm Agent for Use in Wound Care. *Advances in Wound Care (New Rochelle)*, 4, 415-421.
- FITZHENRY, R. J., STEVENS, M. P., JENKINS, C., WALLIS, T. S., HEUSCHKEL, R., MURCH, S., THOMSON, M., FRANKEL, G. & PHILLIPS, A. D. 2003. Human intestinal tissue tropism of intimin epsilon O103 Escherichia coli. *FEMS Microbiology Letters*, 218, 311-316.
- FLAHAUT, S., HARTKE, A., GIARD, J.-C., BENACHOUR, A., BOUTIBONNES, P. & AUFRAY, Y. 1996. Relationship between stress response towards bile salts, acid and heat treatment in Enterococcus faecalis. *FEMS Microbiology Letters*, 138, 49-54.
- FLANAGAN, R. C., NEAL-MCKINNEY, J. M., DHILLON, A. S., MILLER, W. G. & KONKEL, M. E. 2009. Examination of Campylobacter jejuni putative adhesins leads to the identification of a new protein, designated FlpA, required for chicken colonization. *Infection and Immunity* 77, 2399-407.
- FLORKOWSKI, C. M., IKRAM, R. B., CROZIER, I. M., IKRAM, H. & BERRY, M. E. 1984. Campylobacter jejuni myocarditis. *Clinical Cardiology*, 7, 558-9.
- FOX, E. M., RAFTERY, M., GOODCHILD, A. & MENDZ, G. L. 2007. Campylobacter jejuni response to ox-bile stress. *FEMS Immunology & Medical Microbiology*, 49, 165-172.
- FREITAG, C. M., STRIJBIS, K. & VAN PUTTEN, J. P. M. 2017. Host cell binding of the flagellar tip protein of Campylobacter jejuni. *Cellular Microbiology*, 19, e12714.

- FSA. 2013. *Annual Report of the Chief Scientist 2012/13* [Online]. Available: [https://acss.food.gov.uk/sites/default/files/multimedia/pdfs/publication/cstar\\_2013.pdf](https://acss.food.gov.uk/sites/default/files/multimedia/pdfs/publication/cstar_2013.pdf) [Accessed 02.05.2020].
- FSA. 2019a. *PERFORMANCE AND RESOURCES REPORT Q4 2018/19* [Online]. Available: <https://www.food.gov.uk/sites/default/files/media/document/q4-18-19-performance-and-resources-report.pdf> [Accessed 02.05.2020].
- FSA. 2019b. *CAMPYLOBACTER REDUCTION PROGRAMME: UPDATE* [Online]. Available: <https://www.food.gov.uk/sites/default/files/media/document/fsa-19-09-08-campylobacter.pdf> [Accessed 04/05/2020].
- FSA. 2019c. *A microbiological survey of Campylobacter contamination in fresh whole UK-produced chilled chickens at retail sale* [Online]. Available: [https://www.food.gov.uk/sites/default/files/media/document/campylobacter-contamination-in-fresh-whole-uk-produced-chilled-chickens-at-retail-sale-year-3-2016-2017\\_0.pdf](https://www.food.gov.uk/sites/default/files/media/document/campylobacter-contamination-in-fresh-whole-uk-produced-chilled-chickens-at-retail-sale-year-3-2016-2017_0.pdf) [Accessed 04/05/2020].
- GASPERINI, G., BIAGINI, M., ARATO, V., GIANFALDONI, C., VADI, A., NORAI, N., BENSI, G., DELANY, I., PIZZA, M., ARICÒ, B. & LEUZZI, R. 2018. Outer Membrane Vesicles (OMV)-based and Proteomics-driven Antigen Selection Identifies Novel Factors Contributing to *Bordetella pertussis* Adhesion to Epithelial Cells. *Molecular & Cellular Proteomics*, 17, 205-215.
- GAYNOR, E. C., GHORI, N. & FALKOW, S. 2001. Bile-induced 'pili' in *Campylobacter jejuni* are bacteria-independent artifacts of the culture medium. *Molecular Microbiology*, 39, 1546-1549.
- GHOUL, M., POMMEPUY, M., MOILLO-BATT, A. & CORMIER, M. 1989. Effect of carbonyl cyanide m-chlorophenylhydrazone on *Escherichia coli* halotolerance. *Applied and environmental microbiology*, 55, 1040-1043.
- GIBREEL, A., WETSCH, N. M. & TAYLOR, D. E. 2007. Contribution of the CmeABC efflux pump to macrolide and tetracycline resistance in *Campylobacter jejuni*. *Antimicrobial Agents and Chemotherapy*, 51, 3212-3216.
- GILBERT, M., BRISSON, J.-R., KARWASKI, M.-F., MICHNIEWICZ, J., CUNNINGHAM, A.-M., WU, Y., YOUNG, N. M. & WAKARCHUK, W. W. 2000. Biosynthesis of ganglioside mimics in *Campylobacter jejuni* OH4384 identification of the glycosyltransferase genes, enzymatic synthesis of model compounds, and characterization of nanomole amounts by 600-MHz <sup>1</sup>H AND <sup>13</sup>C NMR analysis. *Journal of Biological Chemistry*, 275, 3896-3906.
- GILBERT, M., PARKER, C. T. & MORAN, A. P. 2008. *Campylobacter jejuni* Lipooligosaccharides: Structures and Biosynthesis. *Campylobacter, Third Edition*. American Society of Microbiology.
- GIORDANO, N. P., CIAN, M. B., DALEBROUX, Z. D. & RICHARDSON, A. R. 2020. Outer Membrane Lipid Secretion and the Innate Immune Response to Gram-Negative Bacteria. *Infection and Immunity*, 88, e00920-19.
- GLADMAN, S. & SEEMANN, T. 2012. *VelvetOptimiser, v2.2.5* [Online]. Available: <http://bioinformatics.net.au/software/velvetoptimiser.shtml> [Accessed 2020].
- GOTOH, K., KODAMA, T., HIYOSHI, H., IZUTSU, K., PARK, K.-S., DRYSELIUS, R., AKEDA, Y., HONDA, T. & IIDA, T. 2010. Bile Acid-Induced Virulence Gene Expression of *Vibrio parahaemolyticus* Reveals a Novel Therapeutic Potential for Bile Acid Sequestrants. *PLOS ONE*, 5, e13365.
- GRANT, C., DESZCZ, D., WEI, Y.-C., MARTÍNEZ-TORRES, R. J., MORRIS, P., FOLLIARD, T., SREENIVASAN, R., WARD, J., DALBY, P., WOODLEY, J. M. & BAGANZ, F. 2014. Identification and use of an alkane transporter plug-in for applications in biocatalysis and whole-cell biosensing of alkanes. *Scientific reports*, 4, 5844-5844.
- GRANT, C. C., KONKEL, M. E., CIEPLAK, W., JR. & TOMPKINS, L. S. 1993. Role of flagella in adherence, internalization, and translocation of *Campylobacter jejuni* in nonpolarized and polarized epithelial cell cultures. *Infection and Immunity* 61, 1764-1771.

- GRINNAGE-PULLEY, T., MU, Y., DAI, L. & ZHANG, Q. 2016. Dual Repression of the Multidrug Efflux Pump CmeABC by CosR and CmeR in *Campylobacter jejuni*. *Frontiers in Microbiology*, 7.
- GUERRERO-MANDUJANO, A., HERNÁNDEZ-CORTEZ, C., IBARRA, J. A. & CASTRO-ESCARPULLI, G. 2017. The outer membrane vesicles: Secretion system type zero. *Traffic*, 18, 425-432.
- GUIDI, R., LEVI, L., ROUF, S. F., PUIAC, S., RHEN, M. & FRISAN, T. 2013. *Salmonella enterica* delivers its genotoxin through outer membrane vesicles secreted from infected cells. *Cellular Microbiology*, 15, 2034-2050.
- GUNDOGDU, O., DA SILVA, D. T., MOHAMMAD, B., ELMİ, A., WREN, B. W., VAN VLIET, A. H. M. & DORRELL, N. 2016. The *Campylobacter jejuni* Oxidative Stress Regulator RrpB Is Associated with a Genomic Hypervariable Region and Altered Oxidative Stress Resistance. *Frontiers in microbiology*, 7, 2117-2117.
- GUNDOGDU, O., MILLS, D. C., ELMİ, A., MARTIN, M. J., WREN, B. W. & DORRELL, N. 2011. The *Campylobacter jejuni* transcriptional regulator Cj1556 plays a role in the oxidative and aerobic stress response and is important for bacterial survival in vivo. *Journal of Bacteriology*, 193, 4238-49.
- GUO, B., WANG, Y., SHI, F., BARTON, Y.-W., PLUMMER, P., REYNOLDS, D. L., NETTLETON, D., GRINNAGE-PULLEY, T., LIN, J. & ZHANG, Q. 2008. CmeR Functions as a Pleiotropic Regulator and Is Required for Optimal Colonization of *Campylobacter jejuni* In Vivo. *Journal of Bacteriology*, 190, 1879-1890.
- GUPTA, S., RAY, S., KHAN, A., CHINA, A., DAS, D. & MALLICK, A. I. 2021. The cost of bacterial predation via type VI secretion system leads to predator extinction under environmental stress. *iScience*, 24, 103507.
- HAGEY, L. R., VIDAL, N., HOFMANN, A. F. & KRASOWSKI, M. D. 2010. Evolutionary diversity of bile salts in reptiles and mammals, including analysis of ancient human and extinct giant ground sloth coprolites. *BMC Evolutionary Biology*, 10, 133-133.
- HAMILTON, J. P., XIE, G., RAUFMAN, J.-P., HOGAN, S., GRIFFIN, T. L., PACKARD, C. A., CHATFIELD, D. A., HAGEY, L. R., STEINBACH, J. H. & HOFMANN, A. F. 2007. Human cecal bile acids: concentration and spectrum. *American Journal of Physiology-Gastrointestinal and Liver Physiology*, 293, G256-G263.
- HAMNER, S., MCINNERNEY, K., WILLIAMSON, K., FRANKLIN, M. J. & FORD, T. E. 2013. Bile salts affect expression of *Escherichia coli* O157:H7 genes for virulence and iron acquisition, and promote growth under iron limiting conditions. *PLOS ONE*, 8, e74647.
- HANNU, T., MATTILA, L., RAUTELIN, H., SIITONEN, A. & LEIRISALO-REPO, M. 2005. Three cases of cardiac complications associated with *Campylobacter jejuni* infection and review of the literature. *European Journal of Clinical Microbiology & Infectious Diseases*, 24, 619-22.
- HAO, H., REN, N., HAN, J., FOLEY, S. L., IQBAL, Z., CHENG, G., KUANG, X., LIU, J., LIU, Z., DAI, M., WANG, Y. & YUAN, Z. 2016. Virulence and Genomic Feature of Multidrug Resistant *Campylobacter jejuni* Isolated from Broiler Chicken. *Frontiers in Microbiology*, 7.
- HARA-KUDO, Y. & TAKATORI, K. 2011. Contamination level and ingestion dose of foodborne pathogens associated with infections. *Epidemiology and Infection*, 139, 1505-1510.
- HARDISON, W. G. 1978. Hepatic taurine concentration and dietary taurine as regulators of bile acid conjugation with taurine. *Gastroenterology*, 75, 71-5.
- HAURAT, M. F., ADUSE-OPOKU, J., RANGARAJAN, M., DOROBANTU, L., GRAY, M. R., CURTIS, M. A. & FELDMAN, M. F. 2011. Selective sorting of cargo proteins into bacterial membrane vesicles. *Journal of Biological Chemistry*, 286, 1269-76.
- HAZELEGER, W. C., WOUTERS, J. A., ROMBOUTS, F. M. & ABEE, T. 1998. Physiological activity of *Campylobacter jejuni* far below the minimal growth temperature. *Applied and Environmental Microbiology*, 64, 3917-22.
- HE, X. & AHN, J. 2014. Assessment of conjugal transfer of antibiotic resistance genes in *Salmonella Typhimurium* exposed to bile salts. *Journal of Microbiology*, 52, 716-719.

- HE, Z., GHARAIBEH, R. Z., NEWSOME, R. C., POPE, J. L., DOUGHERTY, M. W., TOMKOVICH, S., PONS, B., MIREY, G., VIGNARD, J., HENDRIXSON, D. R. & JOBIN, C. 2019. Campylobacter jejuni promotes colorectal tumorigenesis through the action of cytolethal distending toxin. *Gut*, 68, 289-300.
- HEIPIEPER, H.-J., KEWELOH, H. & REHM, H.-J. 1991. Influence of phenols on growth and membrane permeability of free and immobilized Escherichia coli. *Applied and Environmental Microbiology*, 57, 1213-1217.
- HENDRIXSON, D. R., AKERLEY, B. J. & DIRITA, V. J. 2001. Transposon mutagenesis of Campylobacter jejuni identifies a bipartite energy taxis system required for motility. *Molecular Microbiology*, 40, 214-24.
- HENDRIXSON, D. R. & DIRITA, V. J. 2003. Transcription of  $\sigma_{54}$ -dependent but not  $\sigma_{28}$ -dependent flagellar genes in Campylobacter jejuni is associated with formation of the flagellar secretory apparatus. *Molecular Microbiology*, 50, 687-702.
- HENDRIXSON, D. R. & DIRITA, V. J. 2004. Identification of Campylobacter jejuni genes involved in commensal colonization of the chick gastrointestinal tract. *Molecular Microbiology*, 52, 471-484.
- HEREDIA, N. & GARCÍA, S. 2018. Animals as sources of food-borne pathogens: A review. *Animal Nutrition*, 4, 250-255.
- HERMANS, D., PASMANS, F., HEYNDRIKX, M., VAN IMMERSEEL, F., MARTEL, A., VAN DEUN, K. & HAESEBROUCK, F. 2012. A tolerogenic mucosal immune response leads to persistent Campylobacter jejuni colonization in the chicken gut. *Critical Reviews in Microbiology*, 38, 17-29.
- HICKEY, T. E., MCVEIGH, A. L., SCOTT, D. A., MICHIELUTTI, R. E., BIXBY, A., CARROLL, S. A., BOURGEOIS, A. L. & GUERRY, P. 2000. Campylobacter jejuni cytolethal distending toxin mediates release of interleukin-8 from intestinal epithelial cells. *Infection and Immunity* 68, 6535-6541.
- HOANG, K., WANG, Y. & LIN, J. 2012. Identification of genetic loci that contribute to Campylobacter resistance to fowlicidin-1, a chicken host defense peptide. *Frontiers in Cellular and Infection Microbiology*, 2.
- HOFFMANN, T. & BREMER, E. 2011. Protection of Bacillus subtilis against cold stress via compatible-solute acquisition. *Journal of Bacteriology*, 193, 1552-62.
- HOFMANN, A. F. & ECKMANN, L. 2006. How bile acids confer gut mucosal protection against bacteria. *Proceedings of the National Academy of Sciences of the United States of America*, 103, 4333.
- HOFMANN, A. F., HAGEY, L. R. & KRASOWSKI, M. D. 2010. Bile salts of vertebrates: structural variation and possible evolutionary significance. *Journal of lipid research*, 51, 226-246.
- HOLMES, K., MULHOLLAND, F., PEARSON, B. M., PIN, C., MCNICHOLL-KENNEDY, J., KETLEY, J. M. & WELLS, J. M. 2005. Campylobacter jejuni gene expression in response to iron limitation and the role of Fur. *Microbiology*, 151, 243-257.
- HOU, J.-J., WANG, X., WANG, Y.-M. & WANG, B.-M. 2021. Interplay between gut microbiota and bile acids in diarrhoea-predominant irritable bowel syndrome: a review. *Critical Reviews in Microbiology*, 1-18.
- HUANG, Y. M. M., MIAO, Y. L., MUNGUIA, J., LIN, L., NIZET, V. & MCCAMMON, J. A. 2016. Molecular dynamic study of MlaC protein in Gram-negative bacteria: conformational flexibility, solvent effect and protein-phospholipid binding. *Protein Science*, 25, 1430-1437.
- HUGHES, G. W., HALL, S. C. L., LAXTON, C. S., SRIDHAR, P., MAHADI, A. H., HATTON, C., PIGGOT, T. J., WOTHERSPOON, P. J., LENEY, A. C., WARD, D. G., JAMSHAD, M., SPANA, V., CADBY, I. T., HARDING, C., ISOM, G. L., BRYANT, J. A., PARR, R. J., YAKUB, Y., JEEVES, M., HUBER, D., HENDERSON, I. R., CLIFTON, L. A., LOVERING, A. L. & KNOWLES, T. J. 2019. Evidence for phospholipid export from the bacterial inner membrane by the Mla ABC transport system. *Nature Microbiology*, 4, 1692-1705.

- HUGHES, R. 2004. Campylobacter jejuni in Guillain-Barré syndrome. *The Lancet Neurology*, 3, 644.
- INDIVERI, C., IACOBAZZI, V., GIANGREGORIO, N. & PALMIERI, F. 1998. Bacterial Overexpression, Purification, and Reconstitution of the Carnitine/Acylcarnitine Carrier from Rat Liver Mitochondria. *Biochemical and Biophysical Research Communications*, 249, 589-594.
- ISOM, G. L., DAVIES, N. J., CHONG, Z. S., BRYANT, J. A., JAMSHAD, M., SHARIF, M., CUNNINGHAM, A. F., KNOWLES, T. J., CHNG, S. S., COLE, J. A. & HENDERSON, I. R. 2017. MCE domain proteins: conserved inner membrane lipid-binding proteins required for outer membrane homeostasis. *Scientific Reports*, 7, 8608.
- JACOBS, J. P., GOUDARZI, M., SINGH, N., TONG, M., MCHARDY, I. H., RUEGGER, P., ASADOURIAN, M., MOON, B.-H., AYSON, A., BORNEMAN, J., MCGOVERN, D. P. B., FORNACE, A. J., JR., BRAUN, J. & DUBINSKY, M. 2016. A Disease-Associated Microbial and Metabolomics State in Relatives of Pediatric Inflammatory Bowel Disease Patients. *Cellular and Molecular Gastroenterology and Hepatology*, 2, 750-766.
- JANG, K.-S., SWEREDOSKI, M. J., GRAHAM, R. L. J., HESS, S. & CLEMONS, W. M. 2014. Comprehensive proteomic profiling of outer membrane vesicles from Campylobacter jejuni. *Journal of Proteomics*, 98, 90-98.
- JAVED, M. A., CAWTHRAW, S. A., BAIG, A., LI, J., MCNALLY, A., OLDFIELD, N. J., NEWELL, D. G. & MANNING, G. 2012. Cj1136 is required for lipooligosaccharide biosynthesis, hyperinvasion, and chick colonization by Campylobacter jejuni. *Infection and Immunity* 80, 2361-2370.
- JERVIS, A. J., BUTLER, J. A., WREN, B. W. & LINTON, D. 2015. Chromosomal integration vectors allowing flexible expression of foreign genes in Campylobacter jejuni. *BMC Microbiology*, 15, 230.
- JIA, W., EL ZOEIBY, A., PETRUZZIELLO, T. N., JAYABALASINGHAM, B., SEYEDIRASHTI, S. & BISHOP, R. E. 2004. Lipid trafficking controls endotoxin acylation in outer membranes of Escherichia coli. *Journal of Biological Chemistry*, 279, 44966-75.
- JIN, S., JOE, A., LYNETT, J., HANI, E. K., SHERMAN, P. & CHAN, V. L. 2001. JlpA, a novel surface-exposed lipoprotein specific to Campylobacter jejuni, mediates adherence to host epithelial cells. *Molecular Microbiology*, 39, 1225-36.
- JIN, S., SONG, Y. C., EMILI, A., SHERMAN, P. M. & CHAN, V. L. 2003. JlpA of Campylobacter jejuni interacts with surface-exposed heat shock protein 90alpha and triggers signalling pathways leading to the activation of NF-kappaB and p38 MAP kinase in epithelial cells. *Cellular Microbiology*, 5, 165-74.
- JOFFRE, E., NICKLASSON, M., ÁLVAREZ-CARRETERO, S., XIAO, X., SUN, L., NOOKAEW, I., ZHU, B. & SJÖLING, Å. 2019. The bile salt glycocholate induces global changes in gene and protein expression and activates virulence in enterotoxigenic Escherichia coli. *Scientific Reports*, 9, 108.
- JOHNSON, W. M. & LIOR, H. 1988. A new heat-labile cytolethal distending toxin (CLDT) produced by Campylobacter spp. *Microbial Pathogenesis*, 4, 115-26.
- JONES, M. A., MARSTON, K. L., WOODALL, C. A., MASKELL, D. J., LINTON, D., KARLYSHEV, A. V., DORRELL, N., WREN, B. W. & BARROW, P. A. 2004. Adaptation of Campylobacter jejuni NCTC11168 to high-level colonization of the avian gastrointestinal tract. *Infection and Immunity* 72, 3769-76.
- JOSHI, N. A. & FASS, J. N. 2011. Sickle: A sliding-window, adaptive, quality-based trimming tool for FastQ files (Version 1.33) [Software].
- JOVER, A., FRAGA, F., MEIJIDE, F., VÁZQUEZ TATO, J., CAUTELA, J., DEL GIUDICE, A. & DI GREGORIO, M. C. 2021. Revealing the complex self-assembly behaviour of sodium deoxycholate in aqueous solution. *Journal of Colloid and Interface Science*, 604, 415-428.
- JUMPER, J., EVANS, R., PRITZEL, A., GREEN, T., FIGURNOV, M., RONNEBERGER, O., TUNYASUVUNAKOOL, K., BATES, R., ŽÍDEK, A., POTAPENKO, A., BRIDGLAND, A., MEYER, C., KOHL, S. A. A., BALLARD, A. J., COWIE, A., ROMERA-PAREDES, B., NIKOLOV, S., JAIN, R.,

- ADLER, J., BACK, T., PETERSEN, S., REIMAN, D., CLANCY, E., ZIELINSKI, M., STEINEGGER, M., PACHOLSKA, M., BERGHAMMER, T., BODENSTEIN, S., SILVER, D., VINYALS, O., SENIOR, A. W., KAVUKCUOGLU, K., KOHLI, P. & HASSABIS, D. 2021. Highly accurate protein structure prediction with AlphaFold. *Nature*, 596, 583-589.
- KAAKOUSH, N. O., CASTAÑO-RODRÍGUEZ, N., MITCHELL, H. M. & MAN, S. M. 2015. Global Epidemiology of Campylobacter Infection. *Clinical microbiology reviews*, 28, 687-720.
- KÄLLBERG, M., WANG, H., WANG, S., PENG, J., WANG, Z., LU, H. & XU, J. 2012. Template-based protein structure modeling using the RaptorX web server. *Nature protocols*, 7, 1511-1522.
- KAMAL, N., DORRELL, N., JAGANNATHAN, A., TURNER, S. M., CONSTANTINIDOU, C., STUDHOLME, D. J., MARSDEN, G., HINDS, J., LAING, K. G., WREN, B. W. & PENN, C. W. 2007. Deletion of a previously uncharacterized flagellar-hook-length control gene fliK modulates the  $\sigma$ 54-dependent regulon in Campylobacter jejuni. *Microbiology*, 153, 3099-3111.
- KAMISCHKE, C., FAN, J., BERGERON, J., KULASEKARA, H. D., DALEBROUX, Z. D., BURRELL, A., KOLLMAN, J. M. & MILLER, S. I. 2019. The Acinetobacter baumannii Mla system and glycerophospholipid transport to the outer membrane. *Elife*, 8.
- KANDELL, R. L. & BERNSTEIN, C. 1991. Bile salt/acid induction of DNA damage in bacterial and mammalian cells: implications for colon cancer. *Nutrition Cancer*, 16, 227-38.
- KAPARAKIS-LIASKOS, M. & FERRERO, R. L. 2015. Immune modulation by bacterial outer membrane vesicles. *Nature Reviews Immunology*, 15, 375-387.
- KAPPES, R. M. & BREMER, E. 1998. Response of Bacillus subtilis to high osmolarity: uptake of carnitine, crotonobetaine and  $\gamma$ -butyrobetaine via the ABC transport system OpuC. *Microbiology*, 144, 83-90.
- KARLYSHEV, A. V., HENDERSON, J., KETLEY, J. M. & WREN, B. W. 1998. An improved physical and genetic map of Campylobacter jejuni NCTC 11168 (UA580). *Microbiology*, 144, 503-508.
- KARLYSHEV, A. V., KETLEY, J. M. & WREN, B. W. 2005. The Campylobacter jejuni glycome\*. *FEMS Microbiology Reviews*, 29, 377-390.
- KARLYSHEV, A. V., LINTON, D., GREGSON, N. A., LASTOVICA, A. J. & WREN, B. W. 2000. Genetic and biochemical evidence of a Campylobacter jejuni capsular polysaccharide that accounts for Penner serotype specificity. *Molecular Microbiology*, 35, 529-541.
- KARLYSHEV, A. V., LINTON, D., GREGSON, N. A. & WREN, B. W. 2002. A novel paralogous gene family involved in phase-variable flagella-mediated motility in Campylobacter jejuni. *Microbiology*, 148, 473-480.
- KARLYSHEV, A. V., MCCROSSAN, M. V. & WREN, B. W. 2001. Demonstration of polysaccharide capsule in Campylobacter jejuni using electron microscopy. *Infection and Immunity* 69, 5921-5924.
- KARLYSHEV, A. V., THACKER, G., JONES, M. A., CLEMENTS, M. O. & WREN, B. W. 2014. Campylobacter jejuni gene cj0511 encodes a serine peptidase essential for colonisation. *FEBS Open Bio*, 4, 468-72.
- KAY, E., CUCCUI, J. & WREN, B. W. 2019a. Recent advances in the production of recombinant glycoconjugate vaccines. *npj Vaccines*, 4, 1-8.
- KAY, S., EDWARDS, J., BROWN, J. & DIXON, R. 2019b. Galleria mellonella Infection Model Identifies Both High and Low Lethality of Clostridium perfringens Toxigenic Strains and Their Response to Antimicrobials. *Frontiers in Microbiology*, 10.
- KEITHLIN, J., SARGEANT, J., THOMAS, M. K. & FAZIL, A. 2014. Systematic review and meta-analysis of the proportion of Campylobacter cases that develop chronic sequelae. *BMC Public Health*, 14, 1203-1203.
- KELLEY, L. A., MEZULIS, S., YATES, C. M., WASS, M. N. & STERNBERG, M. J. E. 2015. The Phyre2 web portal for protein modeling, prediction and analysis. *Nature Protocols*, 10, 845-858.
- KELLY, J., JARRELL, H., MILLAR, L., TESSIER, L., FIORI, L. M., LAU, P. C., ALLAN, B. & SZYMANSKI, C. M. 2006. Biosynthesis of the N-linked glycan in Campylobacter jejuni and addition onto protein through block transfer. *Journal of Bacteriology*, 188, 2427-34.

- KEO, T., COLLINS, J., KUNWAR, P., BLASER, M. J. & IOVINE, N. M. 2011. Campylobacter capsule and lipooligosaccharide confer resistance to serum and cationic antimicrobials. *Virulence*, 2, 30-40.
- KESTY, N. C., MASON, K. M., REEDY, M., MILLER, S. E. & KUEHN, M. J. 2004. Enterotoxigenic *Escherichia coli* vesicles target toxin delivery into mammalian cells. *The EMBO Journal*, 23, 4538-4549.
- KHAN, M. A. & BISHOP, R. E. 2009. Molecular mechanism for lateral lipid diffusion between the outer membrane external leaflet and a beta-barrel hydrocarbon ruler. *Biochemistry*, 48, 9745-9756.
- KIM-ANH LE CAO, FLORIAN ROHART, IGNACIO GONZALEZ, SEBASTIEN DEJEAN WITH KEY CONTRIBUTORS BENOIT GAUTIER, F. & BARTOLO, C. F. P. M., JEFF COQUERY, FANGZOU YAO AND BENOIT LIQUET. (2016). . 2016. *mixOmics: Omics Data Integration Project. R package version 6.1.1*. [Online]. Available: <https://CRAN.R-project.org/package=mixOmics> [Accessed 2020].
- KINSELLA, N., GUERRY, P. & COONEY, J. 1997. The flgE gene of *Campylobacter coli* is under the control of the alternative sigma factor sigma54. *Journal of Bacteriology*, 179, 4647-4653.
- KIRK, M. D., PIRES, S. M., BLACK, R. E., CAIPO, M., CRUMP, J. A., DEVLEESSCHAUWER, B., DÖPFER, D., FAZIL, A., FISCHER-WALKER, C. L. & HALD, T. 2015. World Health Organization estimates of the global and regional disease burden of 22 foodborne bacterial, protozoal, and viral diseases, 2010: a data synthesis. *PLOS Medicine*, 12.
- KOEBNIK, R. 1999. Structural and Functional Roles of the Surface-Exposed Loops of the  $\beta$ -Barrel Membrane Protein OmpA from *Escherichia coli*. *Journal of Bacteriology*, 181, 3688-3694.
- KOEBNIK, R., LOCHER, K. P. & VAN GELDER, P. 2000. Structure and function of bacterial outer membrane proteins: barrels in a nutshell. *Molecular Microbiology*, 37, 239-253.
- KOEPPE, K., HAMPTON, T. H., JAREK, M., SCHARFE, M., GERBER, S. A., MIELCARZ, D. W., DEMERS, E. G., DOLBEN, E. L., HAMMOND, J. H., HOGAN, D. A. & STANTON, B. A. 2016. A Novel Mechanism of Host-Pathogen Interaction through sRNA in Bacterial Outer Membrane Vesicles. *PLOS Pathogens*, 12, e1005672.
- KONKEL, M. E., GARVIS, S. G., TIPTON, S. L., ANDERSON, D. E., JR. & CIEPLAK, W., JR. 1997. Identification and molecular cloning of a gene encoding a fibronectin-binding protein (CadF) from *Campylobacter jejuni*. *Molecular Microbiology*, 24, 953-63.
- KONKEL, M. E., KLENA, J. D., RIVERA-AMILL, V., MONTEVILLE, M. R., BISWAS, D., RAPHAEL, B. & MICKELSON, J. 2004. Secretion of virulence proteins from *Campylobacter jejuni* is dependent on a functional flagellar export apparatus. *Journal of Bacteriology*, 186, 3296-3303.
- KONKEL, M. E., LARSON, C. L. & FLANAGAN, R. C. 2010. *Campylobacter jejuni* FliA binds fibronectin and is required for maximal host cell adherence. *Journal of Bacteriology*, 192, 68-76.
- KOVÁCS, J. K., COX, A., SCHWEITZER, B., MARÓTI, G., KOVÁCS, T., FENYVESI, H., EMÓDY, L. & SCHNEIDER, G. 2020. Virulence Traits of Inpatient *Campylobacter jejuni* Isolates, and a Transcriptomic Approach to Identify Potential Genes Maintaining Intracellular Survival. *Microorganisms*, 8, 531.
- KOWARIK, M., YOUNG, N. M., NUMAO, S., SCHULZ, B. L., HUG, I., CALLEWAERT, N., MILLS, D. C., WATSON, D. C., HERNANDEZ, M., KELLY, J. F., WACKER, M. & AEBI, M. 2006. Definition of the bacterial N-glycosylation site consensus sequence. *The EMBO Journal*, 25, 1957-1966.
- KREUDER, A. J., SCHLEINING, J. A., YAEGER, M., ZHANG, Q. & PLUMMER, P. J. 2017. RNAseq Reveals Complex Response of *Campylobacter jejuni* to Ovine Bile and In vivo Gallbladder Environment. *Frontiers in Microbiology*, 8.
- KRISTOFFERSEN, S. M., RAVNUM, S., TOURASSE, N. J., ØKSTAD, O. A., KOLSTØ, A.-B. & DAVIES, W. 2007. Low Concentrations of Bile Salts Induce Stress Responses and Reduce Motility in *Bacillus cereus* ATCC 14579. *Journal of Bacteriology*, 189, 6741-6741.

- KUEHN, M. J. & KESTY, N. C. 2005. Bacterial outer membrane vesicles and the host-pathogen interaction. *Genes and Development*, 19, 2645-55.
- KULKARNI, H. M., NAGARAJ, R. & JAGANNADHAM, M. V. 2015. Protective role of E. coli outer membrane vesicles against antibiotics. *Microbiology Research*, 181, 1-7.
- KULP, A. & KUEHN, M. J. 2010. Biological functions and biogenesis of secreted bacterial outer membrane vesicles. *Annual Review of Microbiology*, 64, 163-84.
- LANGDON, R. H., CUCCUI, J. & WREN, B. W. 2009. N-linked glycosylation in bacteria: an unexpected application. *Future Microbiology*, 4, 401-412.
- LANGMEAD, B. & SALZBERG, S. L. 2012. Fast gapped-read alignment with Bowtie 2. *Nature Methods*, 9, 357-359.
- LARA-TEJERO, M. & GALAN, J. E. 2001. CdtA, CdtB, and CdtC form a tripartite complex that is required for cytolethal distending toxin activity. *Infection and Immunity* 69, 4358-65.
- LAROCCA, T. J., CROWLEY, J. T., CUSACK, B. J., PATHAK, P., BENACH, J., LONDON, E., GARCIA-MONCO, J. C. & BENACH, J. L. 2010. Cholesterol lipids of *Borrelia burgdorferi* form lipid rafts and are required for the bactericidal activity of a complement-independent antibody. *Cell Host & Microbe*, 8, 331-342.
- LASTOVICA, A. J., ON, S. L. W. & ZHANG, L. 2014. The Family Campylobacteraceae. In: ROSENBERG, E., DELONG, E. F., LORY, S., STACKEBRANDT, E. & THOMPSON, F. (eds.) *The Prokaryotes: Deltaproteobacteria and Epsilonproteobacteria*. Berlin, Heidelberg: Springer Berlin Heidelberg.
- LÊ CAO, K.-A., BOITARD, S. & BESSE, P. 2011. Sparse PLS discriminant analysis: biologically relevant feature selection and graphical displays for multiclass problems. *BMC Bioinformatics*, 12, 253.
- LEE, C.-H. & TSAI, C.-M. 1999. Quantification of Bacterial Lipopolysaccharides by the Purpald Assay: Measuring Formaldehyde Generated from 2-keto-3-deoxyoctonate and Heptose at the Inner Core by Periodate Oxidation. *Analytical Biochemistry*, 267, 161-168.
- LEE, G., PAREDES OLORTEGUI, M., PEÑATARO YORI, P., BLACK, R. E., CAULFIELD, L., BANDA CHAVEZ, C., HALL, E., PAN, W. K., MEZA, R. & KOSEK, M. 2014. Effects of Shigella-, Campylobacter- and ETEC-associated Diarrhea on Childhood Growth. *The Pediatric Infectious Disease Journal*, 33.
- LEE, J., YOON, Y. J., KIM, J. H., DINH, N. T. H., GO, G., TAE, S., PARK, K.-S., PARK, H. T., LEE, C., ROH, T.-Y., DI VIZIO, D. & GHO, Y. S. 2018. Outer Membrane Vesicles Derived From *Escherichia coli* Regulate Neutrophil Migration by Induction of Endothelial IL-8. *Frontiers in Microbiology*, 9.
- LEE, R. B., HASSANE, D. C., COTTLE, D. L. & PICKETT, C. L. 2003. Interactions of *Campylobacter jejuni* cytolethal distending toxin subunits CdtA and CdtC with HeLa cells. *Infection and Immunity* 71, 4883-4890.
- LEON-KEMPIS MDEL, R., GUCCIONE, E., MULHOLLAND, F., WILLIAMSON, M. P. & KELLY, D. J. 2006. The *Campylobacter jejuni* PEB1a adhesin is an aspartate/glutamate-binding protein of an ABC transporter essential for microaerobic growth on dicarboxylic amino acids. *Molecular Microbiology*, 60, 1262-75.
- LEOW, C. Y., KAZI, A., HISYAM ISMAIL, C. M. K., CHUAH, C., LIM, B. H., LEOW, C. H. & BANGA SINGH, K. K. 2020. Reverse vaccinology approach for the identification and characterization of outer membrane proteins of *Shigella flexneri* as potential cellular- and antibody-dependent vaccine candidates. *Clinical and Experimental Vaccine Research*, 9, 15-25.
- LEPORE, B. W., INDIC, M., PHAM, H., HEARN, E. M., PATEL, D. R. & VAN DEN BERG, B. 2011. Ligand-gated diffusion across the bacterial outer membrane. *Proceedings of the National Academy of Sciences of the United States of America*, 108, 10121-10126.
- LERTPIRIYAPONG, K., GAMAZON, E. R., FENG, Y., PARK, D. S., PANG, J., BOTKA, G., GRAFFAM, M. E., GE, Z. & FOX, J. G. 2012. *Campylobacter jejuni* Type VI Secretion System: Roles in Adaptation to Deoxycholic Acid, Host Cell Adherence, Invasion, and In Vivo Colonization. *PLOS ONE*, 7, e42842.

- LETCUMANAN, V., CHAN, K.-G., KHAN, T. M., BUKHARI, S. I., AB MUTALIB, N.-S., GOH, B.-H. & LEE, L.-H. 2017. Bile Sensing: The Activation of *Vibrio parahaemolyticus* Virulence. *Frontiers in Microbiology*, 8.
- LI, C., ZHU, L., WANG, D., WEI, Z., HAO, X., WANG, Z., LI, T., ZHANG, L., LU, Z., LONG, M., WANG, Y., WEI, G. & SHEN, X. 2022. T6SS secretes an LPS-binding effector to recruit OMVs for exploitative competition and horizontal gene transfer. *The ISME Journal*, 16, 500-510.
- LI, H. & DURBIN, R. 2009. Fast and accurate short read alignment with Burrows-Wheeler transform. *Bioinformatics (Oxford, England)*, 25, 1754-1760.
- LI, H., HANDSAKER, B., WYSOKER, A., FENNELL, T., RUAN, J., HOMER, N., MARTH, G., ABECASIS, G., DURBIN, R. & GENOME PROJECT DATA PROCESSING, S. 2009. The Sequence Alignment/Map format and SAMtools. *Bioinformatics (Oxford, England)*, 25, 2078-2079.
- LI, J., HU, F., CHEN, S., LUO, P., HE, Z., WANG, W., ALLAIN, J.-P. & LI, C. 2017. Characterization of novel Omp31 antigenic epitopes of *Brucella melitensis* by monoclonal antibodies. *BMC Microbiology*, 17, 115.
- LIAW, J., HONG, G., DAVIES, C., ELMI, A., SIMA, F., STRATAKOS, A., STEF, L., PET, I., HACHANI, A., CORCIONIVOSCHI, N., WREN, B. W., GUNDOGDU, O. & DORRELL, N. 2019. The *Campylobacter jejuni* Type VI Secretion System Enhances the Oxidative Stress Response and Host Colonization. *Frontiers in Microbiology*, 10.
- LIN, J., MICHEL, L. O. & ZHANG, Q. 2002. CmeABC functions as a multidrug efflux system in *Campylobacter jejuni*. *Antimicrobial agents and chemotherapy*, 46, 2124-2131.
- LIN, J., SAHIN, O., MICHEL, L. O. & ZHANG, Q. 2003. Critical role of multidrug efflux pump CmeABC in bile resistance and in vivo colonization of *Campylobacter jejuni*. *Infection and Immunity* 71, 4250-9.
- LIN, J., CAGLIERO, C., GUO, B., BARTON, Y.-W., MAUREL, M.-C., PAYOT, S. & ZHANG, Q. 2005a. Bile salts modulate expression of the CmeABC multidrug efflux pump in *Campylobacter jejuni*. *Journal of bacteriology*, 187, 7417-7424.
- LIN, J., AKIBA, M., SAHIN, O. & ZHANG, Q. 2005b. CmeR functions as a transcriptional repressor for the multidrug efflux pump CmeABC in *Campylobacter jejuni*. *Antimicrobial Agents and Chemotherapy* 49, 1067-75.
- LINDMARK, B., ROMPIKUNTAL, P. K., VAITKEVICIUS, K., SONG, T., MIZUNOE, Y., UHLIN, B. E., GUERRY, P. & WAI, S. N. 2009. Outer membrane vesicle-mediated release of cytolethal distending toxin (CDT) from *Campylobacter jejuni*. *BMC Microbiology*, 9, 220.
- LIU, L., JOHNSON, H. L., COUSENS, S., PERIN, J., SCOTT, S., LAWN, J. E., RUDAN, I., CAMPBELL, H., CIBULSKIS, R., LI, M., MATHERS, C. & BLACK, R. E. 2012. Global, regional, and national causes of child mortality: an updated systematic analysis for 2010 with time trends since 2000. *The Lancet*, 379, 2151-2161.
- LIU, M. M., BOINETT, C. J., CHAN, A. C. K., PARKHILL, J., MURPHY, M. E. P. & GAYNOR, E. C. 2018. Investigating the *Campylobacter jejuni* Transcriptional Response to Host Intestinal Extracts Reveals the Involvement of a Widely Conserved Iron Uptake System. *MBio*, 9, e01347-18.
- LOCHT, H. & KROGFELT, K. A. 2002. Comparison of rheumatological and gastrointestinal symptoms after infection with *Campylobacter jejuni/coli* and enterotoxigenic *Escherichia coli*. *Annals of the Rheumatic Diseases*, 61, 448-52.
- LOGAN, S. M. & TRUST, T. J. 1982. Outer membrane characteristics of *Campylobacter jejuni*. *Infection and Immunity* 38, 898-906.
- LONG, S. L., GAHAN, C. G. M. & JOYCE, S. A. 2017. Interactions between gut bacteria and bile in health and disease. *Molecular Aspects of Medicine*, 56, 54-65.
- LORENZO-ZÚÑIGA, V., BARTOLÍ, R., PLANAS, R., HOFMANN, A. F., VIÑADO, B., HAGEY, L. R., HERNÁNDEZ, J. M., MAÑÉ, J., ALVAREZ, M. A., AUSINA, V. & GASSULL, M. A. 2003. Oral bile acids reduce bacterial overgrowth, bacterial translocation, and endotoxemia in cirrhotic rats. *Hepatology*, 37, 551-7.

- LOUIS, V. R., GILLESPIE, I. A., O'BRIEN, S. J., RUSSEK-COHEN, E., PEARSON, A. D. & COLWELL, R. R. 2005. Temperature-driven *Campylobacter* seasonality in England and Wales. *Applied and Environmental Microbiology*, 71, 85-92.
- LOVE, M. I., HUBER, W. & ANDERS, S. 2014. Moderated estimation of fold change and dispersion for RNA-seq data with DESeq2. *Genome Biology*, 15, 550.
- LOW, W.-Y. & CHNG, S.-S. 2021. Current mechanistic understanding of intermembrane lipid trafficking important for maintenance of bacterial outer membrane lipid asymmetry. *Current Opinion in Chemical Biology*, 65, 163-171.
- LU, Y.-C., YE, W.-C. & OHASHI, P. S. 2008. LPS/TLR4 signal transduction pathway. *Cytokine*, 42, 145-151.
- LUCCHESI, G. I., LISA, T. A., CASALE, C. H. & DOMENECH, C. E. 1995. Carnitine resembles choline in the induction of cholinesterase, acid phosphatase, and phospholipase C and in its action as an osmoprotectant in *Pseudomonas aeruginosa*. *Current Microbiology*, 30, 55-60.
- LUETHY, P. M., HUYNH, S., RIBARDO, D. A., WINTER, S. E., PARKER, C. T. & HENDRIXSON, D. R. 2017. Microbiota-Derived Short-Chain Fatty Acids Modulate Expression of *Campylobacter jejuni* Determinants Required for Commensalism and Virulence. *MBio*, 8.
- MACHO RENDÓN, J., LANG, B., RAMOS LLORENS, M., GAETANO TARTAGLIA, G. & TORRENT BURGAS, M. 2021. DualSeqDB: the host-pathogen dual RNA sequencing database for infection processes. *Nucleic Acids Research*, 49, D687-D693.
- MAHDAVI, J., PIRINCCIOGLU, N., OLDFIELD, N. J., CARLSOHN, E., STOOF, J., ASLAM, A., SELF, T., CAWTHRAW, S. A., PETROVSKA, L. & COLBORNE, N. 2014. A novel O-linked glycan modulates *Campylobacter jejuni* major outer membrane protein-mediated adhesion to human histo-blood group antigens and chicken colonization. *Open Biology*, 4, 130202.
- MALIK-KALE, P., PARKER, C. T. & KONKEL, M. E. 2008. Culture of *Campylobacter jejuni* with sodium deoxycholate induces virulence gene expression. *Journal of bacteriology*, 190, 2286-2297.
- MALINVERNI, J. C. & SILHAVY, T. J. 2009. An ABC transport system that maintains lipid asymmetry in the gram-negative outer membrane. *Proceedings of the National Academy of Sciences*, 106, 8009-14.
- MAN, L., DALE, A. L., KLARE, W. P., CAIN, J. A., SUMER-BAYRAKTAR, Z., NIEWOLD, P., SOLIS, N. & CORDWELL, S. J. 2020. Proteomics of *Campylobacter jejuni* Growth in Deoxycholate Reveals Cj0025c as a Cystine Transport Protein Required for Wild-type Human Infection Phenotypes. *Molecular & Cellular Proteomics*, 19, 1263-1280.
- MAN, S. M. 2011. The clinical importance of emerging *Campylobacter* species. *Nature Reviews Gastroenterology & Hepatology*, 8, 669-85.
- MANNING, A. J. & KUEHN, M. J. 2011. Contribution of bacterial outer membrane vesicles to innate bacterial defense. *BMC Microbiology*, 11, 258.
- MARI, S. A., KÖSTER, S., BIPPES, C. A., YILDIZ, O., KÜHLBRANDT, W. & MULLER, D. J. 2010. pH-induced conformational change of the beta-barrel-forming protein OmpG reconstituted into native *E. coli* lipids. *Journal of Molecular Biology*, 396, 610-6.
- MARIONI, J. C., MASON, C. E., MANE, S. M., STEPHENS, M. & GILAD, Y. 2008. RNA-seq: an assessment of technical reproducibility and comparison with gene expression arrays. *Genome Research*, 18, 1509-17.
- MARJANOVIC, O., IAVARONE, A. T. & RILEY, L. W. 2011. Sulfolipid accumulation in *Mycobacterium tuberculosis* disrupted in the mce2 operon. *Journal of Microbiology*, 49, 441-7.
- MARKWELL, P. J. & EARLE, K. E. 1995. Taurine: An essential nutrient for the cat. A brief review of the biochemistry of its requirement and the clinical consequences of deficiency. *Nutrition Research*, 15, 53-58.
- MASANTA, W. O., ZAUTNER, A. E., LUGERT, R., BOHNE, W., GROSS, U., LEHA, A., DAKNA, M. & LENZ, C. 2019. Proteome Profiling by Label-Free Mass Spectrometry Reveals Differentiated Response of *Campylobacter jejuni* 81-176 to Sublethal Concentrations of Bile Acids. *PROTEOMICS – Clinical Applications*, 13, 1800083.

- MASHBURN-WARREN, L., HOWE, J., GARIDEL, P., RICHTER, W., STEINIGER, F., ROESSLE, M., BRANDENBURG, K. & WHITELEY, M. 2008. Interaction of quorum signals with outer membrane lipids: insights into prokaryotic membrane vesicle formation. *Molecular Microbiology*, 69, 491-502.
- MASHBURN, L. M. & WHITELEY, M. 2005. Membrane vesicles traffic signals and facilitate group activities in a prokaryote. *Nature*, 437, 422-5.
- MAUE, A. C., MOHAWK, K. L., GILES, D. K., POLY, F., EWING, C. P., JIAO, Y., LEE, G., MA, Z., MONTEIRO, M. A., HILL, C. L., FERDERBER, J. S., PORTER, C. K., TRENT, M. S. & GUERRY, P. 2013. The polysaccharide capsule of *Campylobacter jejuni* modulates the host immune response. *Infection and Immunity* 81, 665-672.
- MAURI, M., SANNASIDDAPPA, T. H., VOHRA, P., CORONA-TORRES, R., SMITH, A. A., CHINTOAN-UTA, C., BREMNER, A., TERRA, V. S., ABOUELHADID, S., STEVENS, M. P., GRANT, A. J., CUCCUI, J., WREN, B. W. & THE GLYCOENGINEERING OF VETERINARY VACCINES, C. 2021. Multivalent poultry vaccine development using Protein Glycan Coupling Technology. *Microbial Cell Factories*, 20, 193.
- MAVRI, A. & SMOLE MOŽINA, S. 2013a. Effects of efflux-pump inducers and genetic variation of the multidrug transporter *cmeB* in biocide resistance of *Campylobacter jejuni* and *Campylobacter coli*. *Journal of Medical Microbiology*, 62, 400-411.
- MAVRI, A. & SMOLE MOŽINA, S. 2013b. Resistance to bile salts and sodium deoxycholate in macrolide- and fluoroquinolone-susceptible and resistant *Campylobacter jejuni* and *Campylobacter coli* strains. *Microbial Drug Resistance*, 19, 168-74.
- MAY, K. L. & SILHAVY, T. J. 2018. The *Escherichia coli* Phospholipase PldA Regulates Outer Membrane Homeostasis via Lipid Signaling. *MBio*, 9, e00379-18.
- MCBROOM, A. J. & KUEHN, M. J. 2007. Release of outer membrane vesicles by Gram-negative bacteria is a novel envelope stress response. *Molecular Microbiology*, 63, 545-58.
- MCMAHON, K. J., CASTELLI, M. E., GARCÍA VESCOVI, E. & FELDMAN, M. F. 2012. Biogenesis of outer membrane vesicles in *Serratia marcescens* is thermoregulated and can be induced by activation of the Rcs phosphorelay system. *Journal of Bacteriology*, 194, 3241-9.
- MCNALLY, D. J., JARRELL, H. C., LI, J., KHIEU, N. H., VINOGRADOV, E., SZYMANSKI, C. M. & BRISSON, J.-R. 2005. The HS:1 serostrain of *Campylobacter jejuni* has a complex teichoic acid-like capsular polysaccharide with nonstoichiometric fructofuranose branches and O-methyl phosphoramidate groups. *The FEBS Journal*, 272, 4407-4422.
- MEADOWS, J. A. & WARGO, M. J. 2015. Carnitine in bacterial physiology and metabolism. *Microbiology (Reading, England)*, 161, 1161-1174.
- MEHDI, H.-F., SHAHIN, N.-P., SEYED DAVAR, S., MOHAMMAD, S. & ASHRAF MOHABATI, M. 2021. Isolation and immunogenicity of extracted outer membrane vesicles from *Pseudomonas aeruginosa* under antibiotics treatment conditions. *Iranian Journal of Microbiology*, 13.
- MEYER, A., STALLMACH, T., GOLDENBERGER, D. & ALTWEGG, M. 1997. Lethal Maternal Sepsis Caused by *Campylobacter jejuni*: Pathogen Preserved in Placenta and Identified by. *Modern Pathology*, 10, 1253-1256.
- MONTE, M. J., MARIN, J. J. G., ANTELO, A. & VAZQUEZ-TATO, J. 2009. Bile acids: chemistry, physiology, and pathophysiology. *World Journal of Gastroenterology*, 15, 804-816.
- MONTEVILLE, M. R., YOON, J. E. & KONKEL, M. E. 2003. Maximal adherence and invasion of INT 407 cells by *Campylobacter jejuni* requires the CadF outer-membrane protein and microfilament reorganization. *Microbiology*, 149, 153-165.
- MORAN, A. P. 1997. Structure and Conserved Characteristics of *Campylobacter jejuni* Lipopolysaccharides. *The Journal of Infectious Diseases*, 176, S115-S121.
- MOREAU, M. R., MASSARI, P. & GENCO, C. A. 2017. The ironclad truth: how in vivo transcriptomics and in vitro mechanistic studies shape our understanding of *Neisseria gonorrhoeae* gene regulation during mucosal infection. *Pathogens and Disease*, 75, ftx057.

- MOSER, I., SCHROEDER, W. & SALNIKOW, J. 1997. Campylobacter jejuni major outer membrane protein and a 59-kDa protein are involved in binding to fibronectin and INT 407 cell membranes. *FEMS Microbiology Letters* 157, 233-8.
- MUKHOPADHYAY, R., HUANG, K. C. & WINGREEN, N. S. 2008. Lipid localization in bacterial cells through curvature-mediated microphase separation. *Biophysical Journal* 95, 1034-49.
- MULCAHY, L. A., PINK, R. C. & CARTER, D. R. F. 2014. Routes and mechanisms of extracellular vesicle uptake. *Journal of Extracellular Vesicles*, 3, 24641.
- MURPHY, K. N. & BRINKWORTH, A. J. 2021. Manipulation of Focal Adhesion Signaling by Pathogenic Microbes. *International Journal of Molecular Sciences*, 22, 1358.
- NACHAMKIN, I., ALLOS, B. M. & HO, T. 1998. Campylobacter Species and Guillain-Barré Syndrome. *Clinical Microbiology Reviews*, 11, 555-567.
- NACHAMKIN, I., YANG, X. H. & STERN, N. J. 1993. Role of Campylobacter jejuni flagella as colonization factors for three-day-old chicks: analysis with flagellar mutants. *Applied and Environmental Microbiology*, 59, 1269-73.
- NAGANA GOWDA, G. A., SHANAIAH, N., COOPER, A., MALUCCIO, M. & RAFTERY, D. 2009. Bile acids conjugation in human bile is not random: new insights from (1)H-NMR spectroscopy at 800 MHz. *Lipids*, 44, 527-35.
- NAKAYAMA, T. & ZHANG-AKIYAMA, Q.-M. 2017. pqiABC and yebST, putative mce operons of Escherichia coli, encode transport pathways and contribute to membrane integrity. *Journal of bacteriology*, 199, e00606-16.
- NARADASU, D., MIRAN, W., SHARMA, S., TAKENAWA, S., SOMA, T., NOMURA, N., TOYOFUKU, M. & OKAMOTO, A. 2021. Biogenesis of Outer Membrane Vesicles Concentrates the Unsaturated Fatty Acid of Phosphatidylinositol in Capnocytophaga ochracea. *Frontiers in Microbiology*, 12.
- NCBI. 2022a. *Compound summary Sodium deoxycholate* [Online]. Available: <https://pubchem.ncbi.nlm.nih.gov/compound/Sodium-deoxycholate> [Accessed 04.01.2022].
- NCBI. 2022b. *PubChem Compound Summary for CID 84703* [Online]. Available: [https://pubchem.ncbi.nlm.nih.gov/compound/3-\\_dodecyl\\_dimethyl\\_azaniumyl\\_propane-1-sulfonate](https://pubchem.ncbi.nlm.nih.gov/compound/3-_dodecyl_dimethyl_azaniumyl_propane-1-sulfonate). [Accessed 04.01.2022 2022].
- NCBI. 2022c. *PubChem Compound Summary for CID 107670, Chaps* [Online]. Available: <https://pubchem.ncbi.nlm.nih.gov/compound/Chaps>. [Accessed 04.01.2022 2022].
- NCBI. 2022d. *PubChem Compound Summary for CID 3423265, Sodium dodecyl sulfate*. [Online]. Available: <https://pubchem.ncbi.nlm.nih.gov/compound/Sodium-dodecyl-sulfate> [Accessed 04.01.2022 2022].
- NCBI. 2022e. *PubChem Compound Summary for CID 23666345, Sodium taurocholate* [Online]. Available: <https://pubchem.ncbi.nlm.nih.gov/compound/Sodium-taurocholate> [Accessed 04.01.2022 2022].
- NEGRETTI, N. M., GOURLEY, C. R., CLAIR, G., ADKINS, J. N. & KONKEL, M. E. 2017. The food-borne pathogen Campylobacter jejuni responds to the bile salt deoxycholate with countermeasures to reactive oxygen species. *Scientific Reports*, 7, 15455.
- NEVERMANN, J., SILVA, A., OTERO, C., OYARZÚN, D. P., BARRERA, B., GIL, F., CALDERÓN, I. L. & FUENTES, J. A. 2019. Identification of Genes Involved in Biogenesis of Outer Membrane Vesicles (OMVs) in Salmonella enterica Serovar Typhi. *Frontiers in Microbiology*, 10.
- NGERNSOMBAT, C., SREESAI, S., HARNVORAVONGCHAI, P., CHANKHAMHAENGDECHA, S. & JANVILISRI, T. 2017. CD2068 potentially mediates multidrug efflux in Clostridium difficile. *Scientific Reports*, 7, 9982.
- NGUYEN, T. T., SAXENA, A. & BEVERIDGE, T. J. 2003. Effect of surface lipopolysaccharide on the nature of membrane vesicles liberated from the Gram-negative bacterium Pseudomonas aeruginosa. *Journal of Electron Microscopy*, 52, 465-469.
- NIELSEN, H., HANSEN, K. K., GRADEL, K. O., KRISTENSEN, B., EJLERTSEN, T., ØSTERGAARD, C. & SCHØNHEYDER, H. C. 2010. Bacteraemia as a result of Campylobacter species: a population-

- based study of epidemiology and clinical risk factors. *Clinical Microbiology and Infection*, 16, 57-61.
- NIKAIDO, H. 2003. Molecular basis of bacterial outer membrane permeability revisited. *Microbiology and Molecular Biology Reviews*, 67, 593-656.
- NORTHFIELD, T. C. & MCCOLL, I. 1973. Postprandial concentrations of free and conjugated bile acids down the length of the normal human small intestine. *Gut*, 14, 513-518.
- NOVIK, V., HOFREUTER, D. & GALÁN, J. E. 2010. Identification of *Campylobacter jejuni* genes involved in its interaction with epithelial cells. *Infection and Immunity* 78, 3540-3553.
- NUIJTEN, P. J., VAN ASTEN, F. J., GAASTRA, W. & VAN DER ZEIJST, B. A. 1990. Structural and functional analysis of two *Campylobacter jejuni* flagellin genes. *Journal of Biological Chemistry*, 265, 17798-804.
- O'DONOGHUE, E. J., SIRISAENGTAKSIN, N., BROWNING, D. F., BIELSKA, E., HADIS, M., FERNANDEZ-TRILLO, F., ALDERWICK, L., JABBARI, S. & KRACHLER, A. M. 2017. Lipopolysaccharide structure impacts the entry kinetics of bacterial outer membrane vesicles into host cells. *PLOS Pathogens*, 13, e1006760.
- OKSANEN, J., KINDT, K., LEGENDRE, P., O'HARA, B., M HENRY H STEVENS, MAINTAINER JARI OKSANEN & SUGGESTS, M. 2007. The vegan package. *Community Ecology Package*, 10, 631-637.
- OLIVER, D. B. & BECKWITH, J. 1982. Identification of a new gene (*secA*) and gene product involved in the secretion of envelope proteins in *Escherichia coli*. *Journal of Bacteriology*, 150, 686-691.
- OLIVER, J. D. 2010. Recent findings on the viable but nonculturable state in pathogenic bacteria. *FEMS Microbiology Reviews*, 34, 415-425.
- PACANOWSKI, J., LALANDE, V., LACOMBE, K., BOUDRAA, C., LESPRIT, P., LEGRAND, P., TRYSTRAM, D., KASSIS, N., ARLET, G., MAINARDI, J.-L., DOUCET-POPULAIRE, F., GIRARD, P.-M. & MEYNARD, J.-L. 2008. *Campylobacter* Bacteremia: Clinical Features and Factors Associated with Fatal Outcome. *Clinical Infectious Diseases*, 47, 790-796.
- PALYADA, K., THREADGILL, D. & STINTZI, A. 2004. Iron acquisition and regulation in *Campylobacter jejuni*. *Journal of Bacteriology*, 186, 4714-29.
- PARKHILL, J., WREN, B. W., MUNGALL, K., KETLEY, J. M., CHURCHER, C., BASHAM, D., CHILLINGWORTH, T., DAVIES, R. M., FELTWELL, T., HOLROYD, S., JAGELS, K., KARLYSHEV, A. V., MOULE, S., PALLAN, M. J., PENN, C. W., QUAIL, M. A., RAJANDREAM, M. A., RUTHERFORD, K. M., VAN VLIET, A. H. M., WHITEHEAD, S. & BARRELL, B. G. 2000. The genome sequence of the food-borne pathogen *Campylobacter jejuni* reveals hypervariable sequences. *Nature*, 403, 665.
- PARTE, A. C. 2018. *LPSN — List of Prokaryotic names with Standing in Nomenclature (bacterio.net), 20 years on* [Online]. International Journal of Systematic and Evolutionary Microbiology. Available: <https://www.bacterio.net/genus/campylobacter> [Accessed 01/05/2020].
- PEAD, P. J. 1979. Electron microscopy of *Campylobacter jejuni*. *Journal of Medical Microbiology*, 12, 383-5.
- PEI, Z., BURUCOA, C., GRIGNON, B., BAQAR, S., HUANG, X.-Z., KOPECKO, D. J., BOURGEOIS, A., FAUCHERE, J.-L. & BLASER, M. J. 1998. Mutation in the *peb1A* locus of *Campylobacter jejuni* reduces interactions with epithelial cells and intestinal colonization of mice. *Infection and Immunity* 66, 938-943.
- PEREZ-RATHKE, A., FAHIE, M. A., CHISHOLM, C., LIANG, J. & CHEN, M. 2018. Mechanism of OmpG pH-Dependent Gating from Loop Ensemble and Single Channel Studies. *Journal of the American Chemical Society*, 140, 1105-1115.
- PEREZ DE LA CRUZ MORENO, M., OTH, M., DEFERME, S., LAMMERT, F., TACK, J., DRESSMAN, J. & AUGUSTIJNS, P. 2006. Characterization of fasted-state human intestinal fluids collected from duodenum and jejunum. *Journal of Pharmacy and Pharmacology*, 58, 1079-89.

- PEREZ VIDA KOVICS, M. L. A., JENDHOLM, J., MÖRGELIN, M., MÅNSSON, A., LARSSON, C., CARDELL, L.-O. & RIESBECK, K. 2010. B Cell Activation by Outer Membrane Vesicles—A Novel Virulence Mechanism. *PLOS Pathogens*, 6, e1000724.
- PHAM, B., CHISHOLM, C. M., FOSTER, J., FRIIS, E., FAHIE, M. A. & CHEN, M. 2021. A pH-independent quiet OmpG pore with enhanced electrostatic repulsion among the extracellular loops. *Biochimica et Biophysica Acta (BBA) - Biomembranes*, 1863, 183485.
- PICKETT, C. L., PESCI, E. C., COTTLE, D. L., RUSSELL, G., ERDEM, A. N. & ZEY TIN, H. 1996. Prevalence of cytolethal distending toxin production in *Campylobacter jejuni* and relatedness of *Campylobacter* sp. cdtB gene. *Infection and Immunity*, 64, 2070-2078.
- POLY, F., EWING, C., GOON, S., HICKEY, T. E., ROCKABRAND, D., MAJAM, G., LEE, L., PHAN, J., SAVARINO, N. J. & GUERRY, P. 2007. Heterogeneity of a *Campylobacter jejuni* protein that is secreted through the flagellar filament. *Infection and Immunity* 75, 3859-3867.
- POPE, L. M., REED, K. E. & PAYNE, S. M. 1995. Increased protein secretion and adherence to HeLa cells by *Shigella* spp. following growth in the presence of bile salts. *Infection and Immunity* 63, 3642-3648.
- POWERS, M. J., SIMPSON, B. W. & TRENT, M. S. 2020. The Mla pathway in *Acinetobacter baumannii* has no demonstrable role in anterograde lipid transport. *ELife*, 9, e56571.
- POWERS, M. J. & TRENT, M. S. 2019. Intermembrane transport: Glycerophospholipid homeostasis of the Gram-negative cell envelope. *Proceedings of the National Academy of Sciences*, 116, 17147-17155.
- PRIETO, A. I., RAMOS-MORALES, F. & CASADESÚS, J. 2004. Bile-induced DNA damage in *Salmonella enterica*. *Genetics*, 168, 1787-1794.
- PUMBWE, L. & PIDDOCK, L. J. V. 2002. Identification and molecular characterisation of CmeB, a *Campylobacter jejuni* multidrug efflux pump. *FEMS Microbiology Letters*, 206, 185-189.
- QUINLAN, A. R. & HALL, I. M. 2010. BEDTools: a flexible suite of utilities for comparing genomic features. *Bioinformatics (Oxford, England)*, 26, 841-842.
- RANGARAJAN, E. S., BHATIA, S., WATSON, D. C., MUNGER, C., CYGLER, M., MATTE, A. & YOUNG, N. M. 2007. Structural context for protein N-glycosylation in bacteria: The structure of PEB3, an adhesin from *Campylobacter jejuni*. *Protein Science*, 16, 990-995.
- RAPHAEL, B. H., PEREIRA, S., FLOM, G. A., ZHANG, Q., KETLEY, J. M. & KONKEL, M. E. 2005. The *Campylobacter jejuni* response regulator, CbrR, modulates sodium deoxycholate resistance and chicken colonization. *Journal of Bacteriology*, 187, 3662-70.
- RATHBUN, K. M., HALL, J. E. & THOMPSON, S. A. 2009. Cj0596 is a periplasmic peptidyl prolyl cis-trans isomerase involved in *Campylobacter jejuni* motility, invasion, and colonization. *BMC Microbiology*, 9, 160.
- REBEIL, R., ERNST, R. K., JARRETT, C. O., ADAMS, K. N., MILLER, S. I. & HINNEBUSCH, B. J. 2006. Characterization of late acyltransferase genes of *Yersinia pestis* and their role in temperature-dependent lipid A variation. *Journal of Bacteriology*, 188, 1381-8.
- RIDLON, J. M., KANG, D.-J. & HYLEMON, P. B. 2006. Bile salt biotransformations by human intestinal bacteria. *Journal of lipid research*, 47, 241-259.
- RIDLON, J. M., KANG, D. J., HYLEMON, P. B. & BAJAJ, J. S. 2015. Gut microbiota, cirrhosis, and alcohol regulate bile acid metabolism in the gut. *Digestive Diseases and Sciences*, 33, 338-45.
- RIDLON, J. M., WOLF, P. G. & GASKINS, H. R. 2016. Taurocholic acid metabolism by gut microbes and colon cancer. *Gut Microbes*, 7, 201-215.
- RITZ, M., GARENAUX, A., BERGE, M. & FEDERIGHI, M. 2009. Determination of rpoA as the most suitable internal control to study stress response in *C. jejuni* by RT-qPCR and application to oxidative stress. *Journal of Microbiological Methods*, 76, 196-200.
- RIVAS, Z. P., TALBOT, K. M., MERSELIS, L. C., MCCORMACK, R. M., ADKINS, B. & MUNSON, G. P. 2020. CexE Is a Coat Protein and Virulence Factor of Diarrheagenic Pathogens. *Frontiers in Microbiology*, 11, 1374-1374.

- RIVERA-AMILL, V., KIM, B. J., SESHU, J. & KONKEL, M. E. 2001. Secretion of the Virulence-Associated Campylobacter Invasion Antigens from Campylobacter jejuni Requires a Stimulatory Signal. *The Journal of Infectious Diseases*, 183, 1607-1616.
- ROBINSON, D. 1981. Infective dose of Campylobacter jejuni in milk. *British Medical Journal (Clinical research ed.)*, 282, 1584.
- ROHART, F., GAUTIER, B., SINGH, A. & LÊ CAO, K.-A. 2017. mixOmics: An R package for 'omics feature selection and multiple data integration. *PLOS Computational Biology*, 13, e1005752.
- ROIER, S., ZINGL, F. G., CAKAR, F., DURAKOVIC, S., KOHL, P., EICHMANN, T. O., KLUG, L., GADERMAIER, B., WEINZERL, K., PRASSL, R., LASS, A., DAUM, G., REIDL, J., FELDMAN, M. F. & SCHILD, S. 2016. A novel mechanism for the biogenesis of outer membrane vesicles in Gram-negative bacteria. *Nature Communications*, 7, 10515.
- ROLHION, N., BARNICH, N., BRINGER, M.-A., GLASSER, A.-L., RANC, J., HÉBUTERNE, X., HOFMAN, P. & DARFEUILLE-MICHAUD, A. 2010. Abnormally expressed ER stress response chaperone Gp96 in CD favours adherent-invasive Escherichia coli invasion. *Gut*, 59, 1355-1362.
- ROLLAUER, S. E., SOORESHJANI, M. A., NOINAJ, N. & BUCHANAN, S. K. 2015. Outer membrane protein biogenesis in Gram-negative bacteria. *Philosophical Transactions of the Royal Society B: Biological Sciences*, 370, 20150023.
- ROLLINS, D. M. & COLWELL, R. R. 1986. Viable but nonculturable stage of Campylobacter jejuni and its role in survival in the natural aquatic environment. *Applied and Environmental Microbiology*, 52, 531-8.
- ROUMIA, A. F., TSIRIGOS, K. D., THEODOROPOULOU, M. C., TAMPOSIS, I. A., HAMODRAKAS, S. J. & BAGOS, P. G. 2021. OMPdb: A Global Hub of Beta-Barrel Outer Membrane Proteins. *Frontiers in Bioinformatics*, 1.
- RUBINCHIK, S., SEDDON, A. & KARLYSHEV, A. V. 2012. Molecular mechanisms and biological role of Campylobacter jejuni attachment to host cells. *European journal of microbiology & immunology*, 2, 32-40.
- RUBINCHIK, S., SEDDON, A. M. & KARLYSHEV, A. V. 2014. A negative effect of Campylobacter capsule on bacterial interaction with an analogue of a host cell receptor. *BMC Microbiology*, 14, 141.
- RUSHTON, S. P., SANDERSON, R. A., DIGGLE, P. J., SHIRLEY, M. D. F., BLAIN, A. P., LAKE, I., MAAS, J. A., REID, W. D. K., HARDSTAFF, J., WILLIAMS, N., JONES, N. R., RIGBY, D., STRACHAN, N. J. C., FORBES, K. J., HUNTER, P. R., HUMPHREY, T. J. & O'BRIEN, S. J. 2019. Climate, human behaviour or environment: individual-based modelling of Campylobacter seasonality and strategies to reduce disease burden. *Journal of Translational Medicine*, 17, 34.
- RUSSELL, D. W. 2003. The enzymes, regulation, and genetics of bile acid synthesis. *Annual Review of Biochemistry*, 72, 137-74.
- SACHER, J. C., JAVED, M. A., CRIPPEN, C. S., BUTCHER, J., FLINT, A., STINTZI, A. & SZYMANSKI, C. M. 2021. Reduced Infection Efficiency of Phage NCTC 12673 on Non-Motile Campylobacter jejuni Strains Is Related to Oxidative Stress. *Viruses*, 13, 1955.
- SAHA, C., MOHANRAJU, P., STUBBS, A., DUGAR, G., HOOGSTRATE, Y., KREMERS, G. J., VAN CAPPELLEN, W. A., HORST-KREFT, D., LAFFEBER, C., LEBBINK, J. H. G., BRUENS, S., GASKIN, D., BEERENS, D., KLUNDER, M., JOOSTEN, R., DEMMERS, J. A. A., VAN GENT, D., MOUTON, J. W., VAN DER SPEK, P. J., VAN DER OOST, J., VAN BAARLEN, P. & LOUWEN, R. 2020. Guide-free Cas9 from pathogenic Campylobacter jejuni bacteria causes severe damage to DNA. *Science Advances*, 6, eaaz4849.
- SAIER, M. H., JR., TRAN, C. V. & BARABOTE, R. D. 2006. TCDB: the Transporter Classification Database for membrane transport protein analyses and information. *Nucleic Acids Research*, 34, D181-6.
- SAIER, M. H., REDDY, V. S., MORENO-HAGELSIEB, G., HENDARGO, K. J., ZHANG, Y., IDDAMSETTY, V., LAM, K. J. K., TIAN, N., RUSSUM, S., WANG, J. & MEDRANO-SOTO, A. 2021. The Transporter Classification Database (TCDB): 2021 update. *Nucleic Acids Research*, 49, D461-d467.

- SAŁAMASZYŃSKA-GUZ, A. & KLIMUSZKO, D. 2008. Functional Analysis of the *Campylobacter jejuni* cj0183 and cj0588 Genes. *Current Microbiology*, 56, 592-596.
- SAŁAMASZYŃSKA-GUZ, A., SERAFIŃSKA, I., BAĆCAL, P. & DOUTHWAITE, S. 2020. Virulence properties of *Campylobacter jejuni* are enhanced by displaying a mycobacterial TlyA methylation pattern in its rRNA. *Cellular Microbiology*, 22, e13199-e13199.
- SALVADOR LÓPEZ, J. M. & VAN BOGAERT, I. N. A. 2021. Microbial fatty acid transport proteins and their biotechnological potential. *Biotechnology and Bioengineering*, 118, 2184-2201.
- SASAKI, K., SASAKI, D., OKAI, N., TANAKA, K., NOMOTO, R., FUKUDA, I., YOSHIDA, K.-I., KONDO, A. & OSAWA, R. 2017. Taurine does not affect the composition, diversity, or metabolism of human colonic microbiota simulated in a single-batch fermentation system. *PLOS ONE*, 12, e0180991.
- SAVAGE, P. B. 2001. Multidrug-resistant bacteria: overcoming antibiotic permeability barriers of gram-negative bacteria. *Annals of Medicine*, 33, 167-71.
- SCANLAN, E., ARDILL, L., WHELAN, M. V. X., SHORTT, C., NALLY, J. E., BOURKE, B. & Ó CRÓINÍN, T. 2017b. Relaxation of DNA supercoiling leads to increased invasion of epithelial cells and protein secretion by *Campylobacter jejuni*. *Molecular Microbiology*, 104, 92-104.
- SCANLAN, E., YU, L., MASKELL, D., CHOUDHARY, J. & GRANT, A. 2017a. A quantitative proteomic screen of the *Campylobacter jejuni* flagellar-dependent secretome. *Journal of Proteomics*, 152, 181-187.
- SCHMIDT, A.-M., ESCHER, U., MOUSAVI, S., TEGTMEYER, N., BOEHM, M., BACKERT, S., BERESWILL, S. & HEIMESAAT, M. M. 2019. Immunopathological properties of the *Campylobacter jejuni* flagellins and the adhesin CadF as assessed in a clinical murine infection model. *Gut Pathogens*, 11, 24.
- SCHMIDT, G. & ZINK, R. 2000. Basic features of the stress response in three species of bifidobacteria: *B. longum*, *B. adolescentis*, and *B. breve*. *International Journal of Food Microbiology*, 55, 41-45.
- SCHMITTGEN, T. D. & LIVAK, K. J. 2008. Analyzing real-time PCR data by the comparative CT method. *Nature Protocols*, 3, 1101-1108.
- SCHONBERG-NORIO, D., MATTILA, L., LAUHIO, A., KATILA, M. L., KAUKORANTA, S. S., KOSKELA, M., PAJARRE, S., UKSILA, J., EEROLA, E., SARNA, S. & RAUTELIN, H. 2010. Patient-reported complications associated with *Campylobacter jejuni* infection. *Epidemiology and Infection*, 138, 1004-11.
- SCHOOLING, S. R. & BEVERIDGE, T. J. 2006. Membrane vesicles: an overlooked component of the matrices of biofilms. *Journal of Bacteriology*, 188, 5945-57.
- SCHROEDER, A., MUELLER, O., STOCKER, S., SALOWSKY, R., LEIBER, M., GASSMANN, M., LIGHTFOOT, S., MENZEL, W., GRANZOW, M. & RAGG, T. 2006. The RIN: an RNA integrity number for assigning integrity values to RNA measurements. *BMC Molecular Biology*, 7, 3.
- SCHURCH, N. J., SCHOFIELD, P., GIERLIŃSKI, M., COLE, C., SHERSTNEV, A., SINGH, V., WROBEL, N., GHARBI, K., SIMPSON, G. G., OWEN-HUGHES, T., BLAXTER, M. & BARTON, G. J. 2016. How many biological replicates are needed in an RNA-seq experiment and which differential expression tool should you use? *RNA (New York, N.Y.)*, 22, 839-851.
- SCHWECHHEIMER, C. & KUEHN, M. J. 2015. Outer-membrane vesicles from Gram-negative bacteria: biogenesis and functions. *Nature Reviews Microbiology*, 13, 605-19.
- SCOTT, N. E., BOGEMA, D. R., CONNOLLY, A. M., FALCONER, L., DJORDJEVIC, S. P. & CORDWELL, S. J. 2009. Mass Spectrometric Characterization of the Surface-Associated 42 kDa Lipoprotein JlpA as a Glycosylated Antigen in Strains of *Campylobacter jejuni*. *Journal of Proteome Research*, 8, 4654-4664.
- SCOTT, N. E., PARKER, B. L., CONNOLLY, A. M., PAULECH, J., EDWARDS, A. V., CROSSETT, B., FALCONER, L., KOLARICH, D., DJORDJEVIC, S. P., HØJRUP, P., PACKER, N. H., LARSEN, M. R. & CORDWELL, S. J. 2011. Simultaneous glycan-peptide characterization using hydrophilic interaction chromatography and parallel fragmentation by CID, higher energy collisional

- dissociation, and electron transfer dissociation MS applied to the N-linked glycoproteome of *Campylobacter jejuni*. *Molecular & Cellular Proteomics*, 10, M000031-mcp201.
- SEBALD, M. & VERON, M. 1963. [BASE DNA CONTENT AND CLASSIFICATION OF VIBRIOS]. *Ann Inst Pasteur (Paris)*, 105, 897-910.
- SEEMANN, T. 2014. Prokka: rapid prokaryotic genome annotation. *Bioinformatics*, 30, 2068-2069.
- SENIOR, N. J., BAGNALL, M. C., CHAMPION, O. L., REYNOLDS, S. E., LA RAGIONE, R. M., WOODWARD, M. J., SALGUERO, F. J. & TITBALL, R. W. 2011. *Galleria mellonella* as an infection model for *Campylobacter jejuni* virulence. *Journal of Medical Microbiology*, 60, 661-669.
- SHOAF-SWEENEY, K. D., LARSON, C. L., TANG, X. & KONKEL, M. E. 2008. Identification of *Campylobacter jejuni* proteins recognized by maternal antibodies of chickens. *Applied and Environmental Microbiology*, 74, 6867-6875.
- SHRIVASTAVA, R. & CHNG, S.-S. 2019. Lipid trafficking across the Gram-negative cell envelope. *The Journal of Biological Chemistry*, 294, 14175-14184.
- SILVA, J., LEITE, D., FERNANDES, M., MENA, C., GIBBS, P. A. & TEIXEIRA, P. 2011. *Campylobacter* spp. as a Foodborne Pathogen: A Review. *Frontiers in Microbiology*, 2, 200.
- SISTRUNK, J. R., NICKERSON, K. P., CHANIN, R. B., RASKO, D. A. & FAHERTY, C. S. 2016. Survival of the Fittest: How Bacterial Pathogens Utilize Bile To Enhance Infection. *Clinical Microbiology Reviews*, 29, 819-836.
- SJÖVALL, J. 1959. Dietary Glycine and Taurine on Bile Acid Conjugation in Man. Bile Acids and Steroids 75. *Proceedings of the Society for Experimental Biology and Medicine*, 100, 676-678.
- SKIRROW, M. B. 2003. CAMPYLOBACTER | *Campylobacteriosis*. In: CABALLERO, B. (ed.) *Encyclopedia of Food Sciences and Nutrition (Second Edition)*. Oxford: Academic Press.
- SONG, T., MIKA, F., LINDMARK, B., LIU, Z., SCHILD, S., BISHOP, A., ZHU, J., CAMILLI, A., JOHANSSON, J., VOGEL, J. & WAI, S. N. 2008. A new *Vibrio cholerae* sRNA modulates colonization and affects release of outer membrane vesicles. *Molecular Microbiology*, 70, 100-111.
- SORG, J. A. & SONENSHEIN, A. L. 2008. Bile salts and glycine as cogerminants for *Clostridium difficile* spores. *Journal of Bacteriology*, 190, 2505-12.
- STACY, A., ANDRADE-OLIVEIRA, V., MCCULLOCH, J. A., HILD, B., OH, J. H., PEREZ-CHAPARRO, P. J., SIM, C. K., LIM, A. I., LINK, V. M., ENAMORADO, M., TRINCHIERI, G., SEGRE, J. A., REHERMANN, B. & BELKAID, Y. 2021. Infection trains the host for microbiota-enhanced resistance to pathogens. *Cell*, 184, 615-627.e17.
- STINTZI, A. 2003. Gene expression profile of *Campylobacter jejuni* in response to growth temperature variation. *Journal of Bacteriology*, 185, 2009-2016.
- STINTZI, A., VAN VLIET, A. H. M. & KETLEY, J. M. 2008. Iron Metabolism, Transport, and Regulation. *Campylobacter*.
- STOLAREK, P., BERNAT, P., SZCZERBIEC, D. & RÓŻALSKI, A. 2021. Phospholipids and Fatty Acids Affect the Colonization of Urological Catheters by *Proteus mirabilis*. *International Journal of Molecular Sciences* 22.
- SU, C.-C., SHI, F., GU, R., LI, M., MCDERMOTT, G., YU, E. W. & ZHANG, Q. 2007. Preliminary structural studies of the transcriptional regulator CmeR from *Campylobacter jejuni*. *Acta crystallographica. Section F, Structural biology and crystallization communications*, 63, 34-36.
- SU, C.-C., RADHAKRISHNAN, A., KUMAR, N., LONG, F., BOLLA, J. R., LEI, H.-T., DELMAR, J. A., DO, S. V., CHOU, T.-H., RAJASHANKAR, K. R., ZHANG, Q. & YU, E. W. 2014. Crystal structure of the *Campylobacter jejuni* CmeC outer membrane channel. *Protein Science*, 23, 954-961.
- SU, C.-C., YIN, L., KUMAR, N., DAI, L., RADHAKRISHNAN, A., BOLLA, J. R., LEI, H.-T., CHOU, T.-H., DELMAR, J. A., RAJASHANKAR, K. R., ZHANG, Q., SHIN, Y.-K. & YU, E. W. 2017. Structures and transport dynamics of a *Campylobacter jejuni* multidrug efflux pump. *Nature Communications*, 8, 171.

- SULAEMAN, S., HERNOULD, M., SCHAUMANN, A., COQUET, L., BOLLA, J.-M., DÉ, E. & TRESSE, O. 2012. Enhanced Adhesion of *Campylobacter jejuni* to Abiotic Surfaces Is Mediated by Membrane Proteins in Oxygen-Enriched Conditions. *PLOS ONE*, 7, e46402.
- SUNG, J. Y., SHAFFER, E. A. & COSTERTON, J. W. 1993. Antibacterial activity of bile salts against common biliary pathogens. *Digestive Diseases and Sciences*, 38, 2104-2112.
- SUZUKI, T., MURAI, T., FUKUDA, I., TOBE, T., YOSHIKAWA, M. & SASAKAWA, C. 1994. Identification and characterization of a chromosomal virulence gene, *vacJ*, required for intercellular spreading of *Shigella flexneri*. *Molecular Microbiology*, 11, 31-41.
- SVENSSON, S. L., DAVIS, L. M., MACKICHAN, J. K., ALLAN, B. J., PAJANIAPPAN, M., THOMPSON, S. A. & GAYNOR, E. C. 2009. The CprS sensor kinase of the zoonotic pathogen *Campylobacter jejuni* influences biofilm formation and is required for optimal chick colonization. *Molecular Microbiology*, 71, 253-272.
- SVENSSON, S. L., PRYJMA, M. & GAYNOR, E. C. 2014. Flagella-Mediated Adhesion and Extracellular DNA Release Contribute to Biofilm Formation and Stress Tolerance of *Campylobacter jejuni*. *PLOS ONE*, 9, e106063.
- SZYMANSKI, C. M., YAO, R., EWING, C. P., TRUST, T. J. & GUERRY, P. 1999. Evidence for a system of general protein glycosylation in *Campylobacter jejuni*. *Molecular Microbiology*, 32, 1022-1030.
- SZYMANSKI, C. M., BURR, D. H. & GUERRY, P. 2002. *Campylobacter* protein glycosylation affects host cell interactions. *Infection and Immunity* 70, 2242-2244.
- TAHERI, N., MAHMUD, A. K. M. F., SANDBLAD, L., FÄLLMAN, M., WAI, S. N. & FAHLGREN, A. 2018. *Campylobacter jejuni* bile exposure influences outer membrane vesicles protein content and bacterial interaction with epithelial cells. *Scientific Reports*, 8, 16996.
- TAHERI, N., FÄLLMAN, M., WAI, S. N. & FAHLGREN, A. 2019. Accumulation of virulence-associated proteins in *Campylobacter jejuni* Outer Membrane Vesicles at human body temperature. *Journal of Proteomics*, 195, 33-40.
- TANG, L., BAI, L., WANG, W.-H. & JIANG, T. 2010. Crystal structure of the carnitine transporter and insights into the antiport mechanism. *Nature Structural & Molecular Biology*, 17, 492-496.
- TANG, X., CHANG, S., QIAO, W., LUO, Q., CHEN, Y., JIA, Z., COLEMAN, J., ZHANG, K., WANG, T., ZHANG, Z., ZHANG, C., ZHU, X., WEI, X., DONG, C., ZHANG, X. & DONG, H. 2021. Structural insights into outer membrane asymmetry maintenance in Gram-negative bacteria by MlaFEDB. *Nature Structural & Molecular Biology*, 28, 81-91.
- TAVEIRNE, M. E., THERIOT, C. M., LIVNY, J. & DIRITA, V. J. 2013. The Complete *Campylobacter jejuni* Transcriptome during Colonization of a Natural Host Determined by RNAseq. *PLOS ONE*, 8, e73586.
- TAYLOR, A. J., ZAKAI, S. A. & KELLY, D. J. 2017. The Periplasmic Chaperone Network of *Campylobacter jejuni*: Evidence that SalC (Cj1289) and PpiD (Cj0694) Are Involved in Maintaining Outer Membrane Integrity. *Frontiers in Microbiology*, 8, 531.
- TERRA, V. S., MAURI, M., SANNASIDDAPPA, T. H., SMITH, A. A., STEVENS, M. P., GRANT, A. J., WREN, B. W., CUCCUI, J. & THE GLYCOENGINEERING OF VETERINARY VACCINES, C. 2022. PglB function and glycosylation efficiency is temperature dependent when the *pgl* locus is integrated in the *Escherichia coli* chromosome. *Microbial Cell Factories*, 21, 6.
- TERRA, V. S., MILLS, D. C., YATES, L. E., ABOUEHADID, S., CUCCUI, J. & WREN, B. W. 2012. Recent developments in bacterial protein glycan coupling technology and glycoconjugate vaccine design. *Journal of Medical Microbiology*, 61, 919-926.
- THAY, B., DAMM, A., KUFER, T. A., WAI, S. N. & OSCARSSON, J. 2014. *Aggregatibacter actinomycetemcomitans* outer membrane vesicles are internalized in human host cells and trigger NOD1- and NOD2-dependent NF- $\kappa$ B activation. *Infection and Immunity* 82, 4034-4046.

- THIBAUT, P., LOGAN, S. M., KELLY, J. F., BRISSON, J. R., EWING, C. P., TRUST, T. J. & GUERRY, P. 2001. Identification of the carbohydrate moieties and glycosylation motifs in *Campylobacter jejuni* flagellin. *Journal of Biological Chemistry*, 276, 34862-70.
- THORNLEY, J. P., JENKINS, D., NEAL, K., WRIGHT, T., BROUGH, J. & SPILLER, R. C. 2001. Relationship of *Campylobacter* Toxigenicity In Vitro to the Development of Postinfectious Irritable Bowel Syndrome. *The Journal of Infectious Diseases*, 184, 606-609.
- TIAN, W., LIN, M., TANG, K., LIANG, J. & NAVEED, H. 2018. High-resolution structure prediction of  $\beta$ -barrel membrane proteins. *Proceedings of the National Academy of Sciences*, 115, 1511-1516.
- TOYOFUKU, M., NOMURA, N. & EBERL, L. 2019. Types and origins of bacterial membrane vesicles. *Nature Reviews Microbiology*, 17, 13-24.
- TRAPNELL, C., WILLIAMS, B. A., PERTEA, G., MORTAZAVI, A., KWAN, G., VAN BAREN, M. J., SALZBERG, S. L., WOLD, B. J. & PACTER, L. 2010. Transcript assembly and quantification by RNA-Seq reveals unannotated transcripts and isoform switching during cell differentiation. *Nature Biotechnology*, 28, 511-515.
- TRUCCOLLO, B., WHYTE, P., BURGESS, C. & BOLTON, D. 2021. Genetic characterisation of a subset of *Campylobacter jejuni* isolates from clinical and poultry sources in Ireland. *PLOS ONE*, 16, e0246843.
- TSATSARONIS, J. A., FRANCH-ARROYO, S., RESCH, U. & CHARPENTIER, E. 2018. Extracellular Vesicle RNA: A Universal Mediator of Microbial Communication? *Trends Microbiology*, 26, 401-410.
- TSIRIGOS, K. D., ELOFSSON, A. & BAGOS, P. G. 2016. PRED-TMBB2: improved topology prediction and detection of beta-barrel outer membrane proteins. *Bioinformatics*, 32, i665-i671.
- UGARTE-RUIZ, M., STABLER, R. A., DOMINGUEZ, L., PORRERO, M. C., WREN, B. W., DORRELL, N. & GUNDOGDU, O. 2015. Prevalence of Type VI Secretion System in Spanish *Campylobacter jejuni* Isolates. *Zoonoses Public Health*, 62, 497-500.
- URDANETA, V. & CASADESÚS, J. 2017. Interactions between Bacteria and Bile Salts in the Gastrointestinal and Hepatobiliary Tracts. *Frontiers in Medicine*, 4.
- VALIENTE, E., DAVIES, C., MILLS, D. C., GETINO, M., RITCHIE, J. M. & WREN, B. W. 2018. *Vibrio cholerae* accessory colonisation factor AcfC: a chemotactic protein with a role in hyperinfectivity. *Scientific Reports*, 8, 8390.
- VAN ALPHEN, L. B., WENZEL, C. Q., RICHARDS, M. R., FODOR, C., ASHMUS, R. A., STAHL, M., KARLYSHEV, A. V., WREN, B. W., STINTZI, A., MILLER, W. G., LOWARY, T. L. & SZYMANSKI, C. M. 2014. Biological Roles of the O-Methyl Phosphoramidate Capsule Modification in *Campylobacter jejuni*. *PLOS ONE*, 9, e87051.
- VAN DEEST, B. W., FORDTRAN, J. S., MORAWSKI, S. G. & WILSON, J. D. 1968. Bile salt and micellar fat concentration in proximal small bowel contents of ileectomy patients. *Journal of Clinical Investigation*, 47, 1314-24.
- VAN DEN BERG, B., BLACK, P. N., CLEMONS, W. M., JR. & RAPOPORT, T. A. 2004. Crystal structure of the long-chain fatty acid transporter FadL. *Science*, 304, 1506-9.
- VAN DER STEL, A.-X. & WÖSTEN, M. M. S. M. 2019. Regulation of Respiratory Pathways in *Campylobacterota*: A Review. *Frontiers in Microbiology*, 10, 1719-1719.
- VAN DEUN, K., HAESEBROUCK, F., HEYNDRICKX, M., FAVOREEL, H., DEWULF, J., CELEN, L., DUMEZ, L., MESSENS, W., LELEU, S., VAN IMMERSEEL, F., DUCATELLE, R. & PASMANS, F. 2007. Virulence properties of *Campylobacter jejuni* isolates of poultry and human origin. *Journal of Medical Microbiology*, 56, 1284-1289.
- VAN VLIET, A. H. 2010. Next generation sequencing of microbial transcriptomes: challenges and opportunities. *FEMS Microbiology Letters* 302, 1-7.
- VAN VLIET, A. H., WOOLDRIDGE, K. G. & KETLEY, J. M. 1998. Iron-responsive gene regulation in a *Campylobacter jejuni* fur mutant. *Journal of Bacteriology*, 180, 5291-5298.
- VANDAMME, P. & DE LEY, J. 1991. Proposal for a New Family, *Campylobacteraceae*. *International Journal of Systematic and Evolutionary Microbiology*, 41, 451-455.

- VAUGHAN-SHAW, P. G., REES, J. R., WHITE, D. & BURGESS, P. 2010. Campylobacter jejuni cholecystitis: a rare but significant clinical entity. *BMJ Case Reports*, 2010, bcr1020092365-bcr1020092365.
- VEITH, P. D., CHEN, Y.-Y., GORASIA, D. G., CHEN, D., GLEW, M. D., O'BRIEN-SIMPSON, N. M., CECIL, J. D., HOLDEN, J. A. & REYNOLDS, E. C. 2014. Porphyromonas gingivalis Outer Membrane Vesicles Exclusively Contain Outer Membrane and Periplasmic Proteins and Carry a Cargo Enriched with Virulence Factors. *Journal of Proteome Research*, 13, 2420-2432.
- VEITH, P. D., GLEW, M. D., GORASIA, D. G., CASCALES, E. & REYNOLDS, E. C. 2021. The Type IX Secretion System and Its Role in Bacterial Function and Pathogenesis. *Journal of Dental Research*, 220345211051599.
- VERHEUL, A., WOUTERS, J. A., ROMBOUTS, F. M. & ABEE, T. 1998. A possible role of ProP, ProU and CaiT in osmoprotection of Escherichia coli by carnitine. *Journal of Applied Microbiology*, 85, 1036-46.
- VICTORA, C. G., ADAIR, L., FALL, C., HALLAL, P. C., MARTORELL, R., RICHTER, L. & SACHDEV, H. S. 2008. Maternal and child undernutrition: consequences for adult health and human capital. *The Lancet*, 371, 340-357.
- WACKER, M., LINTON, D., HITCHEN, P. G., NITA-LAZAR, M., HASLAM, S. M., NORTH, S. J., PANICO, M., MORRIS, H. R., DELL, A. & WREN, B. W. 2002. N-linked glycosylation in Campylobacter jejuni and its functional transfer into E. coli. *Science*, 298, 1790-1793.
- WAI, S. N., LINDMARK, B., SÖDERBLOM, T., TAKADE, A., WESTERMARK, M., OSCARSSON, J., JASS, J., RICHTER-DAHLFORS, A., MIZUNOE, Y. & UHLIN, B. E. 2003. Vesicle-Mediated Export and Assembly of Pore-Forming Oligomers of the Enterobacterial ClyA Cytotoxin. *Cell*, 115, 25-35.
- WALKER, S. P., GRANTHAM-MCGREGOR, S. M., POWELL, C. A. & CHANG, S. M. 2000. Effects of growth restriction in early childhood on growth, IQ, and cognition at age 11 to 12 years and the benefits of nutritional supplementation and psychosocial stimulation. *Journal of Pediatrics*, 137, 36-41.
- WALLACE, J., STANLEY, K., CURRIE, J., DIGGLE, P. & JONES, K. 1997. Seasonality of thermophilic Campylobacter populations in chickens. *Journal of Applied Microbiology*, 82, 219-224.
- WANG, S., LI, W., ZHANG, R., LIU, S. & XU, J. 2016. CoinFold: a web server for protein contact prediction and contact-assisted protein folding. *Nucleic Acids Research*, 44, W361-W366.
- WANG, S., SUN, S., LI, Z., ZHANG, R. & XU, J. 2017. Accurate De Novo Prediction of Protein Contact Map by Ultra-Deep Learning Model. *PLOS Computational Biology*, 13, e1005324.
- WANG, Y. 2002. The function of OmpA in Escherichia coli. *Biochemical and Biophysical Research Communications*, 292, 396-401.
- WASSENAAR, T. M., VAN DER ZEIJST, B. A. M., AYLING, R. & NEWELL, D. G. 1993. Colonization of chicks by motility mutants of Campylobacter jejuni demonstrates the importance of flagellin A expression. *Microbiology*, 139, 1171-1175.
- WATERHOUSE, A., BERTONI, M., BIENERT, S., STUDER, G., TAURIELLO, G., GUMIENNY, R., HEER, F. T., DE BEER, T. A. P., REMPFER, C., BORDOLI, L., LEPORE, R. & SCHWEDE, T. 2018. SWISS-MODEL: homology modelling of protein structures and complexes. *Nucleic Acids Research*, 46, W296-W303.
- WATSON, D., SLEATOR, R. D., CASEY, P. G., HILL, C. & GAHAN, C. G. 2009. Specific osmolyte transporters mediate bile tolerance in Listeria monocytogenes. *Infection and Immunity* 77, 4895-904.
- WATSON, E., SHERRY, A., INGLIS, N. F., LAINSON, A., JYOTHI, D., YAGA, R., MANSON, E., IMRIE, L., EVEREST, P. & SMITH, D. G. E. 2014. Proteomic and genomic analysis reveals novel Campylobacter jejuni outer membrane proteins and potential heterogeneity. *EuPA Open Proteomics*, 4, 184-194.
- WEI, S., LI, X., WANG, J., WANG, Y., ZHANG, C., DAI, S., WANG, X., DENG, X., ZHAO, L. & SHAN, B. 2021. Outer Membrane Vesicles Secreted by Helicobacter pylori Transmitting Gastric Pathogenic Virulence Factors. *American Chemical Society Omega*, 7, 240-258.

- WHO. 2020. *Campylobacter* [Online]. Available: <https://www.who.int/news-room/fact-sheets/detail/campylobacter> [Accessed 01/05/2020].
- WIECZOREK, D., GWIAZDOWSKA, D., STASZAK, K., CHEN, Y.-L. & SHEN, T.-L. 2016. Surface and Antimicrobial Activity of Sulfobetaines. *Journal of Surfactants and Detergents*, 19, 813-822.
- WIMLEY, W. C. 2003. The versatile  $\beta$ -barrel membrane protein. *Current Opinion in Structural Biology*, 13, 404-411.
- WOJCIK, O. P., KOENIG, K. L., ZELENIUCH-JACQUOTTE, A., COSTA, M. & CHEN, Y. 2010. The potential protective effects of taurine on coronary heart disease. *Atherosclerosis*, 208, 19-25.
- WONG, A., LANGE, D., HOULE, S., ARBATSKY, N. P., VALVANO, M. A., KNIREL, Y. A., DOZOIS, C. M. & CREUZENET, C. 2015. Role of capsular modified heptose in the virulence of *Campylobacter jejuni*. *Molecular Microbiology*, 96, 1136-1158.
- WYSZYŃSKA, A., ZYCKA-KRZESINSKA, J., GODLEWSKA, R. & JAGUSZTYN-KRYNICKA, E. 2008. The *Campylobacter jejuni/coli* cjaA (cj0982c) Gene Encodes an N-Glycosylated Lipoprotein Localized in the Inner Membrane. *Current Microbiology*, 57, 181-8.
- YAN, M., SAHIN, O., LIN, J. & ZHANG, Q. 2006. Role of the CmeABC efflux pump in the emergence of fluoroquinolone-resistant *Campylobacter* under selection pressure. *Journal of Antimicrobial Chemotherapy*, 58, 1154-1159.
- YANG, M., LIU, Z., HUGHES, C., STERN, A. M., WANG, H., ZHONG, Z., KAN, B., FENICAL, W. & ZHU, J. 2013. Bile salt-induced intermolecular disulfide bond formation activates *Vibrio cholerae* virulence. *Proceedings of the National Academy of Sciences*, 110, 2348-53.
- YAO, R., BURR, D. H., DOIG, P., TRUST, T. J., NIU, H. & GUERRY, P. 1994. Isolation of motile and non-motile insertional mutants of *Campylobacter jejuni*: the role of motility in adherence and invasion of eukaryotic cells. *Molecular Microbiology*, 14, 883-93.
- YASUGI, M., OKUZAKI, D., KUWANA, R., TAKAMATSU, H., FUJITA, M., SARKER, M. R. & MIYAKE, M. 2016. Transcriptional Profile during Deoxycholate-Induced Sporulation in a *Clostridium perfringens* Isolate Causing Foodborne Illness. *Applied and Environmental Microbiology*, 82, 2929-2942.
- YEOW, J., TAN, K. W., HOLDBROOK, D. A., CHONG, Z.-S., MARZINEK, J. K., BOND, P. J. & CHNG, S.-S. 2018. The architecture of the OmpC-MlaA complex sheds light on the maintenance of outer membrane lipid asymmetry in *Escherichia coli*. *The Journal of biological chemistry*, 293, 11325-11340.
- YIN, C., XIA, B., TANG, S., CAO, A., LIU, L., ZHONG, R., CHEN, L. & ZHANG, H. 2021. The Effect of Exogenous Bile Acids on Antioxidant Status and Gut Microbiota in Heat-Stressed Broiler Chickens. *Frontiers in Nutrition*, 8.
- YODER-HIMES, D. R., CHAIN, P. S., ZHU, Y., WURTZEL, O., RUBIN, E. M., TIEDJE, J. M. & SOREK, R. 2009. Mapping the *Burkholderia cenocepacia* niche response via high-throughput sequencing. *Proceedings of the National Academy of Sciences*, 106, 3976-81.
- YOKOYAMA, K., HORII, T., YAMASHINO, T., HASHIKAWA, S., BARUA, S., HASEGAWA, T., WATANABE, H. & OHTA, M. 2000. Production of Shiga toxin by *Escherichia coli* measured with reference to the membrane vesicle-associated toxins. *FEMS Microbiology Letters*, 192, 139-144.
- YOUNG, K. T., DAVIS, L. M. & DIRITA, V. J. 2007. *Campylobacter jejuni*: molecular biology and pathogenesis. *Nature Reviews Microbiology*, 5, 665.
- YOUNG, N. M., BRISSON, J. R., KELLY, J., WATSON, D. C., TESSIER, L., LANTHIER, P. H., JARRELL, H. C., CADOTTE, N., ST MICHAEL, F., ABERG, E. & SZYMANSKI, C. M. 2002. Structure of the N-linked glycan present on multiple glycoproteins in the Gram-negative bacterium, *Campylobacter jejuni*. *Journal of Biological Chemistry*, 277, 42530-9.
- YU, H., GUO, Z., SHEN, S. & SHAN, W. 2016. Effects of taurine on gut microbiota and metabolism in mice. *Amino Acids*, 48, 1601-1617.
- YURTSEVER, D. & LORENT, J. H. 2020. Structural Modifications Controlling Membrane Raft Partitioning and Curvature in Human and Viral Proteins. *The Journal of Physical Chemistry B*, 124, 7574-7585.

- ZAKHARZHEVSKAYA, N. B., VANYUSHKINA, A. A., ALTUKHOV, I. A., SHAVARDA, A. L., BUTENKO, I. O., RAKITINA, D. V., NIKITINA, A. S., MANOLOV, A. I., EGOROVA, A. N., KULIKOV, E. E., VISHNYAKOV, I. E., FISUNOV, G. Y. & GOVORUN, V. M. 2017. Outer membrane vesicles secreted by pathogenic and nonpathogenic *Bacteroides fragilis* represent different metabolic activities. *Scientific Reports*, 7, 5008.
- ZAMORA, C. Y., WARD, E. M., KESTER, J. C., CHEN, W. L. K., VELAZQUEZ, J. G., GRIFFITH, L. G. & IMPERIALI, B. 2020. Application of a gut-immune co-culture system for the study of N-glycan-dependent host-pathogen interactions of *Campylobacter jejuni*. *Glycobiology*, 30, 374-381.
- ZERBINO, D. R. & BIRNEY, E. 2008. Velvet: Algorithms for de novo short read assembly using de Bruijn graphs. *Genome Research*, 18, 821-829.
- ZGURSKAYA, H. I., YAMADA, Y., TIKHONOVA, E. B., GE, Q. & KRISHNAMOORTHY, G. 2009. Structural and functional diversity of bacterial membrane fusion proteins. *Biochimica et Biophysica Acta (BBA) - Proteins and Proteomics*, 1794, 794-807.
- ZHANG, D. F., LI, H., LIN, X. M., WANG, S. Y. & PENG, X. X. 2011. Characterization of outer membrane proteins of *Escherichia coli* in response to phenol stress. *Current Microbiology*, 62, 777-83.
- ZHANG, M. J., XIAO, D., ZHAO, F., GU, Y. X., MENG, F. L., HE, L. H., MA, G. Y. & ZHANG, J. Z. 2009. Comparative proteomic analysis of *Campylobacter jejuni* cultured at 37C and 42C. *Japanese Journal of Infectious Diseases*, 62, 356-61.
- ZHAO, Z., WANG, L., MIAO, J., ZHANG, Z., RUAN, J., XU, L., GUO, H., ZHANG, M. & QIAO, W. 2022. Regulation of the formation and structure of biofilms by quorum sensing signal molecules packaged in outer membrane vesicles. *Science of The Total Environment*, 806, 151403.
- ZHENG, J., MENG, J., ZHAO, S., SINGH, R. & SONG, W. 2008. *Campylobacter*-induced interleukin-8 secretion in polarized human intestinal epithelial cells requires *Campylobacter*-secreted cytolethal distending toxin- and Toll-like receptor-mediated activation of NF-kappaB. *Infection and Immunity* 76, 4498-4508.
- ZHOU, L., SRISATJALUK, R., JUSTUS, D. E. & DOYLE, R. J. 1998. On the origin of membrane vesicles in Gram-negative bacteria. *FEMS Microbiology Letters*, 163, 223-228.
- ZINGL, F. G., KOHL, P., CAKAR, F., LEITNER, D. R., MITTERER, F., BONNINGTON, K. E., RECHBERGER, G. N., KUEHN, M. J., GUAN, Z., REIDL, J. & SCHILD, S. 2020. Outer Membrane Vesiculation Facilitates Surface Exchange and In Vivo Adaptation of *Vibrio cholerae*. *Cell Host Microbe*, 27, 225-237.e8.
- ZIPRIN, R. L., YOUNG, C. R., STANKER, L. H., HUME, M. E. & KONKEL, M. E. 1999. The absence of cecal colonization of chicks by a mutant of *Campylobacter jejuni* not expressing bacterial fibronectin-binding protein. *Avian Diseases*, 43, 586-9.
- ZWICKER, B. L. & AGELLON, L. B. 2013. Transport and biological activities of bile acids. *The International Journal of Biochemistry & Cell Biology*, 45, 1389-98.

## Appendices



# Sodium Taurocholate Stimulates *Campylobacter jejuni* Outer Membrane Vesicle Production via Down-Regulation of the Maintenance of Lipid Asymmetry Pathway

Cadi Davies<sup>1</sup>, Aidan J. Taylor<sup>2</sup>, Abdi Elmi<sup>1</sup>, Jody Winter<sup>3</sup>, Janie Liaw<sup>1</sup>, Anna D. Grabowska<sup>1</sup>, Ozan Gundogdu<sup>1</sup>, Brendan W. Wren<sup>1</sup>, David J. Kelly<sup>2\*</sup> and Nick Dorrell<sup>1\*</sup>

<sup>1</sup> Faculty of Infectious and Tropical Diseases, London School of Hygiene and Tropical Medicine, London, United Kingdom,

<sup>2</sup> Department of Molecular Biology and Biotechnology, University of Sheffield, Sheffield, United Kingdom, <sup>3</sup> School of Science and Technology, Nottingham Trent University, Nottingham, United Kingdom

## OPEN ACCESS

### Edited by:

D. Scott Merrell  
Uniformed Services University of the  
Health Sciences, United States

### Reviewed by:

Ramesh Vemulapalli,  
Texas A&M University, United States  
Philip R. Hardwidge,  
Kansas State University, United States

### \*Correspondence:

David J. Kelly  
d.kelly@sheffield.ac.uk  
Nick Dorrell  
nick.dorrell@lshtm.ac.uk

### Specialty section:

This article was submitted to  
Bacteria and Host,  
a section of the journal  
Frontiers in Cellular and Infection  
Microbiology

Received: 19 February 2019

Accepted: 09 May 2019

Published: 29 May 2019

### Citation:

Davies C, Taylor AJ, Elmi A, Winter J,  
Liaw J, Grabowska AD, Gundogdu O,  
Wren BW, Kelly DJ and Dorrell N  
(2019) Sodium Taurocholate  
Stimulates *Campylobacter jejuni* Outer  
Membrane Vesicle Production via  
Down-Regulation of the Maintenance  
of Lipid Asymmetry Pathway.  
Front. Cell. Infect. Microbiol. 9:177.  
doi: 10.3389/fcimb.2019.00177

*Campylobacter jejuni* outer membrane vesicles (OMVs) contain numerous virulence-associated proteins including the cytolethal distending toxin and three serine proteases. As *C. jejuni* lacks the classical virulence-associated secretion systems of other enteric pathogens that deliver effectors directly into target cells, OMVs may have a particularly important role in virulence. *C. jejuni* OMV production is stimulated by the presence of physiological concentrations of the bile salt sodium taurocholate (ST) through an unknown mechanism. The maintenance of lipid asymmetry (MLA) pathway has been implicated in a novel mechanism for OMV biogenesis, open to regulation by host signals. In this study we investigated the role of the MLA pathway in *C. jejuni* OMV biogenesis with ST as a potential regulator. OMV production was quantified by analyzing protein and lipid concentrations of OMV preparations and OMV particle counts produced by nanoparticle tracking analysis. Mutation of *miaA* which encodes the outer membrane component of the MLA pathway significantly increased OMV production compared to the wild-type strain. Detergent sensitivity and membrane permeability assays confirmed the increased OMV production was not due to changes in membrane stability. The presence of 0.2% (w/v) ST increased wild-type OMV production and reduced OMV size, but did not further stimulate *miaA* mutant OMV production or significantly alter *miaA* mutant OMV size. qRT-PCR analysis demonstrated that the presence of ST decreased expression of both *miaA* and *miaC* in *C. jejuni* wild-type strains 11168 and 488. Collectively the data in this study suggests *C. jejuni* can regulate OMV production in response to host gut signals through changes in expression of the MLA pathway. As the gut bile composition is dependent on both diet and the microbiota, this study highlights the potential importance of diet and lifestyle factors on the varying disease presentations associated with gut pathogen infection.

**Keywords:** *Campylobacter*, bile salts, outer membrane vesicles, maintenance of lipid asymmetry pathway, *MiaA*

## INTRODUCTION

*Campylobacter jejuni* is a microaerophilic Gram-negative bacterium that is the leading cause of foodborne bacterial gastroenteritis worldwide (Silva et al., 2011; Kaakoush et al., 2015). Whilst *C. jejuni* has a number of potential virulence factors, including a cytolethal distending toxin (Lindmark et al., 2009; Elmi et al., 2012), and multiple proteases (Karlyshev et al., 2014; Elmi et al., 2016, 2018), *Campylobacter jejuni* lacks the classical virulence associated secretion systems of other enteric pathogens that deliver effectors directly to target cells (Parkhill et al., 2000). A Type VI secretion system (T6SS) has been identified in a proportion of strains, however, the function and variability of T6SSs among *C. jejuni* strains is still poorly understood (Bleumink-Pluym et al., 2013; Ugarte-Ruiz et al., 2015). An alternative machinery to deliver potential virulence determinants are outer membrane vesicles (OMVs), which can act as a general secretion pathway among Gram-negative bacteria and maybe are of particular importance for *C. jejuni* virulence and survival.

OMVs are small spherical membrane-bound structures ranging in size from 10 to 500 nm in diameter formed from the outer membrane of Gram-negative bacteria and released into the extracellular environment (Kuehn and Kesty, 2005; Schwechheimer and Kuehn, 2015). OMVs provide a mechanism to deliver cargo in concentrated, selectively packaged parcels, protected from the extracellular environment with the potential for site specific targeting to receptors on cells (Kuehn and Kesty, 2005; Bomberger et al., 2009; Bonnington and Kuehn, 2014; Bitto et al., 2017). OMV production appears evolutionarily conserved in Gram-negative bacteria despite being metabolically energy consuming, suggesting OMVs have vital roles (Kulp and Kuehn, 2010; Roier et al., 2016). OMV production has been observed under a range of conditions in both pathogenic and non-pathogenic Gram-negative bacteria (Mashburn-Warren et al., 2008; Elmi et al., 2012; Altindis et al., 2014; Zakharzhevskaya et al., 2017); both on solid and in liquid media (Schooling and Beveridge, 2006; Schwechheimer and Kuehn, 2015), and in the presence or absence of stress (Schwechheimer and Kuehn, 2015). Conditions or gene mutations resulting in the absence of OMVs have not been identified. OMVs have been suggested to have a variety of functions important in survival and virulence via processes such as competition for growth (Manning and Kuehn, 2011; Kulkarni et al., 2015), immunomodulation (Koeppen et al., 2016; Tsatsaronis et al., 2018), biofilm formation (Schooling and Beveridge, 2006), bacterial communication (Mashburn and Whiteley, 2005; Mashburn-Warren et al., 2008), and the delivery of biomolecules such as toxins (Bielaszewska et al., 2017; Elmi et al., 2018).

Until recently there has been no general regulatory model for OMV biogenesis that could be widely applicable to Gram-negative bacteria. The three main OMV biogenesis models proposed previously have been based on either changes in cell wall to outer membrane (OM) linkages, stress or a species-specific mechanism. One previously proposed model suggests that the build-up of cellular components (such as misfolded proteins due to heat shock, or peptidoglycan fragments due

to cell wall remodeling defects) at the OM result in bulging and subsequent blebbing (Zhou et al., 1998; Mcbroom and Kuehn, 2007). OMVs have since been demonstrated to contain biologically active cargo and not just cell waste (Mashburn and Whiteley, 2005; Bielaszewska et al., 2017; Elmi et al., 2018). A second mechanism proposed that the reduction in cell wall to OM interactions can cause areas prone to blebbing. This has been demonstrated by OMVs being released at cell division sites with high frequency (Kulp and Kuehn, 2010), however, OMV release is not restricted to cell division sites (Elhenawy et al., 2016). Deatherage et al. (2009) studied the effect of removing cell wall to OM linkages on OMV production and found removal of OmpA linkages did not compromise the cell membrane. However, removal of other linkages (*lpp*, *tolA*, *tolB*, and *pal*) did cause membrane defects. Additional studies have found that the down-regulation of *ompA* is dependent on the membrane stress sigma factor,  $\sigma^E$  (Song et al., 2008). A further mechanism has been identified in the OM of *Pseudomonas aeruginosa*, which has increased fluidity compared to the OM of other Gram-negative bacteria. *Pseudomonas aeruginosa* produces a quorum sensing molecule PQS (pseudomonas quinolone signal) which induces membrane curvature through interactions with lipid A to stabilize and reduce fluidity of the OM. Without PQS, *P. aeruginosa* struggles to reach the membrane curvature necessary to form OMVs. However, this proposed mechanism appears specific to *P. aeruginosa* cells (Mashburn and Whiteley, 2005; Mashburn-Warren et al., 2008).

More recently, Roier et al. (2016) have proposed a new general regulatory model based on the maintenance of lipid asymmetry pathway (MLA) that could be widely applicable to Gram-negative bacteria. The MLA pathway has been shown to play a role in the retrograde trafficking of phospholipids (PLs) from the outer leaflet of the OM to the inner membrane. The core components of this pathway are highly conserved in Gram-negative bacteria (Malinverni and Silhavy, 2009). The pathway consists of an inner membrane ABC (ATP binding cassette) transporter consisting of MlaBDEF (MlaB is absent in  $\alpha$  and  $\epsilon$  proteobacteria), a periplasmic chaperone MlaC, and the OM lipoprotein MlaA. The components of the MLA pathway are homologous to YrbBCDEF and VacJ in *Haemophilus influenzae*. Roier et al. proposed that down-regulation or mutation of the MLA pathway or components of this pathway will lead to an accumulation of PLs in the outer leaflet of the OM. This accumulation leads to an asymmetric expansion which eventually results in the formation of an OMV. Roier et al. demonstrated increased OMV production in *mia* mutants, as well as reduced *mia* gene expression in *H. influenzae* under iron-limiting conditions. The same study suggested that iron limitation signaled entry to the host nasopharynx, and the subsequent increase in OMV production was a potential mechanism to defend against antibody and complement-mediated attack.

A range of virulence factors have been identified within *C. jejuni* OMVs, including the cytolethal distending toxin and putative virulence-associated proteases that contribute to *C. jejuni* invasion into intestinal epithelial cells (Lindmark et al., 2009; Elmi et al., 2016, 2018). *C. jejuni* OMVs isolated at 37°C (human body temperature) have also been shown to

differ in protein abundance compared to 42°C (avian body temperature), suggesting *C. jejuni* can alter cargo in response to host signals (Taheri et al., 2019). An important feature of a pathogen is the ability to sense the environment and to appropriately alter and co-ordinate the regulation of virulence factors. We have previously reported the potential significance of the bile salt sodium taurocholate (ST) in the regulation of OMV-mediated virulence in *C. jejuni* (Elmi et al., 2018) and have demonstrated increased OMV production in the presence of physiologically relevant concentrations of ST. In addition, the OMVs isolated from cultures supplemented with ST (ST-OMVs) exhibited increased proteolytic activity, cytotoxicity, and immunogenicity to intestinal epithelial cells. ST has also been shown to up-regulate virulence gene expression in *Vibrio cholerae* by causing alterations in disulphide bond formation in TcpP (transmembrane transcription factor) (Yang et al., 2013).

This study further investigates the link between the MLA pathway and OMV production in Gram-negative bacteria. Increased OMV production without compromising membrane stability was observed in a *C. jejuni* 11168 *mlaA* mutant. This study also builds on previous work linking the bile salt ST to increased OMV production, by identifying a potential mechanism for the ST-OMV phenotype. OMV production was observed to increase in the *C. jejuni* wild-type strain, but not in the *mlaA* mutant in the presence of ST. Growth of *C. jejuni* in the presence of ST also resulted in reduced expression of *mla* genes. The data in this study supports the MLA model of OMV production and the link between bile salts and potential virulence regulation in *C. jejuni*.

## MATERIALS AND METHODS

### Bacterial Strains and Growth Conditions

The *C. jejuni* wild-type strains used in this study were NCTC 11168 (the widely studied human clinical isolate) and 488 (a recent Brazilian human isolate obtained from Daiani Teixeira Da Silva). Cultures were grown in a microaerobic chamber (Don Whitley Scientific, United Kingdom) containing 85% (v/v) N<sub>2</sub>, 10% (v/v) CO<sub>2</sub>, and 5% (v/v) O<sub>2</sub> at 37°C either on blood agar (BA) plates containing Columbia agar base (Oxoid, United Kingdom), 7% (v/v) horse blood (TCS Microbiology, United Kingdom), and *Campylobacter* Selective Supplement (Oxoid), or in Brucella broth (Oxoid) shaking at 75 rpm unless otherwise stated. *C. jejuni* strains were grown on BA plates for 24 h prior to experiments unless otherwise stated. *Escherichia coli* XL2-Blue MRF<sup>+</sup> competent cells (Stratagene, United Kingdom) were used for cloning and were grown at 37°C in aerobic conditions either in Lysogeny broth (LB) (Oxoid) shaking at 200 rpm or on LB agar plates (Oxoid). When required, ampicillin (100 µg/ml), kanamycin (50 µg/ml), apramycin (60 µg/ml), or chloramphenicol (50 µg/ml for *E. coli* or 10 µg/ml for *C. jejuni*) were added to cultures.

### Construction of *C. jejuni* Mutants

The *C. jejuni* 11168 *mlaA* gene was inactivated by deletion of the reading frame by homologous cross-over and replacement with a kanamycin resistance cassette. The mutation vector

was created using the Gibson isothermal assembly method as previously described (Taylor et al., 2017). The *C. jejuni* 11168 wild-type strain was transformed by electroporation and mutant clones selected for kanamycin resistance. Correct insertion and orientation of the kanamycin cassette into the genome was confirmed by PCR.

The *C. jejuni* 488 *mlaA* mutant was constructed by natural transformation using genomic DNA from the *C. jejuni* 11168 *mlaA* mutant spotted onto the *C. jejuni* 488 wild-type strain. Transformations were performed on Mueller-Hinton agar (Oxoid) plates for 5 h under microaerobic conditions at 37°C. Transformants were screened on BA plates supplemented with kanamycin, then putative mutants verified by PCR and sequencing.

### Complementation of *C. jejuni mlaA* Mutants

Complementation of the *C. jejuni* 11168 *mlaA* mutant was performed using the pRRa system to generate a complementation vector as previously described (Taylor et al., 2017). The 11168 *mlaA* mutant was transformed with the complementation vector by electroporation and clones selected for apramycin resistance. Correct insertion of the expression cassette into the genome was confirmed by PCR. In the 11168 *mlaA* complement strain, the inserted *mlaA* gene is under the control of the native promoter.

The *C. jejuni* 488 *mlaA* mutant was complemented using the pCJC1 complementation vector as previously described

TABLE 1 | Primers used in this study.

Primer name	Primer sequence 5' -3'	Source
GSmlaA(F)	TAGGAGTTTTTGTCTGAG	This study
GSmlaA(R)	GCTAAGTTCATTGCGTC	This study
ISAmIaA(F1)	GAGCTCGGTACCCGGGGATCCT CTAGAGTCTGGCACTACAATAAATAGG	This study
ISAmIaA(R1)	AAGCTGTCAAACATGAGAAACCAAGG AGAATGTTTTGGTATTCTTGTTCAA	This study
ISAmIaA(F2)	GAATTGTTTTAGTACCTAGCCGAAGGT GTGCATTATATCCATTCTTGGGT	This study
ISAmIaA(R2)	AGAATACTCAAGCTTGGCATGCGTGCAGG TGGCCAGTTGTTATTATCATTG	This study
pCJC1mlaA(F)	COCCCATGGTTTTAGGAGTTTT TGCTGAGAATAAAATTTATATC	This study
pCJC1mlaA(R)	COCGTAGCTTATTTGCTAAGTTCATTG	This study
pRRAmIaA(F)	ACACTCTAGATTTAGGAGTTTTTGCTTG	This study
pRRAmIaA(R)	ACACCAATTGGATTAATAAATATTTT TTTCATTAA	This study
qRTmlaA(F)	GATCCTACTTGGGCAAGTATAGC	This study
qRTmlaA(R)	ATGCTTACGAGCAAAAGACGCAATG	This study
qRTmlaC(F)	CCACTTCTATGGTAGTAGATGGG	This study
qRTmlaC(R)	GTAGGGCATCAAAGCCTTGGTT	This study
rpoA(F)	CGAGCTTGCTTTGATGAGTG	Fitz et al., 2009
rpoA(R)	AGTTCCACAGGAAACCTA	Fitz et al., 2009

GS, gene specific; ISA, isothermal assembly; pRRa, *C. jejuni* complementation vector; pCJC1, *C. jejuni* complementation vector; qRT, quantitative reverse transcription PCR.

(Gundogdu et al., 2011; Jervis et al., 2015). Briefly, the complete wild-type gene was amplified by PCR to contain the native ribosome binding site, start codon, and stop codon with primers pCJC1mlaA(F/R) (Table 1) to introduce a NcoI site at the 5' end and a NheI site at the 3' end. The amplified gene was digested with NheI and NcoI and ligated into the pCJC1 complementation vector which was used to insert the wild-type gene copy into the 488 ortholog of the *C. jejuni* 11168 pseudogene *cj0223*. Putative clones were selected on BA plates supplemented with chloramphenicol then verified by PCR and sequencing. In the 488 *mlaA* complement strain, the inserted *mlaA* gene is under the control of a constitutive chloramphenicol promoter.

### 3,3'-dipropylthiadicarbocyanine Iodide (DiSC3) Permeability Assay

DiSC3 is a potentiometric fluorescent probe which accumulates on, and translocates into, hyperpolarized lipid bilayers and is frequently used to measure membrane permeability. Fluorescence was monitored at Ex/Em wavelength of 622/670 nm in a Cary Eclipse (Agilent, United States) fluorescence spectrophotometer. *C. jejuni* cells were washed in 20 mM sodium phosphate buffer, pH 7.4, containing 10 mM KCl, and set to an optical density at 600 nm of 0.1. DiSC3 was added to 5 μM final concentration and fluorescence emission followed for 2 min to establish the baseline. Polymyxin B was then added (100 μM final concentration) and emission followed for a further 1 min, before the addition of SDS (20 mM final concentration) to give the maximum fluorescence value. Percentage incorporation of the dye into the membrane was calculated by:

$$100 - \left( \frac{\text{emission after Polymyxin B (minus baseline)}}{\text{maximum emission after SDS (minus baseline)}} \right) \times 100$$

### Growth Kinetics and Membrane Sensitivity Assays

The growth of each *C. jejuni* wild-type, mutant and complement strains was characterized by measuring both the OD<sub>600</sub> value and colony forming units (CFUs) of a liquid culture every 2 h for 18 h. Sensitivity to the bile salt sodium taurocholate at biologically relevant concentrations was analyzed measuring OD<sub>600</sub> and CFU of liquid cultures supplemented with 0.2% (w/v) ST every 2 h for 18 h. Sensitivity to ST at high concentrations was analyzed by comparing the OD<sub>600</sub> and CFU of late-log phase broth cultures in the presence or absence of 2% (w/v) sodium taurocholate. Sensitivity to the zwitterionic detergent lauryl sulfobetain (LSB) was analyzed by comparing CFUs of mid-log phase cultures serially diluted and spotted onto Brucella agar with or without supplementation of LSB (1.25 mM final concentration). Sensitivity to polymyxin B was analyzed by comparing CFUs of mid-log phase cultures serially diluted and spotted onto BA plates with and without supplementation with polymyxin B (2.5 μg/ml final concentration).

### Outer Membrane Vesicle Isolation

*C. jejuni* OMVs were isolated as previously described (Elmi et al., 2012). Briefly, *C. jejuni* from a 24 h BA plate were resuspended in Brucella broth and used to inoculate 50 ml of pre-equilibrated Brucella broth to an OD<sub>600</sub> of 0.1. Cultures were grown to late-log phase, time points determined by growth kinetics for each strain. OD<sub>600</sub> values were normalized to OD<sub>600</sub> 1.0 and the sterile supernatants obtained by pelleting cells and filter-sterilizing supernatants through a 0.22 μm membrane (Millipore, United Kingdom). The supernatants were then concentrated to 2 ml using an Ultra-4 Centrifugal Filter Unit with a nominal 10 kDa cut-off (Millipore). The concentrated filtrate was ultra-centrifuged at 150,000 × g for 3 h at 4°C using a TLA 100.4 rotor (Beckman Instruments, United States). The resulting OMV pellet was washed by resuspending in phosphate buffered saline (PBS) and pelleting by ultra-centrifugation as described above. All isolation steps were performed at 4°C and the resulting OMVs pellet was resuspended in PBS and stored at -20°C.

### Quantification of Outer Membrane Vesicles

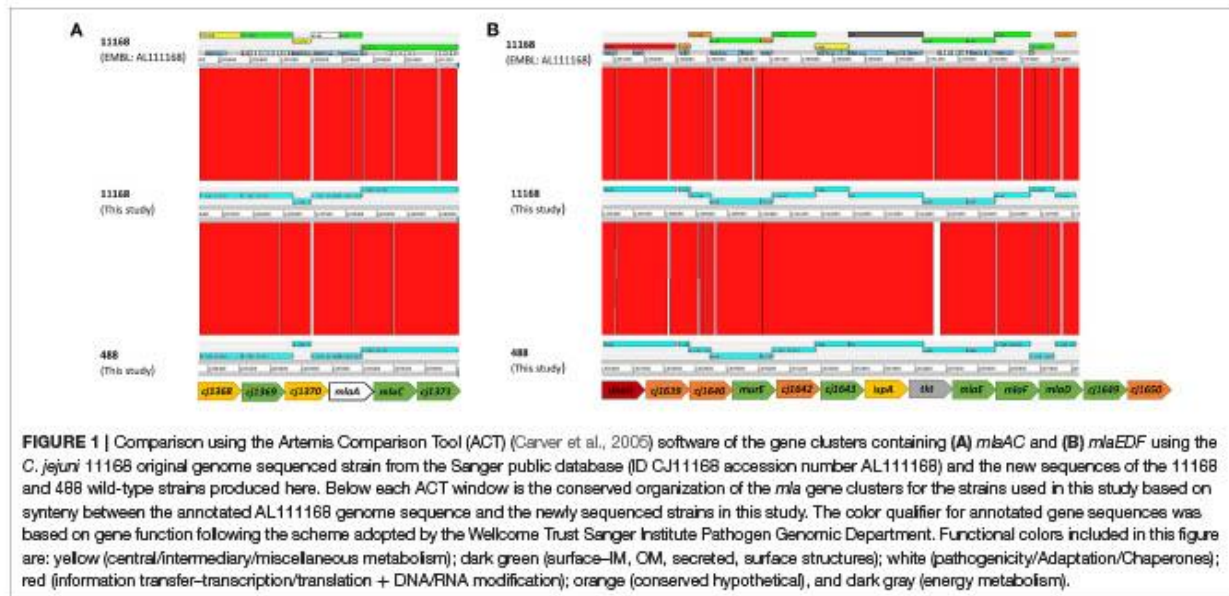
The protein concentration of OMV preparations was quantified using a commercial bicinchoninic-acid (BCA) assay kit according to the manufacturer's protocol (Thermo Fisher Scientific, United Kingdom), using BSA as the protein standard. The lipo-oligosaccharide of OMV preparations was quantified by measuring 2-Keto-3-deoxyoctonate acid (KDO) content as described previously (Lee and Tsai, 1999). Briefly, 50 μl samples were hydrolysed with 50 μl sulphuric acid (0.5 N) at 100°C for 15 min, then mixed with 50 μl 0.1 M periodate reagent (H<sub>5</sub>IO<sub>6</sub>) and incubated at room temperature for 10 min. 200 μl 4% (w/v) sodium arsenite reagent (NaAsO<sub>2</sub>) then 800 μl 0.6% (w/v) thiobarbituric acid was added and samples heated again to 100°C for 15 min. Samples were mixed with 1 ml dimethyl sulfoxide (DMSO) to stabilize the chromophore and OD<sub>548</sub> measurements taken. 2-Keto-3-deoxyoctonate ammonium salt (Sigma-Aldrich, United Kingdom) was used as the KDO standard.

### Analysis of Outer Membrane Vesicles by Nanoparticle Tracking Analysis

Nanoparticle tracking analysis (NTA) was conducted using a ZetaView PMX 110 instrument (Particle Metrix GmbH, Germany) following the manufacturer's instructions. The instrument was calibrated against a known concentration of PS100 nanoparticles with 100 nm diameter (Applied Microspheres B. V., The Netherlands). Nanostandards and OMV samples were suspended in particle-free PBS (Sigma-Aldrich) and diluted appropriately before analysis. Each sample was counted and sized across two cycles of 11 frames per cycle with a flow cell sensitivity of 80%.

### Quantitative Real-Time Polymerase Chain Reaction (qRT-PCR)

To investigate the expression of *mlaA* and *mlaC*, total RNA from both the *C. jejuni* 11168 and 488 wild-type strains, grown in Brucella broth to mid-log phase either in the presence or absence of 0.2% (w/v) sodium taurocholate was extracted using



Invitrogen PureLink RNA kit (Invitrogen, United Kingdom). DNA contamination was removed using the TURBO DNA-free kit (Thermo Fisher Scientific). Purified RNA was quantified using a NanoDrop machine (NanoDrop Technologies, United Kingdom) and used to synthesize complementary DNA (cDNA) using the SuperScript III First-Strand Synthesis kit (Thermo Fisher Scientific). qRT-PCR reactions were performed in triplicate using SYBR green master mix (Thermo Fisher Scientific) and an ABI7500 machine (Applied Biosystems). Relative gene expression comparisons were performed using the  $\Delta\Delta CT$  (cycle threshold) method (Schmittgen and Livak, 2008) and previously published *C. jejuni* *rpoA* primers (Ritz et al., 2009) for internal controls to normalize the mean CT of each gene to the stably expressed housekeeping gene *rpoA*.

### Statistical Analysis

At least three biological replicates were performed each in triplicate for each experiment. Statistical analyses were performed using Prism software (GraphPad Software). Variables were compared using a student's *t*-test or a one sample *t*-test with \* indicating a  $p < 0.05$ , \*\* indicating a  $p < 0.01$ , \*\*\* indicating a  $p < 0.001$ , and \*\*\*\* indicating a  $p < 0.0001$ .

## RESULTS

### Identification of *C. jejuni* Orthologs of the MLA Pathway in *E. coli*

The genomes of *C. jejuni* 11168 and 488 contain sets of genes encoding proteins homologous to components of the MLA pathway in *E. coli* and the VacJ and YrbCEFD proteins in *H. influenzae*. The MLA pathway consists of MlaA (outer membrane lipoprotein), MlaC (periplasmic chaperone), and MlaEFD (inner membrane ABC transporter). In *C. jejuni* these proteins are encoded in two separate regions of the genome (Figure 1).

Cj1371 and Cj1372 in *C. jejuni* 11168 are within the same gene cluster and are homologous to MlaA and MlaC in *E. coli* (amino acid sequence similarity of 29.4 and 21.6%, respectively, to *E. coli* MG1655 MlaA and MlaC) and VacJ and YrbC in *H. influenzae* (amino acid sequence similarity of 25.8 and 22.2%, respectively, to *H. influenzae* KW20 VacJ and YrbC). Homologous proteins were also identified in *C. jejuni* 488 with 97.4 and 96.8% amino acid similarity to Cj1371 and Cj1372, respectively. Cj1646, Cj1647, and Cj1648 in *C. jejuni* 11168 are encoded by the same gene cluster and are homologous to MlaEFD in *E. coli* (amino acid sequence similarity of 27.6, 31.8, and 18.8%, respectively, to *E. coli* MG1655 MlaEFD), and YrbEFD in *H. influenzae* (amino acid sequence similarity of 27.7, 36.4, and 22.8%, respectively, to *H. influenzae* KW20 YrbEFD). Homologous proteins were also identified in *C. jejuni* 488 with 98.1, 99.2, and 97.6% amino acid similarity to Cj1646, Cj1647, and Cj1648, respectively. *miaB* or *yrbB* were absent in the *C. jejuni* strains used in this study.  $\epsilon$  proteobacteria have previously been reported to lack *miaB* homologs (Roier et al., 2016). The MLA nomenclature will be used for this study. The *C. jejuni* 11168 published annotated whole genome sequence (Sanger database: ID CJ11168 accession number AL111168) has assigned color qualifiers based on predicted functionality. MlaDEFC are predicted to be functionally linked to cell surfaces (IM, OM, secreted, surface structures). MlaA is predicted to be functionally linked to pathogenicity, adaptation, and chaperones (Figure 1).

### No Change in Sensitivity of *miaA* Mutant to Detergent Compared to Wild-Type Strains

As the MLA pathway is proposed to play a role in the maintenance of the bacterial OM (Malinverni and Silhavy, 2009), the membrane integrity of the *miaA* mutants was investigated to ensure any changes in OMV production were not an artifact of a fragile OM. Membrane permeability of the *C. jejuni* 11168 parent

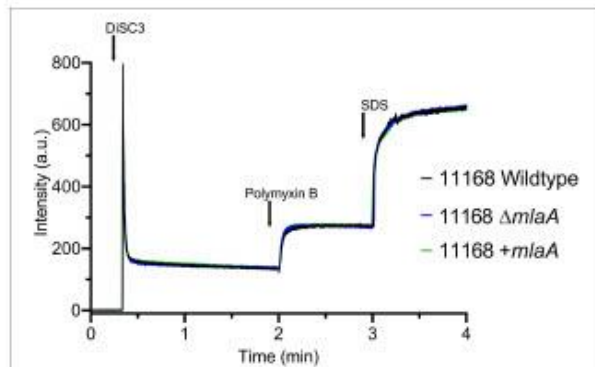


**FIGURE 2 |** Membrane permeability of the *C. jejuni* 11168 wild-type strain, isogenic *m1aA* deletion mutant ( $\Delta m1aA$ ), and complemented ( $+m1aA$ ) strain. Permeability of intact cells was measured using the fluorescent probe 3,3'-Dipropylthiadicarbocyanine iodide (DISC3) which accumulates on, and translocates into, hyperpolarized lipid bilayers. Cells were washed prior to the assay, removing OMVs, to measure parent cell membrane permeability. Polymyxin B was added to the cells at a final concentration of 100  $\mu$ M and release of DISC3 from the membrane was measured. SDS was added at a final concentration of 20 mM to measure maximum fluorescence.

cell membranes in the absence of OMVs was analyzed using the DiSC3 assay. *C. jejuni* cells were washed (removing OMVs) then re-suspended in assay buffer. There was no significant difference in percentage incorporation of the dye after membrane stress with 100  $\mu$ M final concentration polymyxin B between the 11168 wild-type, *m1aA* mutant or complement strain (Figure 2).

Growth or survival during culture conditions in the presence of detergents (LSB and ST) were used to investigate membrane integrity. No significant difference in growth rates measured by either OD<sub>600</sub> readings or CFUs was observed prior to stationary phase for either the *m1aA* mutant or the complemented mutant when compared to the respective wild-type strain. There was also no significant difference observed for any strain when grown in the presence of 0.2% (w/v) ST (biologically relevant concentration) compared to the same strain cultured in Brucella broth alone prior to stationary phase. The *C. jejuni* 11168 strain was able to grow to higher CFU and OD<sub>600</sub> values than the *C. jejuni* 488 strain (Figure S1).

Survival of bacteria in the presence of high concentrations of detergent was investigated either by plating bacteria onto agar supplemented with 1.25 mM LSB or by culturing bacteria in Brucella broth supplemented with 2% (w/v) ST. Survival of both the *m1aA* mutant and complement strains was comparable to the corresponding wild-type strains for both detergents (Figures 3A,B). 1.25 mM LSB caused around a 4-log reduction in growth for 11168 strains compared to around a 2-log reduction for 488 strains. Less than a log reduction in growth was observed for bacteria cultured in 2% (w/v) ST (Figure 3B).

### *m1aA* Mutants Exhibit Increased Resistance to Polymyxin B

Polymyxin B targets cells through binding to LOS or lipopolysaccharide (LPS), meaning OMVs are capable of binding

polymyxin B in the extracellular environment (Manning and Kuehn, 2011). Resistance to a low concentration of polymyxin B (2.5  $\mu$ g/ml) was used as an initial screen for increased OMV production in the *m1aA* mutants compared to the respective wild-type strains. The *C. jejuni* 11168 and 488 *m1aA* mutants were significantly more resistant to polymyxin B compared to their wild-type strains under culture conditions. Complementation of the 11168 *m1aA* mutant with the *m1aA* gene under the control of the native promoter almost completely restored wild-type polymyxin B sensitivity, however, complementation of the 488 *m1aA* mutant with the *m1aA* gene under the control of a constitutive chloramphenicol promoter did not. It would appear that the expression of the inserted *m1aA* gene in the 488 *m1aA* complement is not sufficient to restore the wild-type phenotype under these stress conditions (Figure 3C).

### *m1aA* Mutation Results in Increased OMV Production

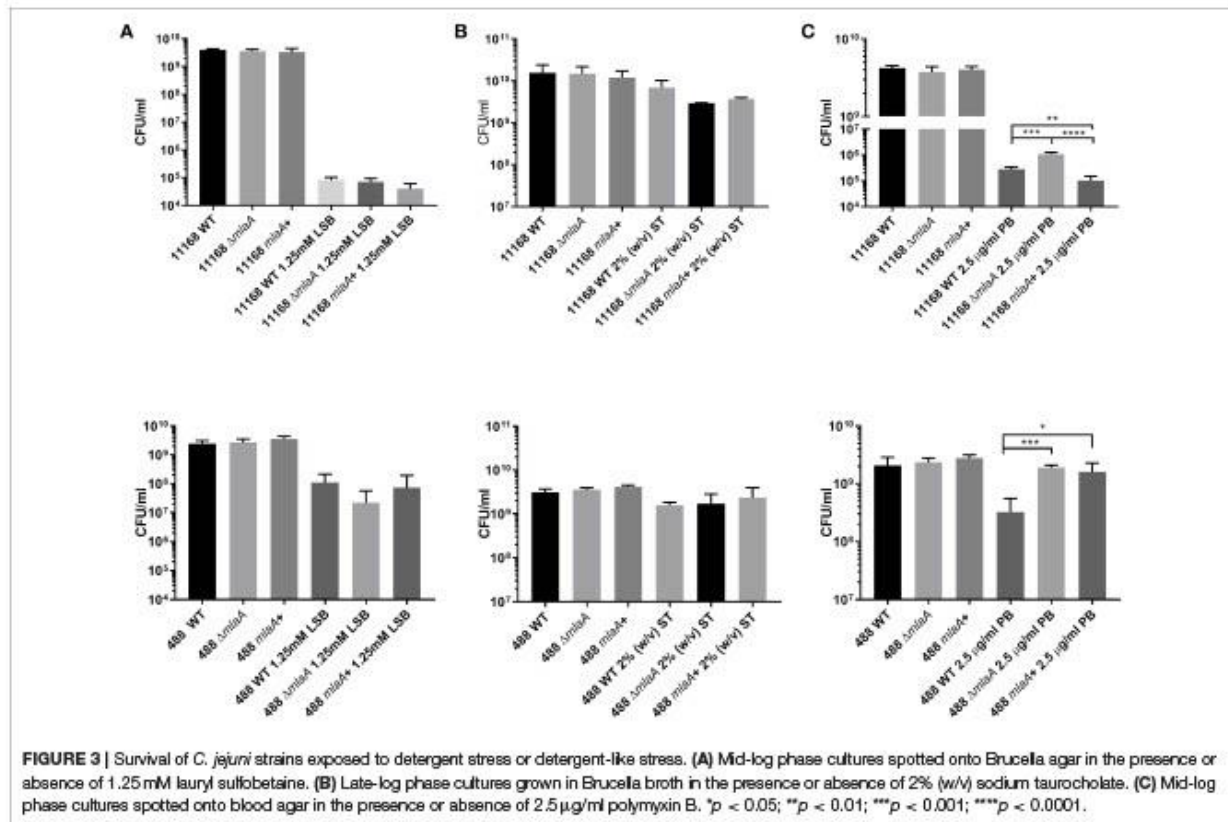
Total protein and KDO concentration were used to quantify OMV preparations. KDO is a component of LOS and can be used to indicate the amount of OM present. As protein and KDO concentrations are unable to determine if OMV preparations contain more OMVs or larger OMVs, NTA was used to verify any changes in production. OMV preparations were from bacterial cultures of equivalent volume and OD<sub>600</sub> readings. OMV preparations isolated from the *C. jejuni* 11168 *m1aA* mutant had significantly higher concentrations of both protein and KDO compared to the wild-type and complement strains (Figure 4). The OMV preparations of the *m1aA* mutant strains were also confirmed to contain more OMVs by NTA particle counts (Figure S2).

### Co-culture With Sodium Taurocholate Increases Lipid and Protein Concentration of *C. jejuni* OMVs

To investigate the link between ST and OMV production proposed by Elmi et al. (2018), OMVs were isolated from *C. jejuni* 11168 wild-type, *m1aA* mutant, and complement strains co-cultured with 0.2% (w/v) ST. OMV preparations isolated from ST supplemented cultures had significantly higher concentrations of KDO for the wild-type and complement strains (Figure 5). ST did not increase the KDO concentration of the *m1aA* mutant OMV preparations. Protein concentrations were significantly higher for the wild-type strain in the presence of ST and higher, but not significantly so for the *m1aA* complement strain. The protein concentration did not increase in the presence of ST for the *m1aA* mutant (Figure 5). The increase in OMVs based on KDO and protein concentrations in the presence of ST for the wild-type and complement strain also correlated to an increase in particle number for NTA (Figure S2).

### Changes in Lipid and Protein Concentration of OMVs Are Inversely Proportional to OMV Size

In addition to quantifying OMV production levels, the size of the OMVs produced were also investigated by NTA. OMV



preparations from all strains and all conditions contained one main size cluster which contained 92–99% of the population. An increase in protein, KDO and particle number either in the presence of ST or in the absence of a complete MLA pathway correlated to a reduction in OMV size. OMVs isolated from the *C. jejuni* 11168 wild-type, *miaA* mutant, and *miaA* complement strain had a mode diameter of 177, 140, and 184 nm, respectively, when isolated from cultures grown in Brucella broth. When co-cultured with 0.2% (w/v) ST, ST-OMV mode diameters were 137, 133, and 159 for the 11168 wild-type, *miaA* mutant, and *miaA* complement strains, respectively (Figure 6). A similar inverse correlation between OMV quantity and size was also observed for mean OMV diameters (Figure S2).

### Co-culture of *C. jejuni* With Sodium Taurocholate Results in Reduced Gene Expression of *miaA* and *miaC*

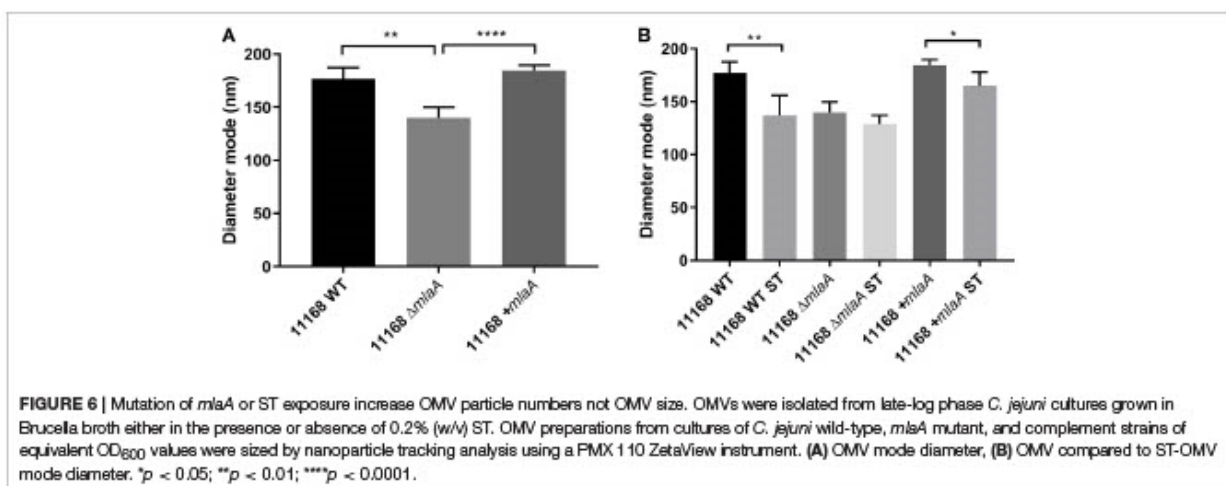
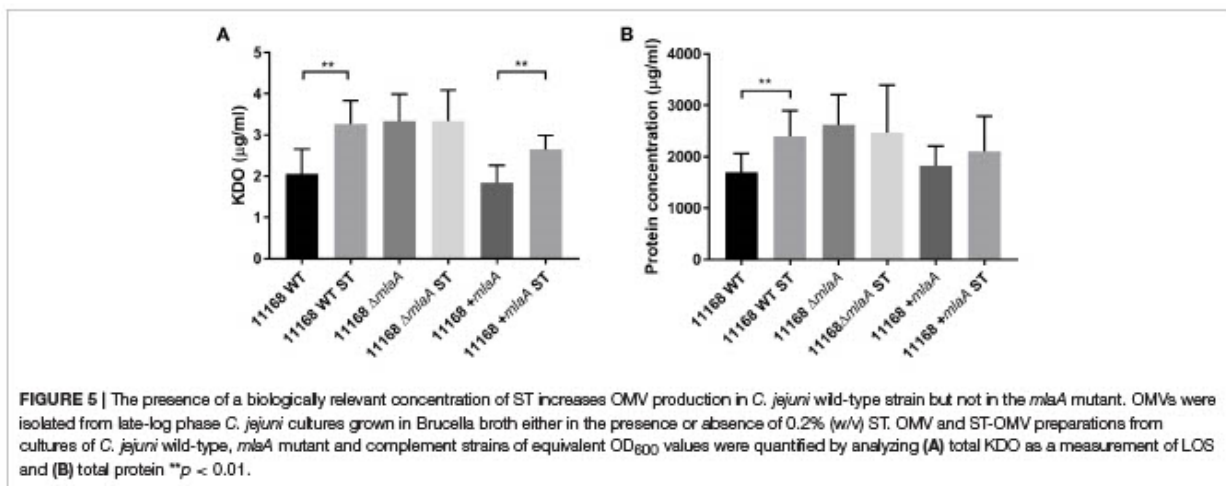
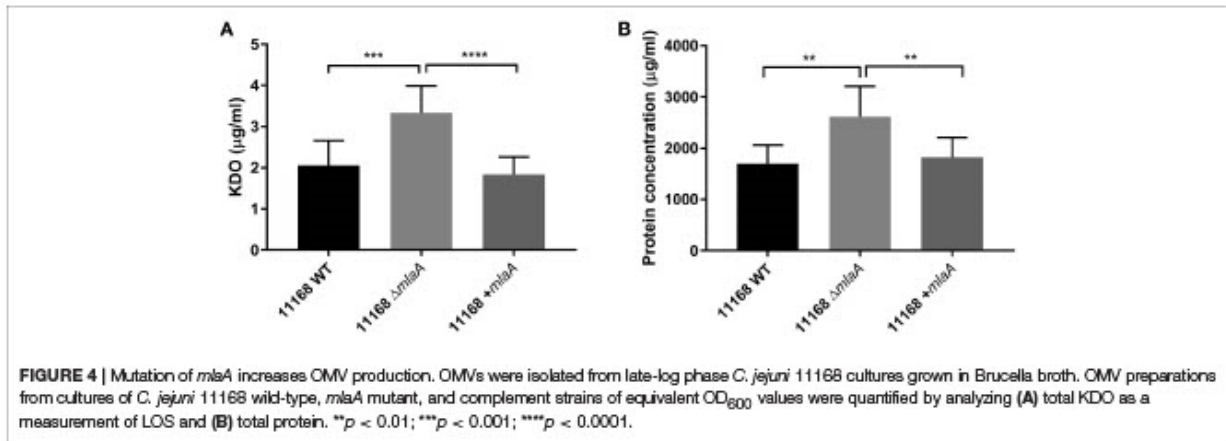
As the *C. jejuni* 11168 *miaA* mutant was not observed to increase OMV production in the presence of 0.2% (w/v) ST in contrast to the wild-type strain, the effect of 0.2% (w/v) ST on the relative expression of genes encoding components of the MLA pathway was investigated. *miaA* and *miaC* were selected for investigation. RNA was isolated from mid-log phase cultures of the *C. jejuni* 11168 and 488 wild-type strains. A

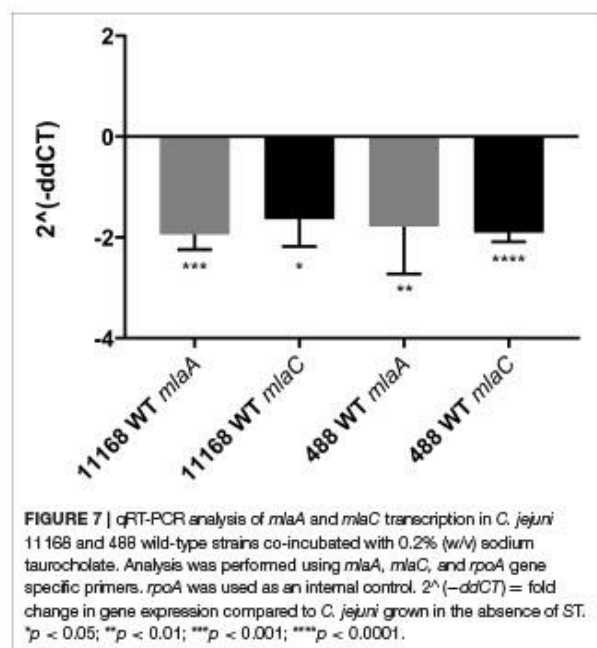
statistically significant approximate 2-fold down-regulation of gene expression of both *miaA* and *miaC* in both wild-type strains (11168 and 488) in the presence of ST compared to the absence of ST, was observed relative to the *rpoA* internal control (Figure 7).

## DISCUSSION

Previous characterizations of the cargo of *C. jejuni* OMVs have identified biologically active compounds that contribute to immunogenicity, cytotoxicity, and the breakdown of the gut barrier mediated by bacterial proteases (Jang et al., 2014; Elmi et al., 2016, 2018). The mechanisms regulating OMV production in *C. jejuni* however, are still poorly understood. In this study, we have characterized both the role of the MLA pathway in *C. jejuni* OMV production, as well as the role of ST in regulating the MLA pathway. OMV production in *C. jejuni* was increased either in the presence of a biologically relevant concentration of ST or in the absence of a complete MLA pathway, linking the model proposed by Roier et al. (2016) with the ST phenotype observed by Elmi et al. (2018).

Despite the bacteriostatic effect of bile salts (Begley et al., 2005), in this study *C. jejuni* was shown to be highly tolerant to ST stress, showing less than a log-reduction in growth at 2% (w/v) ST, a concentration higher than is considered to be biologically relevant (Elmi et al., 2018). This then suggests that much lower





and biologically relevant concentrations of ST could act as stimuli without compromising bacterial growth or membrane integrity. This is in agreement with a previous study (Elmi et al., 2018), which did not observe any defect in growth of *C. jejuni* associated with a biologically relevant concentration of ST (0.2% w/v). The effect of a combination of bile salts similar to that expected to be found in the human gut was not investigated in this study, however, the resistance to ST demonstrated here highlights the exquisite adaptation of *C. jejuni* to the gut environment where localized signals co-ordinate bacterial behavior.

There is conflicting evidence in the literature regarding the impact of *mla* mutations on membrane integrity. Malinverni and Silhavy (2009) observed increased sensitivity of *E. coli mla* mutants to SDS in combination with EDTA, but not to SDS alone. EDTA is a chelating compound that is thought to destabilize LPS to increase membrane permeability (Finnegan and Percival, 2015). The metabolic cost, rather than the membrane integrity of the *E. coli mla* mutants unable to down-regulate OMV production as well as patching areas effected by EDTA, could be the more likely cause of the increased mutant sensitivity. Abellon-Ruiz et al. (2017) observed growth defects in an *E. coli mlaA* mutant compared to the wild-type strain in the presence of both doxycycline and chlorpromazine. This suggested that the PL accumulation at the OM created transient patches of PL bilayer creating windows of opportunity for small molecules that are readily able to diffuse through PL bilayers to enter the cell. However, as an *mla* mutant is unable to down-regulate the creation of these PL bilayer patches, this membrane defect phenotype would be less applicable to a wild-type strain which would be able to up-regulate OMV production without

compromising integrity in favorable conditions and down-regulate production reducing the creation of these patches in unfavorable conditions. Roier et al. (2016) also did not observe any obvious membrane defects for the *mla* mutants in response to detergent stress, supporting the model that increased OMV production is due to a regulated process and is not an artifact of an unstable membrane.

As the membrane of an OMV contains either LOS or LPS, it has been suggested OMVs can confer protection against compounds that target or bind to this component of the bacterial membrane, such as bacteriophage or polymyxin B. This was demonstrated by a study that examined the ability of OMVs to protect against low concentrations of polymyxin B (Manning and Kuehn, 2011). Resistance to this antibiotic is normally achieved through modifications of LOS or LPS preventing the antibiotic binding to the bacterial OM. Manning and Kuehn (2011) observed that only OMVs from polymyxin B sensitive strains conferred protection against polymyxin B when added to a culture of a polymyxin B sensitive bacteria, as polymyxin B was unable to bind to OMVs produced by a polymyxin B resistant strain. Here we demonstrated that there was no significant difference in resistance to polymyxin B between the 11168 wild-type strain and the *mlaA* mutant when cells were washed and supernatant discarded to remove OMVs. The fluorescent probe DiSC3 accumulates on, and translocates into, hyperpolarized lipid bilayers, so the DiSC3 assay was used to investigate changes in bacterial membrane permeability. After the addition of polymyxin B, there was no difference in the change in bacterial membrane permeability of the *mlaA* mutant compared to the 11168 wild-type strain. Based on these results, resistance to a low concentration of polymyxin B (2.5 μg/ml) under culture conditions was investigated as an initial screen for increased OMV production by *mlaA* mutants. A positive correlation between increased OMV production and polymyxin B resistance was observed. As OMV isolation is laborious, this could provide a quick and easy initial screen for OMV production levels.

Both in this study and in a previous study (Elmi et al., 2018), a biologically relevant concentration of ST was shown to stimulate OMV production. 0.2% (w/v) ST was observed to almost double OMV production by the *C. jejuni* 11168 wild-type strain. Mutation of *mlaA* increased OMV production by the same magnitude in the absence of ST, whilst ST did not significantly further stimulate OMV production by the *mlaA* mutant. This increase was also shown by NTA to be due to the presence of increased numbers of OMVs rather than larger OMVs. The increase in OMV production was also associated with a small reduction in OMV size. It is possible that this is due to an increase in PLs in the membrane of the OMVs, based on the model proposed by Roier et al. (2016), altering the membrane curvature during the formation of the OMV. The reduced size of wild-type ST-OMVs was also similar to that of the *mlaA* mutant OMVs. Both the *mlaA* mutant OMVs and wild-type ST-OMVs had comparable diameters. This is in contrast to data from a recent study (Taheri et al., 2018) which did not observe increased OMV production in response to ox bile. Ox bile was used to represent a mixture of bile salts, similar to what would

be found in the gut, whereas ST alone was used in this study, a single component of human bile. Bile composition not only varies between species but also between individuals of the same species, as well as depending on the location in the gut (Sjövall, 1959; Falany et al., 1994; Nagana Gowda et al., 2009; Chiang, 2017). For example, in humans the proportion of taurine to glycine conjugated bile salts is diet determined. Humans with a taurine rich diet (animal-based products) will have a higher proportion of taurine conjugated bile salts compared to low taurine diet (Sjövall, 1959; Wojcik et al., 2010; Ridlon et al., 2016). As oxes are herbivores, the bile pool composition maybe low in taurine conjugated bile salts, such as sodium taurocholate. Previous work by Elmi et al. (2018) found the effect of sodium taurocholate on OMV production to be dose-dependent. The low dose of ox bile used in this other study, along with the potentially low proportion of taurine conjugates within the ox bile, could explain the different results observed between these studies.

Roier et al. proposed that iron limitation regulates the MLA pathway in *H. influenzae*, *V. cholera*, and *E. coli* in a Fur dependent manner. However, a RNA sequencing study did not highlight a link between Fur and the MLA pathway in *C. jejuni* (Butcher et al., 2015). As ST has previously been linked to *C. jejuni* virulence and OMV production, ST was investigated as a potential regulator of the *C. jejuni* MLA pathway. The differential effect ST had on OMV production in the *C. jejuni* 11168 wild-type strain compared to the *m1aA* mutant suggests a direct interaction between ST and the MLA pathway in *C. jejuni*. These are the first data suggesting a role for bile salts in regulating the MLA pathway. The qRT-PCR results in this study showed around a 2-fold down-regulation of *m1aA* and *m1aC* in response to ST exposure, further strengthening the hypothesized interaction between ST and the MLA pathway in *C. jejuni*. As previous studies have suggested removing one component of the MLA pathway prevents functionality (Malinverni and Silhavy, 2009; Roier et al., 2016), this could explain why ST appeared to have no effect on OMV production in a single *m1aA* mutant.

In summary, the data in this study suggests *C. jejuni* can regulate OMV production in response to host gut signals through changes in expression of the MLA pathway. Increased OMV production without compromising membrane stability was observed in a *m1aA* mutant and a potential mechanism for the ST-OMV phenotype was identified. In the presence of ST, OMV production was shown to increase in the wild-type strain, but not in a *m1aA* mutant. Growth of *C. jejuni* in the presence of ST also resulted in reduced expression of both *m1aA* and *m1aC*. Our data supports the MLA model

of OMV production and the link between bile salts and potential virulence regulation in *C. jejuni*. As the gut bile composition is dependent on both diet and the microbiota, this study highlights the potential importance of diet and lifestyle factors on the varying disease presentations associated with gut pathogen infection.

## DATA AVAILABILITY

All datasets generated for this study are included in the manuscript and/or the **Supplementary Files**.

## AUTHOR CONTRIBUTIONS

DK and ND conceived this study. CD, AT, AE, JW, JL, AG, and OG all performed experiments that contributed to this manuscript. CD, DK, and ND wrote the manuscript, with significant input from AT, AE, OG, and BW.

## FUNDING

AT was funded by a Doctoral Training Partnership (DTP) studentship from the UK Biotechnology and Biological Sciences Research Council (BBSRC).

## ACKNOWLEDGMENTS

The authors gratefully acknowledge the support of the Biotechnology and Biological Sciences Research Council Institute Strategic Programme BB/R012504/1 constituent project BBS/E/F/000PR10349.

## SUPPLEMENTARY MATERIAL

The Supplementary Material for this article can be found online at: <https://www.frontiersin.org/articles/10.3389/fcimb.2019.00177/full#supplementary-material>

**Figure S1** | Growth curves of *C. jejuni* 11168 wild-type strain compared to the 488 wild-type strain. Strains were grown in Brucella broth under microaerobic conditions at 37°C. Growth was characterized by measuring (A) OD<sub>600</sub> values and (B) colony forming units (CFUs) every 2 h for 18 h.

**Figure S2** | Mutation of *m1aA* or ST exposure increase OMV particle numbers not OMV size. OMVs were isolated from late-log phase *C. jejuni* cultures grown in Brucella broth either in the presence or absence of 0.2% (w/v) ST. OMV preparations from cultures of *C. jejuni* wild-type, *m1aA* mutant, and complement strains of equivalent OD<sub>600</sub> values were sized by nanoparticle tracking analysis using a PMX 110 ZetaView instrument. (A) Particle counts per ml and (B) OMV mode diameter, mean and median diameters (nm).

## REFERENCES

Abellon-Ruiz, J., Kaptan, S. S., Basle, A., Claudi, B., Bumann, D., Kleinekathofer, U., et al. (2017). Structural basis for maintenance of bacterial outer membrane lipid asymmetry. *Nat. Microbiol.* 2, 1616–1623. doi: 10.1038/s41564-017-0046-x

Altindis, E., Fu, Y., and Mekalanos, J. J. (2014). Proteomic analysis of *Vibrio cholerae* outer membrane vesicles. *Proc. Natl.*

*Acad. Sci. U. S. A.* 111, E1548–E1556. doi: 10.1073/pnas.1403683111

Begley, M., Gahan, C. G. M., and Hill, C. (2005). The interaction between bacteria and bile. *FEMS Microbiol. Rev.* 29, 625–651. doi: 10.1016/j.femsre.2004.09.003

Bielaszewska, M., Ritter, C., Bauwens, A., Greune, L., Jarosch, K.-A., Steil, D., et al. (2017). Host cell interactions of outer membrane vesicle-associated virulence factors of enterohemorrhagic *Escherichia coli* O157: intracellular

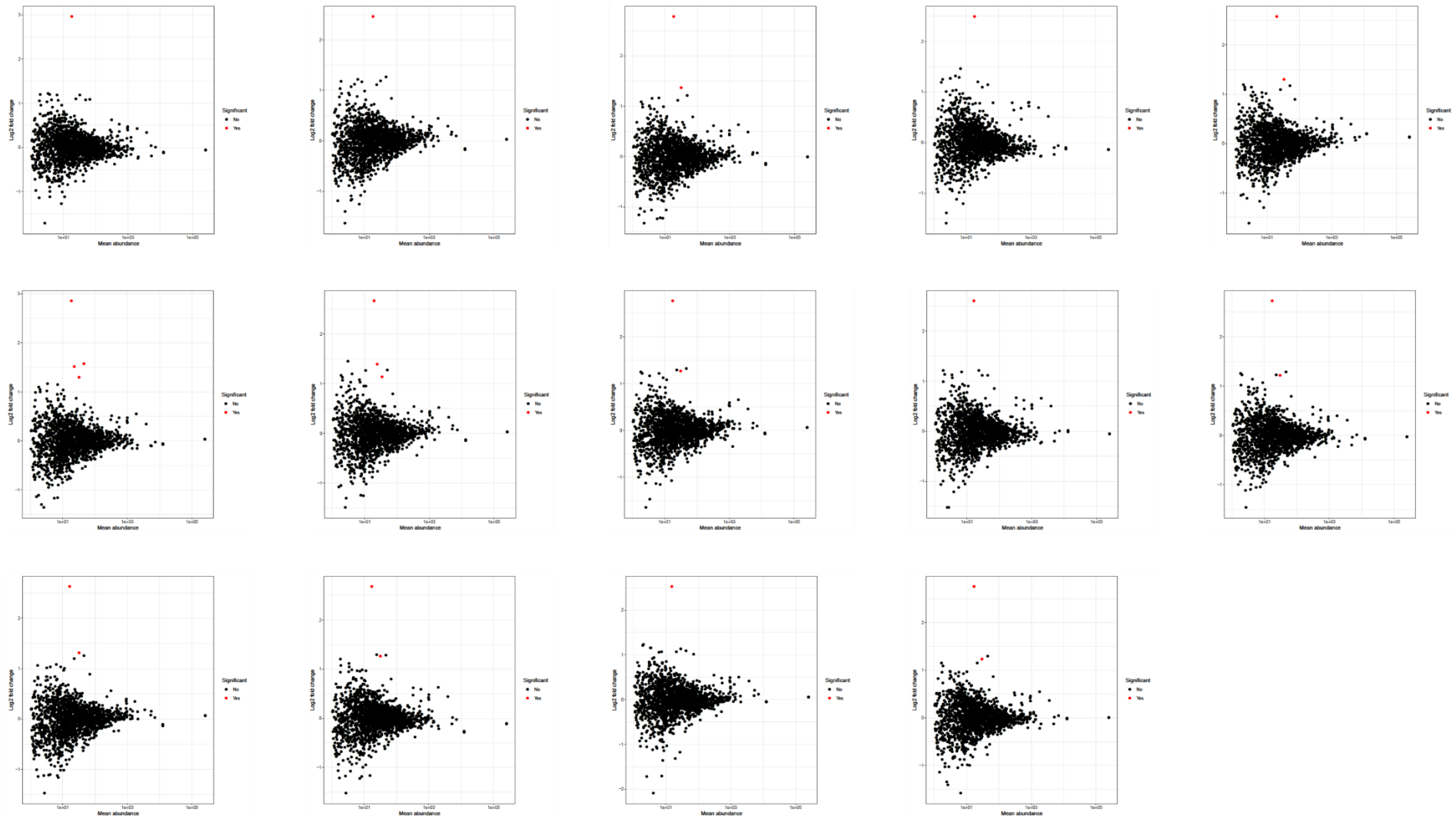
- delivery, trafficking and mechanisms of cell injury. *PLoS Pathog.* 13:e1006159. doi: 10.1371/journal.ppat.1006159
- Bitto, N. J., Chapman, R., Pidot, S., Costin, A., Lo, C., Choi, J., et al. (2017). Bacterial membrane vesicles transport their DNA cargo into host cells. *Sci. Rep.* 7:7072. doi: 10.1038/s41598-017-07288-4
- Bleumink-Pluym, N. M., Van Alphen, L. B., Bouwman, L. I., Wosten, M. M., and Van Putten, J. P. (2013). Identification of a functional type VI secretion system in *Campylobacter jejuni* conferring capsule polysaccharide sensitive cytotoxicity. *PLoS Pathog.* 9:e1003393. doi: 10.1371/journal.ppat.1003393
- Bomberger, J. M., Maceachran, D. P., Coutermarsh, B. A., Ye, S., O'toole, G. A., and Stanton, B. A. (2009). Long-distance delivery of bacterial virulence factors by *Pseudomonas aeruginosa* outer membrane vesicles. *PLoS Pathog.* 5:e1000382. doi: 10.1371/journal.ppat.1000382
- Bonnington, K. E., and Kuehn, M. J. (2014). Protein selection and export via outer membrane vesicles. *Biochim. Biophys. Acta* 1843, 1612–1619. doi: 10.1016/j.bbamcr.2013.12.011
- Butcher, J., Handley, R. A., Van Vliet, A. H., and Stintzi, A. (2015). Refined analysis of the *Campylobacter jejuni* iron-dependent/independent Fur- and PerR-transcriptomes. *BMC Genomics* 16:498. doi: 10.1186/s12864-015-1661-7
- Carver, T. J., Rutherford, K. M., Berriman, M., Rajandream, M.-A., Barrell, B. G., and Parkhill, J. (2005). ACT: the Artemis comparison tool. *Bioinformatics* 21, 3422–3423. doi: 10.1093/bioinformatics/bti553
- Chiang, J. Y. (2017). Recent advances in understanding bile acid homeostasis. *Homeostasis* 6:2029. doi: 10.12688/h0009research.12449.1
- Deatherage, B. L., Lara, J. C., Bergsbaken, T., Rassouljan Barrett, S. L., Lara, S., and Cookson, B. T. (2009). Biogenesis of bacterial membrane vesicles. *Mol. Microbiol.* 72, 1395–1407. doi: 10.1111/j.1365-2958.2009.06731.x
- Elhenawy, W., Bording-Jorgensen, M., Valguamera, E., Haurat, M. F., Wine, E., and Feldman, M. F. (2016). LPS remodeling triggers formation of outer membrane vesicles in salmonella. *MBio* 7:e00940-16. doi: 10.1128/mBio.00940-16
- Elmi, A., Dorey, A., Watson, E., Jagatia, H., Inglis, N. F., Gundogdu, O., et al. (2018). The bile salt sodium taurocholate induces *Campylobacter jejuni* outer membrane vesicle production and increases OMV-associated proteolytic activity. *Cell Microbiol.* 20:e12814. doi: 10.1111/cmi.12814
- Elmi, A., Nasher, F., Jagatia, H., Gundogdu, O., Bajaj-Elliott, M., Wren, B., et al. (2016). *Campylobacter jejuni* outer membrane vesicle-associated proteolytic activity promotes bacterial invasion by mediating cleavage of intestinal epithelial cell E-cadherin and occludin. *Cell Microbiol.* 18, 561–572. doi: 10.1111/cmi.12534
- Elmi, A., Watson, E., Sandu, P., Gundogdu, O., Mills, D. C., Inglis, N. F., et al. (2012). *Campylobacter jejuni* outer membrane vesicles play an important role in bacterial interactions with human intestinal epithelial cells. *Infect. Immun.* 80, 4089–4098. doi: 10.1128/IAI.00161-12
- Falany, C. N., Johnson, M. R., Barnes, S., and Diasio, R. B. (1994). Glycine and taurine conjugation of bile acids by a single enzyme. Molecular cloning and expression of human liver bile acid CoA:amino acid N-acyltransferase. *J. Biol. Chem.* 269, 19375–19379.
- Finnegan, S., and Percival, S. L. (2015). EDTA: an antimicrobial and antibiofilm agent for use in wound care. *Adv. Wound Care* 4, 415–421. doi: 10.1089/wound.2014.0577
- Gundogdu, O., Mills, D. C., Elmi, A., Martin, M. J., Wren, B. W., and Dorrell, N. (2011). The *Campylobacter jejuni* transcriptional regulator Cj1556 plays a role in the oxidative and aerobic stress response and is important for bacterial survival *in vivo*. *J. Bacteriol.* 193, 4238–4249. doi: 10.1128/JB.05189-11
- Jang, K. S., Sweredoski, M. J., Graham, R. L., Hess, S., and Clemons, W. M. Jr. (2014). Comprehensive proteomic profiling of outer membrane vesicles from *Campylobacter jejuni*. *J. Proteomics* 98, 90–98. doi: 10.1016/j.jprot.2013.12.014
- Jervis, A. J., Butler, J. A., Wren, B. W., and Linton, D. (2015). Chromosomal integration vectors allowing flexible expression of foreign genes in *Campylobacter jejuni*. *BMC Microbiol.* 15:230. doi: 10.1186/s12866-015-0559-5
- Kaakoush, N. O., Castano-Rodriguez, N., Mitchell, H. M., and Man, S. M. (2015). Global epidemiology of *Campylobacter* infection. *Chin. Microbiol. Rev.* 28, 687–720. doi: 10.1128/CMR.00006-15
- Karlyshev, A. V., Thacker, G., Jones, M. A., Clements, M. O., and Wren, B. W. (2014). *Campylobacter jejuni* gene cj0511 encodes a serine peptidase essential for colonisation. *FEBS Open Bio.* 4, 468–472. doi: 10.1016/j.fob.2014.04.012
- Koepfen, K., Hampton, T. H., Jarek, M., Scharfe, M., Gerber, S. A., Mielcarz, D. W., et al. (2016). A novel mechanism of host-pathogen interaction through srna in bacterial outer membrane vesicles. *PLoS Pathog.* 12:e1005672. doi: 10.1371/journal.ppat.1005672
- Kuehn, M. J., and Kesty, N. C. (2005). Bacterial outer membrane vesicles and the host-pathogen interaction. *Genes Dev.* 19, 2645–2655. doi: 10.1101/gad.1299905
- Kulkarni, H. M., Nagaraj, R., and Jagannadham, M. V. (2015). Protective role of *E. coli* outer membrane vesicles against antibiotics. *Microbiol. Res.* 181, 1–7. doi: 10.1016/j.micres.2015.07.008
- Kulp, A., and Kuehn, M. J. (2010). Biological functions and biogenesis of secreted bacterial outer membrane vesicles. *Annu. Rev. Microbiol.* 64, 163–184. doi: 10.1146/annurev.micro.091208.073413
- Lee, C.-H., and Tsai, C.-M. (1999). Quantification of bacterial lipopolysaccharides by the purpald assay: measuring formaldehyde generated from 2-keto-3-deoxyoctonate and heptose at the inner core by periodate oxidation. *Anal. Biochem.* 267, 161–168. doi: 10.1006/abio.1998.2961
- Lindmark, B., Rompikuntal, P. K., Vaitkevicius, K., Song, T., Mizunoe, Y., Uhlin, B. E., et al. (2009). Outer membrane vesicle-mediated release of cytolethal distending toxin (CDT) from *Campylobacter jejuni*. *BMC Microbiol.* 9:220. doi: 10.1186/1471-2180-9-220
- Malinverni, J. C., and Silhavy, T. J. (2009). An ABC transport system that maintains lipid asymmetry in the gram-negative outer membrane. *Proc. Natl. Acad. Sci. U. S. A.* 106, 8009–8014. doi: 10.1073/pnas.0903229106
- Manning, A. J., and Kuehn, M. J. (2011). Contribution of bacterial outer membrane vesicles to innate bacterial defense. *BMC Microbiol.* 11:258. doi: 10.1186/1471-2180-11-258
- Mashburn, L. M., and Whiteley, M. (2005). Membrane vesicles traffic signals and facilitate group activities in a prokaryote. *Nature* 437, 422–425. doi: 10.1038/nature03925
- Mashburn-Warren, L., Howe, J., Garidel, P., Richter, W., Steiniger, F., Roessel, M., et al. (2008). Interaction of quorum signals with outer membrane lipids: insights into prokaryotic membrane vesicle formation. *Mol. Microbiol.* 69, 491–502. doi: 10.1111/j.1365-2958.2008.06302.x
- McBroome, A. J., and Kuehn, M. J. (2007). Release of outer membrane vesicles by gram-negative bacteria is a novel envelope stress response. *Mol. Microbiol.* 63, 545–558. doi: 10.1111/j.1365-2958.2006.05522.x
- Nagana Gowda, G. A., Shanaiah, N., Cooper, A., Maluccio, M., and Raftery, D. (2009). Bile acids conjugation in human bile is not random: new insights from (1)H-NMR spectroscopy at 800 MHz. *Lipids* 44, 527–535. doi: 10.1007/s11745-009-3296-4
- Parkhill, J., Wren, B. W., Mungall, K., Ketley, J. M., Churcher, C., Basham, D., et al. (2000). The genome sequence of the food-borne pathogen *Campylobacter jejuni* reveals hypervariable sequences. *Nature* 403:665. doi: 10.1038/35001088
- Ridlon, J. M., Wolf, P. G., and Gaskins, H. R. (2016). Taurocholic acid metabolism by gut microbes and colon cancer. *Gut Microbes* 7, 201–215. doi: 10.1080/19490976.2016.1150414
- Ritz, M., Garenaux, A., Berge, M., and Federighi, M. (2009). Determination of rpoA as the most suitable internal control to study stress response in *C. jejuni* by RT-qPCR and application to oxidative stress. *J. Microbiol. Methods* 76, 196–200. doi: 10.1016/j.mimet.2008.10.014
- Roier, S., Zing, F. G., Cakar, F., Durakovic, S., Kohl, P., Eichmann, T. O., et al. (2016). A novel mechanism for the biogenesis of outer membrane vesicles in gram-negative bacteria. *Nat. Commun.* 7:10515. doi: 10.1038/ncomms10515
- Schmittgen, T. D., and Livak, K. J. (2008). Analyzing real-time PCR data by the comparative CT method. *Nat. Protoc.* 3, 1101–1108. doi: 10.1038/nprot.2008.73
- Schooling, S. R., and Beveridge, T. J. (2006). Membrane vesicles: an overlooked component of the matrices of biofilms. *J. Bacteriol.* 188, 5945–5957. doi: 10.1128/JB.00257-06
- Schwechheimer, C., and Kuehn, M. J. (2015). Outer-membrane vesicles from gram-negative bacteria: biogenesis and functions. *Nat. Rev. Microbiol.* 13, 605–619. doi: 10.1038/nrmicro3525
- Silva, J., Leite, D., Fernandes, M., Mena, C., Gibbs, P. A., and Teixeira, P. (2011). *Campylobacter* spp. as a foodborne pathogen: a review. *Front. Microbiol.* 2:200. doi: 10.3389/fmicb.2011.00200
- Sjövall, J. (1959). Dietary glycine and taurine on bile acid conjugation in man. bile acids and steroids 75. *Proc. Soc. Exp. Biol. Med.* 100, 676–678. doi: 10.3181/00379727-100-24741

- Song, T., Mika, F., Lindmark, B., Liu, Z., Schild, S., Bishop, A., et al. (2008). A new vibrio cholerae sRNA modulates colonization and affects release of outer membrane vesicles. *Mol. Microbiol.* 70, 100–111. doi: 10.1111/j.1365-2958.2008.06392.x
- Taheri, N., Fallman, M., Wai, S. N., and Fahlgren, A. (2019). Accumulation of virulence-associated proteins in *Campylobacter jejuni* outer membrane vesicles at human body temperature. *J. Proteomics* 195, 33–40. doi: 10.1016/j.jpro.2019.01.005
- Taheri, N., Mahmud, A., Sandblad, L., Fallman, M., Wai, S. N., and Fahlgren, A. (2018). *Campylobacter jejuni* bile exposure influences outer membrane vesicles protein content and bacterial interaction with epithelial cells. *Sci. Rep.* 8:16996. doi: 10.1038/s41598-018-35409-0
- Taylor, A. J., Zakai, S. A., and Kelly, D. J. (2017). The periplasmic chaperone network of *Campylobacter jejuni*: evidence that SalC (Cj1289) and PpiD (Cj0694) are involved in maintaining outer membrane integrity. *Front. Microbiol.* 8:531. doi: 10.3389/fmicb.2017.00531
- Tsatsaronis, J. A., Franch-Arroyo, S., Resch, U., and Charpentier, E. (2018). Extracellular vesicle RNA: a universal mediator of microbial communication? *Trends Microbiol.* 26, 401–410. doi: 10.1016/j.tim.2018.02.009
- Ugarte-Ruiz, M., Stabler, R. A., Dominguez, L., Porrero, M. C., Wren, B. W., Dorrell, N., et al. (2015). Prevalence of type VI secretion system in Spanish *Campylobacter jejuni* isolates. *Zoon. Public Health* 62, 497–500. doi: 10.1111/zph.12176
- Wojcik, O. P., Koenig, K. L., Zeleniuch-Jacquotte, A., Costa, M., and Chen, Y. (2010). The potential protective effects of taurine on coronary heart disease. *Atherosclerosis* 208, 19–25. doi: 10.1016/j.atherosclerosis.2009.06.002
- Yang, M., Liu, Z., Hughes, C., Stern, A. M., Wang, H., Zhong, Z., et al. (2013). Bile salt-induced intermolecular disulfide bond formation activates *Vibrio cholerae* virulence. *Proc. Natl. Acad. Sci. U. S. A.* 110, 2348–2353. doi: 10.1073/pnas.1218039110
- Zakharzhevskaya, N. B., Vanyushkina, A. A., Altukhov, I. A., Shavarda, A. L., Butenko, I. O., Rakićina, D. V., et al. (2017). Outer membrane vesicles secreted by pathogenic and non-pathogenic *Bacteroides fragilis* represent different metabolic activities. *Sci. Rep.* 7:5008. doi: 10.1038/s41598-017-05264-6
- Zhou, L., Srisatjaluk, R., Justus, D. E., and Doyle, R. J. (1998). On the origin of membrane vesicles in Gram-negative bacteria. *FEMS Microbiol. Lett.* 163, 223–228. doi: 10.1111/j.1574-6968.1998.tb13049.x

**Conflict of Interest Statement:** The authors declare that the research was conducted in the absence of any commercial or financial relationships that could be construed as a potential conflict of interest.

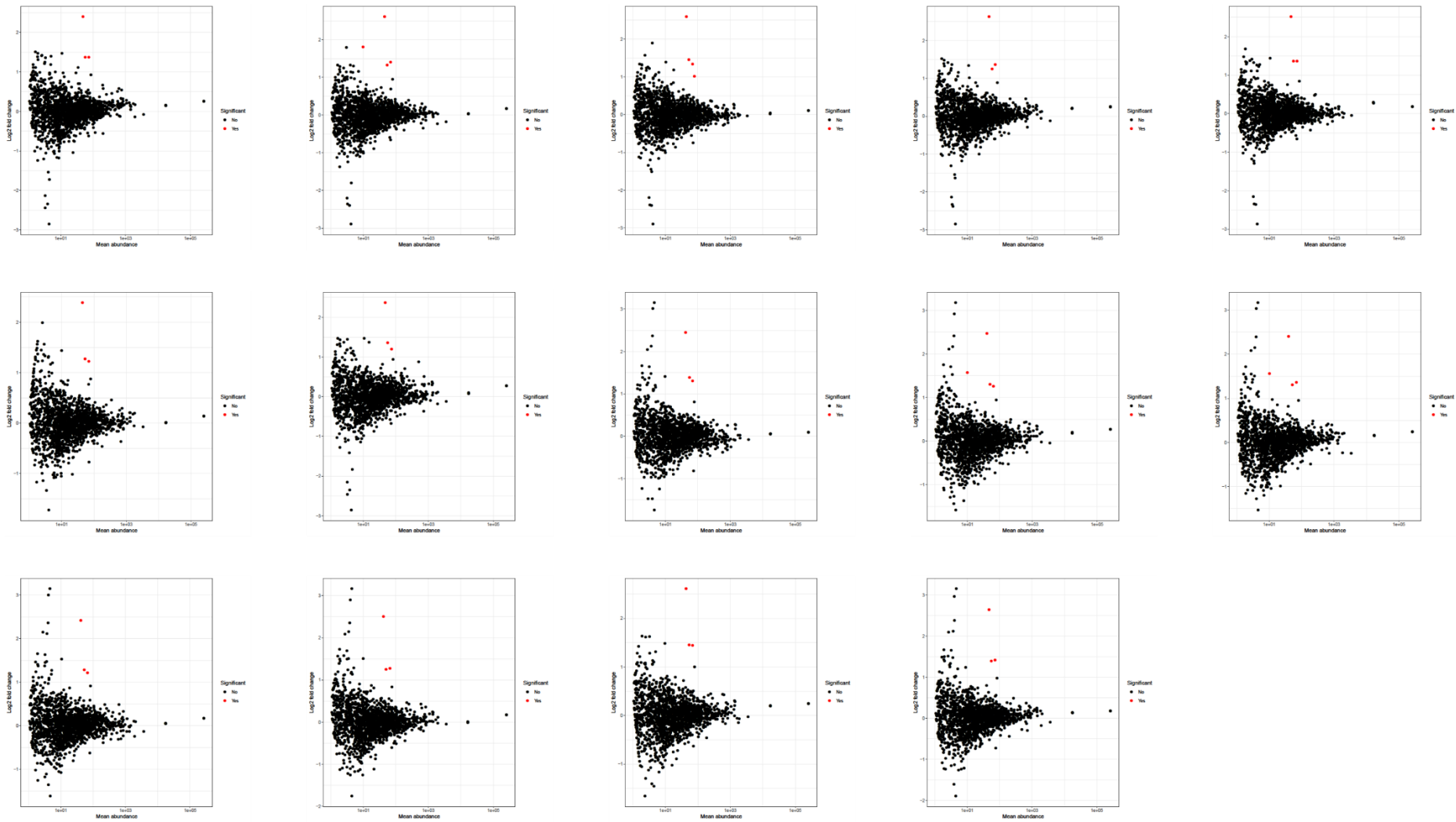
Copyright © 2019 Davies, Taylor, Elmi, Winter, Liaw, Grabowska, Gundogdu, Wren, Kelly and Dorrell. This is an open-access article distributed under the terms of the Creative Commons Attribution License (CC BY). The use, distribution or reproduction in other forums is permitted, provided the original author(s) and the copyright owner(s) are credited and that the original publication in this journal is cited, in accordance with accepted academic practice. No use, distribution or reproduction is permitted which does not comply with these terms.

## Appendix 2:



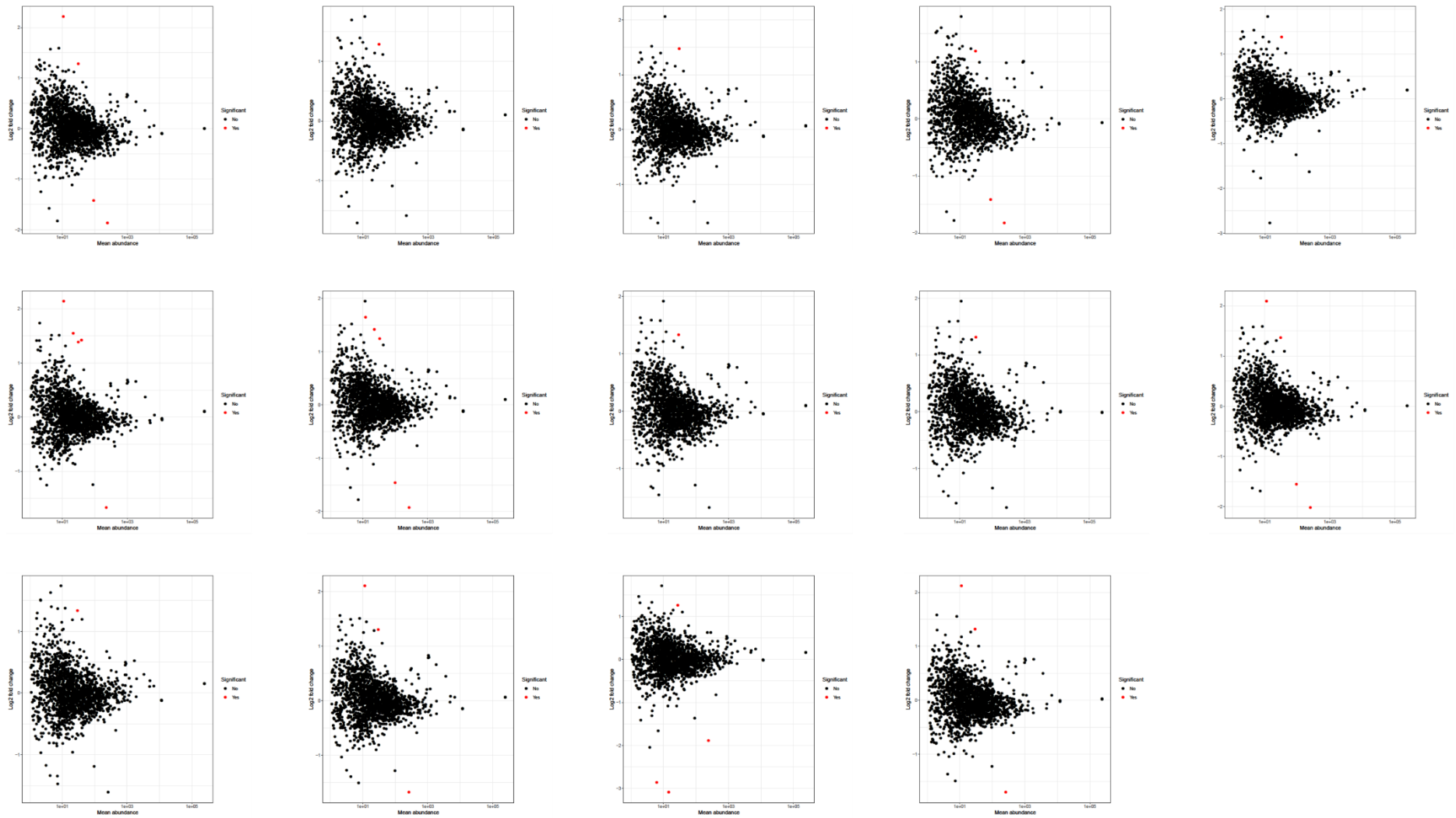
**Appendix 2:** DESeq analysis of *C. jejuni* 11168H wild-type strain grown in the presence of 0.2% (w/v) sodium taurocholate compared to the absence. Results are depicted in MA plots. Each plot represents a single run during LOO (leave one out) cross-validation. Red dots represent differentially expressed genes.

### Appendix 3:



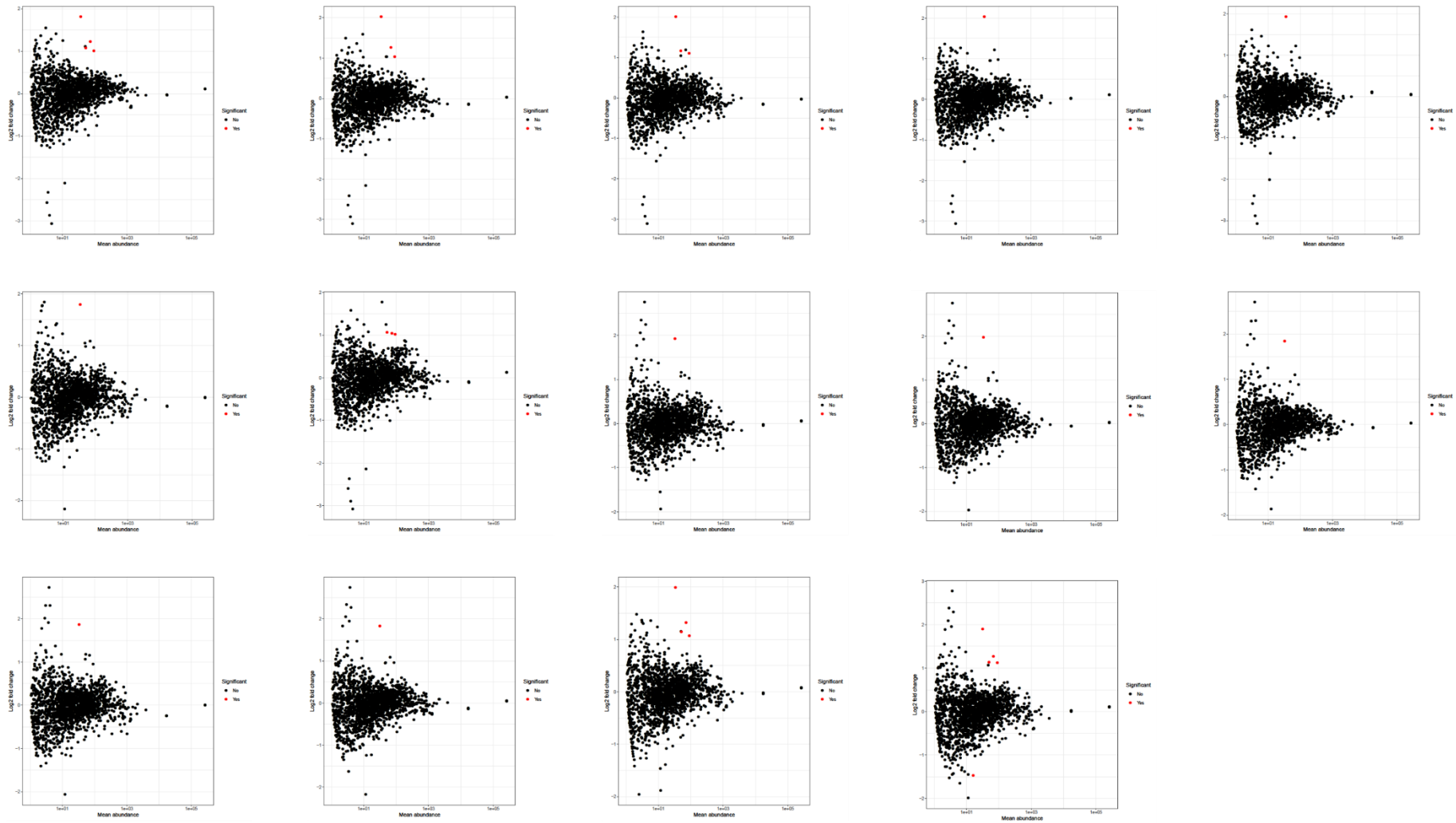
**Appendix 3:** DESeq analysis of *C. jejuni* 488 wild-type strain grown in the presence of 0.2% (w/v) sodium taurocholate compared to the absence. Results are depicted in MA plots. Each plot represents a single run during LOO (leave one out) cross-validation. Red dots represent differentially expressed genes.

## Appendix 4:



**Appendix 4:** DESeq analysis of *C. jejuni* 11168H wild-type strain grown in the presence of 0.05% (w/v) sodium deoxycholate compared to the absence. Results are depicted in MA plots. Each plot represents a single run during LOO (leave one out) cross-validation. Red dots represent differentially expressed genes.

## Appendix 5:



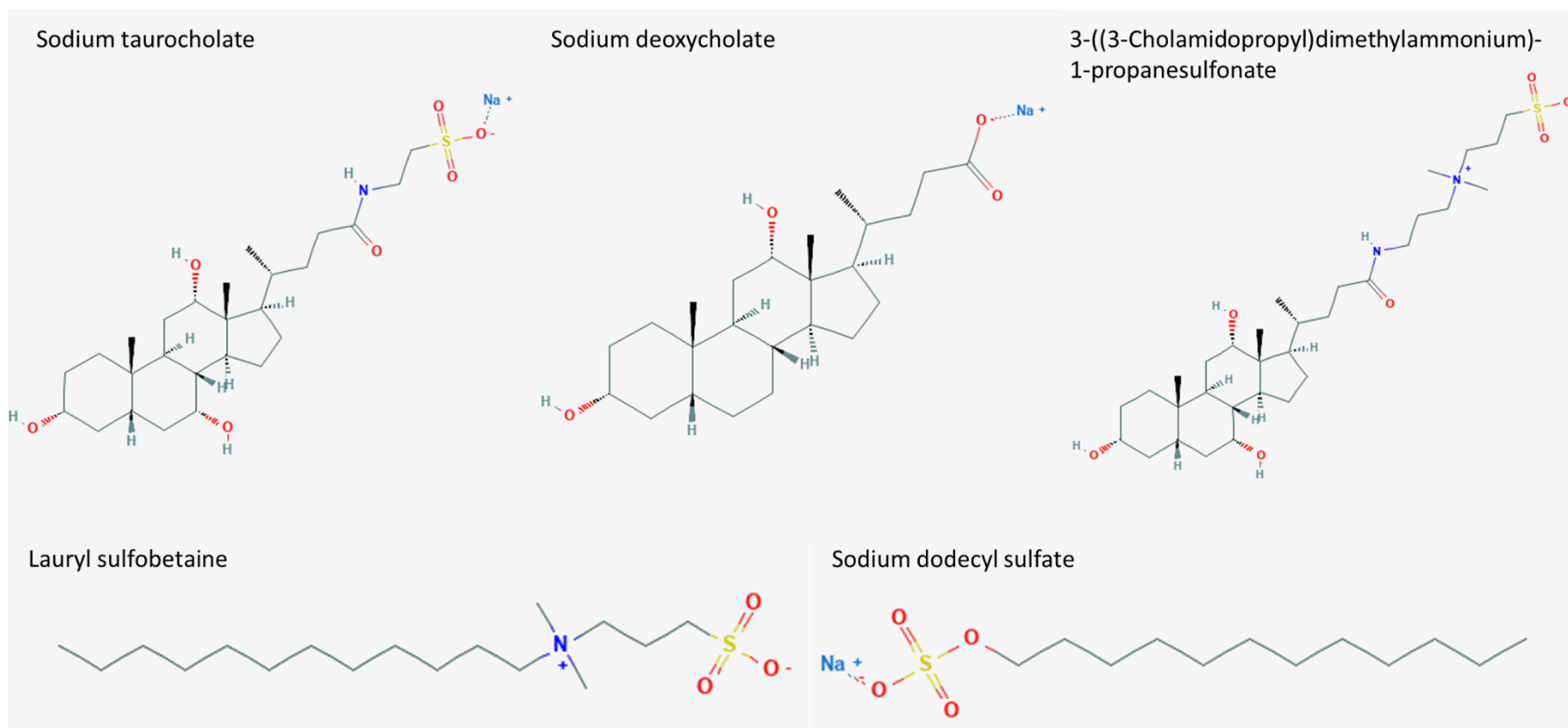
**Appendix 5:** DESeq analysis of *C. jejuni* 488 wild-type strain grown in the presence of 0.05% (w/v) sodium deoxycholate compared to the absence. Results are depicted in MA plots. Each plot represents a single run during LOO (leave one out) cross-validation. Red dots represent differentially expressed genes.

**Appendix 6:**

Strain/condition	Regulation	Individual cross validation runs (1-14)														Maximum	Minimum
		1	2	3	4	5	6	7	8	9	10	11	12	13	14		
11168H 0.2% ST	Up	13	10	11	16	13	12	15	13	11	11	12	10	13	8	16	8
	Down	6	11	11	6	9	8	10	9	8	7	12	11	16	9	16	6
	Total	19	21	22	22	22	20	25	22	19	18	24	21	29	17	29	17
488 0.2% ST	Up	23	21	25	24	24	32	24	29	34	32	28	32	26	27	34	21
	Down	19	18	17	16	11	15	18	7	15	14	10	15	16	13	19	7
	Total	42	39	42	40	35	47	42	36	49	46	38	47	42	40	49	35
11168H 0.05% SDC	Up	26	18	23	32	23	26	28	24	21	22	26	24	15	19	32	15
	Down	9	8	7	10	8	6	8	8	10	9	8	8	15	9	15	6
	Total	35	26	30	42	31	32	36	32	31	31	34	32	30	28	42	26
488 0.05% SDC	Up	21	18	20	22	23	24	21	29	27	22	23	23	21	31	31	18
	Down	27	36	27	23	17	18	30	23	15	17	23	26	24	30	36	15
	Total	48	54	47	45	40	42	51	52	42	39	46	49	45	61	61	39

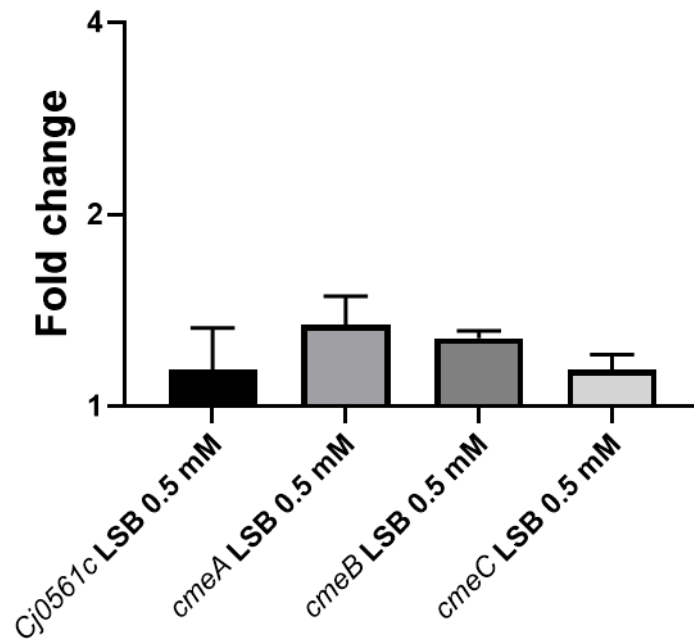
The number of genes exhibiting greater than 1 log fold change during each cross validation run for DESeq analysis. Maximum refers to the maximum number of genes observed during a single cross validation run. Minimum refers to the minimum number of genes observed during a single cross validation run.

## Appendix 7:



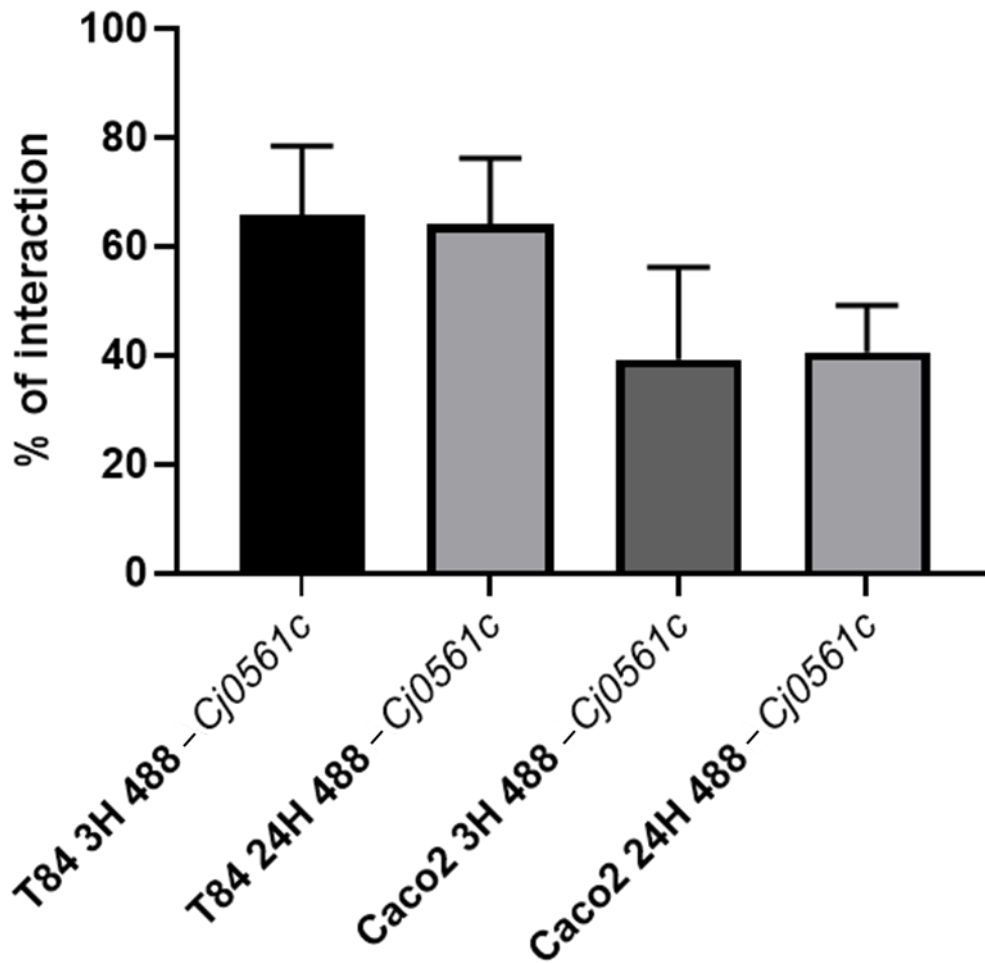
**Appendix 7:** Chemical structure of sodium taurocholate (ST) (NCBI, 2022e), sodium deoxycholate (SDC) (NCBI, 2022a), 3-((3-Cholamidopropyl)dimethylammonium)-1-propanesulfonate (CHAPS) (NCBI, 2022c), lauryl sulfobetaine (LSB) (NCBI, 2022b), and sodium dodecyl sulfate (SDS) (NCBI, 2022d).

**Appendix 8:**



**Appendix 8:** qRT-PCR analysis of *Cj0561c*, *cmeA*, *cmeB* and *cmeC* by the 488 wild-type strain co-incubated with 0.5 mM lauryl sulfobetaine compared to in the absence. *rpoA* was used as an internal control.

Appendix 9:



**Appendix 8:** The scale of the difference in interaction with T84 and Caco-2 cells between the 488 wild-type and 488 *Cj0561c* mutant strain compared to the scale of the difference in invasion between these strains. Results are presented as a percentage of interaction. Less than 100% indicates the difference between wild-type and mutant strain invasion has reduced compared to the difference in interaction.